

University of Warwick institutional repository: <http://go.warwick.ac.uk/wrap>

**A Thesis Submitted for the Degree of PhD at the University of Warwick**

<http://go.warwick.ac.uk/wrap/3494>

This thesis is made available online and is protected by original copyright.

Please scroll down to view the document itself.

Please refer to the repository record for this item for information to help you to cite it. Our policy information is available from the repository home page.

# **FLOW AND HEAT TRANSFER MODELLING OF AN AUTOMOTIVE ENGINE LUBRICATION SYSTEM**

**Volume I**

**Marcus B.M. Fenton**

**Thesis submitted for the degree of Doctor of Philosophy**

**Submitted to the University of Warwick**

**June 1994**

**Advanced Technology Centre  
University of Warwick  
Coventry  
CV4 7AL**

# Table of contents

<b>List of Figures</b>	i
<b>List of Tables</b>	iv
<b>Notation</b>	vi
<b>Acknowledgements</b>	1
<b>Declaration</b>	2
<b>Summary</b>	3
<b>Chapter 1</b>	
<b>Introduction</b>	4
1.1 The Problem	4
1.2 The Proposed Solution	7
1.3 Previous Work by Jaguar	8
1.4 Project Overall Objectives	9
1.5 Program Development Stages	11
<b>Chapter 2</b>	
<b>Literature Search</b>	13
2.1 Introduction	13
2.2 Experimental Investigation of the Lubrication System	13
2.3 Computer Simulation of Lubrication Systems	17
2.4 Computer Simulation of Engine Warm-Up	27
2.4.1 The Determination of Combustion Chamber Temperatures	31
2.4.2 Piston/Cylinder Heat Transfer to the Oil	34
2.4.2.1 Piston/Liner Lubrication	34
2.4.2.2 Oil Spray to Piston Under-Crown	37
2.4.2.3 Oil Spray on the Liner	39
2.4.3 Heat Transfer by the Coolant	40
2.5 Lubrication of Journal Bearings	43
2.5.1 Prediction of Bearing Oil Flow Rate	43

	2.5.2 Heat Transfer Within Bearings . . . . .	46
2.6	Oil Filter . . . . .	48
2.7	Crankshaft and Camshaft Oil Flows . . . . .	48
2.8	Commercial Software for Thermofluid Analysis . . . . .	49
2.9	Conclusions . . . . .	50

## Chapter 3

### Fluid Flow and Heat Transfer Fundamentals Within an Engine

	<b>Lubrication System . . . . .</b>	<b>53</b>
3.1	Introduction . . . . .	53
3.2	Typical Engine Lubrication System Layout . . . . .	54
3.3	Lubricating Oils . . . . .	55
3.4	Flow Passages . . . . .	58
	3.4.1 Flow in Pipes . . . . .	58
	3.4.1.1 Types of Fluid Flow . . . . .	58
	3.4.1.2 Flow Development . . . . .	59
	3.4.1.3 Conservation of Energy . . . . .	60
	Friction losses in pipes and passages . . . . .	61
	Losses from Bends . . . . .	62
	Losses from Junctions and Other Flow Restrictions . . . . .	62
	3.4.2 Heat Transfer in Pipes . . . . .	63
	3.4.2.1 Heat Transfer in Fully Developed Flow . . . . .	64
	3.4.2.2 Equations for Forced Convection . . . . .	66
3.5	Annular Pipes . . . . .	69
	3.5.1 Flow Through an Annuli . . . . .	70
	3.5.2 Heat Transfer in an Annuli . . . . .	70
3.6	Oil Pumps . . . . .	71
3.7	Oil Strainers . . . . .	72
3.8	Oil Filters . . . . .	74
3.9	Engine Bearings . . . . .	74
	3.9.1 Oil Supply . . . . .	75
	3.9.2 Steadily Loaded Journal Bearings . . . . .	76
	3.9.2.1 Supply Grooves . . . . .	79
	3.9.3 Heat Transfer in Journal Bearings . . . . .	82
3.10	Crankshaft and Camshaft Oil Transfer Holes . . . . .	83
	3.10.1 Registry . . . . .	83
	3.10.2 Centrifugal Losses . . . . .	84



	3.10.3 Acceleration of Oil to Journal Surface Speed . . . . .	85
	3.10.4 Acceleration Losses . . . . .	86
3.11	Oil Coolers . . . . .	86
	3.11.1 Heat Exchangers . . . . .	87
	3.11.2 Oil Flow Through an Oil Cooler . . . . .	87
	3.11.3 Heat Transfer in an Oil Cooler . . . . .	89
3.12	Piston/Liner and Valve Train Lubrication . . . . .	91
	3.12.1 Heat Transfer under the Piston . . . . .	92
	3.12.2 Heat Transfer on the Liner . . . . .	94
	3.12.3 Heat Transfer on the cylinder head . . . . .	95
	3.12.4 Prediction of Engine Surface Temperatures . . . . .	95
	3.12.4.1 Boundary Conditions . . . . .	99
	Convection to the Air . . . . .	99
	Convection to Crankcase Gases . . . . .	101
	Convection to the Coolant . . . . .	101
	Convection to the Combustion Gases . . . . .	101
3.13	Conclusions . . . . .	102

## Chapter 4

### Mathematical Model of Flow Conditions Within the Lubrication

	<b>System . . . . .</b>	<b>105</b>
4.1	Introduction . . . . .	105
	4.1.1 Linear and Non-Linear Models . . . . .	106
	4.1.2 Representing the Physical System . . . . .	107
	4.1.2.1 Linear Model . . . . .	108
	4.1.2.2 Non-Linear Model . . . . .	108
	Method One. Continuity of Flow . . . . .	109
	Method Two. Pressure/Flow Rate	
	Combination . . . . .	110
	4.1.3 Component Models . . . . .	112
4.2	Oil Pump . . . . .	114
	4.2.1 Simplified Oil Pump Model . . . . .	115
	4.2.2 Enhanced Oil Pump Model . . . . .	118
	4.2.3 V8 Engine Oil Pump Data . . . . .	123
4.3	Pipes . . . . .	124
	4.3.1 Laminar Pipe Flow . . . . .	125
	4.3.2 Turbulent Pipe Flow . . . . .	126
4.4	Annular Pipes . . . . .	128
4.5	Oil Strainers . . . . .	129

4.6	Oil Filters . . . . .	132
4.7	Journal Bearings . . . . .	133
4.7.1	Partially Grooved Bearings . . . . .	135
4.7.2	Non-Grooved Bearings . . . . .	136
4.8	Crank-Shaft Oil Transfer Holes . . . . .	138
4.9	Cam Bearing Oil Transfer Holes . . . . .	139
4.9.1	Flow Towards Cam-Shaft Centre . . . . .	140
4.9.2	Flow Away from Cam-Shaft Centre . . . . .	141
4.10	Oil Coolers . . . . .	141
4.11	Conclusions . . . . .	143

## Chapter 5

### Mathematical Model of Heat Transfer Within the Lubrication

<b>System . . . . .</b>	<b>146</b>
5.1 Introduction . . . . .	146
5.1.1 Structure of the Heat Transfer and Engine Block Models . . . . .	150
5.2 Pipe Model . . . . .	152
5.3 Journal Bearing Model . . . . .	155
5.3.1 Simple Bearing Oil Temperature Rise Model . . . . .	155
5.3.2 Enhanced Bearing Heat Transfer Model . . . . .	156
5.4 Oil Cooler Model . . . . .	159
5.5 Engine Block Model . . . . .	164
5.5.1 Nodal Resistance Network Model . . . . .	168
5.5.2 Oil Splash Model . . . . .	169
5.5.2.1 Heat Transfer Equation . . . . .	171
5.5.2.2 Continuity Equation . . . . .	173
5.6 Concluding Remarks . . . . .	175

## Chapter 6

<b>Structure of Flow Model Computer Program . . . . .</b>	<b>179</b>
6.1 Introduction . . . . .	179
6.1.1 Programming Language . . . . .	180
6.2 Initiating the Flow Program . . . . .	186
6.3 Representing the Physical System . . . . .	187
6.4 Input of Data . . . . .	193
6.5 Data Processing . . . . .	197
6.5.1 Linear Program . . . . .	197

6.5.2	Non-Linear Program . . . . .	201
6.6	Output of Results . . . . .	206
6.7	User Interface . . . . .	210
6.8	Summary of Chapter 6 . . . . .	213

## Chapter 7

### Structure of Heat Transfer Model and Engine Block Model

<b>Computer Programs . . . . .</b>		<b>218</b>
7.1	Introduction . . . . .	218
7.2	Heat Transfer Program . . . . .	223
7.2.1	Preparation of Bearing Data . . . . .	224
7.2.2	Input of Data . . . . .	226
7.2.3	Data Processing . . . . .	227
7.2.4	Output of Results . . . . .	230
7.2.5	User Interface . . . . .	232
7.3	Engine Block Program . . . . .	233
7.3.1	Representing the Engine Arrangement . . . . .	234
7.3.2	Input of Data . . . . .	238
7.3.3	Data Processing . . . . .	241
7.3.4	Output of Data . . . . .	244
7.3.5	User Interface . . . . .	247
7.4	Summary of Chapter 7 . . . . .	248

## Chapter 8

<b>Flow Analysis of AJ6 Engine Lubrication System . . . . .</b>		<b>252</b>
8.1	Introduction . . . . .	252
8.2	Comparison Between the Two Linear Flow Programs . . . . .	253
8.3	Comparison Between Linear and Non-Linear Flow Programs . . . . .	255
8.4	Modelling the AJ6 Engine Lubrication System . . . . .	258
8.4.1	Pressure and Flow Rate Trends . . . . .	259
8.4.2	Comparison Between Predicted Results and those Provided by Glacier Vandervell . . . . .	260
8.4.3	Discussion of Engine Test Results for the AJ6 Engine . . . . .	264
8.4.3.1	Oil Temperature Observations . . . . .	265
8.4.3.2	Oil Pump Characteristics . . . . .	265
8.4.3.3	Comparison Between Predicted and	



	Measured Values . . . . .	269
8.4.3.4	Influence of Thermal Expansion on Radial Clearance . . . . .	275
8.5	Summary of Chapter 8 . . . . .	279

## Chapter 9

	<b>Modelling the V8 Engine Lubrication System . . . . .</b>	<b>282</b>
9.1	Introduction . . . . .	282
9.2	Comparison with Results from V8 Valve Train Rig Tests .	284
9.2.1	Constant Oil Feed Pressure and Temperature . . . . .	285
9.2.2	Varying Oil Feed Pressures . . . . .	287
9.3	Comparison with Results from V8 Engine Tests . . . . .	291
9.3.1	Pressure and Flow Rate Results . . . . .	292
9.3.2	Oil Temperature Results . . . . .	294
9.4	Modelling the V8 Engine Block. Comparison of Engine Block Temperature Results with Results from an FEA Model . . . . .	296
9.5	Summary of Chapter 9 . . . . .	308

## Chapter 10

	<b>Conclusions and Suggestions for Future Work . . . . .</b>	<b>312</b>
10.1	Overall Conclusions . . . . .	312
10.2	Suggestions for Future Work . . . . .	321

	<b>References . . . . .</b>	<b>328</b>
--	-----------------------------	------------

	<b>Bibliography . . . . .</b>	<b>337</b>
--	-------------------------------	------------

## Appendix A

	<b>Numerical Solution Methods . . . . .</b>	<b>338</b>
A.1	Linear Modelling . . . . .	339
A.1.1	Basic Principles for Solving Sets of Equations . . . . .	340
A.1.2	Gauss-Jordan Elimination . . . . .	342
A.1.3	LU Decomposition . . . . .	343
A.2	Non-Linear Modelling . . . . .	346
A.2.1	Levenberg-Marquardt Algorithm . . . . .	347

## **Appendix B**

### **Lubricant Properties and General**

<b>Modelling Data</b>	351
B.1    Grades of Oil	352
B.2    Oil Additives	353
B.3    Moody Chart	356
B.4    Pipe Roughness Values	357
B.5    Lubrication of Sliding Surfaces	358

## **Appendix C**

<b>Component Performance Characteristics</b>	360
C.1    Thermal Properties of Lubricating Oil	361
C.2    Thermal Properties of Air	366
C.3    Instantaneous Gas Temperature	367
C.4    Journal Centre Orbit Plots	368

## **Appendix D**

<b>Supplementary Calculations</b>	370
D.1    Oil Temperature Rise in the Pump	371
D.2    Typical Reynolds Number for a Falling Oil Film	373
D.3    Oil Filter Characteristics	374
D.4    Oil Cooler Dimensions	376

## **Appendix E**

### **Experimental Investigation of the**

<b>Jaguar AJ6 Engine</b>	377
E.1    Introduction	378
E.2    Engine Modification and Instrumentation	379
E.3    Test Procedure	380

## **Appendix F**

### **Experimental Investigation of the**

<b>Jaguar V8 Engine</b>	383
F.1    Test Schedule	384



# List of Figures

1.1.	Schematic diagram of Jaguar AJ6 engine lubrication system used by Ellinas (1988) . . . . .	10
2.1.	Engine oil flow rate v pump discharge flow rate . . . . .	18
2.2.	Averaged bearing oil flows from various predictive techniques . . . .	46
3.1.	Jaguar AJ6 engine lubrication network . . . . .	56
3.2.	Schematic diagram of Jaguar AJ6 engine lubrication system . . . . .	57
3.3.	Laminar and turbulent velocity profiles . . . . .	59
3.4.	Boundary layer development after a smooth contraction . . . . .	60
3.5.	Typical T and Y junctions . . . . .	63
3.6.	Temperature distribution in pipe flow . . . . .	64
3.7.	Developing temperature profiles in pipe flow . . . . .	65
3.8.	Section through a typical automatic chain tensioner . . . . .	69
3.9.	Oil gear pump design . . . . .	71
3.10.	Ideal oil pump characteristics . . . . .	72
3.11.	AJ6 engine oil filter . . . . .	75
3.12.	Operation of a hydrodynamic journal bearing . . . . .	77
3.13.	Axial hydrodynamic pressure profile . . . . .	77
3.14.	Common supply groove positions . . . . .	80
3.15.	Transfer passage 'in' and 'out' of registry . . . . .	84
3.16.	Flow distribution for dividing manifold . . . . .	88
3.17.	Flow distribution for combining manifold . . . . .	88
3.18.	Temperature variation of unmixed fluids in a cross-flow heat exchanger . . . . .	90
3.19.	Simplified engine arrangement . . . . .	96
3.20.	Example block arrangement and resulting resistance network . . . .	97
4.1.	Jaguar AJ6 engine oil pump characteristic curves . . . . .	116
4.2.	Simplified AJ6 oil pump characteristics . . . . .	116
4.3.	Curve fitting of oil pump characteristics at three engine speeds, using three different iteration techniques . . . . .	119
4.4.	Curve fitting of oil pump data for three engine speeds using the same number of data points to represent each curve . . . . .	120
4.5.	Curve fitting of oil pump data for three engine speeds by breaking down each curve into two second order curves . . . . .	121

4.6.	Variation of measured data for V8 engine oil pump . . . . .	123
4.7.	Laminar flow coefficients - annular cross-sections . . . . .	129
4.8.	Correction factors for eccentric annuli . . . . .	130
4.9.	Influence of Reynolds number on pressure drop across a woven screen . . . . .	132
4.10.	Groove functions for one groove in unloaded region . . . . .	136
4.11.	Cross-section through a finned oil tube in an oil cooler . . . . .	142
5.1	Thermofluid analysis procedure for an engine lubrication system	147
5.2.	Bearing oil temperature rise . . . . .	156
5.3.	Oil temperature rise 'map' for the number 1 main bearing of the V8 engine . . . . .	158
5.4.	Heat transfer data for plate-fin heat exchanger surfaces . . . . .	161
5.5.	Effectiveness - NTU relationship for a cross-flow heat exchanger with both fluids unmixed . . . . .	163
5.6.	Block element and corresponding nodal resistance network for two dimensional conduction and convection . . . . .	166
5.7.	Basic construction of the engine block model . . . . .	168
5.8.	Oil splash onto two elements and resulting oil flow network . . . .	170
6.1.	Flow chart of linear flow program . . . . .	182
6.2.	Flow chart of the non-linear flow program . . . . .	184
6.3.	Simple four element lubrication system . . . . .	190
7.1.	Flow chart of the heat transfer program . . . . .	220
7.2.	Flow chart of the engine block program . . . . .	221
7.3.	Journal bearing oil feed groove extent . . . . .	225
7.4.	Simple two block element arrangement with thermal resistance network . . . . .	236
7.5.	Representative flow network for the two block element arrangement shown in Figure 7.4 . . . . .	238
8.1	Simple two element test system . . . . .	257
8.2	Schematic diagram of the modified AJ6 engine lubrication system - 'Layout1' . . . . .	266
8.3	Schematic diagram of the modified AJ6 engine lubrication system - 'Layout2' . . . . .	267
8.4	Engine speed influence on oil temperature ( $\frac{1}{2}$ load) . . . . .	268
8.5	Engine load influence on oil temperature (2000 rpm) . . . . .	268
8.6	Simplified oil pump characteristics, used to model the AJ6 engine	



	lubrication system . . . . .	269
9.1	Schematic diagram of V8 engine lubrication system . . . . .	283
9.2	Comparison between predicted and measured flow rates for V8 head . . . . .	285
9.3	Comparison of results for the flow rate to the inlet valve side of the V8 engine head. Varying feed pressures. . . . .	288
9.4	Comparison between predicted and measured result trends at cam speed of 2000 rpm. Fixed cam and tappet eccentricity ratios. . . . .	289
9.5	Comparison between predicted and measured result trends at cam speed of 2000 rpm. Varying cam and tappet eccentricity ratios. . . . .	290
9.6	Block element arrangement and nodal resistance network of V8 engine block . . . . .	297
9.7	V8 engine block temperatures and mean oil film temperatures returned by the engine block program (°C) . . . . .	301
9.8	FEA temperature results for the V8 engine block at 6000 rpm (cylinder 1) . . . . .	302
9.9	FEA temperature results for the V8 engine piston at 6000 rpm (cylinder 1, 'A' bank) . . . . .	303
9.10	FEA temperature results for the V8 engine bedplate at 6000 rpm . . . . .	304
9.11	FEA temperature results for the V8 engine cylinder head at 6000 rpm (cylinder 1, 'A' bank) . . . . .	305
B.1.	Moody Chart - Friction Coefficient v Reynolds Number . . . . .	356
B.2.	Idealised lubrication regimes . . . . .	358
C.1.	Kinematic viscosities for an Esso 5W/30 multigrade oil plotted on a standard ASTM chart . . . . .	363
C.2.	Instantaneous gas temperatures for the combustion chamber of the V8 engine . . . . .	367
C.3.	Journal centre orbit plots for the main and big-end bearings of the Jaguar AJ6 engine . . . . .	368
C.4.	Journal centre orbit plot for the No.2 main bearing of the V8 engine at 6000 rpm . . . . .	369
D.1.	Oil filter characteristics at low oil flow rates . . . . .	374
D.2.	Oil filter characteristics at medium oil flow rates . . . . .	375
D.3.	Oil filter characteristics at high oil flow rates . . . . .	375

## List of Tables

2.1.	Engine Friction Losses (Patton et al (1989)) . . . . .	30
3.1.	Heat transfer coefficients for piston oil cooling (Stotter) . . . . .	92
3.2.	Heat transfer coefficients for piston oil cooling (Seale and Taylor) .	93
6.1.	Two-dimensional array BIN with sum of rows . . . . .	190
6.2.	Example of one-dimensional array TYP . . . . .	191
6.3.	Array BIN generated in the fully developed non-linear flow model	191
6.4.	One-dimensional array QNUM . . . . .	192
6.5.	One-dimensional array PNUM . . . . .	193
7.1.	Part of the two-dimensional array IBIN . . . . .	237
7.2.	Part of the one-dimensional array IOILPATH . . . . .	238
7.3.	Part of the one-dimensional array NINLET . . . . .	238
7.4.	Part of the one-dimensional array NOUTLET . . . . .	239
7.5.	Summary of the input data required to model the heat transfer within the engine block . . . . .	240
8.1.	Comparison of oil flow rates predicted by Gauss-Jordan and LU decomposition exact linear methods (AJ6 engine) . . . . .	254
8.2.	Comparison of run times for two non-linear modelling routines . .	256
8.3.	Comparison of results from the LU linear flow program and non- linear flow program (with LU linear matrix solver) . . . . .	257
8.4.	Comparison of results from linear and non-linear flow programs for simple test system . . . . .	258
8.5.	Comparison of bearing hydrostatic flow rates (AJ6 engine) . . . . .	261
8.6.	Comparison of bearing hydrostatic flow rates with cam bearing radial clearance of 0.09 mm . . . . .	263
8.7.	AJ6 engine bearing dimensions and radial clearances . . . . .	270
8.8.	Comparison between measured and predicted values for Layout 1	271
8.9.	Comparison between measured and predicted values for Layout 2	274
8.10.	Thermal properties of cam bearing materials . . . . .	277
8.11.	Calculated hot (120°C) radial clearances for the AJ6 engine cam-shaft bearings . . . . .	278
9.1.	Initial modelling conditions used for the cam bearings and tappets of the V8 head . . . . .	286



9.2.	Calculated hot (120°C) radial clearances for the V8 engine cam-shaft bearings and tappets . . . . .	286
9.3.	Estimated eccentricity ratios for the cam bearings and tappets with varying oil feed pressures . . . . .	290
9.4.	Component dimensions which were used to model the V8 engine lubrication system . . . . .	293
9.5.	Comparison between measured and predicted pressure and flow rate results for the V8 engine . . . . .	293
9.6.	Comparison between measured and predicted oil temperature results for the V8 engine . . . . .	294
9.7.	Modelling conditions used in the nodal resistance network model of the V8 engine block . . . . .	299
9.8.	Summary of the modelling conditions used in the FEA model of the V8 engine (Chang et al (1992)) . . . . .	300
9.9.	Comparison of predicted block temperature results and results obtained from an FEA model of the V8 engine . . . . .	306
B.1.	SAE viscosity numbers for crankcase oils . . . . .	352
B.2.	Pipe roughness values, k (mm) . . . . .	357
C.1.	BP 10W/30 multigrade oil characteristics (AJ6 engine) . . . . .	361
C.2.	Esso 5W/30 multigrade oil characteristics (V8 engine) . . . . .	362
C.3.	Specific heats of lubricating oils (Btu per pound per °F) . . . . .	364
C.4.	Thermal properties of dry air at atmospheric pressure . . . . .	366
D.1.	Modelling conditions for the calculation of the oil temperature rise within a pump . . . . .	372
D.2.	Variable values used to plot the oil filter characteristics . . . . .	374
D.3.	Dimensions of the Jaguar oil cooler . . . . .	376
E.1.	Turbine flow meter calibration data . . . . .	380
E.2.	Brake torque of the Jaguar AJ6 4.0 litre engine . . . . .	381
E.3.	Test schedule for first series of AJ6 engine tests (main bearings 180° groove on the top half) . . . . .	382
F.1.	Test schedule for V8 engine oil system tests . . . . .	384



# Notation

The following notation is used throughout this dissertation. Any special notation is defined in the section to which it applies.

## General

$C$	Intercept on the y-axis by a straight line (general)
$C_p$	Specific Heat (J/Kg°C)
$g$	Acceleration due to gravity (m/s <sup>2</sup> )
$Gr$	Grashof number (dimensionless)
$h$	Heat transfer coefficient (W/m <sup>2</sup> °C)
$M$	Slope of a straight line (dimensionless)
$\dot{m}$	Mass flow rate (Kg/s)
$Nu$	Nusselt number (dimensionless)
$P_1$	Oil pressure at entry to a component (N/m <sup>2</sup> )
$P_2$	Oil pressure at exit from a component (N/m <sup>2</sup> )
$\Delta P$	Change of oil pressure within a component (N/m <sup>2</sup> )
$\Delta P_{bends}$	Change of oil pressure due to losses within bends, junctions and other disturbances (N/m <sup>2</sup> )
$\Delta P_{friction}$	Change of oil pressure due to frictional losses (N/m <sup>2</sup> )
$Pr$	Prandtl number (dimensionless)
$q$	Heat flow rate (W)
$Q_{1,2}$	Oil flow rate through a component (m <sup>3</sup> /s)
$Re$	Reynolds number (dimensionless)
$t_b$	Bulk fluid temperature (°C)
$t_s$	Surface temperature (°C)
$\mu$	Oil dynamic viscosity (Ns/m <sup>2</sup> )
$\rho$	Oil density (Kg/m <sup>3</sup> )
$\sigma$	Standard deviation term used in the Levenberg-Marquardt routine (dimensionless)
$\chi^2$	Merit function used in the Levenberg-Marquardt routine (dimensionless)
$\omega$	Angular speed (rad/s)

**Flow Passages**

$A$	Cross-sectional area of pipe ( $\text{m}^2$ )
$C_f$	Laminar flow coefficient (dimensionless)
$D$	Pipe diameter (m)
$D_h$	Hydraulic diameter (m)
$f$	Friction coefficient (dimensionless)
$f_{\text{circular}}$	Friction coefficient for a circular pipe (dimensionless)
$f_{\text{annular}}$	Friction coefficient for an annular pipe (dimensionless)
$k$ (flow)	Pipe roughness value (m)
$k$ (heat)	Thermal conductivity ( $\text{W/m}^\circ\text{C}$ )
$K_b$	Bend loss coefficient (dimensionless)
$K_{ij}$	Loss coefficient in T and Y junctions (dimensionless)
$L$	Pipe length (m)
$t_{\text{bin}}$	Bulk fluid temperature at inlet ( $^\circ\text{C}$ )
$t_{\text{bo}}$	Bulk fluid temperature at exit ( $^\circ\text{C}$ )
$V$	Fluid velocity (m/s)
$z$	Height above some datum (m)
$\mu$	Oil dynamic viscosity at the pipe surface ( $\text{Ns/m}^2$ )
$\epsilon$	Eccentricity ratio for an annular pipe (dimensionless)

**Oil Strainers**

$d$	Diameter of the wire strands (m)
$K$	Pressure loss coefficient (dimensionless)
$K_\infty$	Pressure loss coefficient at high Reynolds numbers (dimensionless)
$m$	Number of wire strands per metre
$Re_d$	Reynolds number for the flow through a screen (dimensionless)
$U$	Mean fluid velocity approaching the screen (m/s)
$\lambda$	Porosity of a woven screen (dimensionless)
$\phi$	Coefficient of contraction (dimensionless)

**Oil Filters**

$A_f$	Projected area of fibres ( $\text{m}^2$ )
-------	---

$D_f$	Fibre diameter (m)
$L$	Filter bed thickness (m)
$\epsilon$	Porosity of filter element (dimensionless)

### Journal Bearings

$a$	Axial width of oil feed groove (m)
$C_r$	Uniform radial clearance (m)
$D$	Journal diameter (m)
$d_h$	Oil feed hole diameter (m)
$e$	Bearing eccentricity (m)
$f_1, f_2$	Constants of feed groove geometry (dimensionless)
$h$	Oil film thickness (m)
$h_g$	Oil film thickness at groove mid position (m)
$L$	Bearing axial length (m)
$Q^*$	Effective flow factor (dimensionless)
$R_1$	Radius of journal (m)
$R_2$	Inside radius of bearing shell (m)
$U$	Journal peripheral speed (m/s)
$\alpha$	Coefficient of thermal expansion ( $K^{-1}$ )
$C_s$	Effective viscosity (centistokes)
$\epsilon$	Eccentricity ratio (dimensionless)

### Crank-Shaft Oil Transfer Holes

$D$	Diameter of transfer hole (m)
$L$	Length of transfer hole (m)
$r$	Main bearing journal Radius (m)
$R$	Radial distance from crank-shaft centreline to exit from transfer hole (m)
$s$	Minimum distance between oil path and Crank-shaft centreline (m)

### Cam Bearing Oil Transfer Holes

$L_T$	Length of transfer hole (m)
-------	-----------------------------



$D_T$	Diameter of transfer hole (m)
$R_c$	Radius of cam journal (m)
$R_{in}$	Radius of cam-shaft central drilling (m)

### Oil Coolers

$A$	Total surface area ( $m^2$ )
$A_f$	Total surface area of the fins ( $m^2$ )
$A_w$	Total unfinned plate area ( $m^2$ )
$A_x$	Free flow area for each stream ( $m^2$ )
$C_R$	Capacity ratio (dimensionless)
$D_h$	Hydraulic diameter (m)
$f_p$	Fin pitch (fins per metre)
$G$	Mass velocity ( $Kg/sm^2$ )
$k$	Thermal conductivity ( $W/m^\circ C$ )
$L$	Half the length of the fins between the plates (m)
NTU	Number of Transfer Units (dimensionless)
$t$	Fluid temperature ( $^\circ C$ )
$U$	Overall heat transfer coefficient ( $W/m^2^\circ C$ )
$w$	Thickness of the fins (m)
$\varepsilon$	Effectiveness of a heat exchanger (dimensionless)
$\eta$	Surface effectiveness (dimensionless)
$\kappa$	Fin efficiency (dimensionless)

### Subscripts used in the Oil Cooler Model

$c$	Cold fluid (air)
$h$	Hot fluid (oil)
$i$	Inlet condition
$o$	Outlet condition
$av$	Average

### Engine Model

$A_{ij}$	Cross-sectional area for conduction and convection between nodes $i$ and $j$ ( $m^2$ )
----------	--

$C_w$	Width of a falling oil film (m)
$H$	Height of the wetted surface (m)
$k$	Thermal conductivity (W/m°C)
$\dot{m}$	Mass flow rate (Kg/s)
$\dot{m}'$	Mass flow rate per unit length of the upper edge of a surface (Kg/ms)
$R_{ij}$	Total thermal resistance between nodes i and j (°C/W)
$s$	Thickness of the oil film (m)
$t$	Oil temperature (°C)
$t_{sat}$	Saturation temperature (°C)
$\Delta t_x$	Temperature excess (°C)
$\dot{W}'$	Weight flow per unit time over unit length of the upper edge of a surface (N/ms)
$x$	Characteristic length (height) (m)
$\beta$	Coefficient of volume expansion (°C <sup>-1</sup> )
$\gamma$	Specific weight (N/m <sup>3</sup> )
$\delta_{ij}$	Distance between nodes i and j (m)
$\xi$	Dimensionless quantity
$\phi$	Temperature ratio (dimensionless)
$\psi$	Percentage of the flow rate (dimensionless)

### Subscripts used in the Engine Model

ab	Previous element
b	Big-end bearing
c	Cam bearing
m	Main bearing

### Acronyms

ASTM	American Society for Testing Materials
BHRA	British Hydromechanics Research Association
BP	British Petroleum
CFD	Computational Fluid Dynamics
CPU	Central Processing Unit
FEA	Finite Element Analysis



IC	Internal Combustion
MSc	Master of Science
NEL	National Engineering Laboratory
NO <sub>x</sub>	Nitrogen Oxides
PC	Personal Computer
PSI	Pounds per Square Inch
RPM	Revolutions Per Minute
SAE	Society of Automotive Engineers
SLJB	Steadily Loaded Journal Bearing
UHC	Unburned Hydrocarbons
VEC	Vehicle Engine Cooling
VI	Viscosity Index
VMS	Vehicle Mission Simulation

# Acknowledgements

My special thanks go to my project supervisor Dr. Ali Veshagh for his enthusiastic support, help and guidance throughout this project.

Many thanks also to Jaguar Cars for their financial and technical support of the project. In particular I would like to acknowledge Mr Steve Richardson, Mr Chris Jones, and Mr Martin Roskilly for their interest and invaluable advice over the last three years.

I am very grateful to Charles Lai of Leeds University for allowing his computer program to be used in this study. The adapted program proved invaluable for the accurate prediction of the oil temperature rise within the engine journal bearings.

Finally, I wish to acknowledge Mr Richard Carr of Glacier Vandervell, who provided detailed information which was essential for the accurate modelling of the oil flow through the bearings.

# Declaration

I hereby declare that the contents of this dissertation are my own, except where reference is made to any non-original work used in its preparation.



## Summary

This dissertation documents the thermodynamic and fluid mechanic analysis of an engine lubrication system. A comprehensive thermofluid computer model was developed to provide a flexible design analysis tool for the accurate prediction of oil pressures, flow rates and temperatures at any point within any lubrication system. Technical and financial support for the study was provided by Jaguar Cars.

A comprehensive literature review revealed that the past research in this field had concentrated on either the thermofluid analysis of the lubrication system by engine testing, or the detailed analysis of individual components. A small number of computer models were developed for the flow analysis of the whole lubrication system. However, these models had limited heat transfer prediction capabilities, some requiring measured engine temperature data, and were not flexible enough to be employed as design tools.

The objective of this study was to develop a flexible steady-state thermofluid design analysis tool, by integrating a flow analysis approach with a detailed analysis of the heat transfer within the engine block. Mathematical models of the thermofluid behaviour of the lubrication system components were developed and were implemented in a suite of FORTRAN computer programs which formed the design analysis package.

A simple, linear flow model was initially developed to represent the system with a combination of laminar pipes, pumps, filters, journal bearings, crank-shaft transfer holes and cam bearing transfer holes. The linear program provided a rapid analysis tool, but the accuracy of the results were limited by the simplified flow characteristics of the system components. A more comprehensive and flexible non-linear flow model was developed, which solved for the unknowns with an iterative technique. Additional component models with non-linear flow characteristics, such as turbulent pipes, annular pipes, strainers, and oil coolers, were developed. The non-linear solution technique was proven to be robust and flexible and was subsequently used in all the analysis programs.

The heat transfer to the oil within the pressurised part of the lubrication system is modelled by the heat transfer program. The engine block temperatures are calculated by the engine block program. This program accounts for the heat transfer to the oil splashed on to the internal surfaces of the engine. The engine geometry is represented by a series of block elements and modelled as a nodal resistance network. This capability has particular importance during the design stage, rapidly providing an estimate of the temperature profile through the engine block, results which were previously only available from expensive and slow FEA models.

It was shown that both the Jaguar AJ6 and V8 engine lubrication systems could be analyzed in great detail. Engine tests showed that the predicted flow rates, pressures and temperatures were in excellent agreement with measured values. The overall accuracy of the results induced a high degree of confidence in the thermofluid model. The final analysis package was proven to be easy to use, robust, rapid, flexible and accurate.

The design analysis package, developed during the course of this study, represents a unique stand-alone simulation tool which can rapidly analyze any engine lubrication system configuration. This package provides a valuable analysis tool which can be used to optimise system designs at the initial design stage and the diagnosis of performance problems during the development phase. Parametric studies can be easily carried out on the lubrication system and engine block configuration to identify areas which can enhance heat transfer to the oil. The steady-state analysis package forms an excellent platform for the development of a full transient model. This would allow a detailed analysis of the lubrication system during engine warm-up, with the aim of reducing engine emissions and determining minimum oil requirements.

# Chapter 1

## Introduction

### 1.1 The Problem

The modern Internal Combustion (IC) engine operates under extreme mechanical loading and temperature induced environmental conditions. Cycle averaged gas temperatures in the combustion chamber can reach approximately  $800^{\circ}\text{C}$ , with peak flame temperatures as high as  $2600^{\circ}\text{C}$  (Barracough (1991)). At the same time, the engine is expected to start and operate successfully after a night's 'cold soaking' in ambient temperatures as low as  $-30^{\circ}\text{C}$ , or pull large loads in temperatures reaching  $55^{\circ}\text{C}$ . In addition to the operating temperature extremes, a typical automotive four stroke IC engine must successfully operate under high mechanical loading conditions induced by the reciprocating piston masses driving a crank shaft rotating at speeds reaching 7000 rpm. This is in addition to the mechanical loading through the gear box and transmission which is induced by the driving style and road conditions.

Although an engine experiences harsh operating conditions, it must remain reliable and free from mechanical failures. Ideally, the period of time between services needs to be as long as possible, and the services themselves must be easy and cheap. The engine will be expected to have a long life, modern expectations being in the region of approximately 100,000 road miles. These attributes are essential for a marques reputation and marketing appeal.

The key to an automotive IC engine's reliability and long life is the quality



of the lubrication system. Most automotive IC engines have a pressurised oil lubrication system which draws oil from a collection point or 'sump' and delivers it to the various engine components. The primary role of the lubrication system is to provide a continuous supply of filtered oil to the contact between any two sliding surfaces. The oil provides a separation of the surfaces in motion and carries away heat generated by contact resistance. This reduces friction and hence the energy required to achieve that motion.

A result of reduced friction and energy is reduced wear, and hence an enhancement to component life. The main destinations for this oil supply are the various journal bearings, cams, timing chains, tappet sleeves, and the pistons and liners (see Figure 3.1). In addition to providing lubrication between moving surfaces, the oil supply also provides a pressurised oil feed to hydraulically operated components such as self adjusting tappets and hydraulic chain tensioners.

In the past, the design of engine lubrication systems has been based on the experience and judgement of engine design engineers. However, the inevitable advances in technology in engine design means more complex lubrication systems are required. As a result, higher demands are placed on the designer to 'get it right first time'.

If we consider the fluid mechanic characteristics of a lubrication system first. The system design and development requires the designer to accurately predict the oil pressure and oil flow rate which is available to lubricate each engine component. This is essential to ensure that each component obtains a sufficient supply of lubricant not only under normal operating conditions, but also when the pressures and flow rates are affected by system losses. A typical example would be the case of increased flow rate through a worn bearing. In this

case, analysis of the subsequent effect on the oil supply to the rest of the system would be essential for predicting the life of the other engine components.

When considering hydraulically operated components, the designer must predict the pressure available at any point in the system where a tapping is required to feed these components with oil. An accurate prediction of the pressure available allows the designer to size these components to achieve their operating forces and speeds.

The second consideration is the thermodynamic behaviour of the lubrication system. Modern automotive IC engines are designed to operate with low fuel consumption and low exhaust emissions when the engine is in a fully warmed-up condition. At this fully warmed-up condition the engines' metal, coolant, and oil temperatures, are all at their equilibrium operating levels. However, if the engine is started from cold, it takes a varying amount of time, depending on the driving conditions, to achieve the fully warmed-up condition. Eccleston and Hurn (1978)<sup>1</sup> and Andre (1989) found that during the warm-up phase, especially under city driving conditions, engines operate well below their fully warmed-up optimum fuel consumption and emission levels. They reported that it was during these periods that engines emit the largest amount of pollutants such as carbon monoxide (CO) and unburned hydrocarbons (UHC).

The increase in pollutant emissions during the warm-up phase is a result of several factors:

- i, Due to inadequate heat for fuel evaporation, the air and fuel are inadequately mixed, which results in erratic combustion.
- ii, In an attempt to reduce exhaust emissions, many manufactures now fit 3-

---

<sup>1</sup> Dates in parenthesis designate references at the end of the dissertation



way catalytic converters within their car exhaust systems. The catalyst oxidises the UHC to carbon dioxide ( $\text{CO}_2$ ) and water ( $\text{H}_2\text{O}$ ), the CO to  $\text{CO}_2$ , while at the same time reducing nitrogen oxides ( $\text{NO}_x$ ) to nitrogen ( $\text{N}_2$ ). Finley (1991) found that a new 3 way catalyst can, when fully warmed up, achieve levels of conversion efficiency in excess of 98%. Unfortunately when cold the conversion efficiency is zero, resulting in no oxidation of the pollutants.

- iii, Viscosity of the lubricating oil increases with lower temperatures, resulting in higher friction losses and degrading the engine's efficiency, causing increased fuel consumption. Andrews et al (1989) measured the temperature of the engine components during warm-up and found that the oil was generally the last component to reach its equilibrium temperature (approximately  $100^\circ\text{C}$ ). The dynamic viscosity of a typical 10W40 class mineral engine oil at  $-30^\circ\text{C}$  was  $0.156 \text{ Ns/m}^2$ , while at  $100^\circ\text{C}$  it was fell to only  $0.01 \text{ Ns/m}^2$ . It could take in excess of 15 minutes for the oil to reach this equilibrium temperature in some circumstances.

One method of improving these problems is to reduce the warm-up period, in particular, the time taken for the oil to reach its equilibrium temperature. It is both time consuming and expensive to investigate lubricant warm-up by conducting engine tests. For rapid evaluation of the thermal effects on the oil due to various lubrication system design changes, an alternative method of analyzing the system is required which is both fast and accurate.

## 1.2 The Proposed Solution

The above requirements suggest the need for a dedicated computer model which can be used as a design tool to analyze both the thermodynamic and the fluid mechanic characteristics of any lubrication system. The advantages of such



a tool are :

- i, Development costs are minimised because optimised lubrication system design configurations may be defined prior to manufacture.
- ii, During the engine development stage the analytical capability, used in conjunction with simple experimental measurements, can enhance the diagnosis of faults and irregularities.
- iii, As product life extends, the performance requirements and the applications for an engine can change. Demand on, and changes to, the lubrication system become inevitable. For example, a turbo charged engine derivative may require the addition of piston cooling jets and a turbo charger lubrication system. A method of rapidly analyzing the thermodynamic and fluid mechanic effects on the existing lubrication system would be of a great benefit. In addition to analyzing the effect on the whole system, accurate values of the feed pressures and flow rates available to these new components could also be predicted. This would allow their lubrication routes to be sized correctly.

### **1.3 Previous Work by Jaguar**

An initial investigation into the development of a computer model of an engine lubrication system was undertaken by Jaguar in 1987. A computer program written in the programming language FORTRAN was developed at the University of Warwick, and a full report was presented as an MSc thesis by Ellinas (1988).

The primary objective of the investigation was to analyze the overall heat transfer process in the lubrication system of a Jaguar AJ6 six cylinder petrol engine. The model was intended to examine the effect of various design

parameters, and to predict engine warm-up performance.

The limitations with this early work were:

- i, The emphasis on the thermal process without due consideration of the oil flow process.
- ii, The lubrication model was very simplified (see Figure 1.1). The camshaft lubrication was neglected and the bearing model did not take into account the side leakage effect.
- iii, There was limited experimental validation reported.

Considering the limitations with the model it was clear that the requirements, which were discussed above, were not satisfied. To provide a truly flexible lubrication system design analysis tool for the accurate prediction of oil pressures, flow rates and temperatures, a more comprehensive investigation was required. A new three year research study was subsequently proposed and sponsored by Jaguar.

This dissertation represents the research carried out over that three year period.

## **1.4 Project Overall Objectives**

The main objective of the study is to provide a thermofluid analysis of an engine lubrication system resulting in a comprehensive, general purpose, well validated computer simulation program. The program will have the following capabilities:

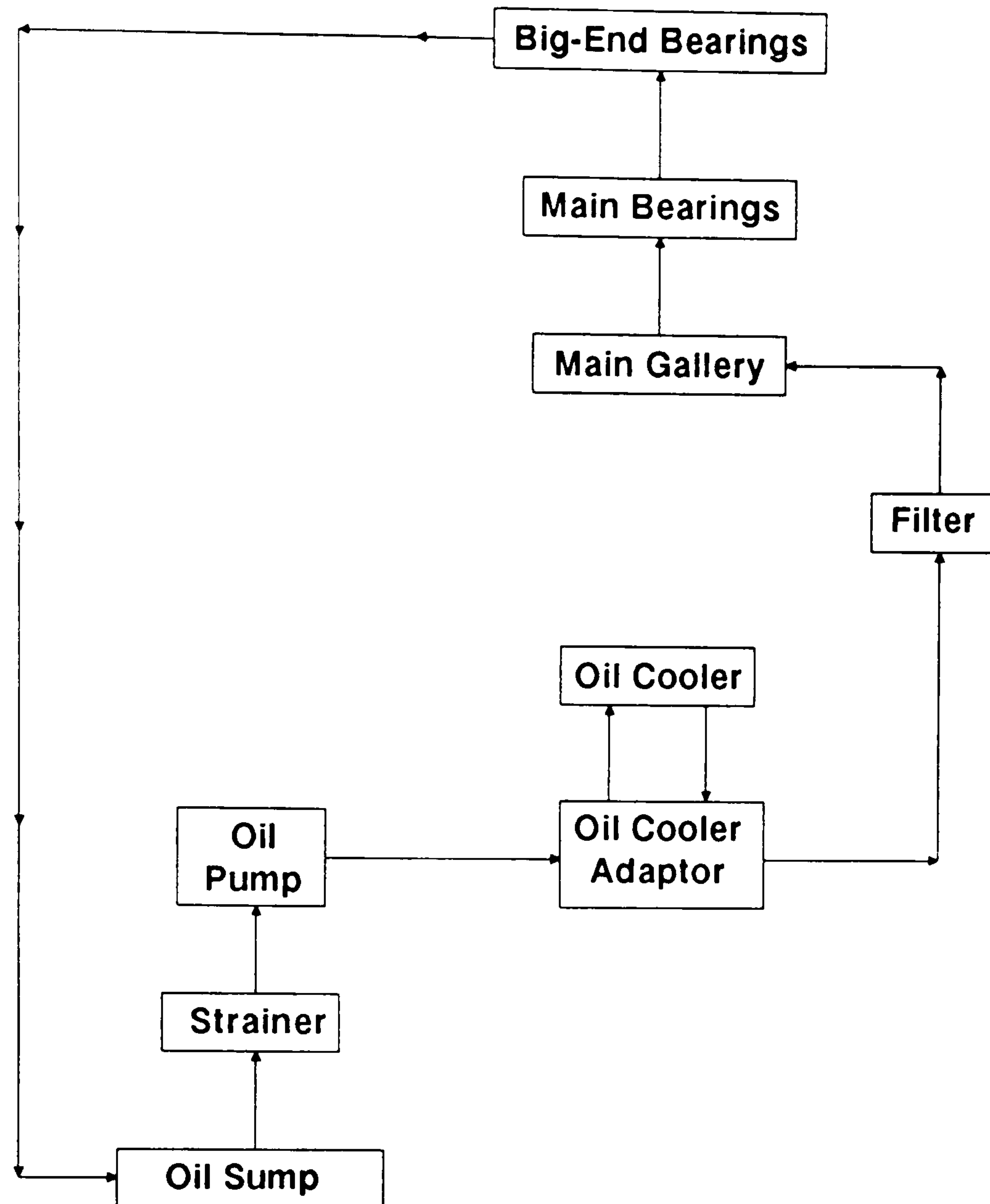


Figure 1.1. Schematic diagram of Jaguar AJ6 engine lubrication system used by Ellinas (1988)

- i, To act as a design and analysis tool to enable the rapid thermofluid study of any lubrication system configuration, and to assess the effect of changes of various design parameters and system layout.
- ii, To predict pressures, temperatures, and flow rates of oil around the chosen lubrication system configuration.
- iii, To analyze the thermal performance of the lubrication system and its components.



- iv, To analyze the role of the lubrication system in the overall engine heat transfer under steady-state conditions.
- v, To predict oil temperatures during engine warm-up and determine time to obtain stabilised temperatures.

## **1.5 Program Development Stages**

- i, The first objective of the project was to develop a steady-state flow model. This model would be developed to a stage where it could be used to provide results for pressures and flow rates, and could be used as a trend analysis tool. The resulting program would form the core for the development of the full thermofluid model. The development of the flow model was broken down into two phases:
  - The first phase was the development of a simple linear flow model which could predict oil flow rates at any point within any proposed lubrication system layout. The model would use simplified linear pressure loss v flow rate relationships to represent the flow of oil through each component element in the lubrication system.
  - During the second phase each element within the lubrication system would be represented by its true pressure loss v flow rate relationship. As this relationship could sometimes be of a non-linear form, a different numerical solution method would be required. A full comparison between the linear and non-linear solution methods could then be carried out.

- ii, The second objective was to use the flow model as a nucleus for the addition of heat transfer calculations. The investigation would initially focus on the heat transfer characteristics of the pressurised side of the lubrication system.
- iii, With a full steady-state thermofluid model of the pressurised side of the lubrication system developed, a method would be found to include heat transfer from heat sources outside the pressurised part of the system, ie. oil splash onto the piston, liner, head etc. This would complete the steady-state thermofluid model.
- iv The thermofluid model would be validated by a comprehensive series of engine tests. These tests would measure the oil pressures, flow rates and temperatures throughout the lubrication system of a Jaguar V8 development engine, over a range of engine speeds and loads.
- v, The feasibility of converting the steady-state thermofluid model into a transient model for the simulation of engine warm-up would be evaluated.

This dissertation reports on the work carried out to achieve these objectives. This includes: an investigation into past work in this field with a comprehensive literature review; a study of the components within a lubrication system and the development of the mathematical models to represent the system. A comparison between the predicted results and measured values will be made.

## **Chapter 2**

### **Literature Search**

#### **2.1 Introduction**

A comprehensive literature search was undertaken to ascertain the amount of work carried out into lubrication system analysis. The emphasis of the search was to gain a greater understanding of the type of research carried out into this field. The literature search focused on achieving two objectives. The first objective was to find out what research had been carried out into the analysis of complete engine lubrication systems. The search covered analysis by testing and analysis by computer simulation. However, the boundary between the two was not so neatly defined, as analysis by numerical methods usually incorporated validation by measurement. This gave an insight into the methods used by various authors, the common findings, and the limitations of their work.

The second objective was to gain detailed knowledge on the oil flow and temperature characteristics through individual engine components. By gaining a greater understanding of these characteristics, the approach to modelling these components would become clearer.

#### **2.2 Experimental Investigation of the Lubrication System**

The literature search revealed that in recent years interest has grown into the influences of the engine lubrication system on the overall performance



of an internal combustion engine. The focus of this research has been to study the influence of oil condition on; engine life, reduction of wear, friction losses, and most recently, engine emissions.

Hayashi (1969) investigated the effects of various engine operating conditions on the engine oil temperature. Oil temperatures were monitored for various engine speeds, loads, and oil feed pressures. The objective of the work was to establish the role the lubricating oil played in dissipating heat from the engine to the air or the cooling water. The heat dissipating capacity of the oil was evaluated by shielding certain areas considered as heat paths (such as the oil sump) with felt. The effect on the oil and coolant temperatures was observed. Testing was conducted on a six cylinder, four stroke, water cooled diesel engine. Some tests were conducted with the engine firing and others were made by rotating the crankshaft of the engine using an electric motor (motoring), to prevent the fluctuation of heat input during firing.

The results of these tests showed that the rise in oil temperature was more greatly influenced by higher engine speeds than by an increase in load. Similar results were found by Andrews et al (1989), whose work concentrated on Spark Ignition (SI) engine warm-up and the influences of water and oil temperatures on engine emissions. Both papers attributed the influence of the engine speed on the overall oil temperature, to the increase in oil temperature within the engine bearings. The rise in temperature of the oil film in the bearings was a result of the increase in oil film shear at high rotational speeds. It was concluded that this had a larger affect on bearing oil film temperature than an increase in oil film pressure at large engine loads.

Hayashi found that the oil pressure had little effect on the lubricating oil temperature rise. However, it was noted that it was essential to maintain

a minimum oil supply pressure to the bearings, as a rapid increase in the bearing metal temperature occurred with inadequate lubrication at low supply pressures. The cooling water was found to be the major contributor to the heat dissipating function of the lubricating oil system, while the heat dissipating properties of the oil sump did not prove to be as effective as expected.

Seth and Field (1984), made an attempt to increase the understanding of the behaviour of the lubrication system of a Ford, four cylinder, petrol engine. The lubrication system was instrumented throughout with pressure sensors. The objective of this study was not to enhance the design process of an engine but to provide a method of detecting lubrication related abnormalities in an existing engine. The signals produced from each of the sensors showed a distinct pulsed wave form. It was suggested that continuous monitoring of these signals would give an indication of the status of the system. A rapid warning could be given for a change in any of the system parameters, such as the failure of a bearing.

Experimental tests showed favourable results, but indicated the limitations of such analysis techniques for lubrication system monitoring. The main weakness of this procedure was that it relied on monitoring pulsed pressure waves travelling through the viscous oil. However, these pressure signatures were found to be extremely sensitive to the oil temperature. As the viscosity of the oil changed due to varying oil temperatures, the direct and reflected wave speeds changed, and the analysis became inaccurate.

Kyto (1989), conducted a comprehensive series of motored engine tests on two petrol engines under cold start-up conditions. Oil pressures, oil temperatures, and engine torque were recorded for 12 different oils. The purpose of the tests was to establish the most suitable oil for cold start



conditions, rather than the analysis of the oil properties within the lubrication system. There were however some interesting observations:

An oil pressure transducer was installed in each engine on the most remote lubrication point on the camshaft bearing. The results showed that it could take a large amount of time for the oil pressure to rise at this point, using some types of oils in cold ambient temperatures. For a typical 10W40 class mineral oil, for example, the maximum pressure was reached at +20°C in 23 seconds, while it took 192 seconds at -30°C. This was primarily due to the oils much higher viscosity at low temperatures, resulting in large pumping losses through the lubrication system.

The torque required to motor the engine at 150 rpm increased from 60 Nm at +20°C, to 125 Nm at -30°C. It was concluded that there were two reasons for this large difference in motored torque:

- i, At low temperatures the oil film within the engine bearings has a high viscosity resulting in large viscous shear losses.
- ii, The more viscous oil also provided better sealing around the piston rings, which increased the compression within the cylinders. This was demonstrated by conducting compression pressure measurements while motoring an engine.

Tran et al (1987) conducted a similar investigation to that of Kyto, but placed the emphasis of their work on the analysis of friction throughout the engine. The friction torque of each engine component was found by dismantling the engine down to the crankshaft and conducting motored tests at various stages of engine rebuild. The effects on the overall torque were measured.



Again, the results showed that, generally, the lower the oil viscosity, the lower the frictional torque. However, it was found to be the inverse in the case of the valve system. It was proposed that the reason for this was that the contact between the cams and the followers was not under fluid lubrication but under boundary lubrication. Thus, the two contact surfaces are only partially 'wetted' by oil, and some of the load is carried by the lubricant and some by surface asperities.

In suggesting methods of solving the problem of boundary lubrication occurring, the authors considered that the use of a separate lubrication system for the valve system, using a different grade of oil of higher viscosity, was impracticable. It was suggested that the friction losses would be minimised if the valve system were supplied with a greater oil feed rate (3-4 l/min) than the crankshaft bearings (1-2 l/min).

## **2.3 Computer Simulation of Lubrication Systems**

Very few of the above researchers made any attempt to use analytical methods to analyze the lubrication system. The following papers were the only papers found which attempted to model the system using computer simulation techniques.

The concept of simulating a series of flow elements by a flow network approach is not new. Petroleum, chemical, and power generating industries have used the network concept in selecting and sizing pipes (eg. Cinque and Sheridan (1968)). The application of the flow network concept to internal combustion engine lubrication systems is relatively recent.

The earliest attempt was made Lo (1971). A simulation program was developed in FORTRAN IV to predict the pressure and flow rate distribution, the minimum bearing oil thickness, and the frictional power loss. The approach taken was based on the conservation of mass, ie, the oil flow rate discharged by the pump must be equal to the engine oil flow rate. Hence, in order to analyze the whole engine lubrication system, it was necessary to find the equilibrium point A as shown in Figure 2.1. This was accomplished by a numerical iteration technique. Firstly, an oil flow rate was assumed and the pump discharge pressure was then found from the oil pump performance curve. The pressure drop and flow rate through each branch of the lubrication system was calculated step by step. The flow rate and pressure on the exit of one section being the input conditions for the next ... etc. The total of the flow rates which 'leaked out' of each section made up the total engine flow rate. If the engine flow rate did not meet the pump discharge flow rate, a new value was assumed. This iteration process was repeated until the equilibrium point, point A, was reached.

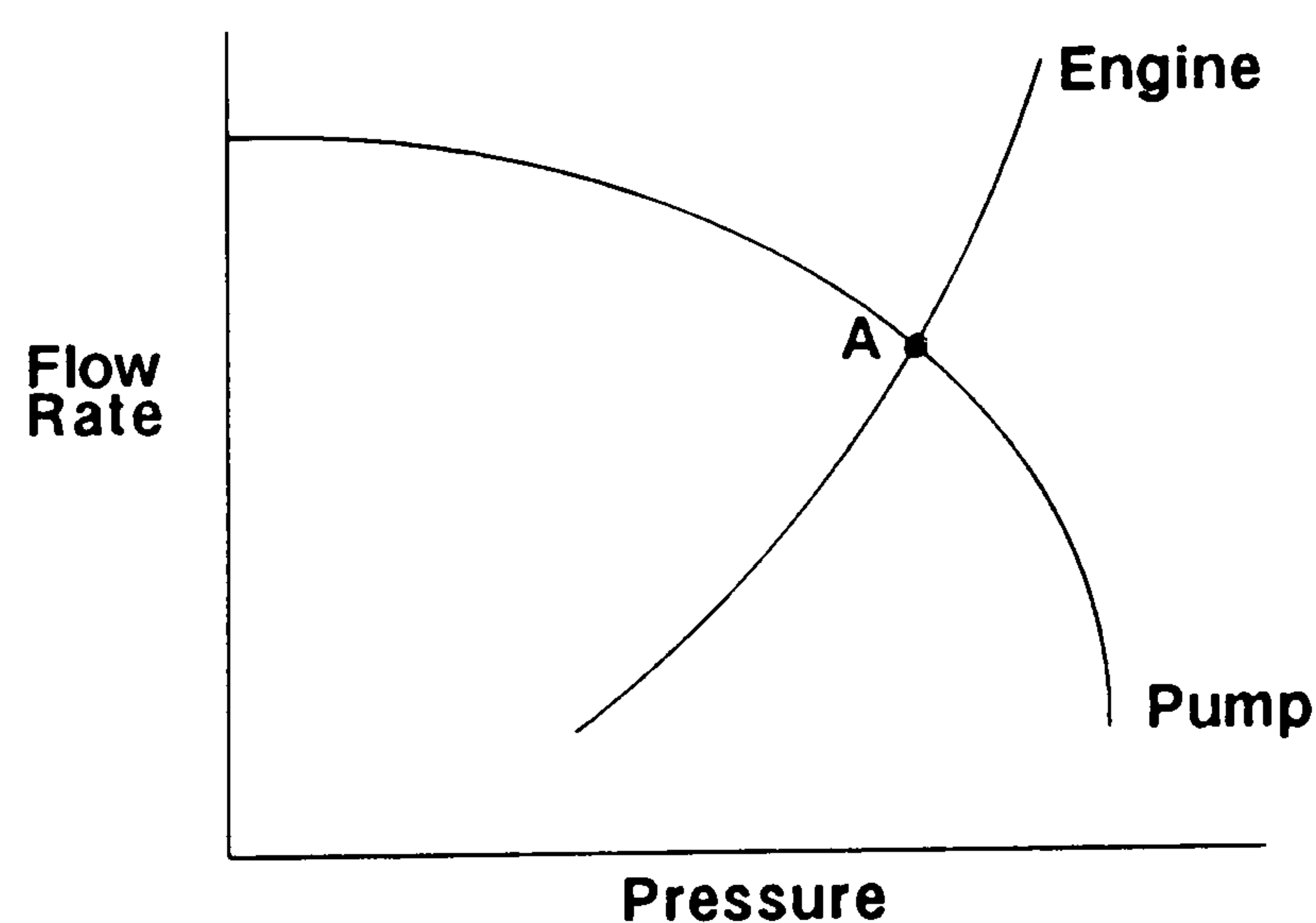


Figure 2.1. Engine oil flow rate v pump discharge flow rate

The main limitation with the above study was the program's lack of flexibility. The lubrication system layout was represented by being broken

down into a few basic hydraulic circuits. A computer subroutine was written for each hydraulic circuit to predict the pressure losses and flow rates. Apart from the case of the bearings, heat transfer and oil temperature effects were ignored in the system. The working temperature of the oil within the journal bearings was estimated by assuming steadily loaded, thermal equilibrium conditions.

Problems would occur if a proposed lubrication system contained a configuration which did not match any of these standard circuits. The study by Lo fails to match the current objective of providing a flexible tool which is capable of modelling any lubrication system at the design stage. However, this paper represents one of the first attempts to model the fluid properties of a lubrication system, and is widely considered as the pioneering work for all subsequent lubrication simulation projects.

Huebner (1975) proposed a more flexible method of flow network analysis for the prediction of pressure drops and flow rates using non-linear programming techniques, in particular Rosenbrocks algorithm (1960). This method was then applied to the analysis of a lubrication system.

Construction of the model centred on developing equations that represented the pressure v flow rate relationship for each component in the system. As these relationships were often in a non-linear form, the non-linear programming technique was required to solve simultaneously for all unknowns. However, many simplifications were made, heat transfer was ignored and the effect of temperature on the oils viscosity was neglected. In addition, when the pressure v flow rate parameters were not fully understood, such as in the case of the bearings, estimated relationships were used. Engine tests showed that the flow rate and pressure predictions were subject to a 15% error.



A similar approach was made by Neu et al (1977). In this work a more comprehensive investigation was made into providing accurate pressure v flow rate relationships for each component. Bearing calculations were made at various crank angles using measured cylinder pressures, and an attempt was made to predict the oil flow and oil temperature differences across the bearings. From engine tests it was found that the flow and pressure predictions were within an accuracy of 4%, for an engine operating under steady-state conditions and using measured oil temperatures. However, when an attempt was made to calculate the oil temperature rise within the bearings, the results were 20-50% below measured values. As a result, the model remained as a steady-state flow analysis tool and no attempt was made to enhance it with the inclusion of heat transfer calculations.

The value of simulation tools in the design and manufacture of engines was addressed by Kluck and Olsen (1986). The paper presented details of a design process, which was applied to optimizing the lubrication system for a heavy-duty diesel engine. It was reported that the first design stage, which was decision analysis, defined objectives and evaluated alternative components for integration into a total lubrication system. Systems resulting from these analysis are further evaluated by value analysis, network simulation, design layouts, and engine testing.

Little detail was provided of the simulation model which was used, but reference was made to a linear flow analysis program developed at Wright-Patterson Aeronautical Laboratories (Ref. 'SSFAN' (1980)). The lubrication system was represented as a flow network, built-up from component elements. These elements included pipes, filters, pumps, oil coolers, and regulating valves. The steady-state analysis operated with an initial estimate of flow through the system. An iteration procedure commenced until continuity was

satisfied at each junction. The program returned branch flow rates, and the pressure at each junction.

Although correlation with test data was reported to be 'reasonably good', the model assumed a constant oil temperature throughout the system, with no heat transfer considerations. No information was given on the method used for calculating the oil flow characteristics through the bearings. A journal bearing finite element analysis program, developed by Das and Dancer (1982), was used to calculate the viscosity effect on bearing eccentricity ratio. This was used for input to the network simulation. However, this model was limited to the linear equations used to represent the pressure resistance through each component, and remained a steady-state flow network analysis tool with no heat transfer capability.

Chiang et al (1982<sub>a</sub>) reported on an investigation into the thermodynamic properties of diesel engines, which initially concentrated on the development of a Vehicle Engine Cooling (VEC) system computer simulation model. This model was subsequently used in the study of the transient performance of the control devices and the effect of their activation temperature settings on the oil, coolant, and cab temperatures (Chiang et al (1982<sub>b</sub>)). Using the results obtained from this work, a computer controlled cooling system was developed which controlled the operation of the vehicles thermostat, cooling fan, and radiator shutter system.

The VEC model was used to make comparison simulation tests between the conventional cooling system and the computer controlled system, under various ambient temperatures and route conditions (Chiang et al (1984)). The emphasis of the work was to use realistic transient data. A Vehicle Mission Simulation (VMS) program was developed. This was used to determine realistic



engine and vehicle operating conditions for the VEC system computer simulation model.

By 1987 the authors had started work on the design of a microprocessor controlled lubricating oil cooling system for the Cummins NTC series truck diesel engine (Hovin et al (1988)). The microprocessor controlled oil cooling system was designed to improve the transient capacities of the oil cooling system. In the past, a wax bulb oil thermostat had been used to control the flow of oil through the oil cooler. In this investigation the thermostat was replaced by a microprocessor controller, and valve controlled by the microprocessor. The objectives of the microprocessor controlled oil cooling system were:

- i, To maintain the oil sump temperature at approximately 105°C under transient and steady-state operation. The authors considered that 105°C was the optimal oil temperature for maximum engine performance, emissions, and durability. It was found that this temperature was sufficient to vaporise any water carried in the oil circuit. In addition, the set temperature of 105°C was within the operating range of the oil, where the viscosity was sufficient to provide adequate lubrication while lowering the pumping losses.
- ii, To improve the heating of the oil during start-up conditions. The microprocessor controller was designed to allow the coolant to heat the oil when required, in an oil/coolant heat exchanger. Total oil flow through the heat exchanger was available, provided the coolant temperature was higher than the oil temperature.



A computer simulation program was developed to model the microprocessor controlled oil cooling system, and this was integrated with the VEC program. Simulation run results were used to set the activation temperatures of the various coolant and oil temperature control devices of the diesel engine. The authors reported that this greatly improved the temperature stability of the system. The oil sump temperatures reached steady-state levels approximately 80 seconds faster than the conventionally controlled system during warm-up, and the system was able to hold the oil temperatures at a constant value of 105°C during engine testing.

The VEC model concentrated on the specific analysis of the overall effects of the microprocessor controllers on the coolant and oil temperatures. The model included a simple lubrication system analysis, but there was no evidence of any attempt to model oil flow or oil pressure influences. The heat transfer to the oil from engine components such as bearings, pistons, and liners were considered simply lumped as a percentage of the total energy balance. It was not an objective of the work to develop an accurate simulation model of the lubrication system. The lubrication system model which was developed was specific to the diesel engine used by the authors and was not a flexible design analysis tool.

Perkins Technology have developed a flexible design tool for the analysis of high speed diesel engine lubrication systems. Haddock (1991) reported on work which had been carried out eight years previously on the development of this tool. The approach taken was similar to that employed by Neu et al (1977). The lubrication system was represented as a network of oil flow elements which were joined at nodal points. Pressure v flow rate equations for each of the element types were used to generate the flow resistances. The linear simultaneous equations which were produced were solved to yield nodal flows

and pressures.

The program solution strategy relied on an iterative approach. Following an initial estimate of the flow rates through the network, an iterative procedure was undertaken until convergence of the element resistance was consistent with the flow prediction. When this was complete the resistance of the whole oil circuit was determined. The circuit resistance was then matched to the pump characteristics, and the instantaneous point of operation was found. A new estimate of the flow rates through the network was made, and the process repeated. This approach was taken because of the reliance on using a linear solution technique. The author found that the pressure loss ( $\Delta P$ ) v flow rate,  $Q$ , relationships for the individual component elements were often of a non-linear form. For example:

$$\Delta P = R \cdot Q^n \quad (2.1)$$

The element flow resistance,  $R$ , was re-written in terms of a linear flow rate:

$$Q = \frac{1}{R'} \cdot \Delta P \quad (2.2)$$

where

$$R' = R \cdot Q^{n-1} \quad (2.3)$$

The flow characteristics through the various component elements were either calculated from component dimensional data, sometimes using published friction and loss coefficients, or obtained from rig tests. Haddock reported that the pressure v flow rate characteristics for the engine bearings were obtained by linking with a bearing model which was also developed at Perkins. The bearing model took into account feed hole and groove geometry, bearing film extent, and bearing eccentricity.



Although the work by Haddock only reported steady-state modelling, Fenton (1984) reported that the model has since been developed further and can now cover transient response. No evidence was found of the inclusion of the heat transfer effects. This model achieves the objectives of being a truly flexible design tool, but it is handicapped by the approach of using a linear solution technique, and no heat transfer calculations. With no published validation results available, the accuracy of the predicted results remains unknown.

Trapy and Damiral (1990) reported on research which closely matched the objectives of this study. A computer simulation model (TRANSLUB) was developed that could predict oil flow rates, pressures, and temperatures throughout any proposed lubrication system. The main objective of the paper was to provide an analysis tool for the study of the thermal behaviour of the lubricant, and the lubrication system, during engine warm-up.

Trapy and Damiral approached the modelling problem by breaking down the lubrication system into small elements, representing each element by a pressure loss v flow rate relationship. For steady-state simulation, the pressures and flow rates were calculated simultaneously using the Levenberg-Marquardt mean least squares non-linear method (a detailed description of the Levenberg-Marquardt routine is given in Appendix A.2.1). For transient simulation, quasi-steady development of the system was assumed. ie, the oil properties at any point in time were assumed to be in a temporary steady-state condition. Thus, the model computed a sequence of steady-states located at constant time steps. The iteration loop for the prediction of pressures and flow rates was nested in an iteration loop for temperatures. The lubricant temperature was allowed to change according to the heat balance computed at each step.



The model required as input data the values of the engine wall temperatures. A comprehensive series of engine tests were carried out on a Renault F2N 4 cylinder 1.7 litre petrol engine to validate the model and to provide the required temperature measurements. The results from the simulation runs and the engine tests indicated similar findings to those of Hayashi (1969) and Andrews et al (1989). It was found that the lubricant temperature during warm-up was influenced much more by engine speed than by engine load.

Tests were also carried out with varying amounts of oil in the sump. It was found that reducing the quantity of oil in the sump did reduce the warm-up duration of the oil. However, the reduction in the warm-up time was very small. Reducing the oil mass from 4Kg to 1Kg reduced the warm-up period from 23 minutes to 19 minutes. It was found that the amount of heat lost by the lubricant, probably through the sump walls, increased when the oil mass decreased. As a result, the expected reduction in warm-up duration was inhibited.

Some tests were also carried out with a heat exchanger between the coolant and the lubricant flow networks. Under cold start conditions heat was exchanged between the coolant and the lubricant in order to accelerate the warm-up period of the lubricant. The results obtained showed a 30% improvement of both engine warm-up efficiency and heat recovery efficiency. Heat recovery efficiency was described as the ability to use the heat produced by engine combustion and friction, which is otherwise wasted to ambient, for 'useful work', ie, heating the engine components to their optimum working temperature.

The model only took account of the heat generated by friction within the bearings and heat exchanged with the passage walls. As this produced results which were lower than those measured on the engine tests, it was evident that there was an additional heat source which had not been accounted for. Therefore, heat transfer to the oil from other sources was represented in the computer model as an adjustment factor, simply classed as 'complementary heat'. Using an adjustment factor in the model, the predicted values for the oil flow rates were reported to be 98% accurate and the oil temperatures and pressures were within 99% of the measured values.

As the Renault engine used for the engine testing was fitted with oil nozzles which sprayed oil under the piston to improve their cooling, it was found on later engine testing that the source of this 'complementary heat' was the heat exchange to the oil sprayed on to the piston and liners. It accounted for as much as 39% of the heat received by the oil during the warm-up period, and reduced to 9% under steady-state conditions. It was concluded that this reduction under steady-state conditions was due to the oil receiving a larger amount of heat from the walls of the oil passages, when the engine block had reached its fully warmed-up temperature.

Apart from the discrepancies which were discussed above, this paper represents the most comprehensive computer simulation of the lubrication system to date, and it sets the standard for future simulation work.

## **2.4 Computer Simulation of Engine Warm-Up**

The representation of engine geometry and the generation of temperature distributions can be carried out using a Finite Element Analysis (FEA) package. The thermal analysis of engine structures, using such an FEA



tool, was reported by Cornforth (1985). However, the computational costs with such an approach are generally high. Solution times are dependent upon the number of finite elements which are used. However, reducing the number of finite elements causes problems in maintaining an accurate description of the surfaces and volumes. This leads to additional difficulties in efficiently coupling segments of the model together.

Several authors have reported methods of simulating the engine warm-up process by using a lumped capacitance method. Although these methods do not generally include the same level of detail as the FEA approach, comparable results have been reported, at a fraction of the run-time. The common objective has been to predict component temperatures, heat flow, and friction characteristics. The area of interest to this study was the approach taken by each author in determining the heat transfer to the oil flows.

Kaplan and Heywood (1991) developed a model which predicted the mean temperature of the 'major components' of an engine during the warm-up process. In this case the 'major components' were; piston, head, block, oil reservoir, and the coolant reservoirs in the head, block and radiator. The model was simplified to one-dimensional heat flow, and a lumped thermal capacitance was used for each component. The combustion gas heat transfer was predicted using a previously developed SI cycle simulation program (Poulos (1982)). The limitation of this approach, with respect to the present study, was the method of accounting for the heat transfer to the oil. The heat transfer paths to the oil were; convection on the under-side of the piston; convection on the head and thermal energy generated by the pump and crankshaft. Although the approach taken was suitable for the calculation of the temperature trends of the major components, the model was not capable of detailed temperature analysis.



A more detailed and flexible approach was taken by both Veshagh and Chen (1993), and Shayler et al (1993). Both authors adopted a similar method of representing a piston/liner/block arrangement by a series of solid elements. In Shaylers model each element is assumed to have a spatially uniform temperature. Each element is thermally coupled to adjacent elements and to any adjacent fluid. 23 elements were used to represent a piston/liner arrangement. The results were reported to 'agree favourably' with results obtained from an FEA package which used 3500 elements to describe the same geometry.

The heat transfer to the oil was estimated from frictional power dissipation and contact with parts of the engine structure. The frictional power dissipation losses were considered in the main bearings, the valve train, and the piston skirt. There was no evidence that heat transfer through oil splash onto the piston and liner was accounted for.

The approach used by Veshagh and Chen was very similar. The piston/liner/block arrangement was represented as a thermal network consisting of fluid circuits separated by solid walls. The solid walls were represented by hexahedral elements with lumped heat capacitance. Each wall element had seven temperatures, one for the centre, and one at each of the six surfaces. The engine model included four fluid circuits; engine combustion gas, under-bonnet air, coolant, and lubrication flows. The model was reported to have a high resolution of temperature variation of the whole engine system during warm-up.

Heat transfer to the oil was calculated by accounting for heat transfer within flow passages, heat transfer to the piston under-crown, and frictional power losses. The total engine friction was first calculated and divided into the

following five heat paths; crankshaft, liner, valve train, oil pump, and water pump. The proportions used were those reported by Patton et al (1989), as shown in Table 2.1.

Crankshaft	11 %
Liner	53 %
Valve Train	15 %
Oil Pump	10 %
Water Pump	11 %

Table 2.1. Engine Friction Losses (Patton et al (1989))

It was assumed that all the heat generated by friction on the crankshaft, and half the heat generated by friction on the piston/liner surface, was dissipated to the oil. The remaining heat was dissipated through heat conduction.

Both of these papers give a clear insight into the heat flow paths which must be considered when evaluating engine heat transfer. The lubricating oil is just one of the convective fluids which must be considered. For proper evaluation of the heat transfer aspects of the lubrication system, consideration must be made of the heat transfer paths of the whole engine system. Ideally, the oil temperatures and the block metal temperatures must be solved for simultaneously. This can only be achieved if the other convective fluids are also accounted for. The primary convective fluids in engine heat transfer are; the lubricant; the combustion chamber gases; the coolant, and the ambient air.

Detailed research has been conducted into these individual heat transfer paths by many authors. The work which is of most relevance to this study is documented in the sub-sections below. Seale and Taylor (1970), however, investigated three primary heat flow paths in a single study. The heat transfer

coefficients were measured on the gas side of the piston and liner, the water side of the liner, and the oil side of the piston. A significant radial variation in the heat transfer across the piston crown was found. Seale reported that heat transfer coefficients at the exposed section of the liner were similar to the values at the outer edge of the piston. The position of the maximum heat transfer coefficient on the piston crown was coincident with:

- i, The position of maximum air turbulence.
- ii, The position the tips of the fuel sprays have reached at the time of ignition.

The heat transfer between the piston under-crown and the cooling oil was measured for various types of cooling arrangement. An expression was suggested for the heat transfer with oil jet cooling. Equations were also derived to enable heat transfer coefficients to be predicted between the liner and the cooling water.

#### **2.4.1 The Determination of Combustion Chamber Temperatures**

Many papers have been published on the measurement and prediction of the temperature of the combustion chamber gases. The focus of the majority of the work has been to predict the cylinder convective heat transfer coefficients.

The in-cylinder heat transfer is associated with the distribution of heat flux. The heat flux through the combustion chamber wall varies with time and space. The early models developed by Nusselt (1923<sub>p</sub>) and Eichelberg (1923), emphasized the overall heat balance. These models used empirical relations between the total heat flux and the operating conditions. Later models were



based on the correlations of the steady-state incompressible pipe flow, and were based on the following relation:

$$Nu = a Re^n Pr^m \quad (2.4)$$

Sitkei (1962) and Annand (1963) proposed a power law of 0.7 for the Reynolds number term, both Taylor and Toong (1957) and Alcock (1962) used exponent 0.75, and Woschni (1967) employed exponent 0.8. The objective of these models was to predict an overall instantaneous heat transfer coefficient with reasonably good time varying resolution.

To expand the versatility of this type of model, various modifications were proposed by the authors. Annand used the mean piston speed as the representative velocity in the Reynolds number. Woschni suggested that the representative velocity is different for different parts of the cycle, and is dependent on the pressure in the cylinder. Poulos and Heywood (1980) included an additional turbulent kinetic energy term. Annand and Ma (1971) introduced a term for the effect of bulk temperature variation. Rao and Bardon (1985) related the convective heat transfer coefficient to the turbulence intensity.

Recent models have concentrated on the local behaviour of in-cylinder heat transfer. Borgnakke et al (1980) suggested a new type of model based on the one-dimensional theory of unsteady compressible thermal boundary layer. Yang and Martin (1989) found an approximate solution of the linearized one-dimensional energy equation for transient, compressible, non-chemically reacting, turbulent boundary layer flows. Jennings and Morel (1990) integrated the multi-dimensional flow code with the thin-shear-layer approximation to calculate convective heat transfer. The in-cylinder bulk flow was calculated using a Computational Fluid Dynamics (CFD) code, while the near-wall flow was calculated based on the boundary layer theory. Chen and Veshagh (1992)

proposed a model which was based on the solution of the full one-dimensional equations of transient compressible boundary layer. The boundary layer development was governed by the bulk flow and the interaction between the velocity and thermal boundary layers. The effect of flame penetration inside the boundary layer was also taken into consideration.

A detailed analysis of the combustion process, and the prediction of the in-cylinder heat transfer coefficients, was considered to be outside the scope of this study. It was assumed that cycle averaged temperatures and heat transfer coefficients could be obtained using simplified methods. The possible methods of predicting these temperatures and heat transfer coefficients are demonstrated by the other studies of modelling engine warm-up.

For example, Shayler et al (1993) used a simplified method to calculate the cycle averaged gas temperature and heat transfer coefficient, in their overall engine warm-up model. The in-cylinder heat flow was estimated from a prediction of the amount of heat rejected to the coolant, under steady-state conditions. A correlation developed by Taylor and Toong (1957) was used to predict the latter.

In the engine warm-up model developed by Veshagh and Chen (1993), the cycle averaged heat transfer coefficient and averaged gas temperature was calculated using a previously developed cycle simulation program (Chen (1990)). The cycle simulation program used the Woschni correlation (1967) to calculate the in-cylinder heat transfer coefficient. The Woschni correlation was adapted in the model, to account for in-cylinder radiation.

For the purpose of the present study, it was assumed that cycle averaged temperatures and heat transfer coefficients could be obtained by

using existing cycle simulation tools. The simulation model used at Jaguar, which was developed by the National Engineering Laboratory (NEL) (Bingham (1987)), and the cycle simulation model developed by Chen (1990), are examples of the simulation tools which are available (see section 9.4 for the values used).

### **2.4.2 Piston/Cylinder Heat Transfer to the Oil**

Documented research into the behaviour of oil around the piston/liner assembly can be broken down into three main categories; oil behaviour between piston and liner; piston cooling by oil jet, and the thermal analysis of spray cooling.

#### **2.4.2.1 Piston/Liner Lubrication**

The two principal heat transfer paths from a piston are:

- i, Heat transfer to the liner.
- ii, Heat transfer to the oil spray on the piston under-crown.

Little knowledge is available of the factors controlling the heat transfer processes between the piston and liner. These processes are complicated by the presence of an oil film and piston rings, as well as the occurrence of reciprocating motion, piston friction and side thrust. Much research has been conducted into the analysis of the lubricant behaviour between the piston and liner. The majority of this work has concentrated on the investigation of oil consumption.



Generally, oil consumption is induced by two reasons; one is oil loss via the piston rings and the other is oil loss via the valve guides. The greatest oil consumption path is reported to be caused by oil loss via the piston rings (Saito et al (1989)). The mechanism of oil passing between the piston and liner, and entering the combustion chamber, consists of the following three flow paths:

- i, Oil flow through the ring gap,
- ii, Oil flow through the ring groove,
- iii, Oil flow as an oil film between the piston ring and cylinder liner.

The majority of the research into this field has concentrated on measuring the amount of oil which is consumed. For example, Maeda et al (1986) developed an oil consumption meter which used sulphur as a tracer in the oil. Johren and Newman (1988) used a method of continuously weighing of the oil in a specially modified dry sump engine. Wong and Hoult (1991) used a radioactive tracer method for analyzing the oil film behaviour between the rings and the liner, in conjunction with the measurement of oil consumption.

The papers of most interest to this study were those which focused on the detailed analysis of the oil film between the rings and liner, and investigated the heat transfer mechanism through this film. Both Parker (1989) and Pachernegg (1971) reported that the piston rings are generally hydrodynamically lubricated. The lubricant condition is very similar to that found in an engine journal bearing, with distinct convergent/divergent sections across the ring face. However, at the top and bottom of the piston strokes, the velocity of the piston rings relative to the liner becomes zero. Under these conditions, 'squeeze' effects can reduce the oil film thickness, and boundary lubrication can come into effect.

Manganiello and Bogart (1945) reported on an experimental study of the heat transfer coefficients across the oil film between the piston rings and liner. Tests were conducted with a heat transfer apparatus that simulated the piston/liner relation. This was achieved by means of a stationary, electrically heated, smooth-walled aluminium piston and a reciprocating steel sleeve. The tests showed that the piston heat transfer coefficient increased rapidly under the following conditions:

- i, With an increase in the average oil-film temperature,
- ii, With an increase in speed,
- iii, With an increase in the supply of oil to the piston clearance space.

It was reported that an increase in side thrust had no significant effect on the piston heat transfer coefficient. These findings supported the lubricant condition analogy between a piston ring and a journal bearing. As reported in section 2.2, the oil temperature rise in a journal bearing is more greatly influenced with journal rotational speed than with journal load.

The lubricant condition between the rings and liner is further complicated with the dynamic behaviour of a reciprocating piston. To further the understanding of this dynamic behaviour, Li et al (1982) developed a computer model of an automotive piston in 1982. The emphasis of this work was the analysis of piston slap. The analysis incorporated a hydrodynamic lubrication model. The variation of piston transverse position and rotation with crank angle, and the piston skirt frictional power loss, were calculated. The calculations incorporated different gudgeon pin locations, piston/cylinder clearances, and lubricant viscosities. The results showed that the piston motion was greatly influenced by the location of the gudgeon pin.



Li reported that piston dynamics were also sensitive to piston/cylinder clearances and lubricant viscosity. Skirt eccentricity was reduced with a decrease in the clearance and an increase in lubricant viscosity. Both of these resulted in an increase in viscous friction.

#### **2.4.2.2 Oil Spray to Piston Under-Crown**

The above work concentrated on the oil behaviour between the piston and liner. This area covers the first heat transfer path from the piston. This heat transfer path is of great importance to the overall engine heat transfer. However, due to the relatively small amounts of oil involved, very little heat is transferred directly to the oil by this path. The second heat transfer path from a piston is of more interest to this study. This is the heat transfer to oil splash/spray on the piston under-crown. Several authors have reported investigations into piston cooling by various forms of oil jets and sprays.

Flynn and Underwood (1945) conducted an investigation into the cooling of a diesel engine piston by an oil jet. The oil jet was achieved by drilling a feed hole through the centre of the connecting rod (con rod). The oil which was ejected from the top of this drilling was directed to the piston under-crown. To aid heat transfer to the oil, a baffle was installed at the bottom of the piston skirt. With high oil flow rates ( $> 3.8 \times 10^{-5} \text{ m}^3/\text{s}$ ) the baffle was shown to be beneficial to piston cooling because it retained the cooling oil through a 'cocktail shaker' action. At lower oil flow rates the baffle actually obstructed the cooling oil thrown from the crankshaft. This resulted in higher piston temperatures compared with the case where no oil cooling and no piston baffle had been used.



The piston cooling method referred to as a 'cocktail shaker' action, was investigated in greater detail by Bush and London (1965). In a cocktail shaker piston the oil is drawn into a closed chamber below the piston crown and released from the chamber to the crankcase through overflow holes. The overflow is arranged such that the volume of the chamber is only partly filled with oil. The oil is agitated violently by the piston reciprocating movement. The turbulence of the oil motion produces a high heat transfer coefficient between the oil and the piston.

The effectiveness of the 'cocktail shaker' method in comparison with other oil cooling methods was demonstrated by the research carried out by Stotter (1966). The author conducted an experimental investigation into various methods of cooling pistons with oil. This investigation included the analysis of the following piston cooling methods:

- i,      Pistons with no oil cooling,
- ii,     Cooling from the oil spray from a pressure lubricated small-end bearing,
- iii,    'Cocktail shaker' pistons,
- iv,     Jet cooling.

The results from this investigation are shown in Table 3.1. The best cooling method was found to be the oil jet. The 'cocktail shaker' method, and oil spray from the small-end bearing method, were found to produce very similar results. It was concluded that the oil ejected from the small-end bearing provided an effective means of cooling, and that for moderate loads no special provisions for oil cooling have to be made.

The values for the heat transfer coefficient obtained with no direct piston cooling were very much lower than those obtained by any other type of

cooling. This was explained by the fact that the inside surface of the piston crown remained 'dry'. The heat was transferred to the air and the oil, which was in the form of a vapour or a fine mist. It was stated that there was little or no solid-liquid contact but only solid-gaseous contact. However, Stotter remarked that further investigations had shown a ten fold increase in the heat transfer coefficient values. This was explained by improved solid-liquid contact under some engine conditions. Although a full explanation of this improvement was not given, it was concluded that the oil thrown from the bearings on the crankshaft could be the source of additional oil. Seale and Taylor (1970) obtained similar results in their study. The results of the study by Seale and Taylor, of various piston oil cooling methods, are presented in Table 3.2.

#### 2.4.2.3 Oil Spray on the Liner

Very little research has been carried out on the analysis of the heat transfer to oil droplets which are thrown onto the liner and other hot engine surfaces. In the case of the liner, this heat transfer mechanism is further complicated by the reciprocating motion of the piston, which removes the oil from the surface on each stroke. The study of the hydrodynamics of droplet impingement on a heated surface is not new. The cooling of hot surfaces by liquid droplets is an effective process since large heat fluxes are involved (Tio and Sadhal (1992)).

In the field of automotive engine research, most attention has focused on the behaviour of fuel droplets within the combustion chamber. For example, Naber and Farrell (1993) examined the impact of single droplets on a heated surface. The droplet impingement was photographed with a high speed 'cine' camera to obtain the history of the hydrodynamics of the impingement process. No attempt was made to predict the heat transfer of this flow mechanism.



Other research has concentrated on the detailed thermal analysis of droplet sprays on heated surfaces. For example, Tio and Sadhal (1992) calculated the Nusselt number for droplet spray evaporation, and Pais et al (1992) examined the effect of surface roughness on the heat transfer mechanism in spray cooling.

Much research has been carried out in this area over the past three decades. However, a detailed analysis of this literature was considered to be beyond the scope of this study. Although the above papers gave an insight into the possible conditions found on the surface of a liner, no data was available which was specific to oil droplet effects. The heat transfer to the oil through the liner remains a 'grey area', where little or no past research has been undertaken. It was assumed that the heat transfer mechanism in this area could be accounted for by using one of the following approximations.

- i, The heat transfer coefficients can be the same as those found for piston cooling with oil splash.
- ii, The droplet/spray impingement mechanism can be simplified to a thin film of liquid flowing down a heated surface. This mechanism is well documented by Jakob (1963), and is discussed in more detail in section 3.12.2.

### **2.4.3 Heat Transfer by the Coolant**

Many researchers have concentrated on the analysis and simulation of engine cooling systems. For example, both Tenkel (1974) and Ninoyu et al (1993) described methods of predicting cooling system performance at the design stage. The emphasis of their work was to obtain the optimum design of the cooling system and front-end shape of the vehicle. Couëtouse and Gentile



(1992) re-examined traditional cooling system configurations and their control. A new electronically controlled cooling system with the associated control strategy was proposed. The emphasis of this work was to optimise the transfer of the available heat within an engine. By maintaining engine temperatures at their optimum operating levels under all operating conditions, and utilising the available heat more efficiently, fuel consumption and passenger compartment comfort could be improved.

Although the cooling system remains the primary heat transfer path within an engine, the analysis of the whole cooling system remains outside the scope of this study. The research of most interest is that which concentrates on the detailed analysis of the heat transfer process within the water jacket of the engine. This process is well documented by authors such as Finlay et al (1987) and Kays (1989). Both authors report that heat transfer from the engine block to the coolant takes place by a combination of forced convection and nucleate boiling.

Kays (1989) reports that the bulk temperature of the coolant is generally maintained at 10 to 20 °C below the saturation temperature. Meanwhile, the surface temperature is generally 20 to 30 °C above the saturation temperature. Boiling occurs at the surface, but the vapour condenses as the vapour bubbles mix with the cooler water, so there is no net boiling. The onset of nucleate boiling in local areas of the cylinder head may be beneficial as it enables an increase in heat flux to occur. This occurs with relatively small increases in surface temperature.

Finlay et al (1987) investigated heat transfer by forced convection and nucleate boiling with the use of a test rig. Measurements of heat transfer to water/ethylene glycol mixtures were reported for a range of coolant velocities

and heat fluxes, with a fixed pressure drop across the test section. These measured results were shown to be in good agreement with a heat transfer model proposed by Chen (1966). It was found that at the highest flow velocities (3 to 5.5 m/s) forced convection was the dominant mode of heat transfer. At lower velocities, particularly below 1.0 m/s, strong nucleate boiling occurred which had a significant influence on heat transfer.

The results showed that at coolant velocities below 0.5 m/s the intensity of boiling increased and intermittent vapour flashing within the test section created some flow instability. Further increases in heat flux increased the rate of vapour production within the test section causing larger instabilities in the flow until eventually the rate of production of vapour prevented the flow of coolant through the test section. This condition was called 'dryout', and was accompanied by a large increase in the surface temperature.

When the test section was changed from a copper to an aluminium tube, dryout did not occur until flow velocities dropped to below 0.1 m/s. It was reported that it was difficult to maintain a constant pressure drop across the test section under these conditions. The reported levels at which dryout occurs under these conditions must, therefore, be treated with some caution. The authors concluded that under typical engine operating conditions where the coolant flow rate is approximately 1.0 m/s, the heat transfer can be regarded as a combination of forced convection and nucleate boiling. The heat transfer model proposed by Chen (1966) was found to produce accurate results for these heat transfer conditions.

## 2.5 Lubrication of Journal Bearings

The principal role of any engine lubrication system is to deliver an adequate supply of oil to the various engine journal bearings. Therefore, the accurate prediction of the flow and heat transfer properties within these components lies at the heart of any lubrication system simulation model. A very large amount of work has been conducted into the analysis of the lubricant condition within journal bearings.

### 2.5.1 Prediction of Bearing Oil Flow Rate

Jones et al (1982) conducted a study into the accurate prediction of oil flow rates through engine crankshaft bearings. Jones reported that many of the techniques currently used for the analysis of dynamically loaded bearings, made use of the 'mobility method' (eg. Campbell et al (1967)). This approach gave components of journal centre velocity for the instantaneous load at each time step considered. Various mobility equations are available, the most commonly used are those based on the short bearing approximation, which were derived by Booker (1965).

Jones reported that one disadvantage of using the short bearing approximation is that it is only accurate for narrow bearings and for moderate eccentricity ratios. For other conditions it tends to overestimate the film thickness. Booker (1971) referred to a solution method developed by Moes (1971), which overcame this problem by using a finite bearing theory.

The mobility method cannot adequately take into account the influence of oil feed features, as the solution assumes an uninterrupted oil film. If the lubricant is supplied via an oil hole, the bearing has to be considered plain. For



a full circumferential groove, the bearing can be treated as two plain bearings. For a partial circumferential groove (usually  $180^\circ$ ) an approximation can be used where the bearing is treated as a full width plain bearing when the load is in the plain part, and as a full circumferentially grooved bearing when the load is in the grooved part.

Analysis techniques were improved with the use of finite bearing models. The bearing surface is divided into a rectangular mesh. The pressures at the nodes of this mesh are then determined for any given journal position and velocity. From this pressure distribution, the load capacity, oil flow and friction torque are obtained. Oil feed holes and grooves within the bearing can be modelled by applying predetermined pressures at the position of these features. This automatically takes account of the effect on the generated hydrodynamic pressure when the hole is in the load carrying film. Conway-Jones et al (1990) reported that this procedure takes 10,000 times longer than the mobility method and cannot be used on a daily basis. However, it can be used in the study of specific problems, such as the effects on the hydrodynamic pressure profile due to the oil holes or grooves.

Jones (1982) reported that the greatest step forward in modelling the bearing was the inclusion of the oil film history. In brief, oil film history is the movement of the oil between the two loaded surfaces of the bearing, prior to the instant being considered. As the transport of oil within a bearing takes time, it is the movement of oil prior to the instant being considered that governs the availability of oil around the bearing. Under the action of a dynamic load, situations can arise where there is inadequate oil to fill the clearance space in some of those regions where potentially high pressures could have been generated. This leads to smaller oil film extent, which in turn affects the oil film characteristics, such as load capacity and oil flow.

Martin and Lee (1982) reported the development of an approximate, but fast method of solution. A new procedure for predicting the flow due to the supply pressure (hydrostatic flow) was developed. Martin (1983) noted that the previous attempts at the prediction of feed pressure flow by Cameron (1981), did not apply directly to rectangular feed grooves and circular oil holes. Cameron's feed pressure flow equations were based on dimensionless terms derived from theory, together with a flow factor based on the experiments of Hirano and Shodai (1958). Martins approach was based on geometric plotting techniques and the results compared extremely well with Hiranos experimental results.

The feed pressure flow predicted by Martin, when coupled with the flow caused by the pumping action of the bearing (hydrodynamic), gave predictions which were in good agreement with those of more rigorous mobility models. Figure 2.2 shows diagrammatically the predicted flows obtained by the various methods outlined above, compared with the measured flows obtained from experiments on the main bearings of a 1.8 litre 4 cylinder in-line petrol engine.

The experimental flows are designated  $Q_x$ . The flows from the rapid method are the feed pressure flow  $Q_p$ , the hydrodynamic flow  $Q_H$ , and the equivalent flow  $Q_s$ . The equivalent flow is an adjusted value for the sum of hydrostatic and hydrodynamic flows.  $Q_R$  is the flow calculated using the rigorous model without oil film history, where  $Q_F$  is the predicted flow when oil film history is taken into account.

The flow  $Q_F$  predicted by the rigorous model using oil film history, is in much closer agreement with experimental results than the other predictions. However, it can be clearly seen that the feed pressure flows  $Q_p$  are only slightly less than the values of experimental flow  $Q_x$  for all the cases considered. As a



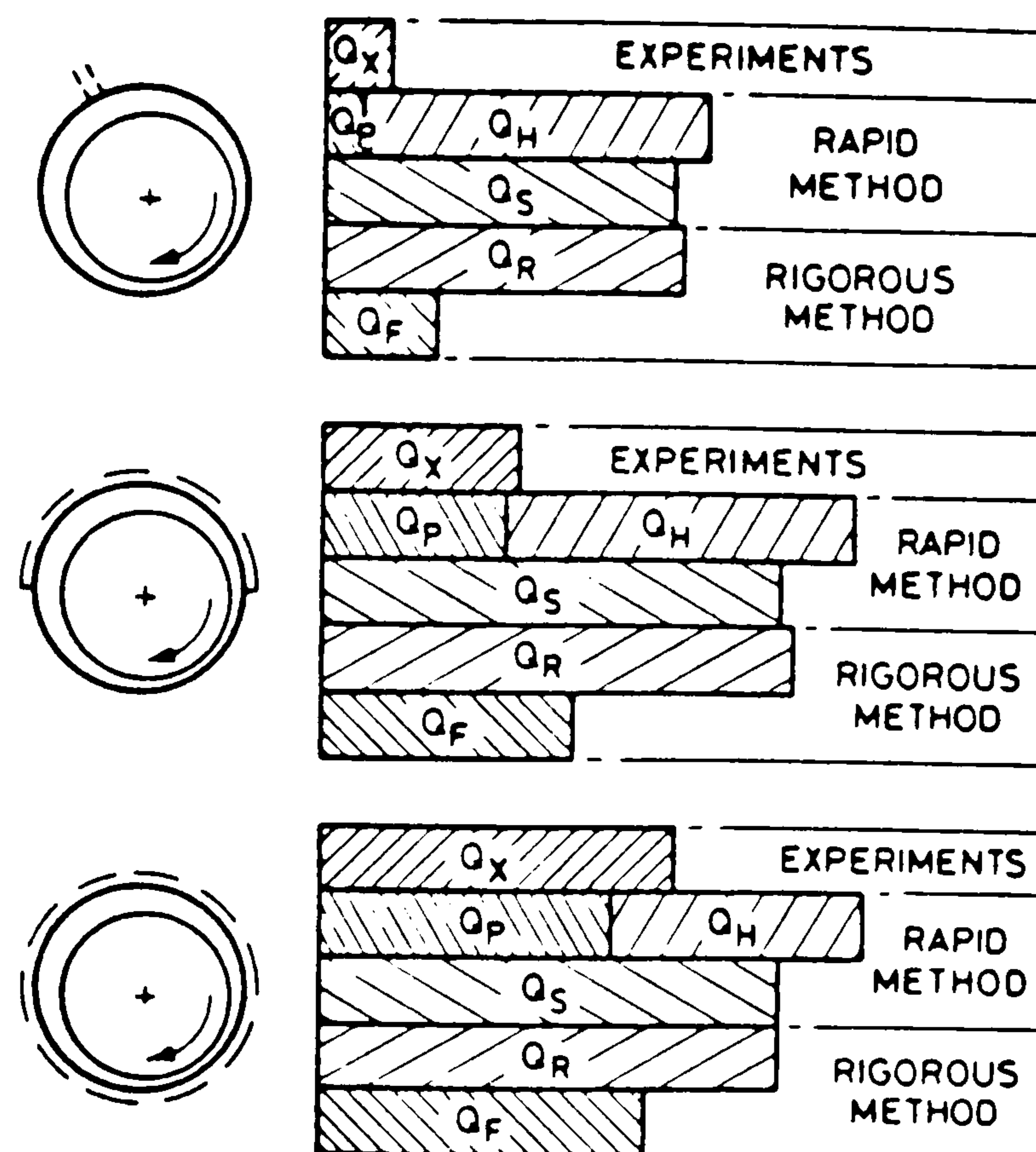


Figure 2.2. Averaged bearing oil flows from various predictive techniques compared with experiment

result, Glacier recommended the equations for the prediction of feed pressure flow which were developed by Martin and Lee (1982), be used for the prediction of the total flow in this study.

### 2.5.2 Heat Transfer Within Bearings

As discussed in the above section, many techniques have been established for the prediction of bearing oil flow rates. However, they all involve an estimate of the viscosity of the working oil, which in turn depends on its temperature. This is set by the heat balance within the bearing system, in which the heat generated through shearing and squeezing of the oil is equated to the heat carried away by the oil flow and conduction through the bearing and housing.



Conway-Jones et al (1990) reported that a typical assumption for a hydrodynamically lubricated bearing is that 85-95% of the heat generated in the oil is carried away by the oil flow. It was reported that there is only a small variation in temperature around the bearing, with the bearing and the journal being at approximately the same temperature. The heat generated within an oil film depends on the oil viscosity and the rate of shear of the oil. This in turn depends on the speed of rotation and inversely upon the oil film thickness. Thus, the heat generated within an oil film is directly related to the bearing power loss.

The authors conducted tests on a 1.3 litre petrol engine to analyze the heat transfer paths in crankshaft bearings. The oil flow to the connecting rod was found to be significantly less than through the main bearing. Thus, the big-end bearings ran at higher temperatures than the main bearings, although the temperature difference was controlled by the thermal conductivity of the crankshaft. It was found that 30-50% of the heat generated within the connecting rod was conducted through the crankshaft to the main bearings. The oil flow through the main bearings carried away most of the additional heat.

The authors suggested a method of predicting the heat generated within the oil film of a journal bearing. The proposed method was developed by Martin et al (1987), and relied on relating the bearing power loss to dimensionless bearing and engine load parameters. Bearing load diagrams were defined by dimensionless groups in which the reciprocating and rotating masses were accounted for. Having calculated the power loss through the bearing by this method, the mean temperature rise of the oil can be found for the given oil flow rate.

## 2.6 Oil Filter

Although much literature is available in the field of fluid filtration, very few papers were found which concentrated on the detailed analysis of the thermofluid conditions within an automotive oil filter. Many authors concentrated their attention on the discussion about whether there is in fact a need for an engine oil filter in the first place. This was demonstrated by Nostrand (1974), who made an historical review of the papers published on oil filtration to that date. It was not until approximately 1946 that the engine and filter manufacturers agreed that lubricant filtration played a significant role in the reduction of wear and prolonged engine life. Nostrand continued to discuss the various filtration methods and types, these are discussed in more detail in Chapter 3.8.

Jaisinghani (1981) presented a paper on the resistance of flow of oil through a cartridge filter. An empirical expression for the pressure drop due to liquid flow through fibrous beds, under conditions expected in liquid cartridge filtration, was developed. This expression was validated over a period of more than three years and it was found that the results were always within 15% of values obtained from filter rig tests.

## 2.7 Crankshaft and Camshaft Oil Flows

Lubricant supply to the crankshaft connecting rod bearings (big-end) of current automotive engines is obtained from the main bearing supply via transfer holes in the crankshaft. Meernik (1986) proposed a method of calculating the oil pressure requirements to overcome the frictional and centrifugal forces within the big-end bearing. More significantly, the analysis included a study of the force required to overcome the inertia force of the oil in

the transfer hole between the 180° (partial) grooved main bearings and the big-end bearings.

The study proposed that crankshaft oil flow was primarily controlled by the following items:

- i, Registry between the bearing and the crankshaft flow paths.
- ii, Centrifugal losses.
- iii, Losses associated with accelerating the oil to journal surface speed.
- iv, Viscous flow losses.
- v, Acceleration losses in the transfer passage due to pulsed nature of the flow.

The author used data from an oil flow test rig to determine explicit correlations for each of the above items. These relationships are discussed in more detail in section 3.10.

## **2.8 Commercial Software for Thermofluid Analysis**

The literature search revealed a commercial software package called 'FLOWMASTER' which was jointly developed by Amazon computers and the British Hydromechanics Research Association (BHRA). FLOWMASTER was developed to provide a means of predicting the fluid behaviour in piping networks. The detailed analysis of the fluid flow through each individual element relies on data published by Miller (1990). It is an ideal package for the flow analysis of the piping installations in the petrochemical, process, water and power industries.



FLOWMASTER, however, is a very general pipe flow analysis package, it can only analyze flow networks which can be represented by; pipes, bends, valves, junctions, pumps, and orifices. As such, it is of no practical use for the specialist analysis of a lubrication system, which in addition to containing pipes, pumps, and bends, also contains journal bearings, filters, heat exchangers, and centrifugally affected components such as the crank-shaft oil transfer holes. In addition, FLOWMASTER has a very limited heat transfer prediction capability, which would be insufficient for the prediction of heat transfer within a lubrication system.

## 2.9 Conclusions

The literature search revealed that much research has been conducted into the analysis of both the thermodynamic and the fluid mechanic properties of the various components within the lubrication system. The majority of the work has concentrated on the detailed oil flow and heat transfer analysis of the oil film within the journal bearings and between the piston rings and the liner.

It was found that very little research has been conducted into the prediction of the amount of oil splashed onto the liner surface, or the calculation of the heat transferred to this oil before it is scraped off by the oil piston rings. The heat transfer process between the oil spray and the liner and other internal engine surfaces remains a 'grey area', where little or no research has been conducted.

Some researchers did attempt to analyze the whole lubrication system, mainly by engine testing, but very few tried to bring together the existing detailed knowledge of the flow and heat transfer conditions within the individual components, and construct a simulation model for the analysis of the

whole system.

The majority of the computer simulation models which were constructed, were either specific to a particular engine, or were found to be inaccurate in the prediction of oil flow rates and pressures through individual components, in particular, the journal bearings.

The most comprehensive study was undertaken by Trapy and Damiral (1990), whose research closely matched the objectives of this study. The authors reported that a computer simulation model had been developed which could predict oil flow rates, pressures, and temperatures throughout any proposed lubrication system. Although the model produced accurate results for the oil pressures and the flow rates, there was a discrepancy in the calculation of the oil temperatures because the model neglected the heat transfer to the oil from the liners, pistons and valve train.

Trapy and Damiral calculated the heat transfer to the oil within the flow passages by using measured engine block temperatures. However Veshagh and Chen (1993) and Shayler et al (1993) have demonstrated a method of predicting the heat transfer role of the lubrication system during engine warm-up. Their approaches were similar, in that they represented a piston/cylinder arrangement by a series of block elements. Using a nodal resistance network approach, the nodal temperatures and convective fluid temperatures were calculated simultaneously at discrete time steps.

The method of using a representative nodal resistance network allowed the heat transfer paths to the oil to be accounted for, and the oil temperatures to be predicted. This allowed the heat transfer to the oil within the oil passages, and the oil splashed onto the piston and liner surfaces, to be

calculated at the design stage.

In conclusion, it was proposed that a truly flexible thermofluid design analysis tool could be developed by integrating a flow analysis approach similar to that employed by Trapy and Damiral, with a detailed heat transfer modelling method similar to that documented by Veshagh and Chen. This would allow the rapid analysis of any engine lubrication system configuration at the design stage, without the need for any measured block temperature data.



## **Chapter 3**

# **Fluid Flow and Heat Transfer Fundamentals Within an Engine Lubrication System**

### **3.1 Introduction**

The simulation model documented in this dissertation was developed for use in the design and development of Jaguar IC petrol engines. Two families of engines were under production at Jaguar; a 12 cylinder 'V' configuration, and a six cylinder in-line configuration. The six cylinder family of engines was named the AJ6. As the AJ6 family of engines were of a more simple design than the V12, Jaguar recommended that the lubrication system simulation model would initially be developed for the analysis of this engine. However, the model was structured in such a manner as to easily facilitate the analysis of any other lubrication system configuration.

Following initial development of the model, using the AJ6 engine's lubrication system as a benchmark, attention was switched to a new 8 cylinder 'V' configuration engine being developed at Jaguar. It was believed that more test data would become available for this engine, which could be used for validation of the model. In addition, the switch to a different lubrication system layout was an excellent test of the flexibility of the model. This led to the development of additional component models.

An engine lubrication system is comprised of two types of components; those which are lubricated, and those which help to provide that lubrication. On the pressurised side of the lubrication system, the main destinations for the oil supply were the engine journal bearings and the automatic chain tensioners. Some designs of chain tensioners provide an oil jet onto the timing chains.

The remaining components help provide the required oil supply. These components include; flow passages, bends, junctions, pumps, strainers/filters, oil coolers, and crank-shaft and cam bearing oil transfer holes.

In addition to providing a pressurised oil feed to the journal bearings and chain tensioners, the lubrication system also provides lubrication to components in the form of oil splash and oil spray. This usually originates from the oil spraying out of the various journal bearings. A typical example of this type of lubrication is the oil spray onto the piston and liner. However, these components remain outside the pressurised side of the lubrication system and were not included in the initial fluid model. Only the heat transfer aspects of these components needed to be considered and this was done separately from the thermofluid model of the pressurised side.

In order to accurately model a lubrication system, a detailed knowledge of the oil flow through the various components within the system was required. A detailed analysis of the fluid flow and heat transfer within the component elements discussed above is presented in this chapter.

## **3.2 Typical Engine Lubrication System Layout**

The lubrication system of the AJ6 engine will be used as an example. The AJ6 engine is a naturally aspirated, spark ignited (SI) IC petrol engine.

The AJ6 family of engines include 3.2 litre, 3.6 litre and 4.0 litre capacity variants. The lubrication system of the AJ6 engine is shown in diagrammatic form in Figure 3.1 and in a more detailed schematic form in Figure 3.2. The pressurised side of the system is shown in solid lines in Figure 3.2, while the broken lines represent the areas lubricated by oil splash and spray. The flow network which was used to represent the pressurised side of this system, is shown in schematic form in Figure 8.2.

Although the AJ6 engines which are currently in production include an oil cooler in the lubrication circuit, it was not an objective of the project to model the flow of oil through the oil cooler, as it was intended to be phased-out on future models. The flow network used to represent the pressurised side of the lubrication system of the V8 development engine, is shown in schematic form in Figure 9.1.

### 3.3 Lubricating Oils

The lubricating oil lies at the heart of any engine lubrication system. The lubricant provides the necessary fluid film between sliding surfaces, and removes heat which is generated through friction.

Jaguar recommend the use of Castrol 10W/40 multigrade oil for in-service engines. However a different grade of oil, a BP 10W/30 multigrade, was used in engine tests carried out at Jaguar. It was decided to model the AJ6 engine lubrication system with this grade of oil. The V8 engine was modelled with an Esso 5W30 multigrade oil. This grade of oil was used in the engine tests and Jaguar planned to recommend the same grade of oil for in-service engines. The characteristics and properties of the oils used to model the AJ6 and the V8 engines are presented in Appendix B.1, B.2 and C.1.



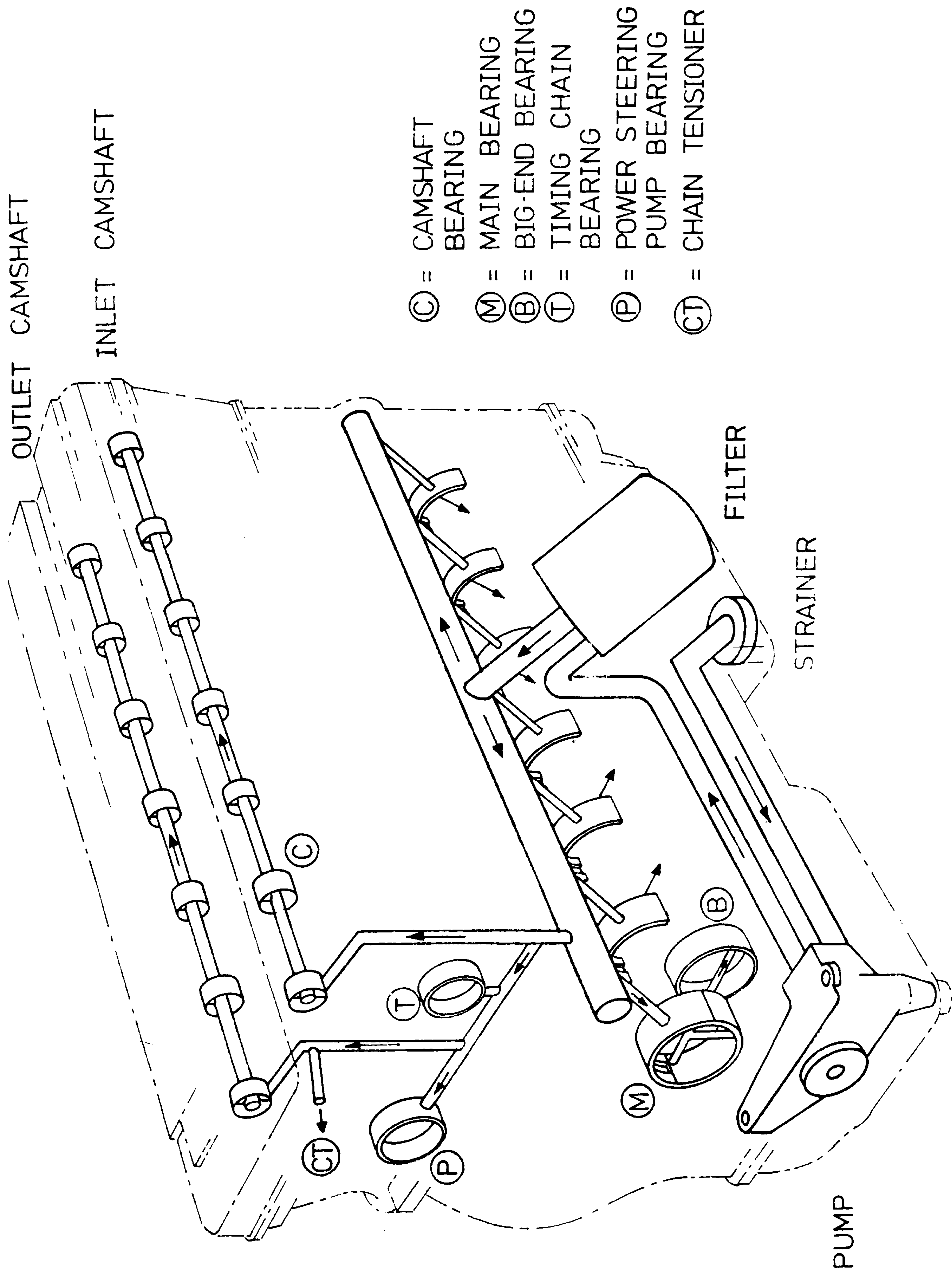


Figure 3.1. Jaguar AJ6 engine lubrication network

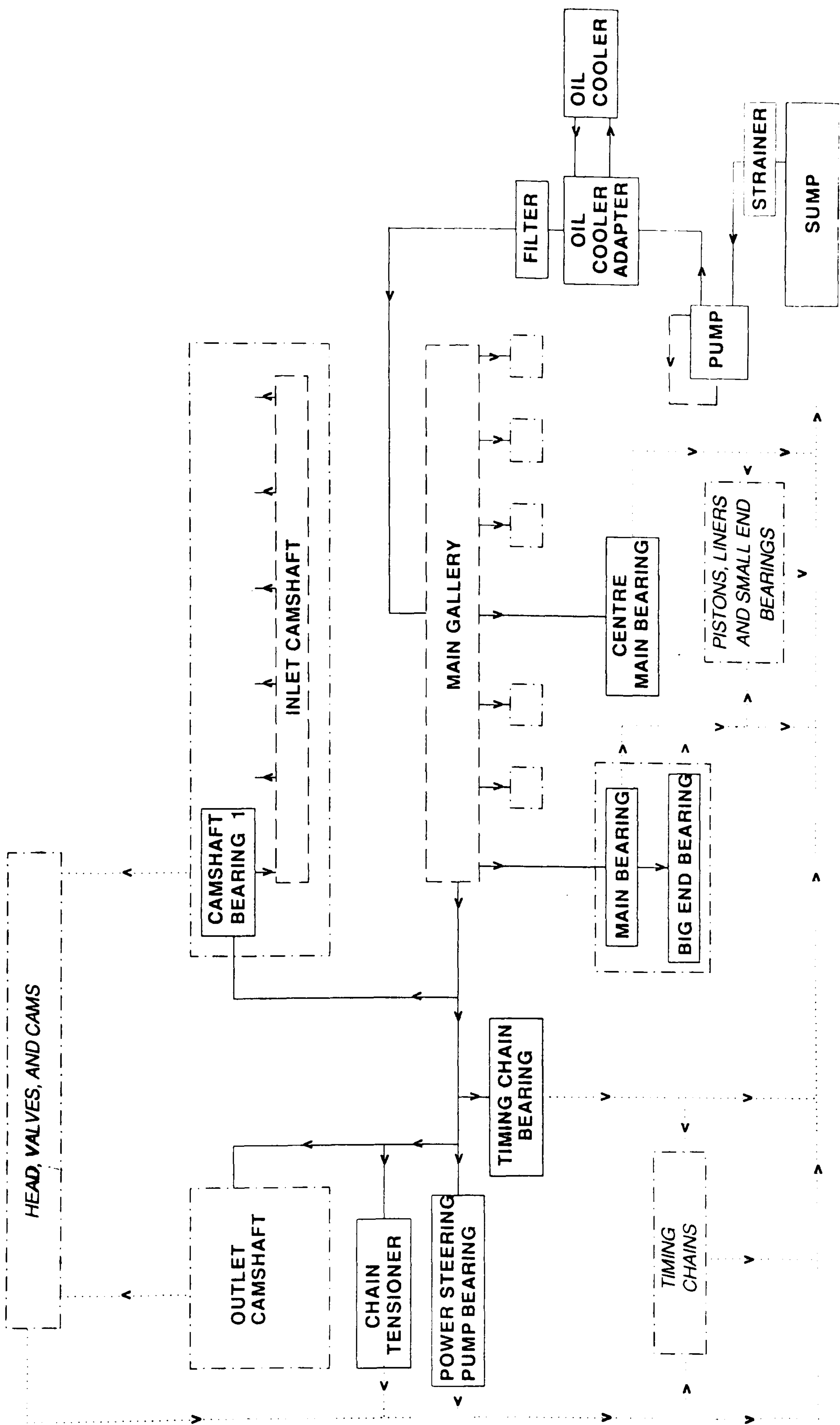


Figure 3.2. Schematic diagram of Jaguar AJ6 engine lubrication system

## **3.4 Flow Passages**

The oil is transported to the lubricated components through a complex series of pipes and drillings within the structure of the engine block. This network of pipes and drillings was simplified to a fluid flow network, in which each of the flow sections were represented as a straight pipe of constant circular cross-section.

### **3.4.1 Flow in Pipes**

The manner in which the oil is transported within a pipe is dependent upon the type of flow. It was assumed that each flow passage was of constant cross-sectional area, and that a sufficient amount of oil would always remain in the sump to ensure that the oil strainer was always completely covered. This assumption assured no air would be drawn into the system, and the pipes would always run full of oil. Thus, the flow of oil in the lubrication system passages was uniform and incompressible.

#### **3.4.1.1 Types of Fluid Flow**

Viscosity causes fluid particles immediately adjacent to a rigid surface to be brought to rest. The area of low energy fluid that forms is termed the 'boundary layer'. With increasing distance from the surface, the velocity of the fluid particles increases up to a maximum which is usually at the passage centreline.

There are two distinct types of fluid flow which occur; turbulent flow, and laminar flow. Figure 3.3 shows the difference in the velocity profiles for



fully developed laminar and turbulent flow in a circular pipe. Developed laminar flow is characterised by a peak to mean velocity ratio of 2. This is compared with a developed turbulent profile which has a peak to mean velocity ratio of about 1.2 (Miller (1990)).

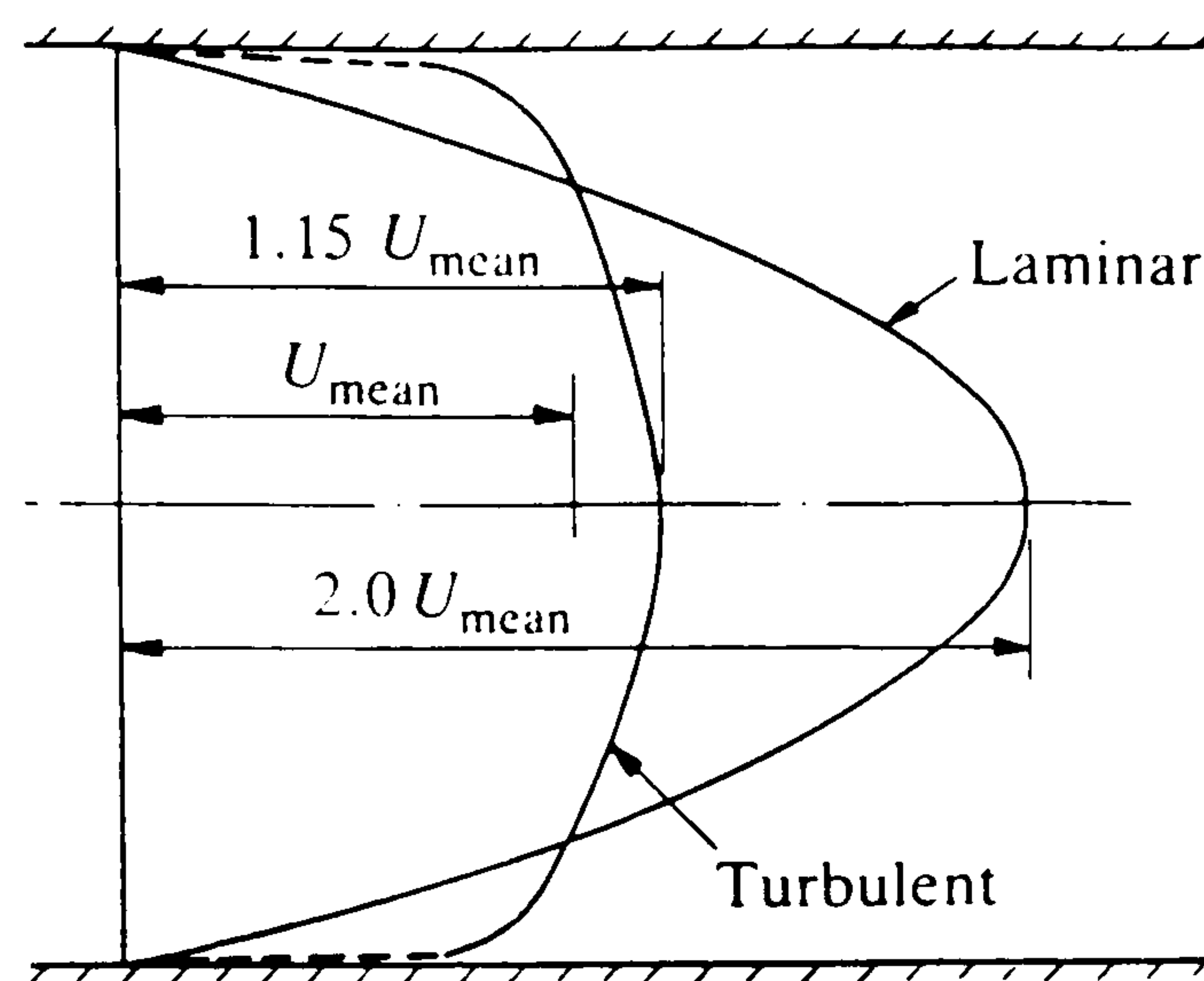


Figure 3.3. Laminar and turbulent velocity profiles

The type of flow is determined by the value of the Reynolds number, which can be expressed as follows:

$$Re = \frac{\rho V D}{\mu} \quad (3.1)$$

In pipes, flow is laminar if  $Re < 2100$ . For  $2100 < Re < 5000$ , any turbulence generated by a disturbance is likely to persist. A  $Re > 5000$  normally guarantees turbulent flow in tube sections.

#### 3.4.1.2 Flow Development

The various stages of flow development in a straight pipe, preceded by

a well designed contraction with minimum pressure losses and disturbances, are shown in Figure 3.4.

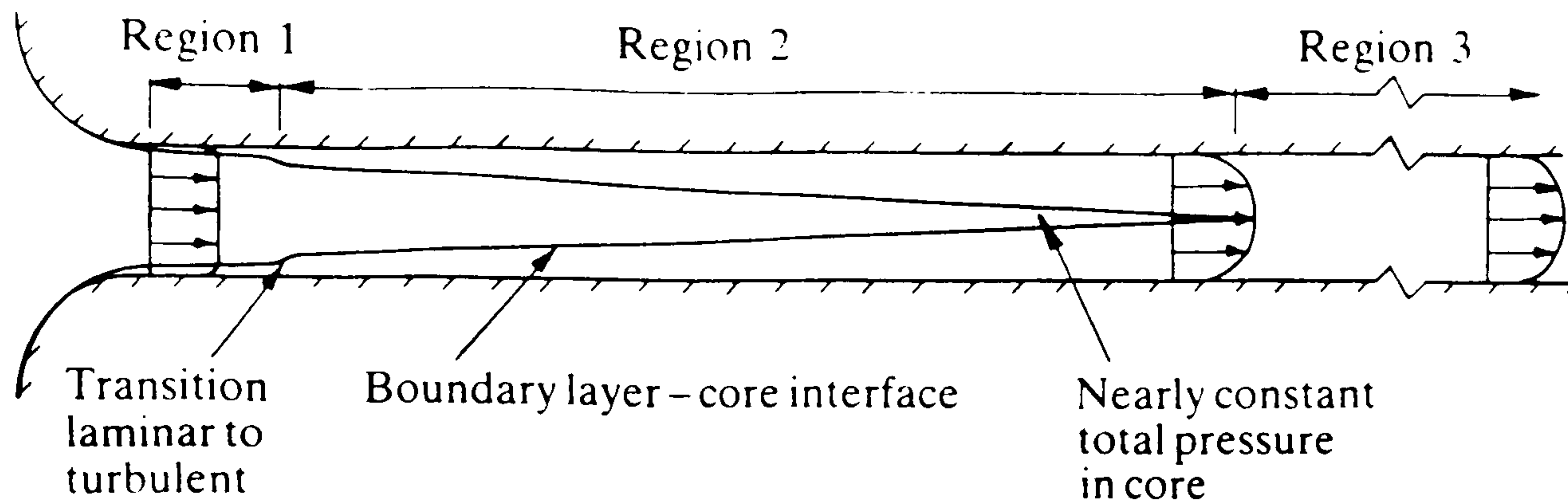


Figure 3.4. Boundary layer development after a smooth contraction

In region 1, close to the inlet, the velocity profile is virtually one-dimensional with a thin boundary layer. If the flow is laminar leaving the contraction, it will become turbulent in this region. Region 2 extends to the point where the boundary layers merge at the centre of the pipe. At a Reynolds number of  $10^6$  the boundary layers merge 30 diameters from the inlet (Miller (1990)).

### 3.4.1.3 Conservation of Energy

The conservation of energy between any two points in a pipe can be represented by the Bernoulli equation:

$$P_1 + \frac{\rho V_1^2}{2} + \rho g z_1 = P_2 + \frac{\rho V_2^2}{2} + \rho g z_2 + \text{losses} \quad (3.2)$$

The losses in Equation 3.2 are a result of both fluid friction and disturbances from bends and junctions. These losses are discussed in more detail below.

### Friction losses in pipes and passages

The pressure loss due to friction in a length of pipe is given by the Darcy-Weisbach formula:

$$\Delta P = f \frac{L}{D} \rho \frac{V^2}{2} \quad (3.3)$$

The value of the friction coefficient,  $f$ , depends on the type of fluid flow. For laminar flow the friction coefficient can be expressed as:

$$f = \frac{C_f}{Re} \quad (3.4)$$

Where  $C_f$  is 64 for circular cross-sections, 56 for square cross-sections, and 96 for an infinitely wide two-dimensional passage.  $C_f$  values for other cross-sectional shapes can be obtained in graphical form from Miller (1990).

For turbulent flow, the accepted presentation of friction coefficients for pipes of circular cross-section is the Moody chart (Appendix B.3), which is based on the Colebrook-White equation (1939). However, as this equation requires an iterative solution, it is not suitable for use in a model which uses a linear solution method. Instead, an equation of similar accuracy to the Colebrook-White equation, which was derived by Swamee and Jain (1976), may be used:

$$f = \frac{0.25}{\left[ \log \left( \frac{k}{3.7D} + \frac{5.74}{Re^{0.9}} \right) \right]^2} \quad (3.5)$$

Where  $k$  is the roughness value, and is obtained from published data (Miller (1990)). A selection of roughness values for different types of pipes is



given in Appendix B.4.

### Losses from Bends

The pressure losses due to a bend are made up of losses within the bend, and losses associated with the redevelopment of the flow after the bend. The equation which represents this pressure loss, is of the form:

$$\Delta P = \frac{K_b \rho V^2}{2} \quad (3.6)$$

The bend loss coefficient,  $K_b$ , for a Reynolds number of  $10^6$ , is obtained in graphical form from published data for various types of pipe bends (Miller (1990)). Correction factors are given to correct the loss coefficients to any other Reynolds numbers, and for bends which are in close proximity to other components.

### Losses from Junctions and Other Flow Restrictions

'T' junctions are often the highest loss components in a piping system. The energy losses are predominantly due to turbulent mixing. The method of calculating the pressure losses within these junctions is very similar to the method employed for bends. Equation 3.6 is used, and the loss coefficient,  $K$ , is obtained from graphical data by Miller (1990). Typical T and Y junctions which are covered by this data are shown in Figure 3.5.

The loss coefficients  $K_{ij}$  shown in Figure 3.5 are defined as:

$$K_{ij} = \frac{\text{Total pressure in leg } i - \text{Total pressure in leg } j}{\text{Mean velocity pressure in leg } 3} \quad (3.7)$$

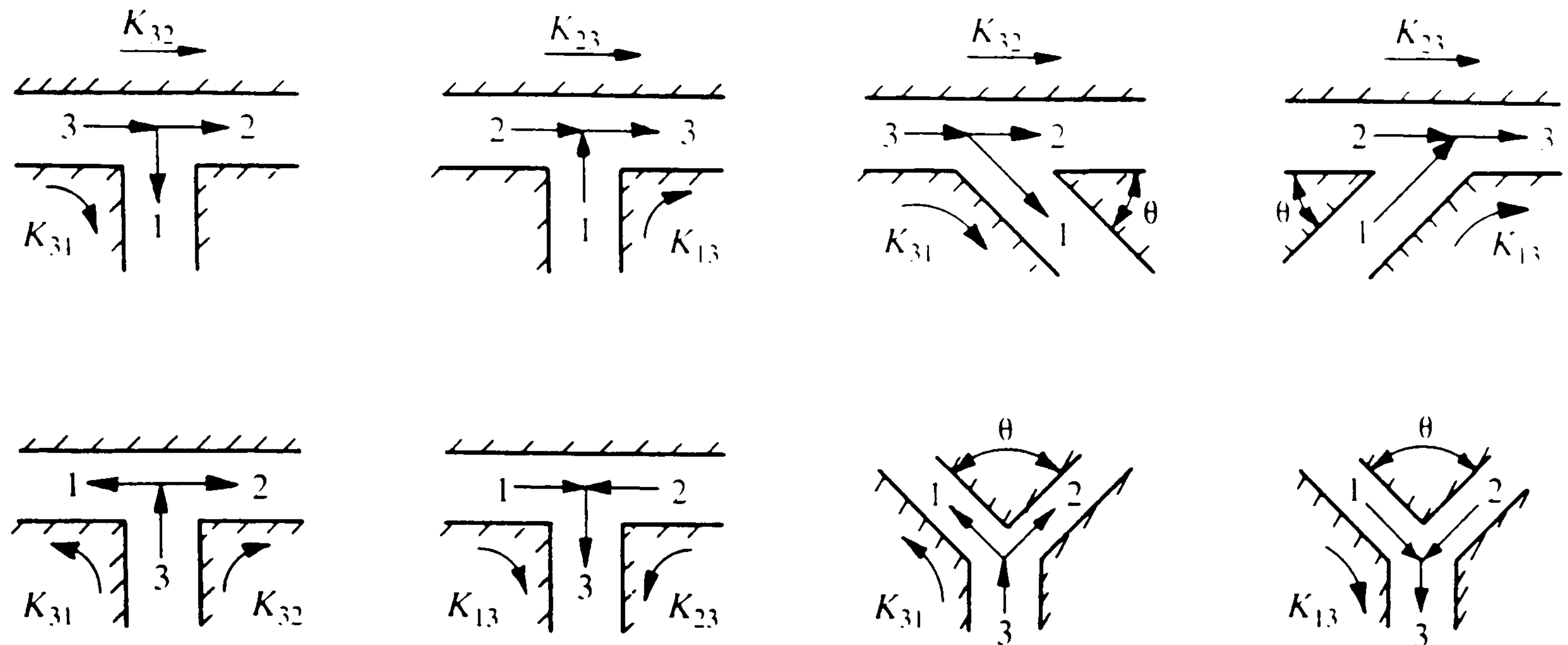


Figure 3.5. Typical T and Y junctions

Pressure losses due to abrupt changes in cross-sectional area of the pipe, including the flow through an orifice plate, are predicted in a similar way. The loss coefficients are again obtained from graphical data published in Miller (1990)

Miller (1990) found that the pressure losses in bends and junctions under laminar flow conditions are negligible. In laminar flow, the onset of turbulence within the bend or junction is suppressed, and the secondary flows are stronger and more stable.

### 3.4.2 Heat Transfer in Pipes

The primary mode of heat transfer for internal flow in a pipe is convection. Although the process of conduction by molecular exchange is still present in a moving fluid, the transport of energy is greatly influenced by the fluid motion. When the fluid motion is induced from an outside force such as a pump, the transfer of heat is termed 'forced convection'. Even when no flow is induced by an outside force, fluid motion may still occur as a result of density differences produced by local heating of the fluid. This process of heat

transfer is called 'free convection'. When the fluid velocity is low, situations arise where heat transfer is neither 'forced' or 'free' in nature, but a combination of the two. A summary of combined free and forced convection effects in tubes was given by Metais and Eckert (1964).

For the purpose of this study it was assumed that the flow velocity in the pipe sections within the lubrication system would always remain high enough to neglect the effects of free convection. This assumption simplified the approach taken for representing the pipe elements in the model. Heat transfer by forced convection is independent of the attitude angle of the pipe. This reduces the amount of input data required from the user while forming the layout of the system.

#### 3.4.2.1 Heat Transfer in Fully Developed Flow

In the case of flow in a pipe in which heat transfer is taking place, there is a difference between the pipe wall temperature and the fluid temperature. As shown in Figure 3.6, this difference produces a temperature profile in the fluid.

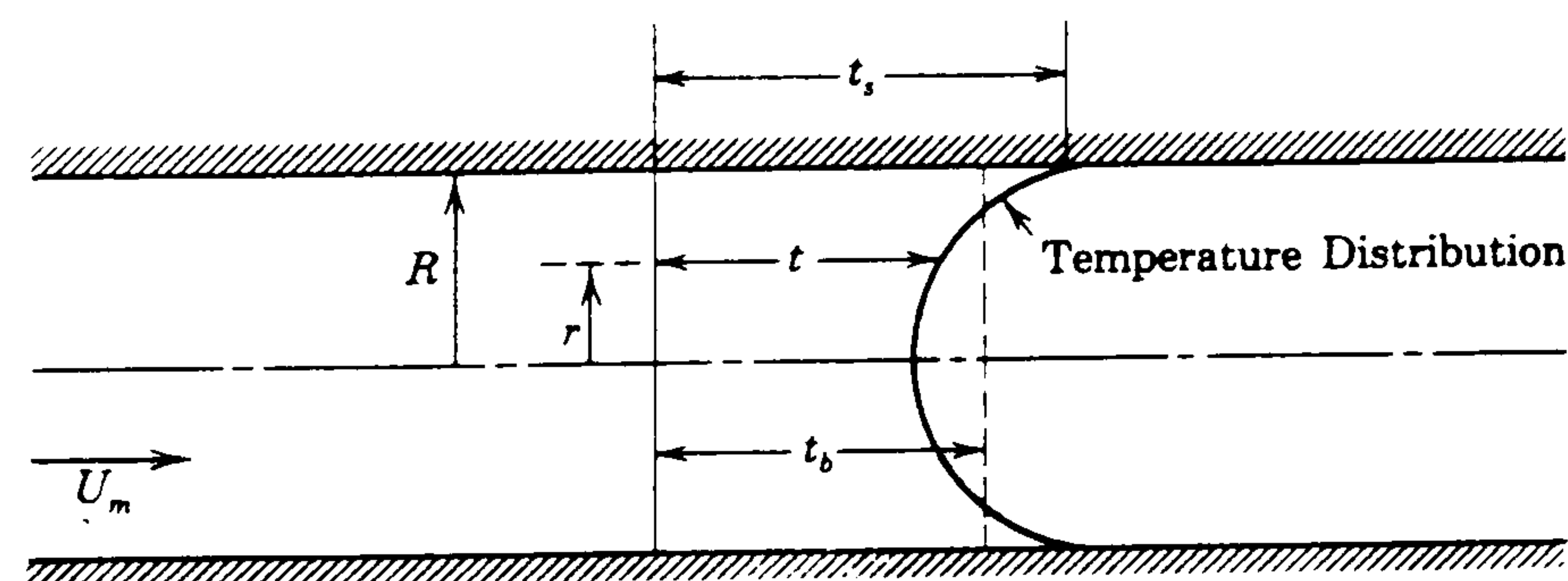


Figure 3.6. Temperature distribution in pipe flow



The exact form of the temperature profile depends on; the thermal boundary conditions imposed on the surface; whether the flow is laminar or turbulent, and entry length effects. To characterize the fluid temperature for the calculation of the heat transfer coefficient, the 'bulk' fluid temperature,  $t_b$ , is defined. This temperature is the energy averaged temperature across the cross-section, as defined in Equation 3.8.

$$t_b = \frac{\int_0^R v \rho C_p 2\pi r t \, dr}{\int_0^R v \rho C_p 2\pi r \, dr} \quad (3.8)$$

As in the case of the development of the velocity profile, discussed in section 3.4.1.2, there are also 'starting length' considerations with respect to the temperature profile in pipe flow. Figure 3.7 depicts a fluid of initially uniform temperature entering a pipe, the wall of which is hotter than the fluid.

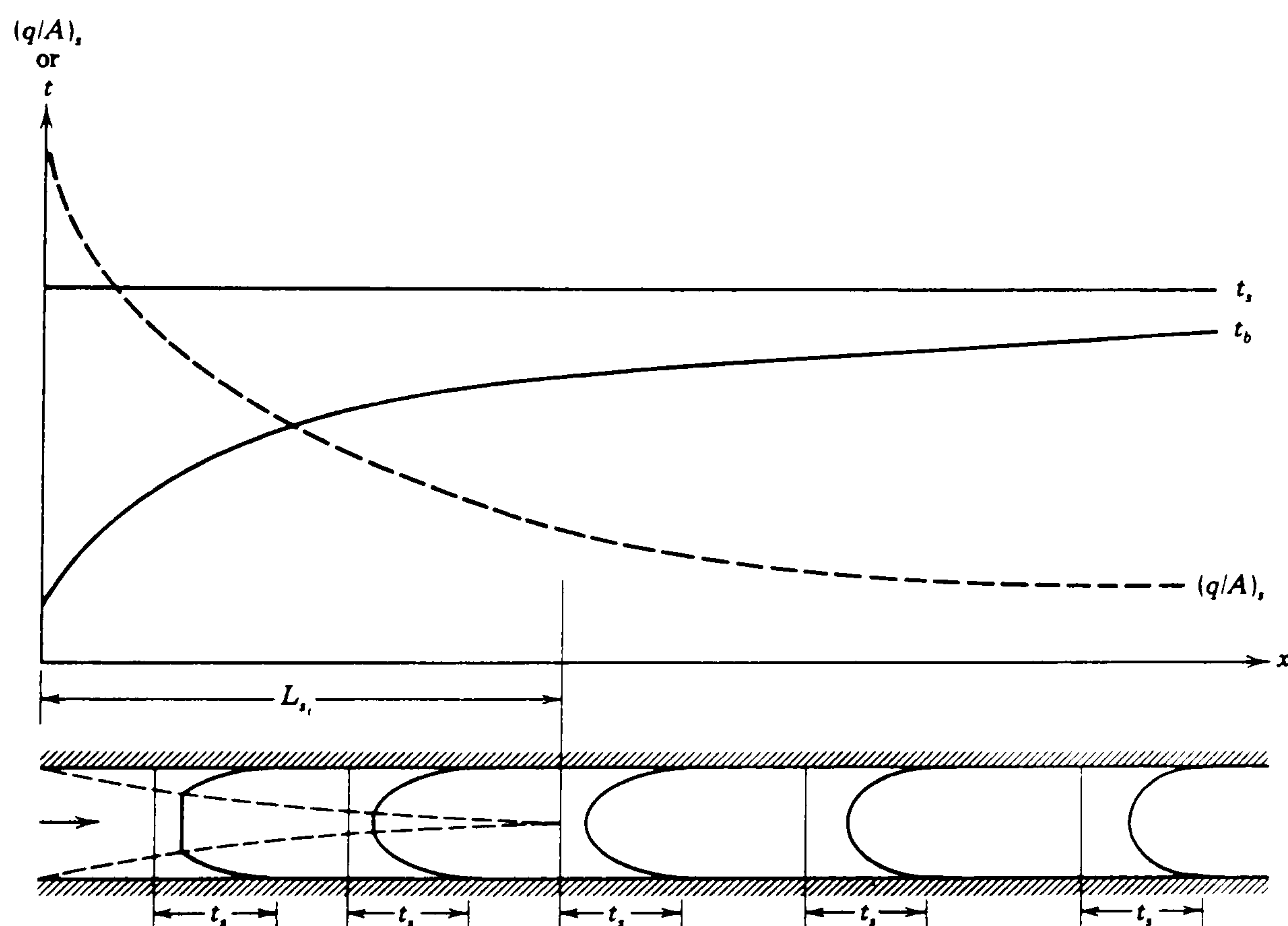


Figure 3.7. Developing temperature profiles in pipe flow

The wall temperature,  $t_s$ , in this example is held fixed. As the flow proceeds down the pipe, a thermal boundary layer develops at the surface. The fluid temperature within the boundary layer is altered by heat transfer with the surface, while the fluid in the central core remains at the inlet temperature. Eventually, the thermal layer completely fills the pipe at the thermal starting length  $L_s$ , and the temperature profile becomes fully developed.

The exact nature of the shape of the developing and the fully developed temperature profile is dependent on whether the flow is laminar or turbulent.

### 3.4.2.2 Equations for Forced Convection

The total heat transferred over a pipe length  $L$  is given by the energy balance equation:

$$q = h\pi DL(t_s - t_b)_m = \dot{m}C_p(t_{bo} - t_{bin}) \quad (3.9)$$

where  $(t_s - t_b)_m$  is the mean of the temperature difference  $(t_s - t_b)$  over the length  $L$ . In preference to the arithmetic mean, the appropriate mean value for  $(t_s - t_b)$  as it varies from  $(t_s - t_{bin})$  to  $(t_s - t_{bo})$  is the log mean as given in Equation 3.10.

$$(t_s - t_b)_m = \frac{(t_s - t_{bin}) - (t_s - t_{bo})}{\ln \left( \frac{t_s - t_{bin}}{t_s - t_{bo}} \right)} \quad (3.10)$$

The key variable in Equation 3.9 is the heat transfer coefficient,  $h$ . The following correlations yield methods of predicting the dimensionless Nusselt number,  $Nu$ . The value of  $h$  can then be calculated from Equation 3.11.

$$h = Nu \frac{k}{D} \quad (3.11)$$

For fully developed laminar flow with a constant tube surface temperature, the Nusselt number is given by Equation 3.12. This equation is applicable to tubes that are so long that the starting length may be ignored.

$$Nu = 3.66 \quad (3.12)$$

For 'short' tubes in which the starting lengths are important, the empirical relation of Sieder and Tate (1936) is preferred:

$$Nu = 1.86 \left[ \left( \frac{D}{L} \right) Re Pr \right]^{\frac{1}{3}} \left( \frac{\mu}{\mu_s} \right)^{0.14} \quad (3.13)$$

Where:  $0.48 < Pr < 16,700$

$(D/L)RePr > 10$

All properties, except  $\mu_s$ , at mean  $t_b$

$\mu_s$  at  $t_s$

Equation 3.13 gives the average  $h$  to be applied over the pipe length  $L$ . The quoted limit of  $(D/L)RePr > 10$  establishes what is meant by a short tube. For values below this limit, Equation 3.12 may be used.



The most widely used equation for turbulent flow is the Dittus-Boelter (1930) equation:

$$Nu = 0.023 Re^{0.8} Pr^n \quad (3.14)$$

Where:  $n = 0.4$  for  $t_s > t_b$   
 $n = 0.3$  for  $t_s < t_b$   
 $(t_s - t_b) < 6^\circ\text{C}$  for liquids

One advantage with the Dittus-Boelter equation is that knowledge of the pipe surface temperature,  $t_s$ , is not required, only whether the fluid is being heated or cooled. However, the greatest limitation for its use with liquids, is the limitation of the temperature difference,  $t_s - t_b$ . For differences greater than  $6^\circ\text{C}$ , the following empirical equation of Sieder and Tate (1936) is preferred, although knowledge of the surface temperature is required:

$$Nu = 0.027 Re^{0.8} Pr^{\frac{1}{3}} \left( \frac{\mu}{\mu_s} \right)^{0.14} \quad (3.15)$$

Where: All properties are at the temperature,  $t_b$ , except for the property  $\mu_s$ , which is calculated at the temperature,  $t_s$ .

The above equations can only be used when the ratio  $L/D \geq 60$ . For short tubes it may be necessary to account for starting length effects. Very little information is available on turbulent starting lengths other than they are usually shorter than in laminar flow. Nusselt (1931) found the following expression to be applicable for shorter tubes:

$$Nu = 0.036 Re^{0.8} Pr^{\frac{1}{3}} \left( \frac{D}{L} \right)^{\frac{1}{18}} \quad (3.16)$$

Where:  $10 < L/D < 400$   
properties at  $t_b$

### 3.5 Annular Pipes

Annular pipes were included in the list of component elements within an engine lubrication system due to the requirement to model the flow of oil through automatic chain tensioners. Chain tensioners on the AJ6 engine were of a similar design to those on the V8. Figure 3.8 depicts a section through a typical chain tensioner assembly.

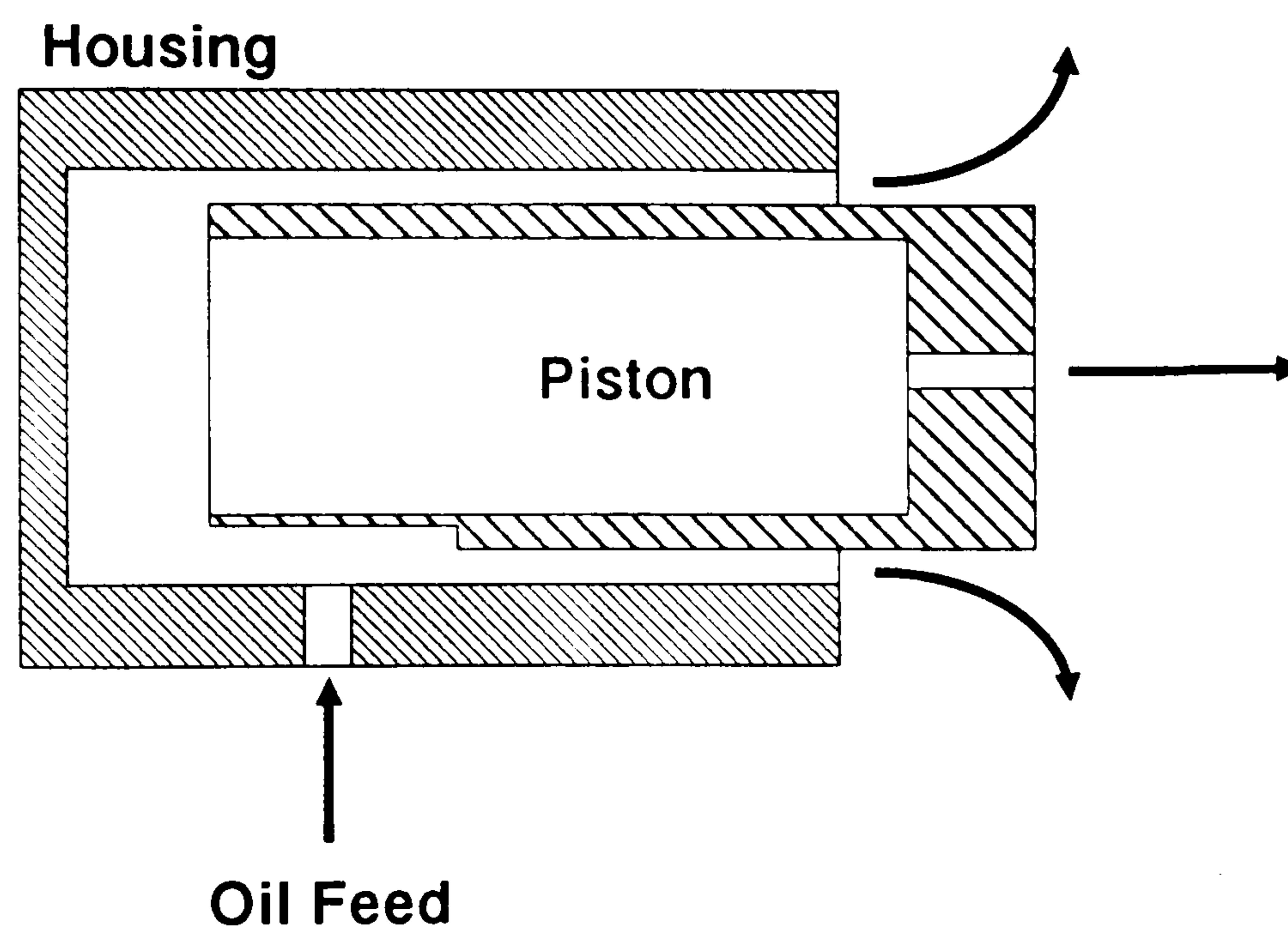


Figure 3.8. Section through a typical automatic chain tensioner

From a flow network point of view, there are two flow paths of interest. The primary flow path is through the small drilling in the centre of the piston. The oil jet from this hole lubricates the timing chains and guides. It can be seen from Figure 3.8 that there is no seal between the piston and cylinder, and

the oil flow through this gap forms the second flow path, which must also be accounted for. This flow path can be considered as an annular pipe.

### 3.5.1 Flow Through an Annuli

The method of modelling flow through an annuli is very similar to that of a circular pipe, described in section 3.4.1.3. Using the hydraulic diameter concept, friction coefficients for concentric annuli lie within a factor of about 1.05 of those for a normal pipe.

$$f_{annular} = 1.05 f_{circular} \quad (3.17)$$

The hydraulic diameter is given by  $(D_2 - D_1)$ , where  $D_1$  and  $D_2$  are the inner and outer annulus diameters, respectively. To allow for eccentricity, correction factors are applied to Equation 3.3, which are obtained from graphical data by Miller (1990). This data is shown in Figure 4.8.

### 3.5.2 Heat Transfer in an Annuli

Annular pipes were included for the express purpose of representing the oil flow through the chain tensioners. The heat transfer process between the cylinder, the piston, and the oil, is of a complex nature for this type of component. To simplify the model, the heat transfer calculations used for an annular pipe were similar to those of a circular pipe, as detailed in section 3.4.2.



### 3.6 Oil Pumps

The oil pump fitted to Jaguar engines is of a gear pump design similar to that shown in Figure 3.9. Gear pumps are positive displacement pumps which are ideal for the pumping of lubricating oil, as the pumping fluid provides the required lubrication. In addition, the relatively high viscosity of oil assists in reducing leakage.

The AJ6 engine oil pump characteristics were obtained from pump test bed measurements at Jaguar in 1980 and are shown in Figure 4.1. The V8 engine pump characteristics were provided by the pump supplier. The AJ6 engine pump was driven at a pump speed to engine speed drive ratio of 0.636:1. For the V8 engine this ratio was 1:1.

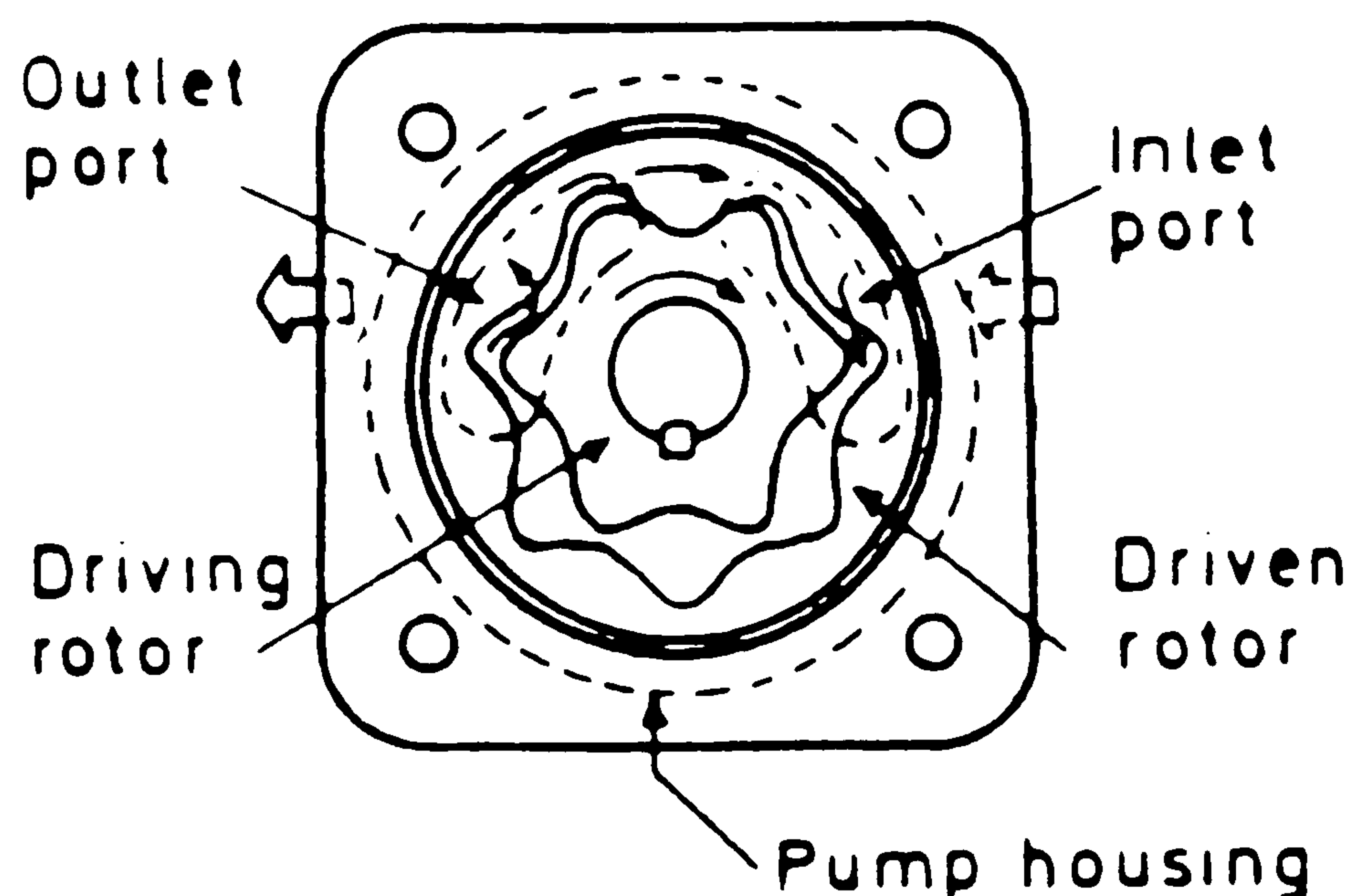


Figure 3.9. Oil gear pump design

Each oil pump characteristic curve is comprised of two distinct regions. This is demonstrated in a simplistic form in Figure 3.10. As the pump is of a fixed displacement type, the output characteristics would normally lie somewhere along the line in region 1. Under ideal conditions the line would be vertical, but the deviation is attributed to leakage past the rotor face.

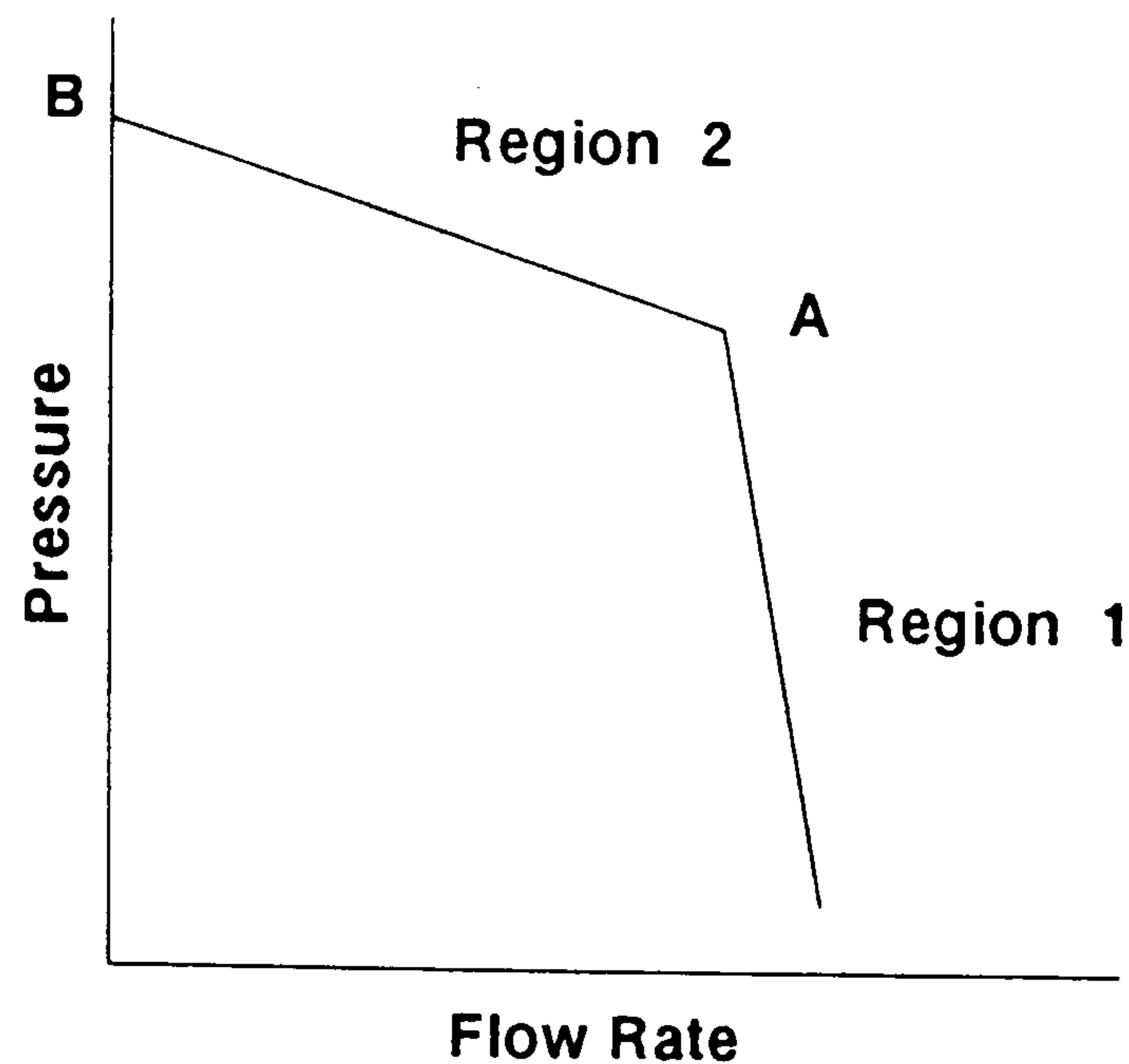


Figure 3.10. Ideal oil pump characteristics

Of course, the linear pressure rise in region 1 can not be allowed to continue indefinitely otherwise a theoretically infinite pressure will be achieved if the oil flow was in some way blocked. Therefore, the oil pump incorporates a pressure relief valve which starts to 'crack open' when the pressure reaches point A. The flow above pressures at point A follow the characteristics of region 2 up to point B. Here, the maximum oil pressure is reached, and all the oil flow is by-passed through the relief valve back to the input side of the pump.

It was assumed that heat transfer within the pump was negligible compared to the rest of the flow network. This assumption was made following the simple calculation of the energy required to drive the pump. This calculation is included in Appendix D.1.

### 3.7 Oil Strainers

A typical engine lubrication system contains two levels of oil filtration. The first level is the 'coarse' filtering of the oil before it is drawn into the oil pump. This filtration stage is intended to remove any 'large' particles or debris,

which may have collected in the sump. The oil strainers fitted to Jaguar engines strain the oil through a round wire square mesh.

The pressure loss through a round wire square mesh can be calculated using a method developed by Annand (1953). It is assumed that the flow of oil is at an angle of incidence of 90° to the plane of the mesh. The pressure loss is dependent on the porosity of the mesh. The porosity is the ratio of the projected free area of the wire gauze to the cross-sectional area of the duct in which the gauze is placed. The porosity,  $\lambda$ , of a woven screen of square mesh composed of wire strands of diameter,  $d$ , with  $m$  wires per unit length, is given by:

$$\lambda = (1 - md)^2 \quad (3.18)$$

The pressure loss can then be calculated from:

$$\Delta P = K \frac{\rho U^2}{2} \quad (3.19)$$

Where

$$K = K_{\infty} \times \left( \frac{K}{K_{\infty}} \right) \quad (3.20)$$

The parameter  $K/K_{\infty}$  is obtained from graphical data (see Figure 4.9) and the pressure drop coefficient,  $K_{\infty}$ , is found from an empirical correlation by de Vahl Davis (1964):

$$K_{\infty} = \left( \frac{1 - \phi \lambda}{\phi \lambda} \right)^2 \quad (3.21)$$



A full description of the mathematical model derived to represent the flow characteristics through an oil strainer, is given in section 4.5. As the oil strainer remains immersed in the oil in the sump, the heat transfer within the strainer was considered to be negligible, and was ignored.

### **3.8 Oil Filters**

The second filtration stage is usually carried out after the pump. Due to space constraints the pump is usually housed within the body of the engine, while the oil filter is positioned on the outside of the engine block for easier access during servicing. A filter is required in a lubrication circuit to remove foreign matter exceeding the thickness of the oil film separating the moving parts (Nostrand (1975)).

Jaguar engines utilise full flow oil filter systems, the filter being of a pleated paper construction (see Figure 3.11). A pressure relief valve is included within the filter canister which starts to 'crack open' when the pressure difference across the filter element reaches approximately 0.9 bar. No pressure loss v flow rate characteristics were available for the oil filters used by Jaguar. The pressure loss is calculated using empirical equations published by Jaisinghani and Sprenger (1981). These equations were derived for viscous oil flow through a new, uncontaminated, filter element. No data was found for the prediction of pressure losses through contaminated filter elements.

### **3.9 Engine Bearings**

Plain, fluid film lubricated journal bearings are widely used in automobile engines. Their function is to support rotating parts and transfer loads between components. A journal bearing essentially consists of a bearing

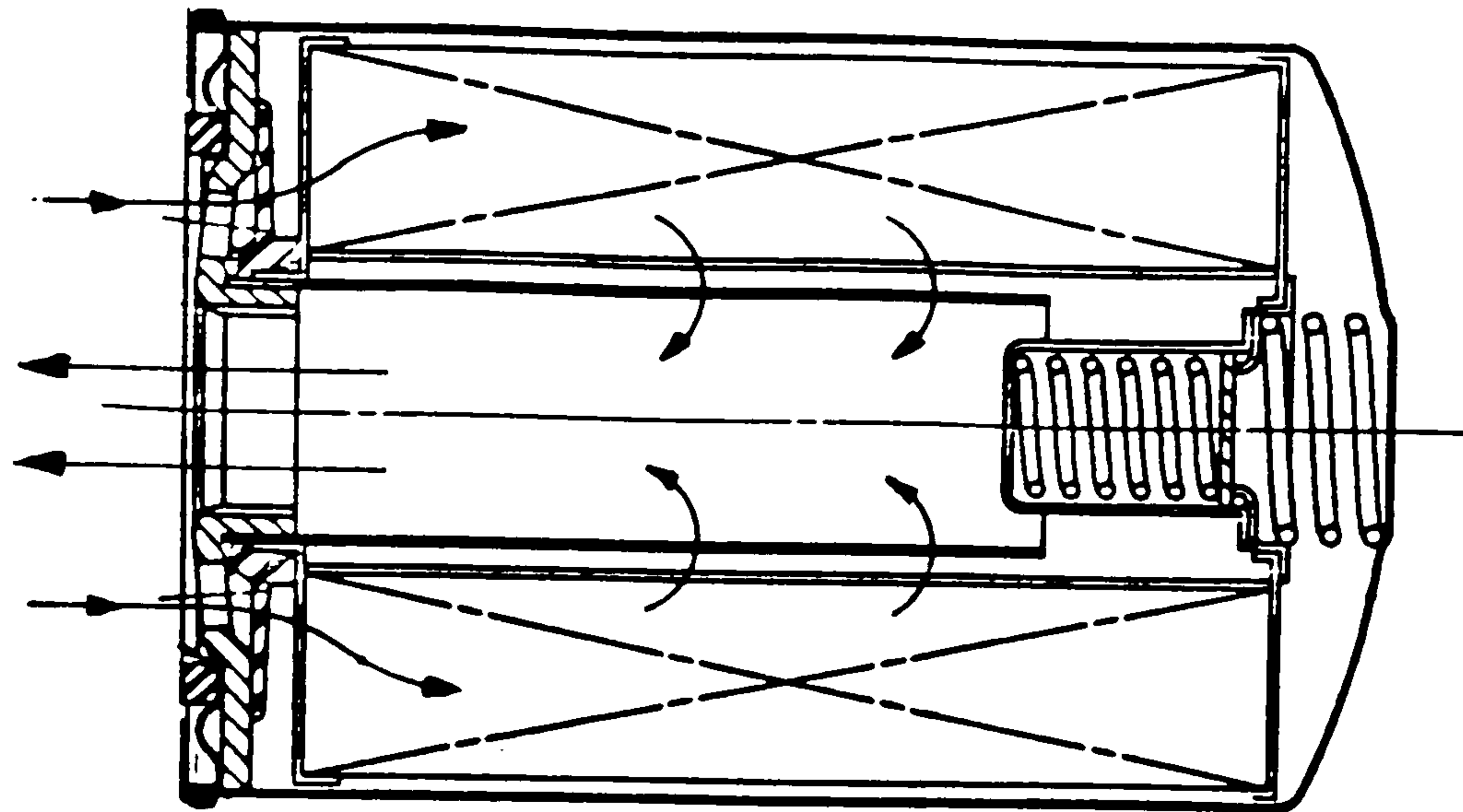


Figure 3.11. AJ6 engine oil filter

shell seated between a rigid housing and a rotating shaft. Lubricant is supplied through a groove or hole, and is drawn into the bearing by the relative motion of the surfaces.

A detailed description of the four different types of lubrication conditions; hydrodynamic, thin film, boundary, and dry, is given in Appendix B.5. Journal bearings are designed to operate in the hydrodynamic regime. Hydrodynamic pressure is generated within the oil in the bearing to balance the applied load.

### 3.9.1 Oil Supply

There are different methods of supplying oil to a bearing. The main oil supply methods are; pumped, pumped oil mist, gravity, capillary systems, and dipping systems. For plain journal bearings oil mists, capillaries, and gravity feeds are unlikely to provide sufficient flow rate. In Jaguar engines, all the journal bearings have a pumped oil supply apart from the gudgeon pins, or 'small-end bearings', in the pistons. The small-end bearings are lubricated by

the same method as the piston rings and liners. This is achieved by a combination of oil splash and oil mist, generated primarily by oil thrown out of the big-end and main bearings.

### 3.9.2 Steadily Loaded Journal Bearings

The basic operating principle of a steadily loaded journal bearing (SLJB) is shown in Figure 3.12. The lubricant is drawn into the region between the moving parts of the bearing, and a hydrodynamic pressure is generated within the fluid which keeps the bearing surfaces separated. Consider the geometry of the mutually eccentric circles of similar diameter shown in Figure 3.12, which represents a SLJB. In this diagram the outer circle of radius  $OE$ , equal to  $R_1$ , represents the bore of the journal bearing shell. The inner circle of slightly smaller radius  $CF$ , equal to  $R_2$ , represents the periphery of the rotating circular shaft. The shaft is rotating clockwise with a peripheral velocity  $U_0$  within the journal bearing. The eccentricity between the shaft and the journal bearing is represented by the distance,  $e$ , between the centre of the journal  $O$  and the centre of the shaft  $C$ . The straight line  $EOCF$  is known as the 'line of centres'.

In an operating hydrodynamic journal bearing, the space between the two surfaces is filled with a fluid, and  $h$  corresponds to the varying film thickness in the bearing.  $R_1 - R_2$  is recognised as the uniform radial clearance,  $c$ , between the bearing and the shaft. The ratio  $e/c$  is known as the 'eccentricity ratio',  $\epsilon$ , a dimensionless parameter which describes the shape of the fluid film between the surfaces of the journal bearing and shaft.

The existence of the combined 'convergent-divergent' geometry of the film shown in Figure 3.12, produces a circumferential hydrodynamic pressure



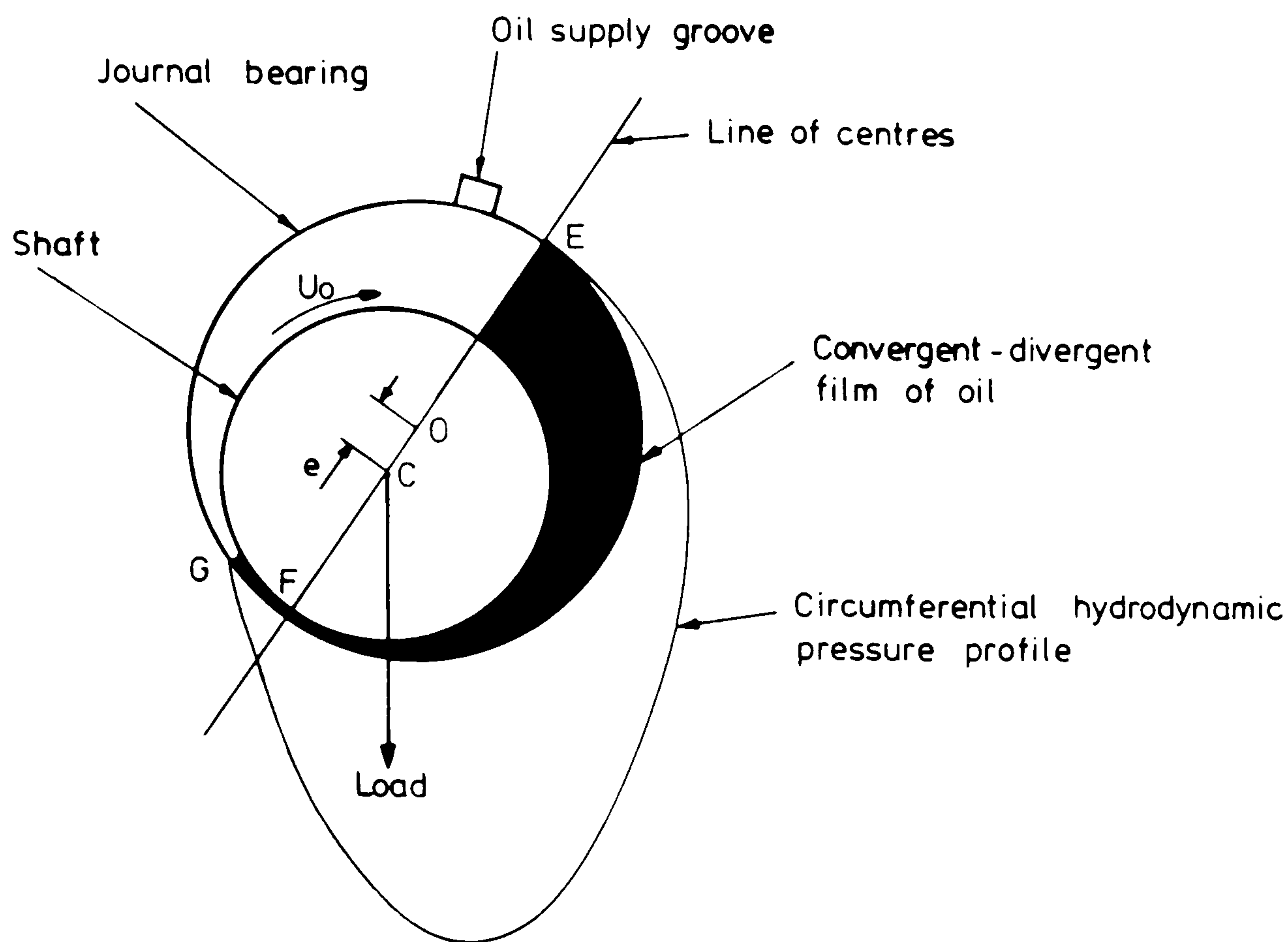


Figure 3.12. Operation of a hydrodynamic journal bearing

profile. In addition, as most bearings have an axial length,  $b$ , which is usually less than their diameter, a flow of liquid occurs in the axial direction. Therefore pressure profiles of the shape given in Figure 3.13 exist in the axial direction.

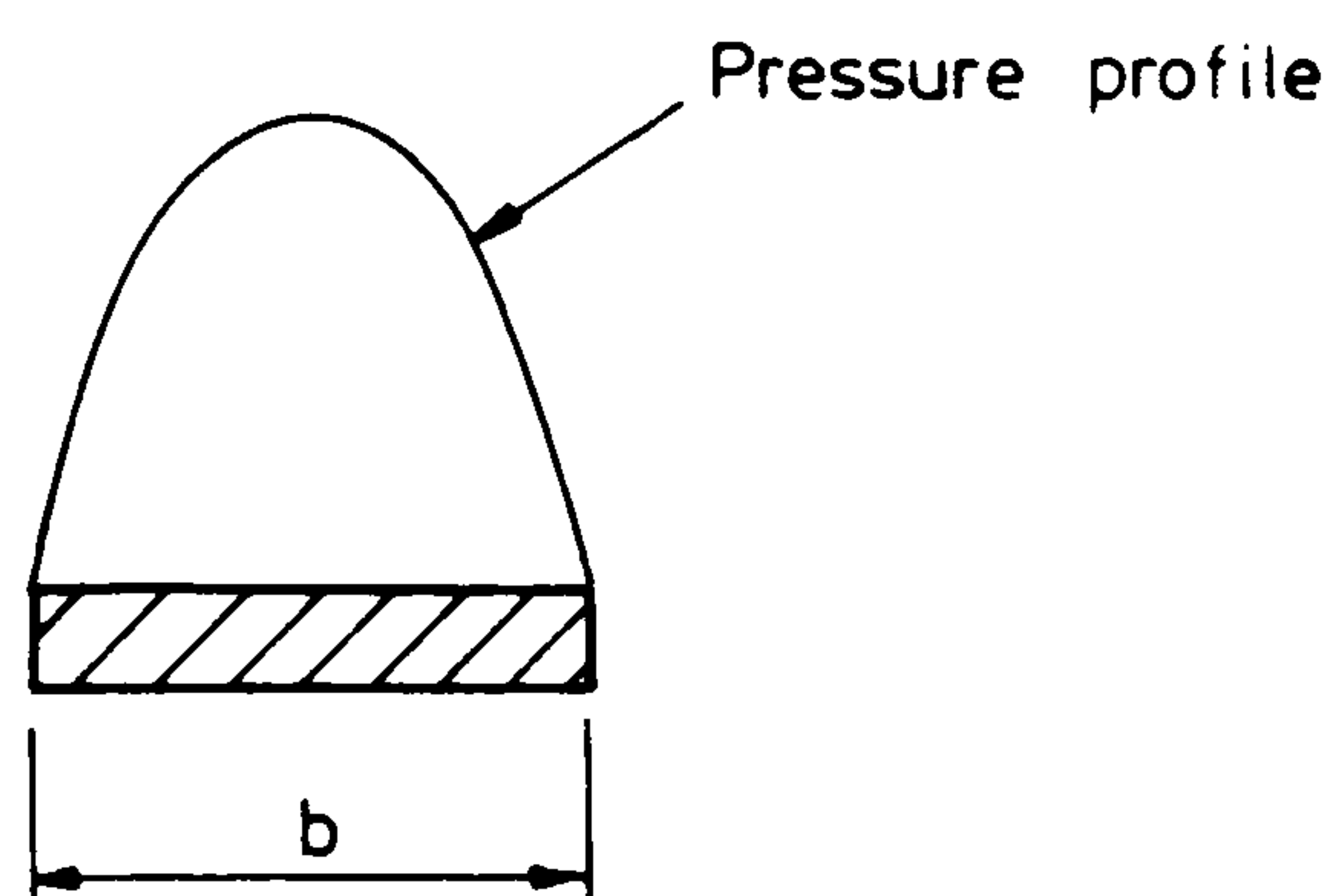


Figure 3.13. Axial hydrodynamic pressure profile

Some of the fluid which is drawn into the converging section flows completely through the bearing to emerge at G (see Figure 3.12). However, complete recirculation of the fluid does not occur, as some fluid can escape from the bearing by flowing in the axial direction. It is necessary to continually

replace the fluid which escapes in the axial direction by introducing replacement fluid into the bearing.

Oil behaviour within the bearing is further complicated by sub-ambient pressures generated within the divergent section. When the oil pressure falls below the saturation pressure, dissolved gases are emitted from the solution. In addition, air will be drawn into the bearing from the surrounding atmosphere. This phenomenon is known as gaseous cavitation (Lai (1993)). The second, but less common form of cavitation is vaporous cavitation. This occurs when the lubricant pressure drops to the vapour pressure. Boiling of the lubricant will occur and vapour will form within the oil film.

The occurrence of cavitation markedly affects the hydrodynamic performance of a journal bearing. Gas and vapour cavities will collapse almost instantaneously if the journal shifts orbit and hydrodynamic pressure rises. This can result in serious erosion damage to the bearing and the journal surface. A proper consideration of cavitation is essential in the design of fluid film lubricated journal bearings. The onset of cavitation is suppressed by careful positioning of oil feed grooves and maintaining a sufficient oil supply pressure and oil flow rate to the bearing. Modelling the phenomenon of cavitation was considered to be outside the scope of this study. However, it can be seen that the prediction of the bearing feed pressures and oil flow rates are essential at the design stage, to ensure the suppression of cavitation.

Engine bearings, such as crankshaft main bearings, big end bearings and camshaft bearings, experience dynamic loading. The load magnitude and direction are a function of time. Consequently, instead of taking up a fixed location, the journal will orbit within the clearance space. The first step towards analyzing a dynamically loaded bearing is the prediction of the journal

orbit. With this established, the minimum oil film thickness, the power loss and oil flow rate can be determined.

Booker (1965) developed the 'Mobility Method' for predicting the journal centre orbit in a dynamically loaded situation. In this method, the motion of the shaft is determined by balancing the generated hydrodynamic force with the externally applied load.

It is apparent that the dynamic behaviour of a journal bearing is extremely complex. Mobility analysis of the bearings within an engine lubrication system would be very time consuming in both programming and computer run time. Therefore, it was considered to be outside the scope of this study. The primary objective of the lubrication system simulation model was to provide a design tool for the rapid analysis of the whole engine lubrication system. For this reason, the journal bearings were considered to be steadily loaded.

### **3.9.2.1 Supply Grooves**

Fluid may be introduced into a bearing through various configurations of supply grooves. The principal positions for the supply grooves, which are adopted in many journal bearings, are shown in Figure 3.14. The basic principle is that the larger the oil supply groove the better the oil delivery to the bearing. Unfortunately the presence of an oil groove in the bearing surface affects the hydrodynamic pressure profile and reduces the load carrying capacity of the bearing. For this reason, bearings of different oil supply groove configurations are used for the various load conditions experienced throughout an automotive engine.



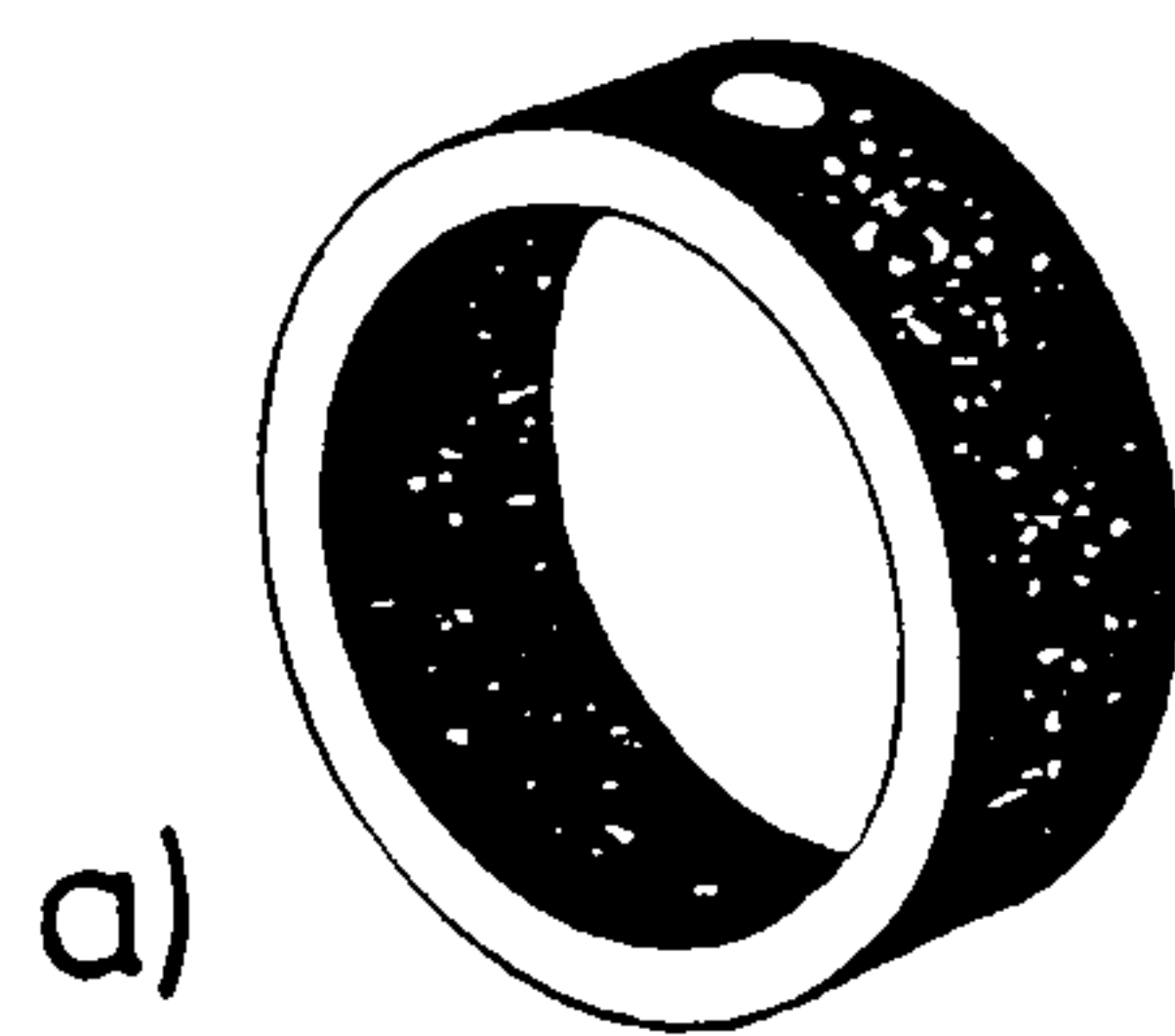
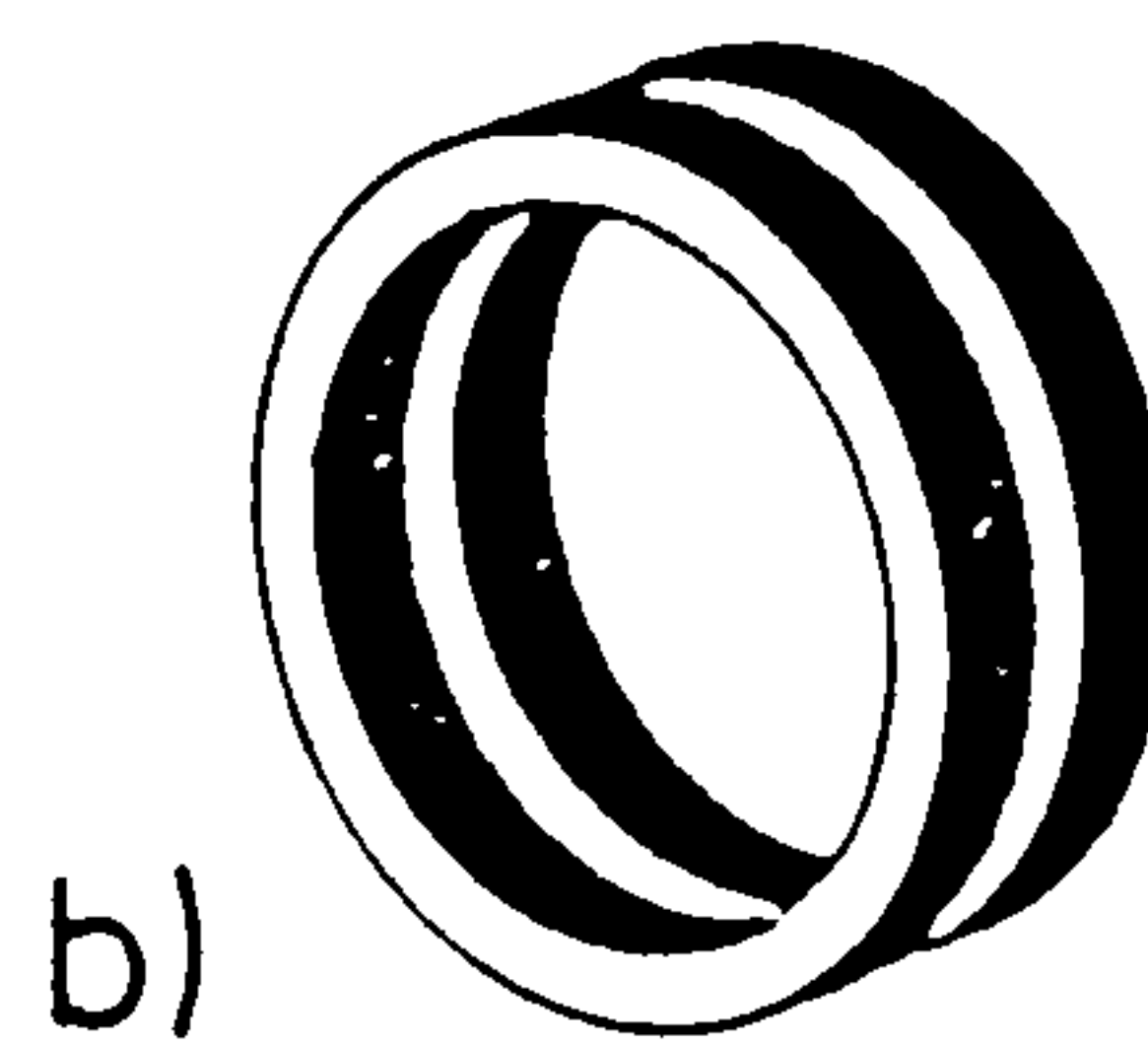
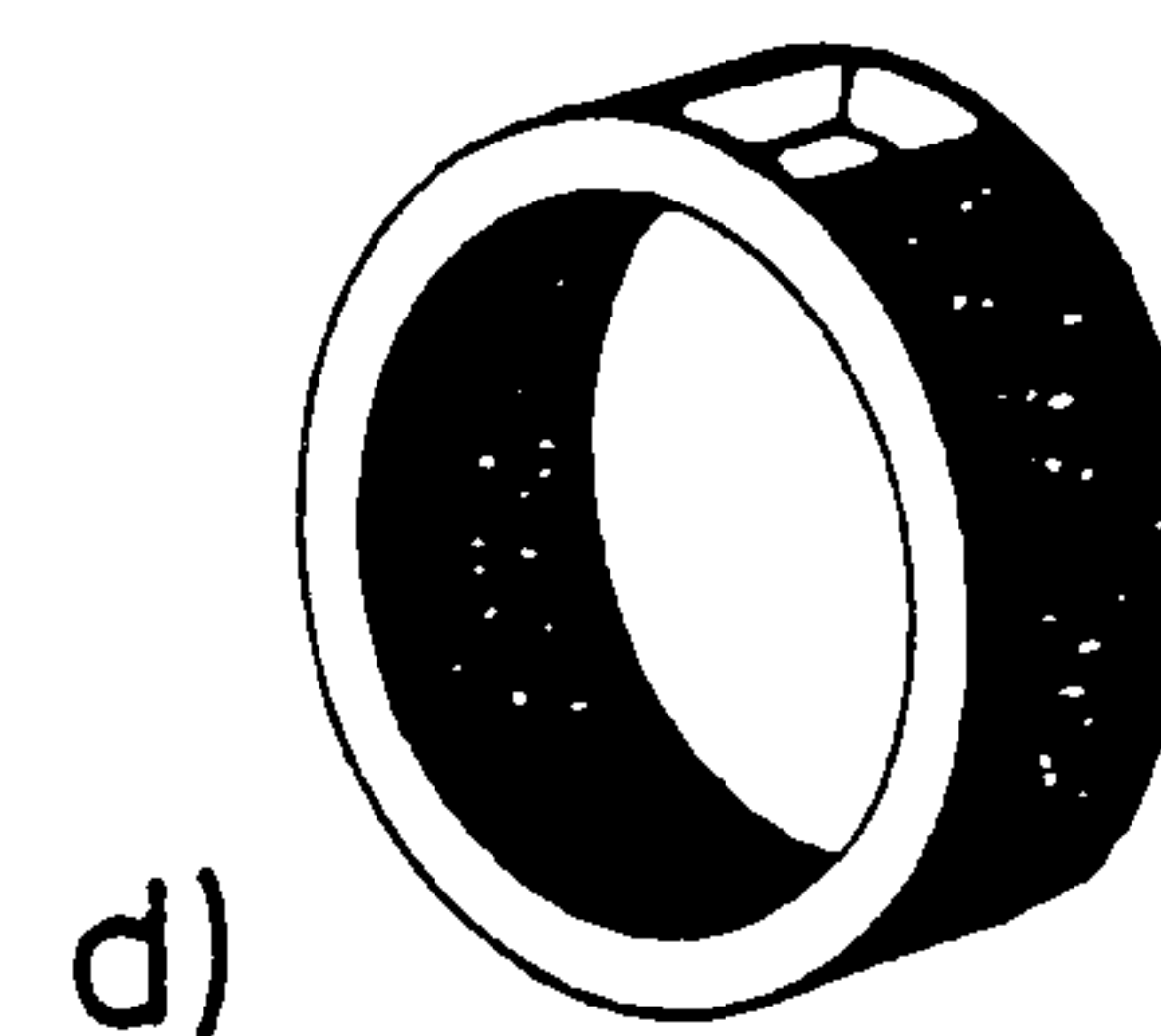
SINGLE  
CIRCULAR  
OIL HOLECIRCUMFERENTIAL  
GROOVE (360°)RECTANGULAR FEED  
GROOVE (LARGE  
ANGULAR EXTENT)RECTANGULAR  
FEED GROOVE  
(SMALL ANGULAR  
EXTENT)

Figure 3.14. Common supply groove positions

The provision of a single circular hole in a bearing, as shown in Figure 3.14(a), represents the simplest form of grooving. The presence of a complete circumferential groove of the type shown in Figure 3.14(b) allows loads to be applied in any direction and accepts shaft rotation in both directions. However, the load capacity of the bearing is reduced as the groove disturbs the hydrodynamic pressure profile of the 'plain surface'. A variation of this arrangement is shown in Figure 3.14(c), a partially grooved bearing which accepts shaft rotation in either direction provided the loads are applied in the non-grooved portion. Figure 3.14(d) illustrates the general arrangement of a rectangular groove in its basic form. Bearings equipped with only a single rectangular groove are not suitable for shafts which are able to rotate in both directions or for loads which vary significantly in direction.

The majority of journal bearings used in Jaguar engines are of the single circular supply hole construction. The exception is the crankshaft main

bearings, where all but one of the bearings have a  $180^\circ$  circumferential groove. The principal reason for this is to aid the oil transfer to the drillings within the crankshaft. These drillings transfer oil through the crankshaft to the big-end bearings. The  $180^\circ$  circumferential groove gives  $180^\circ$  registry between the oil supply in the groove and each drilling within the journal. The centre main bearing does not transfer oil to a big-end bearing, and therefore, has a simple circular oil supply hole.

Oil supply to the camshaft bearings is provided by a simple oil supply hole. In the AJ6 engine the camshaft bearing is supplied with oil from a drilling running down the centre of the entire camshaft. In turn, this central feed hole is supplied with oil by oil transfer through the first camshaft bearing, in a similar manner to that employed in the transfer of oil through the main bearings to the big-end bearings. The first bearing on each camshaft of the AJ6 engine is of a similar design to the main bearings, and has a  $180^\circ$  circumferential oil supply groove. The oil supply to the camshaft bearings on the V8 engine is of a more simple design. The oil is supplied through a simple oil supply hole, from an oil gallery running through the head.

The equations used to represent the pressure loss v flow rate relationships for the various bearings were recommended by Glacier Vandervell, the bearing suppliers to Jaguar. These equations were presented in a paper by Martin and Lee (1982), and were shown to predict hydrostatic flow rates reasonably accurately. The equations ignore hydrodynamic pumping effects and assume steadily loaded bearing conditions. However, as discussed in section 2.5.1, the results from these equations were found to compare favourably with measured values from engine tests. The equations are discussed in detail in section 4.7.

### 3.9.3 Heat Transfer in Journal Bearings

Heat transfer to the lubricant in a bearing is directly related to the power loss within the bearing. Major sources of power loss in engine bearings arise from; the shearing of lubricant; the work done on the lubricant due to hydrodynamic pressure flow, and the journal translation effect.

One of the most comprehensive equations for predicting bearing power loss was given by Booker et al (1982). This was presented in vector form and Martin (1985) rearranged it into algebraic form to make it more understandable. The expressions for instantaneous power loss due to shear, pressure and squeeze were presented. Martin found that over 90% of the power dissipation was due to shear.

It is clear that an iterative procedure is required for predicting the working temperature of the bearing. Given the input oil conditions, power dissipation due to film shear can be estimated, and new oil working properties can be calculated. Given these new oil working conditions, a new power loss can be calculated leading to refined values of oil properties. The iteration procedure will commence until an equilibrium condition is reached and the working temperature of the oil within the bearing is found.

Heat transfer to the oil within a dynamically loaded bearing was considered to be outside the scope of this study. However, an estimation of the working properties of the oil within a SLJB was made for the purpose of calculating the bearing flow characteristics in the initial flow model. A simple temperature rise model was derived from a method reported by Cameron (1981). This method is described in detail in section 5.3.1.



For the purpose of the heat transfer model, a more precise method was required that would account for mobility effects within a dynamically loaded bearing. This was achieved by using pre-prepared bearing 'maps' as input data for each engine bearing. The maps contained temperature rise data for a given engine speed and load condition, over a range of oil input temperatures and feed pressures. They were generated from an adapted bearing mobility analysis model, developed for Jaguar by Lai (1993).

### **3.10 Crankshaft and Camshaft Oil Transfer Holes**

The transfer of oil to the central drilling of the camshaft of the Jaguar AJ6 engine is by a similar mechanism to that employed within the crankshaft. For this reason this section will only refer to the mechanism of oil transfer to the crankshaft. However, the points discussed are equally relevant to oil transfer into and out of the camshaft central supply hole. The equations discussed below were derived by Meernik (1986). They were determined from explicit correlations using data obtained from an oil flow test rig. Meernik suggests that in addition to the friction losses normally associated with the flow through a pipe, the oil flow is primarily controlled by bearing registry, centrifugal effects, and oil acceleration losses. The effects of these are described in the following sections.

#### **3.10.1 Registry**

Registry of bearing and crankshaft flow paths denotes that a reasonable flow passage exists between them. For example, a bearing with a full circumferential oil groove would have continuous registry. However, for a 180° partially grooved bearing, and only one oil transfer hole, the transfer hole experiences both periods of registry and non-registry (see Figure 3.15). During

non-registry the inlet flow to the transfer hole will be negligible.

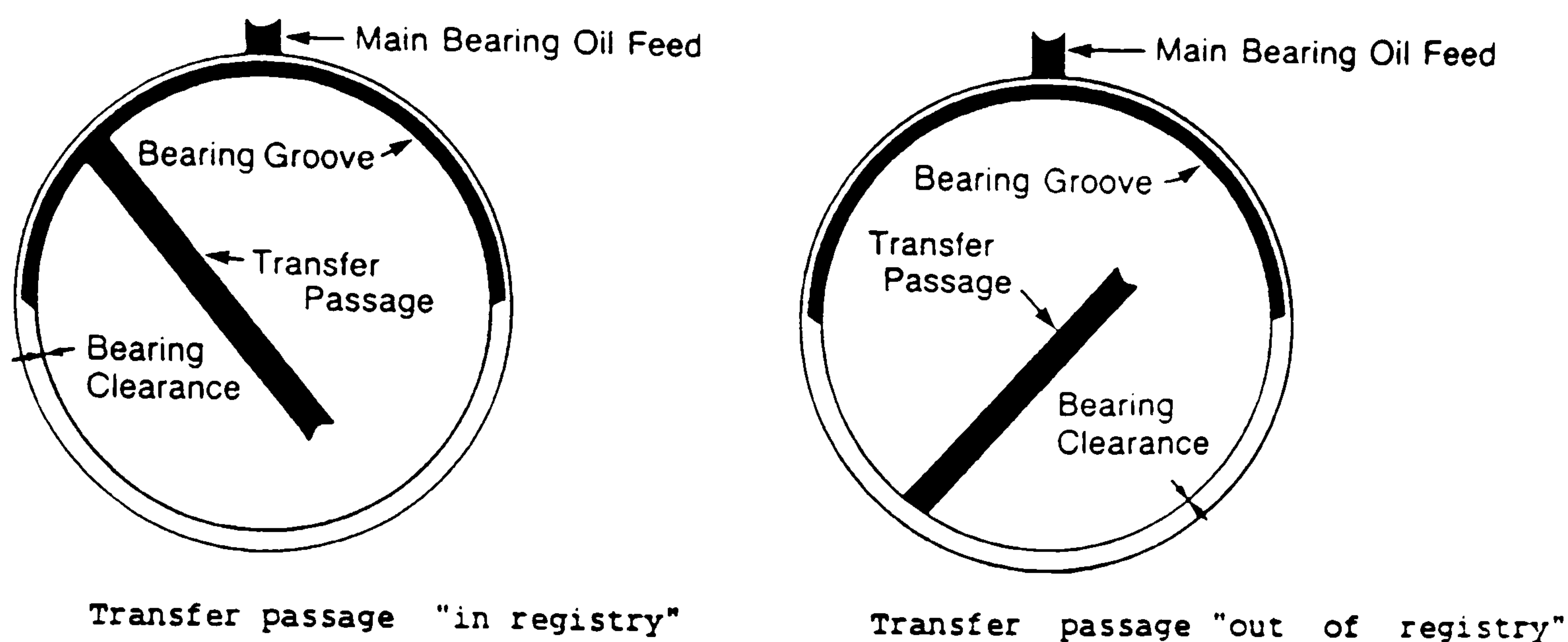


Figure 3.15. Transfer passage 'in' and 'out' of registry

The crankshafts on Jaguar engines are fitted with two transfer holes,  $180^\circ$  apart. The two transfer holes join to form a single transfer hole at approximately the centre of rotation of the crankshaft. The two transfer holes ensure almost continuous registry.

### 3.10.2 Centrifugal Losses

The typical crankshaft hole between the main bearings and the big-end bearings is a straight path. Functionally, however, it has two distinct sections. The region from the main journal surface to the point of closest approach to the crankshaft centreline, can be considered an entrance section. The centrifugal force in this region opposes the flow entering the hole. The remaining portion of the transfer hole functions as an oil reservoir and centrifugal pump, to feed the big-end bearings.

To push oil into the reservoir portion during crankshaft rotation, the centrifugal forces on the oil in the entrance section must be overcome. The necessary driving pressure to overcome this is:

$$\Delta P = \frac{1}{2}\rho\omega^2(r^2 - s^2) \quad (3.22)$$

### 3.10.3 Acceleration of Oil to Journal Surface Speed

Oil at the entrance to the transfer hole of the rotating journal has a kinetic energy per unit volume of  $\frac{1}{2}\rho(\omega r)^2$ . However, the oil in the bearing groove has essentially zero kinetic energy. For a typical journal with a simple transfer hole, there are two possible sources from which the required increase in energy can be obtained:

- i, Viscous shear originating from the journal surface.
- ii, Oil supply pressure.

The relative extent to which these sources are utilised depends on the oil contained in the bearing groove. If there is minimal or no oil flow, the thin layer of oil lying next to the journal, having been accelerated to nearly surface velocities by viscous forces, will be adequate to supply the small requirements. However, if an appreciable fraction of the groove volume is removed on each revolution, the oil supply must provide some of the energy required to accelerate the oil to journal surface speed. In the limiting case, due to either high oil flow rate and/or negligible viscosity, the oil supply provides virtually all the necessary energy. The resulting demand on pressure would be:

$$\Delta P = \frac{1}{2}\rho(\omega r)^2 \quad (3.23)$$



To counter the problems associated with having to accelerate the oil to journal surface speed, some journals are machined with lead-in grooves to the entrance to the transfer hole. However, none of the bearings in Jaguar engines have such a lead-in groove in the journals, and this element was not considered any further.

#### **3.10.4 Acceleration Losses**

If the bearing and journal geometry is such that there is any non-registry time, there will be a pressure loss associated with accelerating the oil already in the transfer hole each time flow is re-established. However, Meernik noted that for the theoretically worst case of a typical crank speed of 6000 rpm, and a driving pressure of 2 bar, it would only take  $3 \times 10^{-5}$  seconds, or about  $1^\circ$  of revolution, to accelerate the oil to a full flow rate of 10 ml/sec. This was assumed to be a negligible effect, and consequently acceleration losses were ignored.

### **3.11 Oil Coolers**

Under some engine operating conditions the temperature of the oil begins to rise above its desired working level. This leads to increased engine temperatures, high temperature conditions within the bearings, and a breakdown of the additives within the oil (see Appendix B.2 for a discussion of oil properties). The Jaguar V8 engine utilises an oil cooler in the lubrication system to cool the lubricant before it enters the engine.

### 3.11.1 Heat Exchangers

An oil cooler operates on the principle of exchanging heat between two different fluid streams without physically mixing them. In the case of Jaguar engine oil coolers, the two working fluids are the lubricant and the ambient air. In this case the oil is the 'hot' fluid and the air is the 'cold' fluid.

Ordinary heat exchangers may be divided into two general groups, depending on the relative orientation of the flow direction of the two fluid streams. The first group is reserved for orientations which allow the two fluids to flow in parallel directions. If both fluids enter at the same end and flow in the same direction as each other, the arrangement is termed a 'parallel flow' heat exchanger. If the two fluids flow parallel to each other but in opposite directions, the arrangement is termed a 'counterflow' heat exchanger.

The second group of heat exchangers comprise those in which the two streams cross one another in space, usually at right angles. This arrangement is termed a 'cross-flow' heat exchanger. An automotive oil cooler and cooling system radiator, are two examples of this type of heat exchanger.

### 3.11.2 Oil Flow Through an Oil Cooler

A typical oil cooler construction is comprised of an inlet manifold section which delivers oil to a series of flattened tubes, which converge into an exit manifold. The distribution of flow between branches depends on the following criteria:

- i, Length of the manifold, and hence friction losses.
- ii, Either, the ratio of the inlet velocity pressure of the manifold to the

losses in the branches or, the ratio of total branch area to manifold area.

Trends in flow distribution for constant area dividing manifolds are shown in Figure 3.16 and for constant area combining manifolds in Figure 3.17.

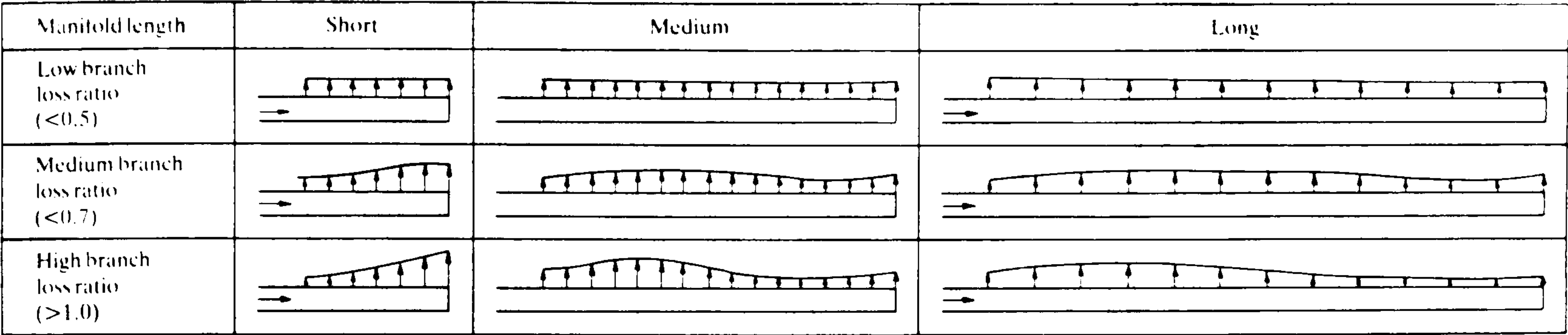


Figure 3.16. Flow distribution for dividing manifold

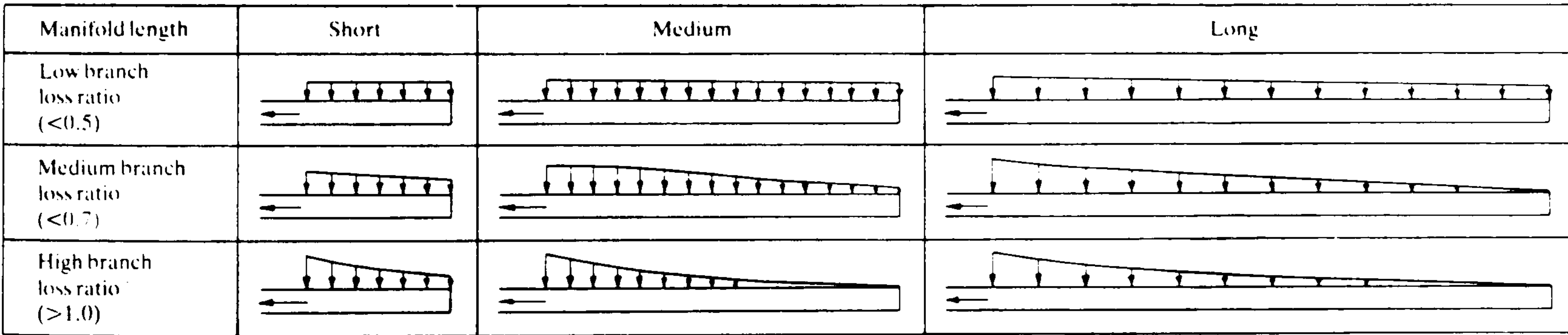


Figure 3.17. Flow distribution for combining manifold

The loss ratio in Figure 3.16 and Figure 3.17 can be defined as:

$$Loss\ ratio = \left( \frac{velocity\ pressure}{pressure\ losses\ in\ branches} \right) \text{ or } \left( \frac{total\ branch\ cross\ sectional\ area}{manifold\ cross\ sectional\ area} \right) \tag{3.24}$$



The oil cooler fitted to Jaguar engines has a manifold length to branch length ratio of 0.52 and a loss ratio of 0.5 (see Appendix D.4). It was assumed that the manifold could be considered to be 'short', with even flow distribution through the branches. When flow divides and recombines, the continuity and energy equations, along with estimates for junction loss coefficients, allow the flow distribution and pressure loss to be calculated:

$$Q_A = Q_B = Q_1 + Q_2 + \cdots + Q_n \quad (3.25)$$

$$\Delta P_{A-B} = \Delta P_{path\ 1} = \Delta P_{path\ 2} = \Delta P_{path\ n} \quad (3.26)$$

The pressure loss is a combination of both friction and junction losses. Under laminar flow conditions, the junction losses were considered to be negligible and the total pressure losses were due solely to friction. The equations used to represent the pressure loss v flow rate relationship for an oil cooler, were the same as those for a flow passage. These equations were documented in section 3.4.1.

### 3.11.3 Heat Transfer in an Oil Cooler

The oil cooler fitted to Jaguar engines is comprised of thin flat oil tubes. The area between the tubes is finned to aid heat transfer to the cooling air. Heat transfer to the oil within the tubes is assisted with the inclusion of a thin corrugated plate. For modelling purposes this arrangement was simplified to the cross-flow heat exchanger shown in Figure 3.18.

The temperature effects on the two working fluids for this type of heat exchanger are shown in Figure 3.18. Heat transfer in this arrangement is through forced convection to the fluids and conduction through the walls. Both fluid temperatures vary through the heat exchanger. There is no satisfactory

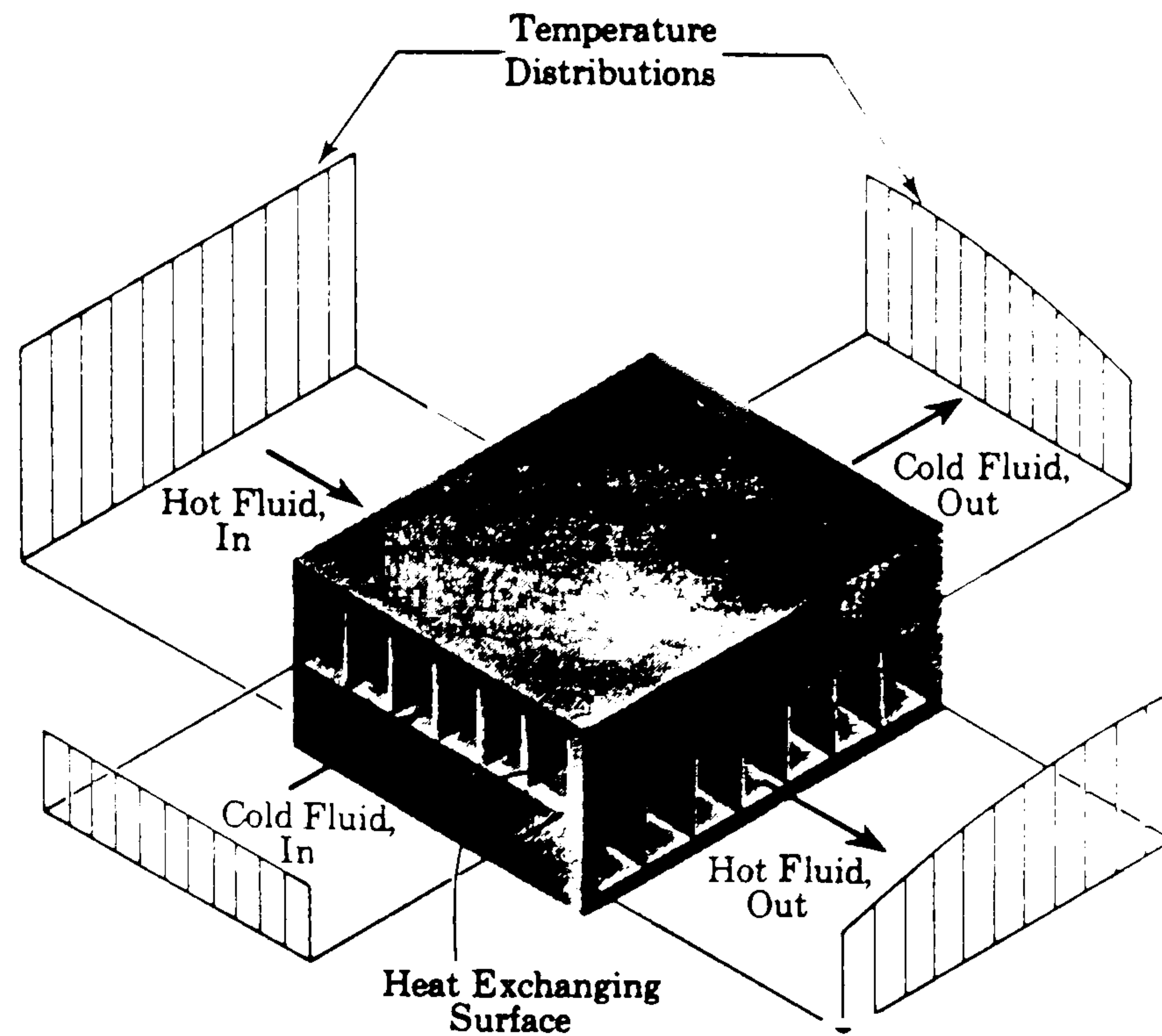


Figure 3.18. Temperature variation of unmixed fluids in a cross-flow heat exchanger analytical method available for the solution of this type of arrangement with two sets of finned surfaces. The chosen solution method utilises the concept known as the 'number of transfer units' (NTU) solution. This concept has been developed extensively by Kays and London (1964), for a range of plate and fin geometries.

For a given heat exchanger geometry with known hot and cold fluid inlet conditions, the heat transfer coefficients on the hot and cold side can be calculated. This is achieved by an iterative procedure following an initial selection of 'trial' values for the hot and cold fluid exit temperatures. The Reynolds number is based on the hydraulic diameter,  $D_h$ :

$$D_h = \frac{4 \times \text{flow area}}{\text{wetted perimeter}} \quad (3.27)$$

and the mass velocity,  $G$ :

$$G = \frac{\text{mass flow rate}}{\text{flow area}} \quad (3.28)$$

Thus the Reynolds number is expressed as:

$$Re = \frac{D_h G}{\mu} \quad (3.29)$$

Given the Reynolds number, the parameter  $(h/Gc_p)Pr^{2/3}$  can be found from graphical data for the required plate-fin geometry. The heat transfer coefficient,  $h$ , can be then extracted. The process continues with the calculation of the NTU, the capacity ratio,  $C_R$ , and the 'effectiveness',  $\epsilon$ , of the heat exchanger. The outlet oil temperature can then be found from the solution of the equation:

$$\epsilon = \frac{t_{hin} - t_{hout}}{t_{hin} - t_{cin}} \quad (3.30)$$

A full description of this process, and the equations and graphical data used, is given in section 5.4.

### 3.12 Piston/Liner and Valve Train Lubrication

The pistons and liners are lubricated by the same process that lubricates the small-end bearing in Jaguar engines. Lubrication of these items relies on a combination of oil splash from the crankshaft and oil mist within the engine block. These are two areas which have been classed as 'grey areas'. No evidence was found of any past research into the measurement or prediction of the amount of oil which is deposited on to the surfaces of these components. In addition, little research has been carried out into the analysis of the chemical composition of this oil. It is possible that the oil mist in particular could contain an amount of water, fuel, and combustion products. Little is known about the possible effect these contaminants have on the heat transfer between



the oil mist and the engine surfaces. The calculation of the heat transfer to the oil is further complicated by the scraping effect of the piston as it moves down the liner on every stroke. The scraping effect not only removes oil, but transfers heat to the oil film through friction.

The valve train is lubricated solely by the oil which has flowed out of the camshaft bearings. The amount of oil which is deposited on to the valve train could be assumed to be the total oil flow to the head. However, no evidence was found that any author had attempted to analyze the complicated oil flow paths across the head of the engine, or predict the heat transfer to this oil.

None of these fields were directly concerned with the pressurised oil feed side of the lubrication system model, but were considered to be of utmost importance to the heat transfer model.

3.12.1 Heat Transfer under the Piston

Stotter (1966) compared heat transfer coefficients between the oil and the piston under-crown surface, for four types of oil cooling conditions. The results are shown in Table 3.1.

Oil Cooling Method	Heat Transfer Coefficient (W/m <sup>2</sup> K)	
	Minimum Value	Maximum Value
No direct oil supply to the piston.	245	327
Cooling due to oil emerging from the small-end bearings	2126	2780
Oil jet directed at under-crown surface	4088	8994
'Cocktail shaker' piston	2044	2944

Table 3.1. Heat transfer coefficients for piston oil cooling (Stotter)

When no oil is specifically directed at the piston under-crown, the heat transfer coefficients remain low. Stotter reported that for the test engine used in his study, the inside surface of the piston crown remained 'dry' under these conditions. Heat was transferred to the air and the oil, which was either in the form of a vapour or a fine mist.

For the purpose of this study, the piston under-crown oil conditions were estimated from observations made during engine testing by Jaguar. Jaguar reported that during an engine test which used a 'glass sided' engine, the oil was observed to flow out of the big-end and main bearings in the form of a sheet. This sheet of oil was reported to spray out of the sides of the bearings uniformly around the circumference. As such, it was independent of the crank angle and piston motion.

The under-crown oil conditions are, therefore, a combination of oil mist and oil spray from the main and big-end bearings. The value for the heat transfer coefficient was expected to lie somewhere between the value for no oil impingement and that resulting from the spray from the small-end bearings. The heat transfer coefficients for these conditions were suggested by Seale and Taylor (1970), and are shown in Table 3.2.

Oil Cooling Method	Heat Transfer Coefficient (W/m <sup>2</sup> K)		
	Min. Value	Max. Value	Average Value
Oil Splash	1172	1172	1172
Oil Jet	2051	3223	2637
Cocktail Shaker	-	-	1406

Table 3.2. Heat transfer coefficients for piston oil cooling (Seale and Taylor)

### 3.12.2 Heat Transfer on the Liner

In an attempt to model the heat transfer to the oil sprayed onto the liner, the lubricant condition was simplified to that of a falling liquid film. This approach is based on the falling liquid film cooling theory developed by Nusselt (1923<sub>a</sub>). The theory assumes that the fluid film is in laminar flow and that the effect of inertia of the fluid is negligible compared with the effect of friction. Thus, no oil acceleration occurs, but equilibrium exists between the weight of the liquid and the frictional force. Since the thickness of the film does not change, the velocity of the liquid element depends only on the distance from the wall, and not on the vertical distance from the top of the wall.

A more recent and general theory, covering laminar and turbulent films, was developed by Dukler and Bergelin (1952). The equations of Nusselt were confirmed up to a Reynolds number of approximately 1000, even in cases where waves were visible at the gas-liquid interface. Wave motion may start at Reynolds numbers as low as 25, but it does not disturb the laminar motion up to a Reynolds number of 1000. The Reynolds number for this situation is defined as:

$$Re = \frac{4 \dot{m}}{\mu C_w} \quad (3.31)$$

where  $C_w$  is the width of the fluid film.

It was found that typical values for the Reynolds number in this application were in the order of about 10 (see Appendix D.2). The assumption of laminar flow in the fluid film, and the use of Nusselts theory, is therefore justified. A detailed description of the equations used to predict the heat transfer coefficient of the oil film is given in section 5.5.2.1.



### **3.12.3 Heat Transfer on the cylinder head**

The heat transfer mechanism between the oil and the components on the engine head, is not fully understood. The oil which is thrown from the camshaft bearings experiences a variety of temperature sources. These include; the cams, the valve stems, the cam followers, and the body of the cylinder head.

Heat transfer to this oil was accounted for by simplifying the oil flow to that of a falling fluid film. The same approach was taken as that used for the heat transfer to the liner. The complicated flow path on the head includes 'pockets' in which the oil can lie. This can be accounted for by adjustment of the value of the contact surface area (see the listing of the data file 'v8bloc.fil' in Volume II, for the values used to model the V8 engine head)

### **3.12.4 Prediction of Engine Surface Temperatures**

For the calculation of the heat transfer to the oil splash and spray, the contact surface temperatures must either be fixed, or calculated simultaneously, to ensure thermal stability. The approach taken was to develop a model for the simulation of the oil and metal temperatures through a cross-section of a representative piston/cylinder/block arrangement. An example of such an arrangement, where the piston is assumed stationary at its mid-stroke position, is shown in Figure 3.19. The model is not inherently restricted to one cylinder, but cylinder-to-cylinder differences are usually sufficiently small to have a negligible effect on the temperature predictions. A similar approach was taken by Shayler et al (1993).

The engine section shown in Figure 3.19 can be represented as a thermal system which is governed by heat convection and conduction. The



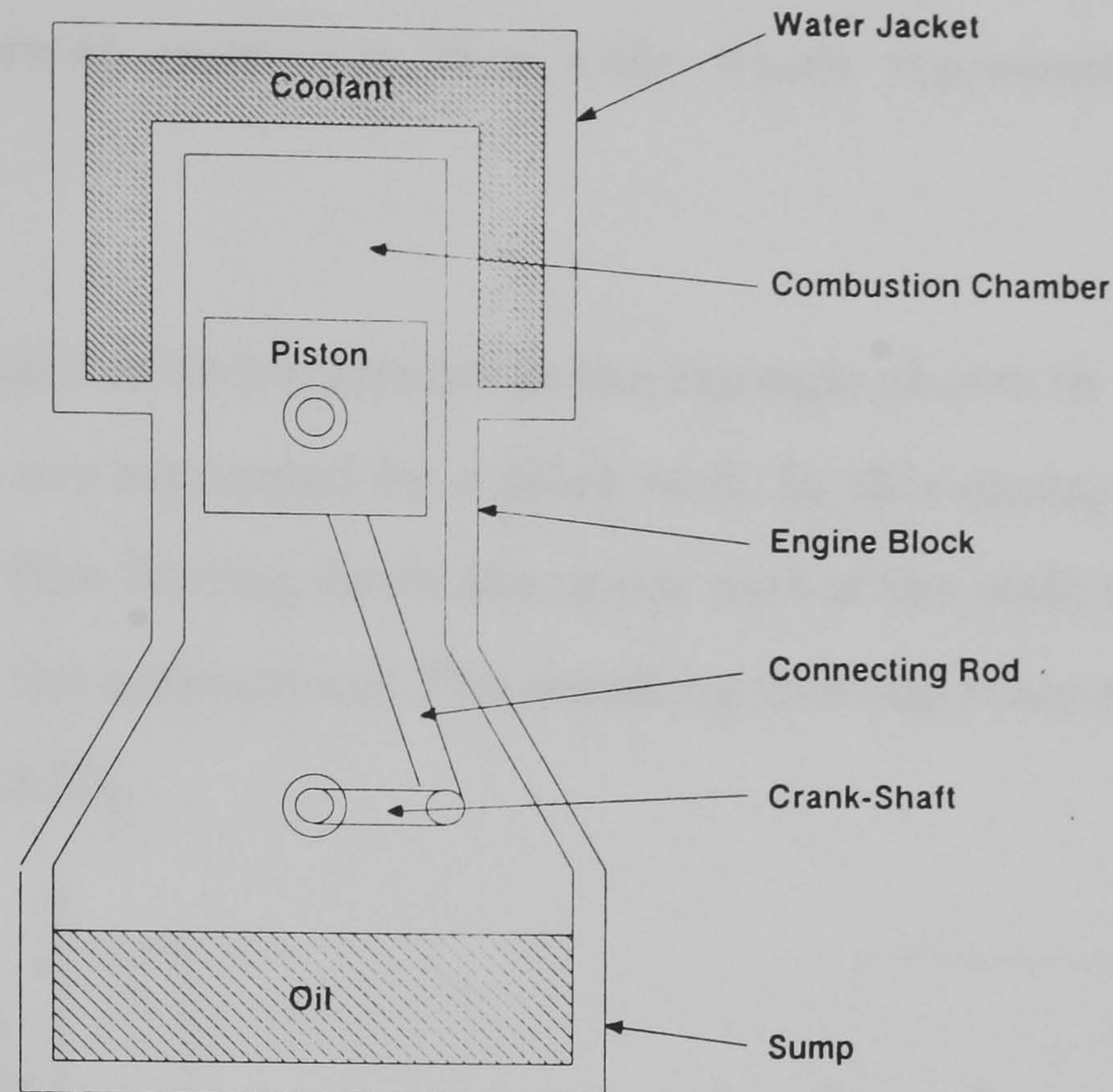


Figure 3.19. Simplified engine arrangement

approach taken was similar to that documented by Chapman (1987). By taking a suitable cross-section through the engine, the model can be further simplified by analyzing the required heat transfer paths in only two dimensions.

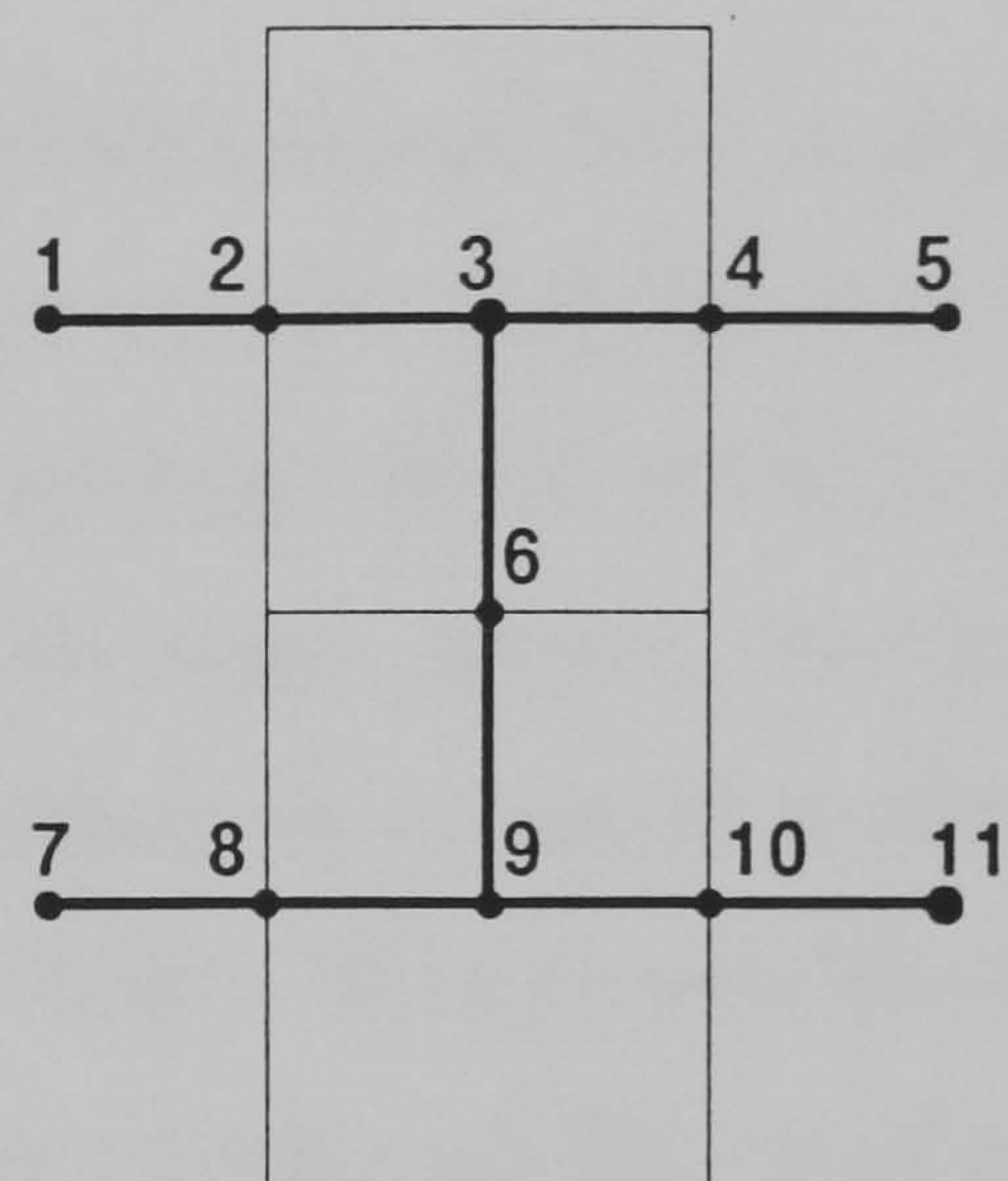
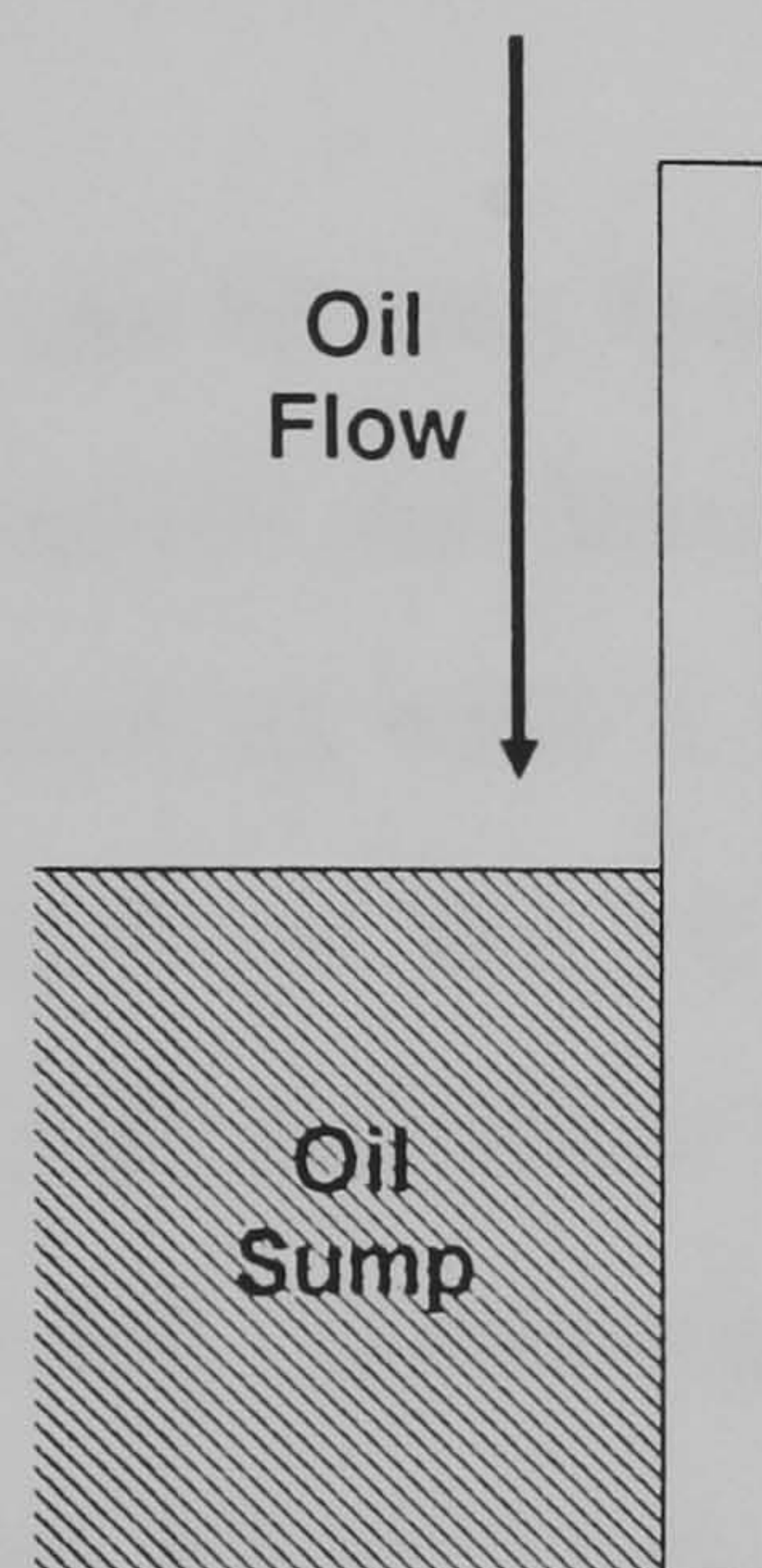
The thermal system consists of several different fluid circuits which are separated by solid walls. The solid walls are represented by rectangular elements which are linked together to form a network. Each element has five representative temperatures, one at the centre of the element and one at each of the four surfaces.

Using an electrical network analogy, a thermal resistance network can be formed. Each node in the network represents a temperature, and a thermal resistance joins adjacent nodes. Each element is either joined to a neighbouring



element or it is subject to forced or natural convection. Therefore, the surface nodes of each element are either shared with the neighbouring element or are linked by a thermal resistance to a node which represents a bulk fluid temperature.

This approach is demonstrated in the example shown in Figure 3.20<sub>a</sub>, in which two fluids are separated by a solid wall. In this example the working fluids are; the oil film flowing down the upper part of the wall; the oil collected in the sump, and the ambient air. The resulting thermal resistance network is shown in Figure 3.20<sub>b</sub>.



- 1 - 2    Convection to Oil
- 7 - 8    Convection to Sump
- 4 - 5, 10 - 11    Convection to Air

Figure 3.20<sub>a</sub>. Example block arrangement.    Figure 3.20<sub>b</sub>. Resulting resistance network.

The expression which must be satisfied at each node,  $i$ , takes the form:

$$\sum_j \frac{t_j - t_i}{R_{ij}} + q_i = 0 \quad (3.32)$$



where

$$R_{ij} = \begin{cases} \frac{\delta_{ij}}{kA_{kij}} & \text{for conduction} \\ \frac{1}{h_{ij}A_{cij}} & \text{for convection} \end{cases} \quad (3.33)$$

In Equation 3.32,  $q_i$  represents the heat added at a node other than surface convection, ie. the heat flux necessary to maintain the node at the desired temperature. For the purposes of this study no internal heat generation will be considered, and the  $q_i$  term will be ignored.

It can be seen from Figure 3.20 that the oil temperatures in the falling film are solved simultaneously with the contact surface temperatures. The oil temperature at node 1, for example, is the average of the inlet and outlet temperatures of the oil film flowing down the upper section. The use of a separate inlet condition for the lower section allows new inlet oil conditions to be calculated. This accounts for a quantity of 'fresh' oil to be introduced from spray from the bearings. This fresh oil will mix with the oil film running down the upper section, resulting in a new oil flow rate and new oil inlet temperature conditions.

Under steady-state conditions, the oil in the sump can be calculated using a similar method. The only difference to the method used for the oil film is that the flow rate is the total flow rate through the lubrication system, and the inlet temperature conditions are calculated from every oil source.

### 3.12.4.1 Boundary Conditions

In addition to convection to the oil, the other boundary condition of interest to this study is that of convection to other boundary fluids. For simplicity, the temperatures of these fluids are assumed to be known. For a typical water cooled IC petrol engine, these boundary fluids are; the water in the cooling jacket; the ambient air; the air within the crankcase, and the combustion gases.

#### Convection to the Air

Estimation of the heat transfer to the ambient air is complicated by the uncertainty of the air flow conditions around the engine. At very low air velocities free convection can be assumed, but with increasing air speed, mixed and forced convection regimes are encountered.

For forced convection, only laminar flow conditions were considered, due to the relatively low air velocities encountered around the engine block, even at high vehicle speeds. Laminar flow can be assumed if the Reynolds number is less than  $5 \times 10^5$ . Jaguar suggested that under-bonnet air velocities were typically 20% of the vehicle speed. Using this assumption, air velocities were generally no greater than 7.1 m/s, which equates to a vehicle speed of 80 miles/hr.

The average Nusselt number for laminar flow over a flat surface is given by:

$$Nu = 0.664 Re^{\frac{1}{2}} Pr^{\frac{1}{3}} \quad (3.34)$$

where  $0.6 < Pr < 50$   
 properties at  $t_m$

For free convection conditions on a vertical plane surface, with a laminar boundary layer, the average Nusselt number is given by Equation 3.35. Laminar boundary conditions are present if the Rayleigh number,  $Ra < 10^9$ . The Rayleigh number is a function of the Grashof and Prandtl numbers, and is defined as  $Ra = GrPr$ .

$$Nu = 0.637 Ra^{\frac{1}{4}} \left( 1 + \frac{0.861}{Pr} \right)^{-\frac{1}{4}} \quad (3.35)$$

where

$$Gr = \frac{x^2 g B \Delta t}{\nu^2} \quad (3.36)$$

For gases, the coefficient of expansion,  $\beta$ , can be defined as:

$$\beta = \frac{1}{\text{absolute bulk temperature}} \quad (3.37)$$

Veshagh and Chen (1993) suggest that for an air temperature of 27 °C a typical value for the heat transfer coefficient between the water jacket and the air is only 12 W/m<sup>2</sup>K. This was calculated using the equations for forced convection, but with an under-bonnet air velocity of only 1.1 m/s.

### Convection to Crankcase Gases

The gases within the crankcase are a mixture of air, oil vapour, fuel vapour and combustion gases. The degree of heat transfer to these gases is not



clear. However, following the assumption that a significant amount of oil is thrown from the bearings onto the various engine interior surfaces, the surface area exposed to this gaseous mixture is assumed to be minimal. For the purpose of this study, the gas was assumed to be air, and the heat transfer was calculated in a similar method to that described above.

### Convection to the Coolant

On the coolant side of the liner and cylinder, convective heat transfer must also include the effect of boiling. The total heat transfer is equal to the sum of forced convection and nucleate boiling. The heat transfer from nucleate boiling is calculated from the McAdams formula (1954):

$$h = 0.002253 \frac{(\Delta t_x)^{3.96}}{t_s - t_b} \quad (3.38)$$

where the temperature excess,  $\Delta t_x = t_s - t_{sat}$ .

Chen suggests that a typical value for the heat transfer coefficient between the water jacket and the coolant is 330 W/m<sup>2</sup>K. In addition, it was suggested that steady-state coolant temperatures could justifiably be taken to be 100°C.

### Convection to the Combustion Gases

On the gas side of the combustion chamber, the cycle-averaged heat transfer coefficient and cycle averaged gas temperatures are used to replace the time varying values. Calculation of these values was considered to be outside the scope of this study. Instead, these characteristics can be obtained from cycle simulation programs such as those used by Jaguar (Bingham (1987)), or

developed by Chen (1990). Chen reported that a typical cycle-averaged heat transfer coefficient on the cylinder gas side is  $0.19 \text{ kW/m}^2\text{K}$ , with an averaged cylinder gas temperature of approximately  $1080^\circ\text{C}$ .

### 3.13 Conclusions

This chapter has presented a preliminary investigation into the engine components which are directly affected by the lubrication system. It has been shown that the lubrication system remains at the heart of the design of a modern automotive IC engine. To accurately simulate the lubrication system, each environment experienced by the lubricant, must be accounted for.

The pressurised side of the lubrication system can be represented as a flow network, which is formed from the following component elements:

- i, Circular straight pipes. Laminar and turbulent flow conditions will be accounted for. Under turbulent flow conditions losses from bends and junctions can be included using published pressure loss coefficients. The heat transfer through forced convection will initially assume constant wall temperatures.
- ii, Annular straight pipes. These can be modelled in a similar way to that of a circular pipe. Eccentricity can be accounted for by using graphical correction factors. The heat transfer calculations can be considered to be the same as for a straight pipe.
- iii, Oil pumps. Measured or predicted operating characteristics are required. These characteristics will include the effect of the pressure relief valve.

- iv, Oil strainers. The most common form of oil strainer is of round wire square mesh construction. Heat transfer within the strainer is negligible.
- v, Oil filters. Oil filters of pleated paper construction with full oil flow, will be modelled. Heat transfer aspects within the filter will be ignored for the present study, but remain a long term objective.
- vi, Journal bearings. The engine bearings are the key component within a lubrication system and are the primary recipient of the oil supply. The bearings will be considered to be steadily loaded, with two types of oil grooves; single feed hole, and  $180^\circ$  partially grooved. Heat transfer within the bearing must be accounted for, to estimate the working oil properties, and the oil temperature rise through the bearing.
- vii, Crankshaft and camshaft oil transfer holes. The flow through these centrifugally effected components will account for; friction, registry, and oil acceleration effects. The heat transfer calculations can be considered to be the same as for a straight pipe.
- viii, Oil cooler. The oil cooler will be considered as a cross-flow oil to air heat exchanger with fins on the hot and cold fluid surfaces. Given inlet oil and air temperatures, the exit temperatures will be solved by an iterative procedure. The pressure losses through the cooler can be calculated in a similar way to that used for a pipe, using the hydraulic diameter principle and junction loss coefficients.

The lubrication of the piston, liner and valve train is outside the scope of the pressurised lubrication system model. Lubrication of these components



is achieved primarily through oil spray from the various engine bearings. The heat transfer to the oil in these situations will be accounted for with the development of an engine block model.

A section through an engine block, which includes the combustion chamber, the piston, and the liner, can be represented by a series of block elements. The conduction of heat through these elements, and the heat convection to boundary fluids, can be solved simultaneously using an equivalent thermal resistance network approach. The oil splashed on to the inside surfaces of the engine can be modelled as a falling liquid film. This oil film represents one of the boundary fluids of the engine block elements. The remaining boundary fluids are; the ambient air, the crankcase gases, the coolant, and the combustion gases.

Cycle averaged heat transfer coefficients can be calculated by using suitable cycle averaged bulk fluid temperatures. This enables the temperatures of the oil film and the block temperatures to be calculated simultaneously.

Each of the environments experienced by the lubrication system have been accounted for. The flow and heat transfer aspects of each of the component elements within the pressurised side of the system have been analyzed. It has been shown that the heat transfer to the oil outside the pressurised side of the system, must also be accounted for, and a method of achieving this has been proposed.

## **Chapter 4**

# **Mathematical Model of Flow Conditions Within the Lubrication System**

### **4.1 Introduction**

In order to simulate any physical system, a mathematical model of the system needs to be formulated. A mathematical model can be broadly defined as a formulation of equations that express the essential features of the physical system or process in mathematical terms. The actual mathematical model can range from a simple algebraic relationship to large complicated sets of differential equations.

For the purpose of this study, a mathematical model of the flow conditions in the lubrication system needed to be set up, in order to solve for the two type of unknowns, ie. the pressures and flow rates. When modelling the lubrication system of an engine, the pressure losses and the resulting oil flow rate in one section, had an effect on the pressures and flow rates in the other sections. This implied three requirements:

- i, Each section within the system needed to be represented by a pressure loss v flow rate mathematical relationship.
- ii, The continuity of flow between adjacent sections needed to be maintained, with 'the algebraic sum of flows into each node being zero'.
- iii, All the pressures and flow rates needed to be solved simultaneously for

the whole system.

Thus, the entire lubrication system was represented by a set of simultaneous equations, which were solved using a numerical technique.

#### 4.1.1 Linear and Non-Linear Models

The first objective of this study was to develop a flexible linear flow model that could be used as a trend analysis tool. The model would provide a means of rapidly evaluating of the oil flow characteristics, predict performance trends, and produce reasonably accurate results for oil pressures and flow rates. This was achieved by formulating the pressure loss v flow rate relationships for the various elements within the system into a simplified linear form, constructing a set of linear simultaneous equations, and solving for them simultaneously using a linear routine (these routines are described in Appendix A.1).

The linear flow model was structured in such a way as to easily facilitate the use of different linear solving routines. Gauss-Jordan elimination linear routine was selected for initial model development. Although this routine is reported by Chapra and Canale (1985) to be slow in raw operation count, it was considered to be straightforward, understandable and robust. To investigate the benefits of a faster linear routine, a second linear flow model was developed which incorporated the LU decomposition algorithm. A discussion of the differences between these two linear models, with respect to run times and accuracy of results, is given in section 8.2.



The second objective of this study was to develop a more precise flow model, placing the emphasis on the prediction of accurate values for the oil pressures and flow rates, even if it was at the expense of modelling speed. The purpose of this model was to provide a precise flow analysis tool which would form the nucleus for the addition of further component elements. This allowed the true pressure loss v flow rate relationships to be used to represent each element in the system. As these relationships could realistically be of a non-linear form, this would result in a set of non-linear equations. A different approach for solving for the unknowns was required than that used for the linear case.

The Levenberg-Marquardt algorithm (described in detail in Appendix A.2.1) was selected for use in solving the sets of non-linear simultaneous equations in the non-linear flow model. The algorithm was extracted from Press et al (1990). The Levenberg-Marquardt algorithm represents one of the most concise and stable non-linear solution methods for simultaneous equations available today. In addition, it was the method employed and tested by Trapy and Damiral (1990) in their model of an engine lubrication system. Consequently it has been proven for solving for a system of a similar size to a typical Jaguar engine lubrication system. A comparison of the run times and accuracy of results, for the linear and non-linear models, is given in section 8.3.

#### **4.1.2 Representing the Physical System**

The physical system was represented by being broken down into component elements which were connected at nodal points (see Figures 8.2 and 9.1 for the AJ6 and V8 engine lubrication networks). It was assumed that the pressures at entry and exit from the system were atmospheric. As the

remaining pressures within the system were solved as gauge pressures, the entry and exit pressures for the system were, therefore, assumed to be zero.

#### 4.1.2.1 Linear Model

In the linear model, the physical system was represented by six types of component elements; pumps, laminar pipes, filters, bearings, crankshaft oil transfer holes, and cam bearing oil transfer holes. Each element in the system was represented by a linear pressure loss v flow rate equation. In addition, flow continuity was represented at every dividing node in the system. The equation which represented the flow continuity was of the form:

$$Q_{x,y} - Q_{y,z_1} - Q_{y,z_2} \cdots - Q_{y,z_n} = 0 \quad (4.1)$$

Where n = number of flow paths out of node y.

Thus, the entire system was represented by a M x N set of simultaneous algebraic equations, where the number of equations, M, and the number of unknowns, N, were equal. This set of simultaneous equations was solved by either the Gauss-Jordan elimination or the LU decomposition routines (these routines are described in Appendix A.1). Either routine returned the values for the pressures at the nodes within the system, and the flow rates in each flow branch.

#### 4.1.2.2 Non-Linear Model

Modelling flexibility was improved in the non-linear model with the inclusion of additional component elements; turbulent pipes, laminar or turbulent annular pipes, oil strainers, and laminar or turbulent oil coolers. Two methods of representing and processing the pressure loss v flow rate

relationships for all the component elements were investigated:

### Method One. Continuity of Flow

Each element in the system was represented by a pressure loss v flow rate mathematical relationship in the form of Equation 4.2.

$$f(\Delta P, Q) = 0 \quad (4.2)$$

Equation 4.2 was re-arranged in terms of flow rate, Q, which yielded:

$$Q = f(\Delta P) \quad (4.3)$$

The whole lubrication system was therefore modelled by a set of equations which represented the continuity of flow for each node in the system, in the form of Equation 4.4.

$$Q_{x,y} - Q_{y,z_1} - Q_{y,z_2} \cdots - Q_{y,z_n} = 0 \quad (4.4)$$

Where n = number of flow paths out of node y.

By replacing each Q term in Equation 4.4 with the relevant mathematical relationship in the form of Equation 4.3, the Levenberg-Marquardt algorithm (described in Appendix A.2.1) returned the values for the pressures throughout the system. Once these pressures were known, the flow rates, Q, could be calculated by substituting the relevant calculated pressures into Equation 4.3, for each element in the system.

The advantages with this method were:



- i, As it was only the values for the pressures which were returned from the Levenberg-Marquardt routine, the size of the matrices  $[\beta]$  and  $[\phi']$  (see Appendix A.2.1) were smaller than they would be if the flow rates,  $Q$ , were included. This could result in shorter overall run times.
- ii, Again, as the parameters to be fitted were all pressures, they were all approximately of the same order of magnitude. Therefore, a single value for the standard deviation term,  $\sigma$ , could be derived, for use in the calculation of the  $\chi^2$  merit function.

The disadvantages were:

- i, If more complex pressure loss v flow rate relationships were used in the future, it may become increasingly difficult (maybe prohibitively so) to rearrange the equations from the form of Equation 4.2 into the form of Equation 4.3.
- ii, Equally, if Equation 4.4 became more complicated, the task of providing the required partial derivatives for the Hessian matrix at each step, would become more demanding.

### **Method Two. Pressure/Flow Rate Combination**

Again, each element was represented by a pressure loss v flow rate relationship. However, instead of representing the system with a set of continuity of flow equations for each node, the system was represented by a combination of the pressure loss v flow rate equation for each element (Equation 4.2) and a simple continuity of flow relationship for each dividing node (similar to Equation 4.4). The Levenberg-Marquardt algorithm returned the values for all the pressures and the flow rates directly.

The advantages with this method were:

- i, The values for all the pressures and the flow rates were returned directly.
- ii, The system was represented in a similar manner to that employed in the linear model. Many of the subroutines written for the linear model could be used directly in the non-linear model.
- iii, There was no requirement to re-arrange the pressure loss v flow rate relationships (Equation 4.2) into the possibly more complicated form of Equation 4.3.

The disadvantages were:

- i, With all the pressures and the flow rates to be solved for simultaneously, the number of parameters to be fitted could be larger than that of method one. Subsequently the run times could be greater, and the accuracy of the results could be reduced.
- ii, There was a considerable order of magnitude difference between the two types of parameters which would be returned. For example the pressures would be of the order of magnitude of  $10^5 \text{ N/m}^2$ , while the flow rates would be of the order of magnitude of  $10^{-6} \text{ m}^3/\text{s}$ . Therefore, difficulty may have arisen in deriving a suitable value for the user supplied standard deviation term,  $\sigma$ , for use in the calculation of the  $\chi^2$  merit function.

The present non-linear program was developed utilising method two, It was considered to be the simpler of the two methods to implement. The majority of the subroutines written for the linear program could be used in the non-linear program construction, and in addition, this method returned both

the pressures and the flow rates directly. A second stage of calculating the flow rates separately, after the values for the pressures was obtained, was not needed.

To overcome the difficulty of deriving a single standard deviation,  $\sigma$ , for use in any type of equation, two different values were used. For the pressure loss v flow rate relationships, a value of  $10 \times 10^5$  was used, while for the continuity of flow equations a value of  $10 \times 10^{-5}$  was selected. These values were derived by a trial and error procedure, using the returned values for the sum of flows through the dividing nodes as an indication of the accuracy of the results. Lubrication systems of various sizes were modelled, no problems were encountered and the values for  $\sigma$  appeared to be suitable for general use.

### 4.1.3 Component Models

Referring back to the main requirements of this study, ie. to develop a simple, rapid, flow model, it was intended that simplifications and approximations would be made to derive equations which were all of a simple linear form. These equations would be solved by either the Gauss-Jordan or the LU decomposition linear matrix solving techniques. The lubrication system was represented in the linear flow model by six types of elements/components; oil pumps, pipes, oil filters, bearings, cam-shaft oil transfer holes and crankshaft oil transfer holes. However, it was found that many of the pressure loss v flow rate relationships were of a linear form and only a few equations, for example, the pipe flow and pump characteristics, needed to be simplified by linearisation.

The non-linear model was initially developed using the same linear equations to represent the pressure loss v flow rate relationships of each



component. The purpose of this was to aid the development of the non-linear method, and enable the results obtained for a particular system to be checked against those predicted by the linear model.

The first non-linear model was developed to a stage where the results obtained were in exact agreement with those obtained by the linear method which utilised the LU decomposition linear matrix solver. A full comparison of these results is given in section 8.2. Further development of the non-linear model resulted in a re-evaluation of the oil pump model and turbulent pipe flow model. In addition, new models were developed to represent oil strainers, annular pipes, and oil coolers.

The oil pump characteristics which were initially available, were for an oil pump operating with an oil temperature of  $100^{\circ}\text{C}$ . For this reason, the linear model and the initial non-linear model were developed with the assumption of the oil being at a steady  $100^{\circ}\text{C}$  throughout the system. The value of  $100^{\circ}\text{C}$  was close to the oil equilibrium temperature, found by Andrews et al (1989). The only exception, was the oil temperature within the journal bearings and the crankshaft oil transfer holes. As the oil flow through the bearings was sensitive to oil viscosity, simple calculations are made initially, to estimate the oil temperature and viscosity within the bearings.

As the oil entering the crankshaft oil transfer holes was fed directly from the oil within the main bearings, the temperature of the oil within the bearings had an effect on the oil temperature within these sections as well. For this reason, the oil temperature within the crank-shaft oil transfer holes was assumed to be the same as the value calculated within the main bearings.

The later non-linear model improved modelling flexibility by allowing the user to select the sump oil temperature. In addition, the oil temperature within each of the component elements was calculated by the heat transfer model. The heat transfer model, which is described in more detail in Chapter 5, predicted the oil temperature within each component element. The predicted oil temperatures could be used to provide more realistic oil properties in the non-linear flow model. A description of the interaction between the flow program and the heat transfer program is presented in Chapter 6 and Chapter 7. The use of the predicted oil temperatures allowed a far more accurate prediction of the flow rates and pressure losses within these components. The new predictions for the flow conditions within the system were fed back to the heat transfer model and an iterative procedure commenced.

This Chapter presents the mathematical models which were derived to represent the pressure loss v flow rate characteristics for each component element within the flow model. The differences between the component models which were derived for use in the linear model and the non-linear model (if any) are also presented. The partial derivatives of each equation are also presented. These derivatives were considered to be a fundamental part of the individual component models. They were used, in conjunction with the pressure loss v flow rate relationship, to represent the flow characteristics of each component in the non-linear flow model.

## 4.2 Oil Pump

From a modelling point of view, the oil pump was the critical component within an engine lubrication system. The sum of the pressure losses from the other parts of the lubrication system were matched by the pump performance at the equilibrium operating condition. This was demonstrated by the



modelling approach taken by Lo (1971), which was documented in section 2.3. Therefore, an accurate representation of the oil pump performance was required, if an accurate calculation were to be made of the pressure losses and flow rates in the complete system.

No attempt was made to model the oil pump using an analytical approach. It was assumed that a far more accurate representation of the performance of an existing oil pump would be achieved using measured data. It was assumed that this data would always be available to the engine designer, obtained either from the pump suppliers, or from in-house rig testing. Measured oil pump characteristics were used during the development of the flow model. However, the pump model which was developed allowed theoretical characteristics to also be used. It was considered that if no measured data were available, for example at the early design stage of an engine, theoretical oil pump performance characteristics could be used. The lubrication system could be modelled and the approximate lubrication requirements could be found. Parametric studies could be carried out on the oil pump, using different pump performance characteristics, and the optimum pump operating characteristics could be determined.

#### **4.2.1 Simplified Oil Pump Model**

The linear flow model used measured pressure v flow rate characteristics for the Jaguar AJ6 engine oil pump. These were obtained from oil pump performance tests carried out at Jaguar (Bush (1980)). Characteristics were obtained for various engine speeds, as shown in Figure 4.1, using a BP 10W/30 multigrade oil at 100°C, and with a pump to engine speed ratio of 0.636:1.



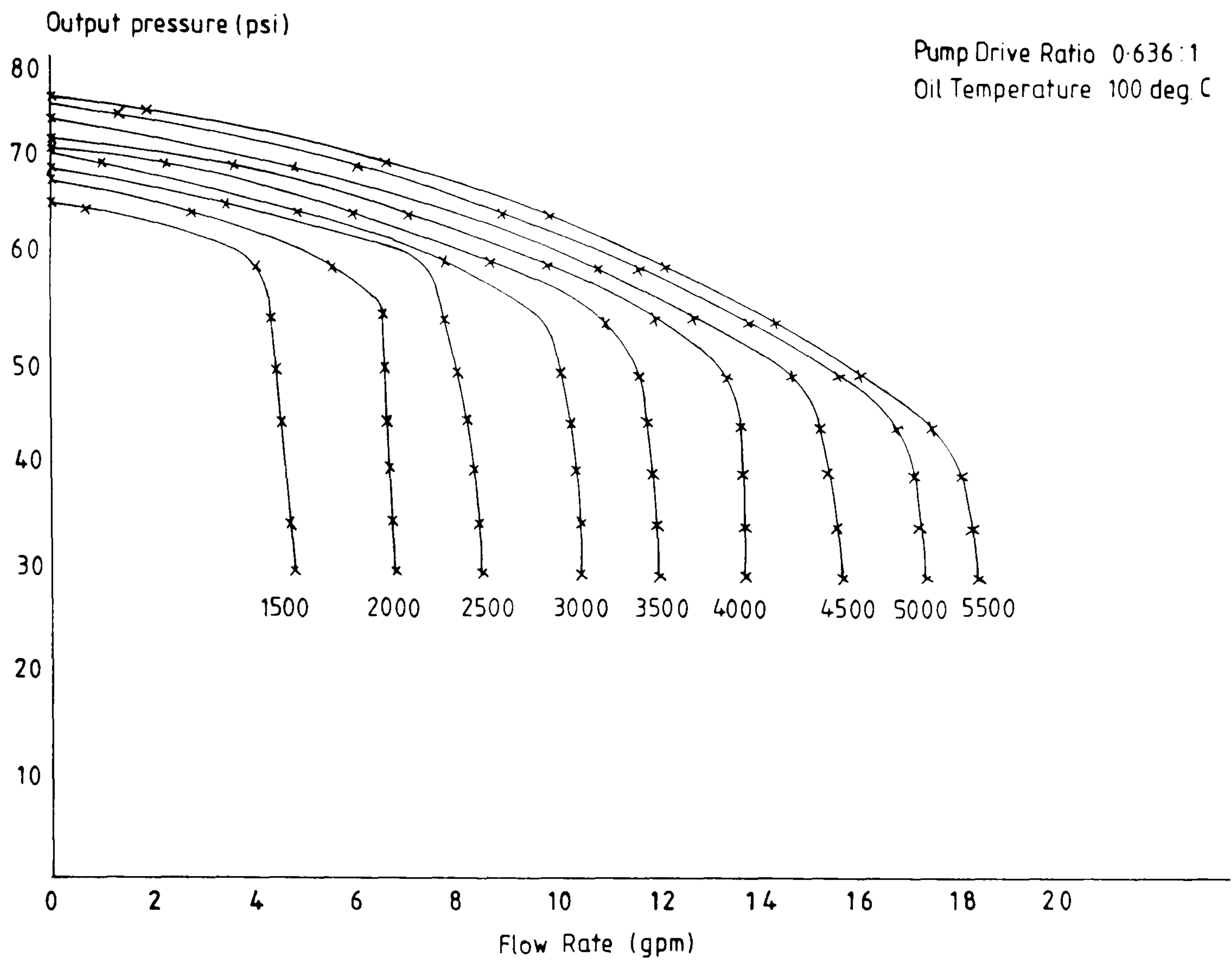


Figure 4.1. Jaguar AJ6 engine oil pump characteristic curves

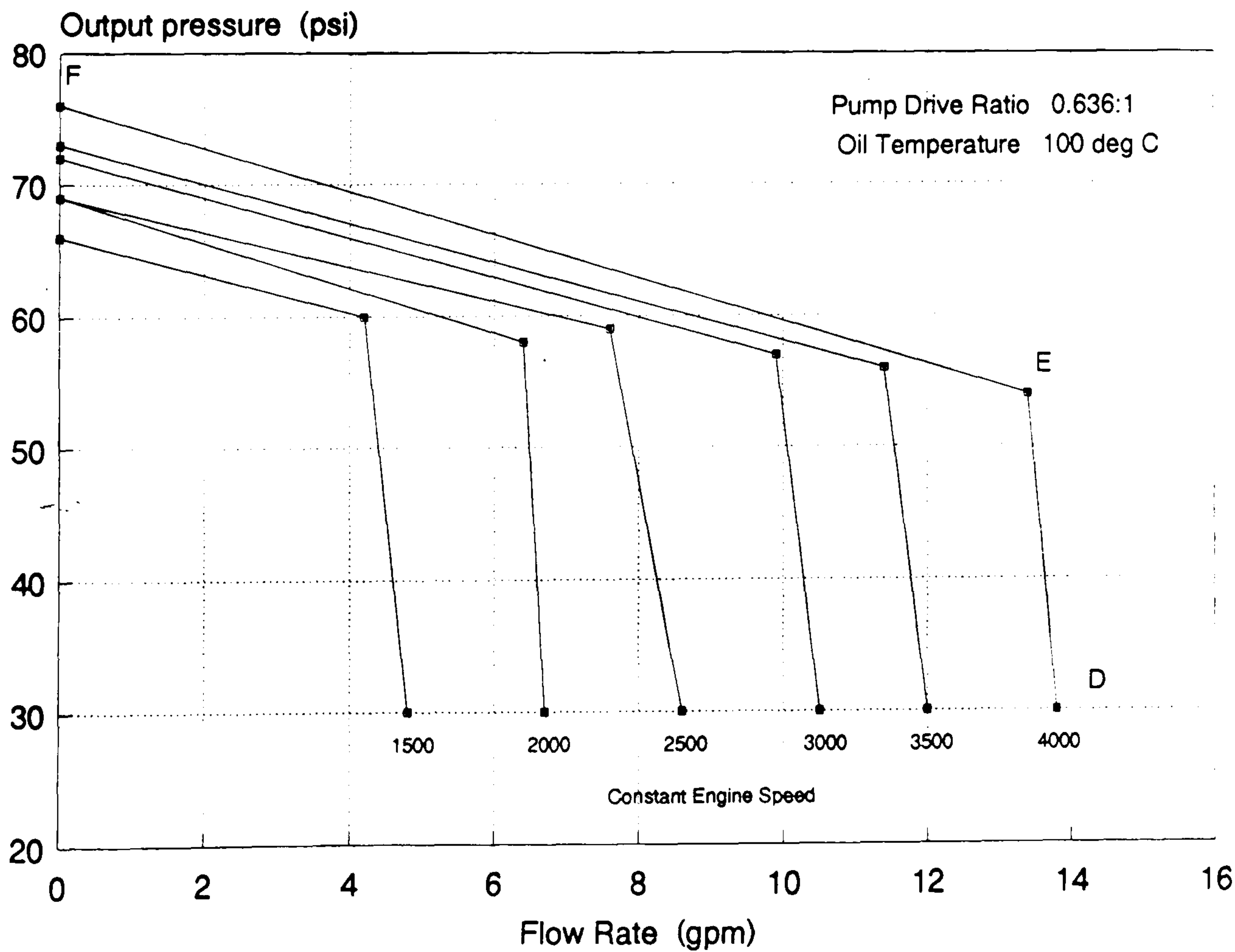


Figure 4.2. Simplified AJ6 oil pump characteristics

The oil pump characteristics were simplified into the general 'ideal' linear relationships shown in Figure 4.2, by simple visual curve fitting. No data was available for engine speeds below 1500 rpm, and the characteristics departed too far from the linear simplification at engine speeds in excess of 4000 rpm. The characteristic for each speed consisted of two straight lines, which were represented by the pressure and flow rate co-ordinates of the three points on the curve, D, E, F. Any combination of engine speed and pump drive ratio could be selected, providing the resulting pump speed lay within the known range. Using interpolation, the co-ordinates at points D, E and F were derived for any resulting pump speed. Following the calculation of the co-ordinates of these three points, the equations for the two straight lines ( $Y=MX+C$ ) were calculated.

It was assumed that the pump would operate in the lower section initially. The slope,  $M$ , and the constant,  $C$ , for the lower section of the chosen pump speed curve were calculated by solving a simple set of two simultaneous equations. These values for  $M$  and  $C$  were then placed in the general linear equation which represented the pressure v flow rate relationship of the pump, operating in the lower linear region:

$$Y = 0 = P_2 - P_1 - MQ_{1,2} - C \quad (4.5)$$

The flow characteristics for each component element were represented in the non-linear model by a combination of a pressure loss v flow rate relationship and the partial derivatives of this relationship. The partial derivatives of Equation 4.5, which were used in the Levenberg-Marquardt routine in the non-linear flow model, were:

$$\frac{dY}{dP_1} = -1 \quad (4.6)$$

$$\frac{dY}{dP_2} = 1 \quad (4.7)$$

$$\frac{dY}{dQ_{1,2}} = -M \quad (4.8)$$

At the end of each set of calculations, the calculated pump output pressure was compared to the value of the pressure at point E. If the calculated pressure was greater than this switch pressure, the oil pump was assumed to be operating in the second linear region. The oil pump characteristics were then re-calculated to match the upper linear portion of the curve, in a similar manner to that described above.

#### 4.2.2 Enhanced Oil Pump Model

A detailed investigation was made to enhance the oil pump model into a more representative form, for use in the non-linear flow model. At the early stages of the project, the oil pump model was based on the AJ6 engine oil pump characteristics. As the only data available were the measured pressure and flow rate co-ordinates at discrete points along each curve, it was concluded that the best representation of this curve was a method which incorporated each data point.

A similar linear interpolation method was used as before to determine a unique set of data points for any given engine speed and pump drive ratio. An investigation was made into methods of fitting a more representative curve through these data points for the chosen pump speed. Three interpolation



techniques were investigated for predicting the pressure and flow rates between each point on the characteristic curve; polynomial, cubic spline, and linear. The resulting curves are shown in Figure 4.3.

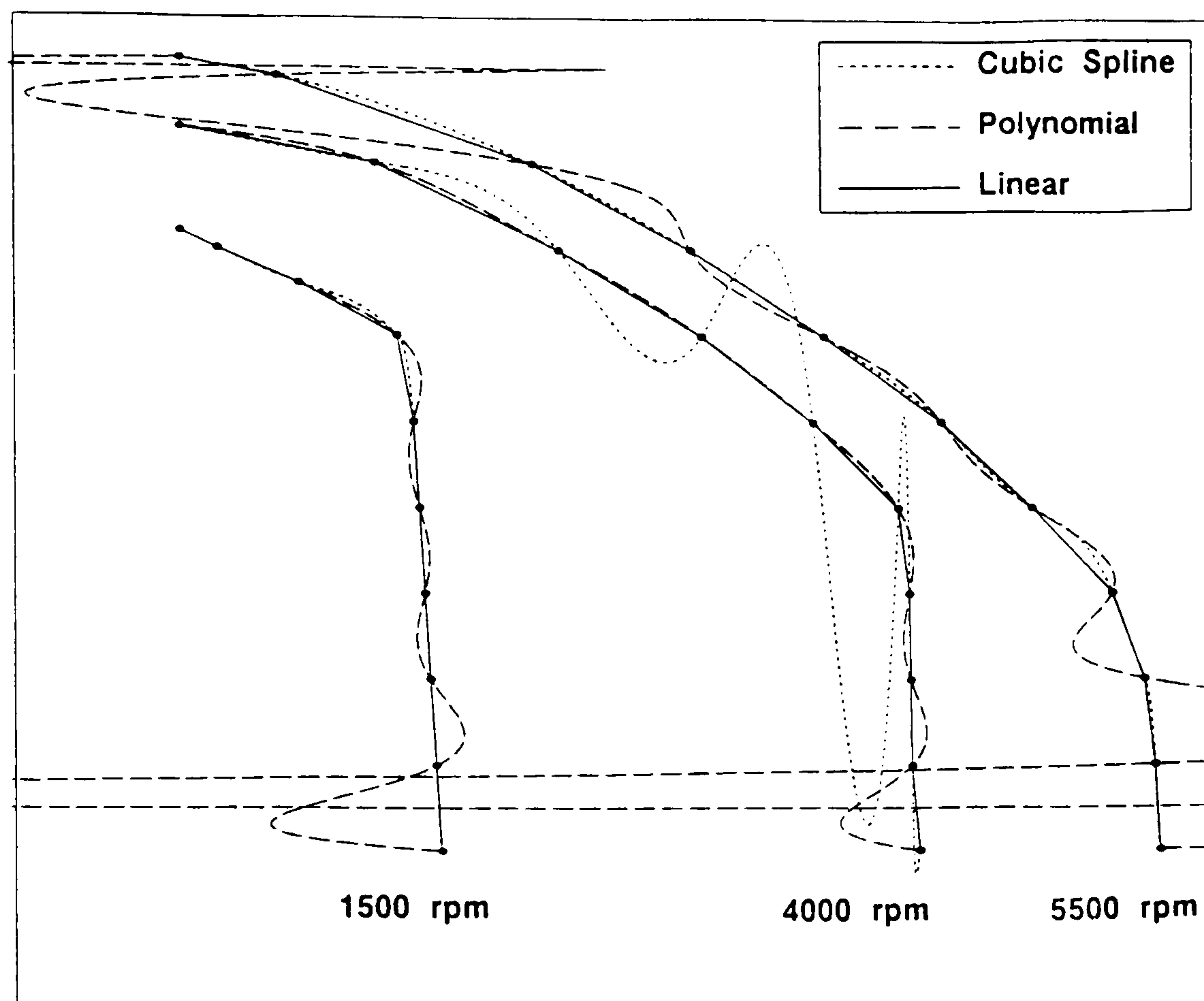


Figure 4.3. Curve fitting of oil pump characteristics at three engine speeds, using three different iteration techniques.

Figure 4.3 shows the data points which represent the pump characteristics at three engine speeds; 1500 rpm, 4000 rpm, and 5500 rpm. These speeds were selected as they represented the full range of known data. Cubic spline interpolation gave a very close fit to the 'ideal' curve in both the low and high speed cases. However, excessive instability occurred in the 4000 rpm speed curve. As this curve was very similar to the 1500 rpm curve, being represented by the same number of data points, it was concluded that the instability was primarily due to the steep slope of the lower section of the curve. As it would have been unrealistic to assume that a pump with similar

characteristics was not used in such simulation studies in future, it was concluded that this was not a viable solution.

Polynomial interpolation produced results which were also highly unstable, especially in the case of the 5500 rpm curve. However, it was found that if this particular curve was represented by 10 data points, similar to the number of points on the 1500 rpm and 4000 rpm curves, rather than 11, the instability reduced by a large amount. The resulting curves are shown in Figure 4.4. Although the lower order approach resulted in a more stable curve, the curve fit was still far from the 'ideal' curve, especially in the lower section.

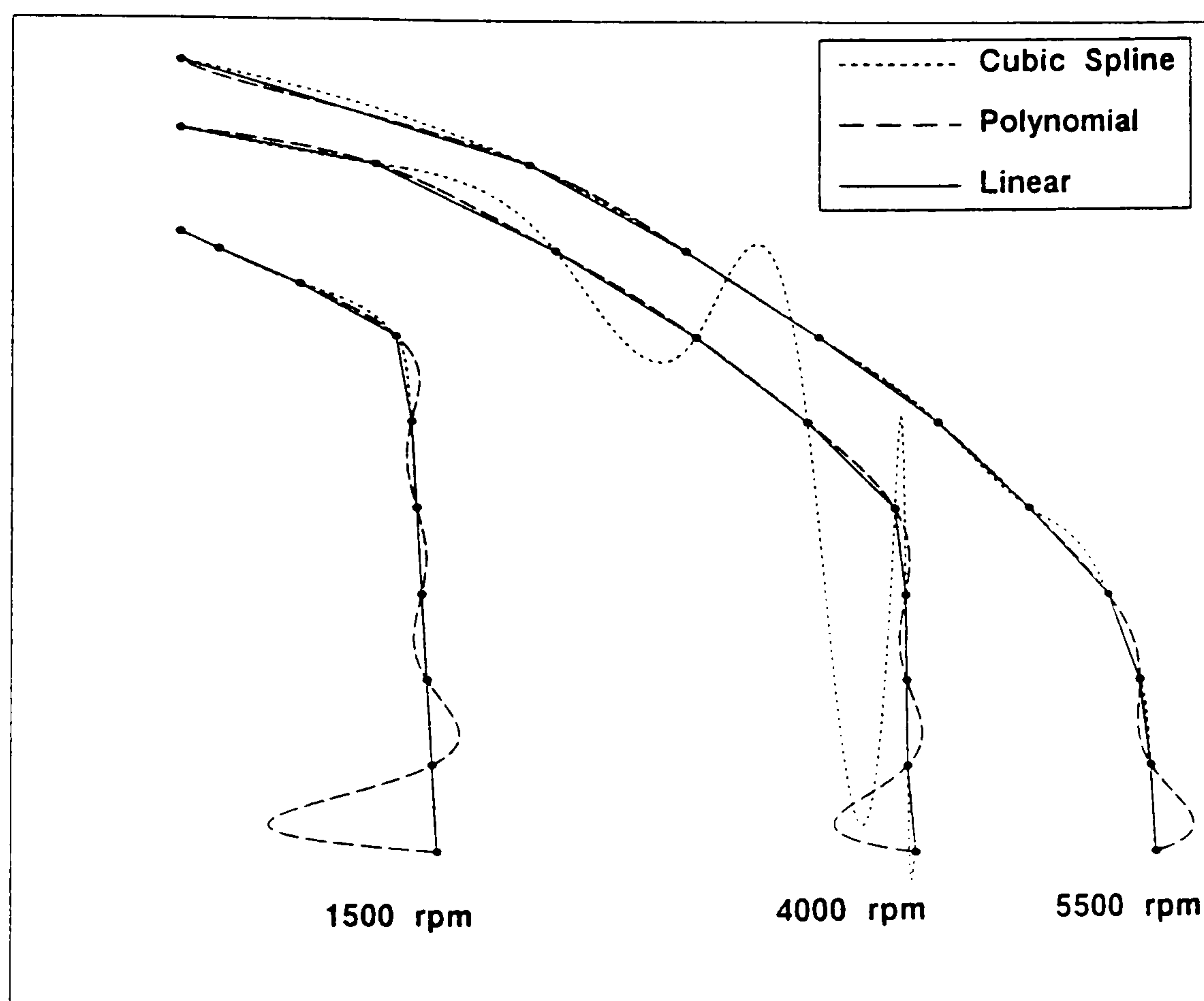


Figure 4.4. Curve fitting of oil pump data for three engine speeds using the same number of data points to represent each curve.

A second investigation showed that if the characteristic curve was broken down into two distinct sections, each section being represented by three

data points, the resulting second order curve provided a close fit to the remaining points. This is shown in Figure 4.5, the five points chosen to represent each curve are shown as double circles.

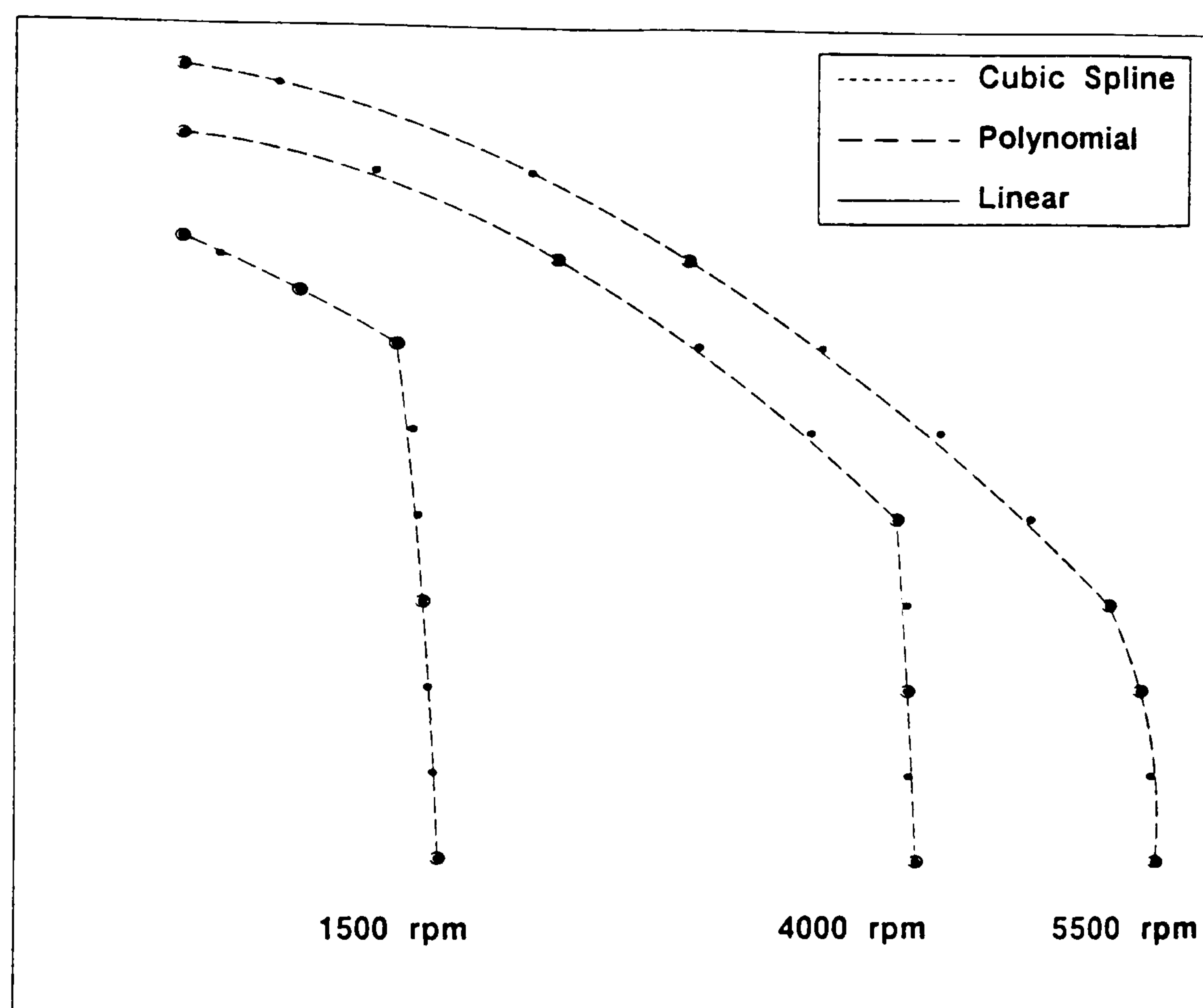


Figure 4.5. Curve fitting of oil pump data for three engine speeds by breaking down each curve into two second order curves.

It was found that the initial approach to modelling the oil pump, by breaking down each characteristic curve into two linear regions, could be improved. The two linear region simplification approach led to errors caused by fitting a straight line through a set of points which usually lay in a curve. It was found that a smoother fit could be obtained by splitting each curve into two distinct sections and representing each section by a second order equation.

Some doubt remained as to the practical use of such a method. The benefits of such an approach were that each characteristic curve was still



represented by only two sections. This would have kept the program run time to a minimum by minimising the number of iterations required to represent the pump (the program construction is described in Chapter 6). The disadvantage with this approach was that although the resulting curves gave a close fit through the data points, the curve did not pass through every data point. It was concluded that a method which included each data point was required, to ensure an accurate representation of the measured pump characteristics and that an accurate representation of the known data had a greater importance than program run time.

As can be seen from Figures 4.3, 4.4, and 4.5, a good representation of the curve was obtained using a piece wise linear approach. The pump characteristic curve was represented by a series of linear sections joining each data point. This approach was similar to that employed for the two linear region simplification described above. It was assumed that the oil pump would initially be operating in the linear region which was closest to the central point of the curve and could be represented by a simple linear equation described earlier.

Following the calculation of the system pressures and flow rates, the predicted pump output pressure was checked against the upper and lower pressure values for the linear region in which it was assumed to be operating. If the predicted pressure lay outside this region, it was assumed that the pump was operating in the neighbouring section, and the process was repeated. This process continued until convergence occurred and the pump output pressure lay within the chosen linear region.

Naturally, given the possible increase in the number of iterations which were required, the program run times could increase. It is difficult to give a

true comparison, as the run times depended on the number of data points used to represent each pump characteristic and the position on the curve where the pump was operating.

### 4.2.3 V8 Engine Oil Pump Data

The oil pump characteristics for the V8 engine were provided by Jaguar from a series of six repeat rig tests. Each set of data represented the pressure v flow rate measurements with a HP10 grade test oil maintained at a temperature of 53°C. This equated to a 5W/30 multigrade oil at 120°C. Data was provided for eight different engine speeds ranging from 400 rpm to 7000 rpm, with a pump drive ratio of 1:1.

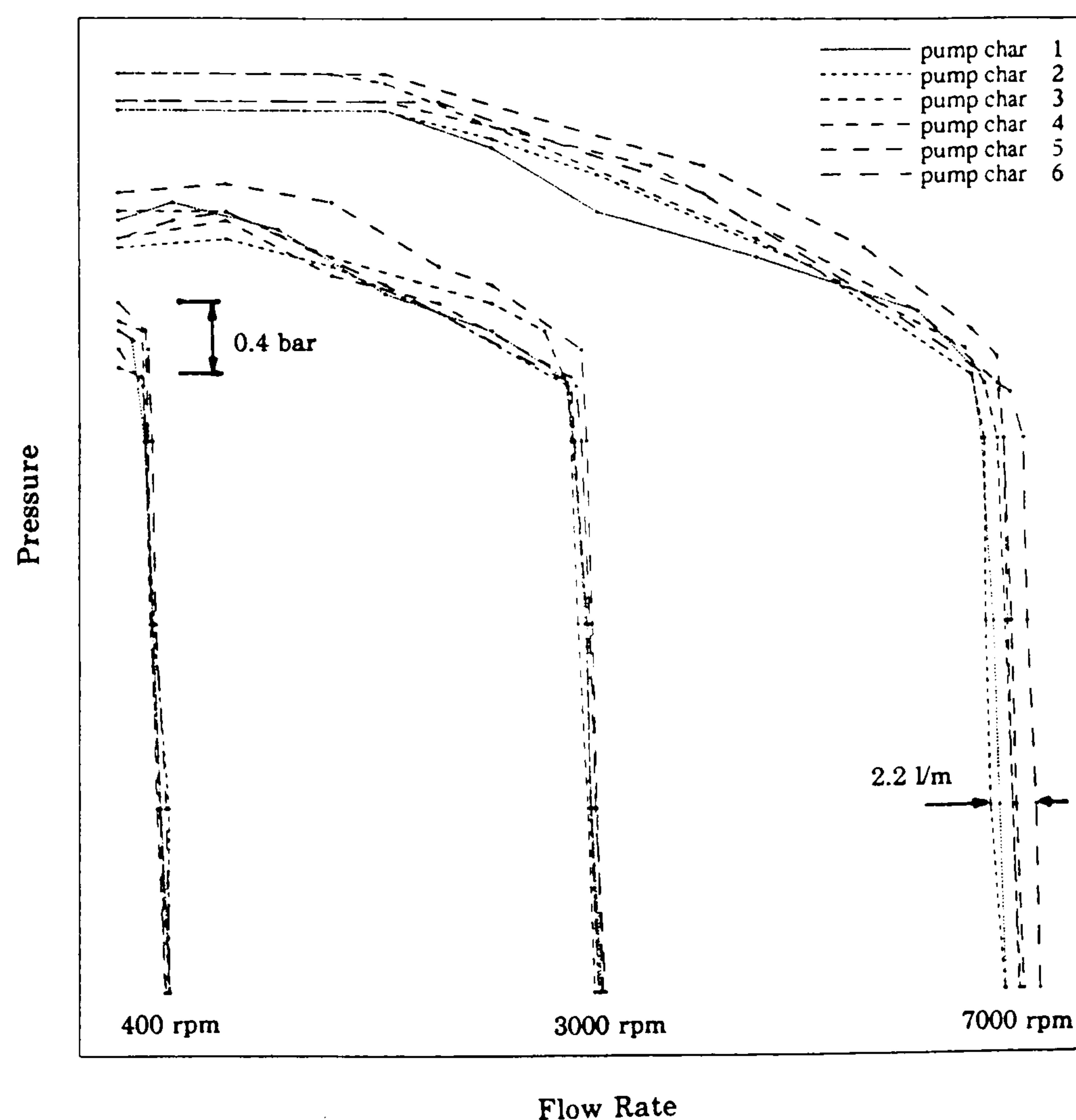


Figure 4.6. Variation of measured data for V8 engine oil pump

For comparison purposes, Figure 4.6 shows the degree of variation between the measured characteristic curves at three different engine speeds. It can be seen that the measured flow rates varied by more than 2.2 l/min, and the measured pressures by more than 0.4 bar. Instead of estimating the 'best fit' curve through the scattered data, characteristic curve number 4 was chosen to represent the best compromise.

### 4.3 Pipes

The equation to represent the pressure loss v flow rate relationship of the flow of oil through the pipes, was derived from Bernoulli's pressure equation. Thus, the conservation of energy between any two points in a pipe was represented by an equation of the form:

$$P_1 + \frac{\rho V_1^2}{2} + \rho g z_1 = P_2 + \frac{\rho V_2^2}{2} + \rho g z_2 + \text{losses} \quad (4.9)$$

Assuming incompressible flow, constant cross section, negligible changes of height and ignoring the effects of density changes, Equation 4.9 was reduced to:

$$P_1 = P_2 + \text{losses} \quad (4.10)$$

The 'losses' in the above equation were a result of both fluid friction and disturbances from bends and junctions. Initially, only the losses due to fluid friction were included. The primary reason for this was that the addition of the bend and junction losses would create a non-linear relationship which could not be solved by the linear model. In addition, these losses were considered to be negligible if the flow through the lubrication system was laminar. The pipe model was enhanced later by developing the non-linear model to allow for



turbulent flow and pressure losses from bends.

### 4.3.1 Laminar Pipe Flow

The pressure losses in laminar pipe flow was expressed as:

$$\Delta P = \Delta P_{friction} \quad (4.11)$$

The friction losses through the pipe were represented by an adaption of the Darcy-Weisbach formula:

$$\Delta P = f \frac{L}{D} \rho \frac{V^2}{2} \quad (4.12)$$

where the friction coefficient,  $f$ , was calculated from:

$$f = \frac{C_f}{Re} \quad \text{and} \quad Re = \frac{\rho V D}{\mu} \quad (4.13)$$

while

$$V = \frac{Q}{A} \quad \text{and} \quad A = \frac{\pi D^2}{4} \quad (4.14)$$

The laminar flow coefficient,  $C_f$ , was 64 for circular cross-sections, 56 for square cross-sections, and 96 for an infinitely wide two dimensional passage. Assuming circular cross-section pipes throughout the lubrication system, Equation 4.12 became:

$$\Delta P = \frac{128 \mu L}{\pi D^4} Q \quad (4.15)$$

Substituting Equation 4.15 into Equation 4.10, yielded the equation which was used to represent the pressure loss v flow rate relationship for a laminar pipe element:

$$Y = 0 = P_1 - P_2 - \frac{128\mu L}{\pi D^4} Q_{1,2} \quad (4.16)$$

The partial derivatives of Equation 4.16, which were used in the non-linear flow model, were of the form:

$$\frac{dY}{dP_1} = 1 \quad (4.17)$$

$$\frac{dY}{dP_2} = -1 \quad (4.18)$$

$$\frac{dY}{dQ_{1,2}} = - \frac{128\mu L}{\pi D^4} \quad (4.19)$$

### 4.3.2 Turbulent Pipe Flow

The pressure losses in turbulent pipe flow were expressed as:

$$\Delta P = \Delta P_{friction} + \Delta P_{bends} \quad (4.20)$$

The friction losses through the pipe were again represented by an adaptation of the Darcy-Weisbach formula (Equation 4.12), with the friction coefficient,  $f$ , expressed by the Colebrook-White equation (1939):

$$f = 4 \times 0.001375 \left[ 1 + \left( 20000 \frac{k}{D} + \frac{10^6}{Re} \right)^{\frac{1}{3}} \right] \quad (4.21)$$

Substituting Equations 4.13 and 4.14 into Equation 4.21 yields:

$$f = 5.5 \times 10^{-3} \left[ 1 + \left( 20000 \frac{k}{D} + \frac{\mu \pi D \times 10^6}{4 \rho Q} \right)^{\frac{1}{3}} \right] \quad (4.22)$$

and Equation 4.12 was represented as

$$\Delta P_{friction} = \frac{8L \rho Q^2}{\pi^2 D^5} \cdot 5.5 \times 10^{-3} \left[ 1 + \left( 20000 \frac{k}{D} + \frac{\mu \pi D \times 10^6}{4 \rho Q} \right)^{\frac{1}{3}} \right] \quad (4.23)$$

It was assumed that the pipes and drillings were equivalent to new steel pipes with a roughness value,  $k$ , of  $2.5 \times 10^{-5}$  m (Miller (1990)). A selection of roughness values for different types of pipes is given in Appendix B.4.

The pressure losses due to bends, junctions, and other disturbances were accounted for by using the general expression given by Equation 4.24. The pressure loss due to the disturbance was represented by the dimensionless loss coefficient,  $K_b$ , which was obtained from published data such as Miller (1990).

$$\Delta P_{bends} = \frac{K_b \rho V^2}{2} \quad (4.24)$$

Substituting Equation 4.14 into Equation 4.24 showed that:

$$\Delta P_{bends} = \frac{8K_b \rho Q^2}{\pi^2 D^4} \quad (4.25)$$

Substituting Equations 4.23 and 4.25 into Equation 4.10 gave the general pressure loss equation for turbulent pipe flow:



$$Y = 0 = P_1 - P_2 - \frac{8K_b Q Q_{1,2}^2}{\pi^2 D^4} - \left( \frac{L Q Q_{1,2}^2}{\pi^2 D^5} \cdot 0.044 \left[ 1 + \left( 20000 \frac{k}{D} + \frac{\mu \pi D \times 10^6}{4 Q Q_{1,2}} \right)^{\frac{1}{3}} \right] \right) \quad (4.26)$$

The partial derivatives of Equation 4.26, which were used in the non-linear model, were of the form:

$$\frac{dY}{dP_1} = 1 \quad (4.27)$$

$$\frac{dY}{dP_2} = -1 \quad (4.28)$$

$$\frac{dY}{dQ_{1,2}} = -2Q_{1,2}(a + b) - \frac{(5bd + 6bcQ_{1,2})}{3 \left( c + \frac{d}{Q_{1,2}} \right)^{\frac{2}{3}}} \quad (4.29)$$

where

$$a = \frac{8K_b Q}{\pi^2 D^4} \quad b = \frac{0.044 L Q}{\pi^2 D^5} \quad c = 20000 \frac{k}{D} \quad d = \frac{\mu \pi D \times 10^6}{4 Q} \quad (4.30)$$

## 4.4 Annular Pipes

The modelling approach for annular pipes was very similar to that used for circular cross-section pipes documented in section 4.3. The pipe diameter,  $D$ , used in Equations 4.12 to 4.30 was replaced by the hydraulic diameter,  $D_h$ . Given the geometry of the annular pipe shown in Figure 4.8, the hydraulic diameter was expressed as:

$$D_h = d_2 - d_1 \quad (4.31)$$

For laminar flow, the flow coefficient,  $C_f$ , used in Equation 4.13, was obtained from graphical data extracted from Miller (1990), as shown in Figure

4.7. For turbulent flow, the friction coefficient,  $f$ , for a concentric annulus lay within a factor of about 1.05 of that given by Equation 4.22. Therefore:

$$f_{\text{annular}} = 1.05 f_{\text{circular}} \quad (4.32)$$

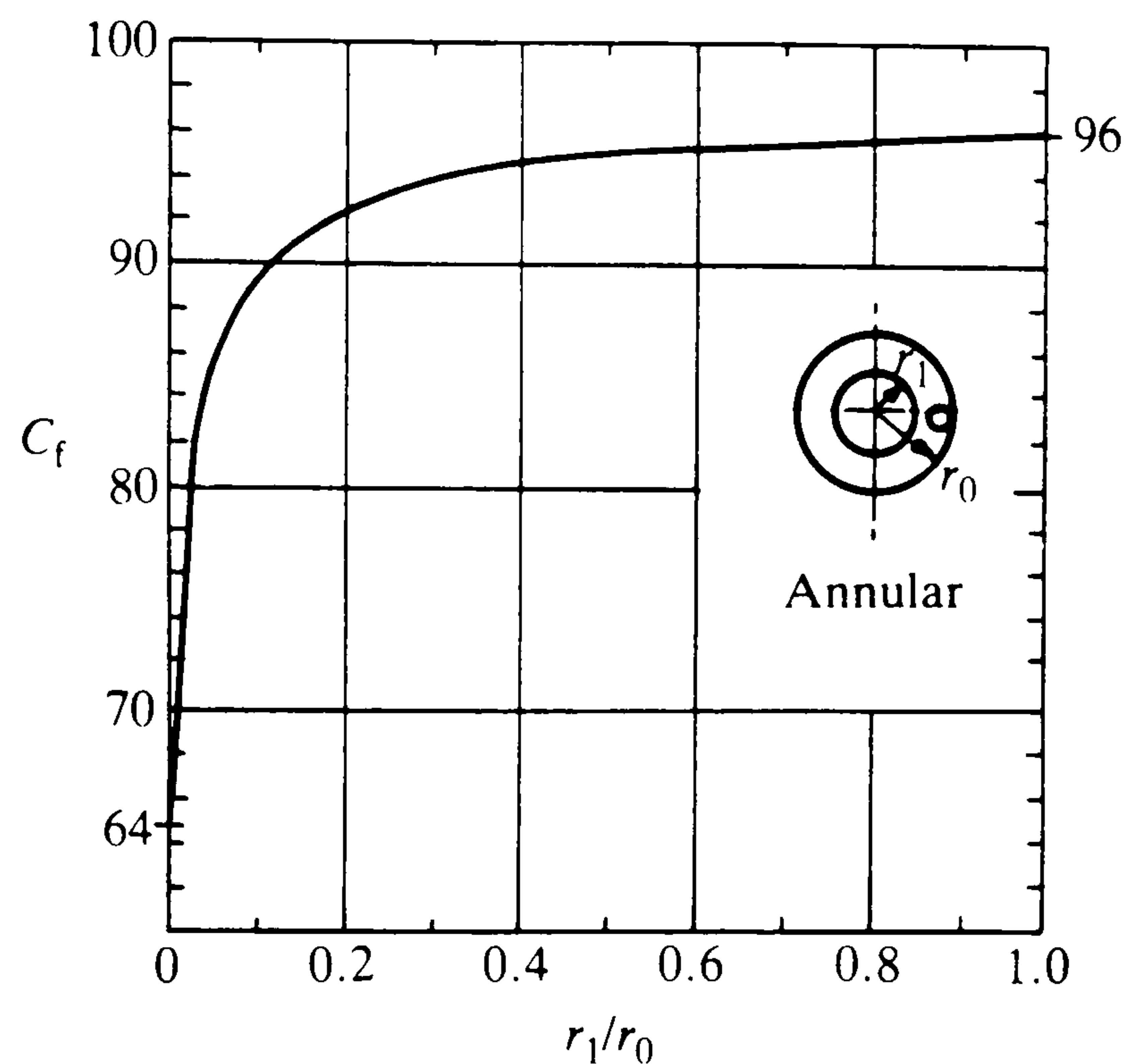


Figure 4.7. Laminar flow coefficients - annular cross-sections

Eccentricity within an annuli, with turbulent flow conditions, was accounted for by using graphical data extracted from Miller (1990). A modified friction coefficient was obtained by multiplying Equation 4.22 by the correction factor,  $C_f$ , obtained from data shown in Figure 4.8.

## 4.5 Oil Strainers

The pressure loss v flow rate relationship through an oil strainer was represented by the general pressure loss equation:

$$\Delta P = K \frac{\rho V^2}{2} \quad (4.33)$$

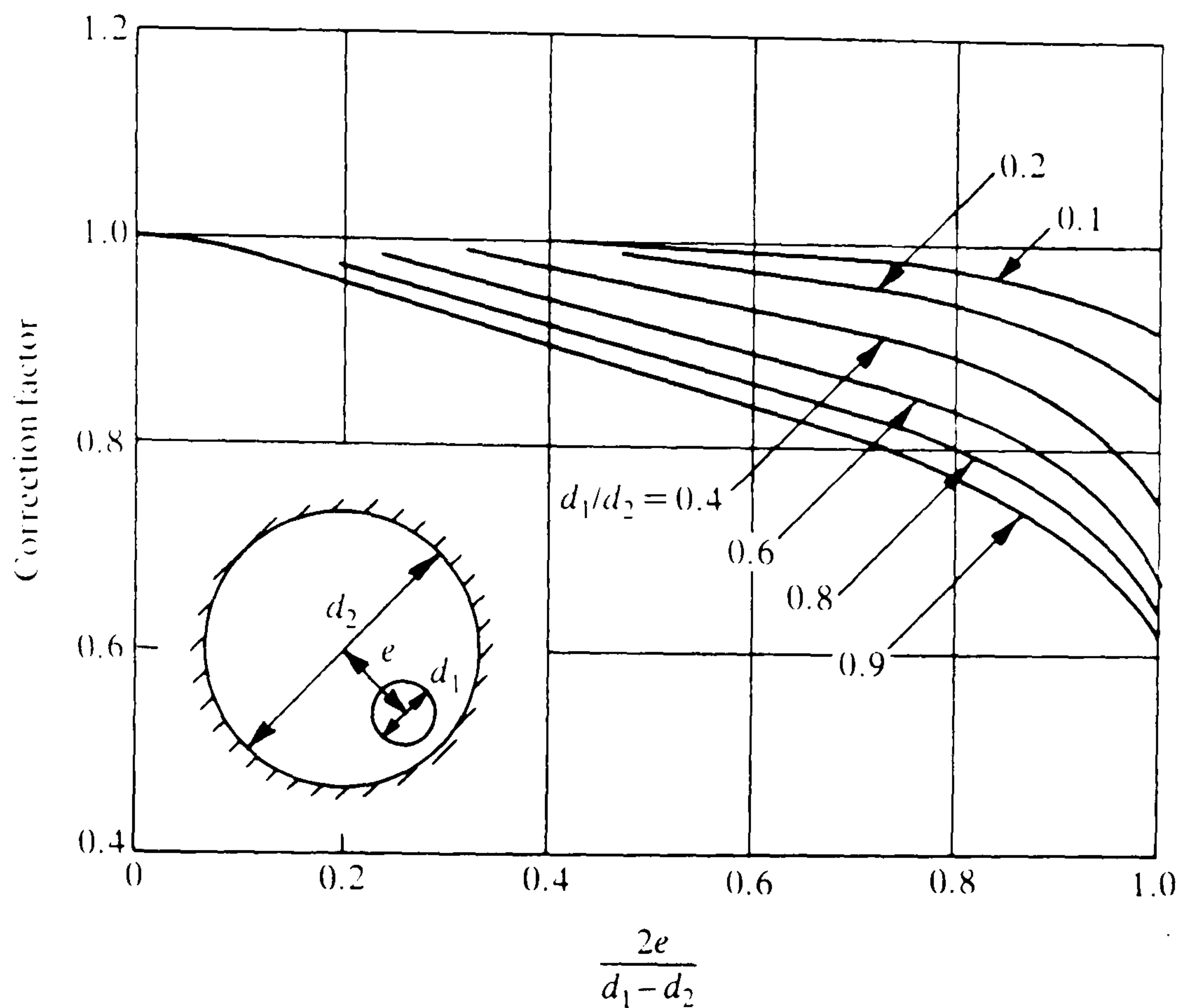


Figure 4.8. Correction factors for eccentric annuli

Substituting Equation 4.14 into Equation 4.33 resulted in the following expression:

$$Y = 0 = P_1 - P_2 - \frac{K 8 \rho Q^2}{\pi^2 D^4} \quad (4.34)$$

The partial derivatives of Equation 4.34, which were used in the non-linear model, were of the form:

$$\frac{dY}{dP_1} = 1 \quad (4.35)$$

$$\frac{dY}{dP_2} = -1 \quad (4.36)$$

$$\frac{dY}{dQ_{1,2}} = - \frac{16 K \rho Q_{1,2}}{\pi^2 D^4} \quad (4.37)$$

The dimensionless loss coefficient,  $K$ , was calculated from a method developed by Annand (1953). It was assumed that the strainer was comprised of round wires, woven to form a square mesh, and that the flow of oil was at



an angle of incidence of 90° to the plane of the mesh. Thus,

$$K = K_{\infty} \times \left( \frac{K}{K_{\infty}} \right) \quad (4.38)$$

The loss coefficient at high Reynolds numbers,  $K_{\infty}$ , was found from an empirical correlation by de Vahl Davis (1964):

$$K_{\infty} = \left( \frac{1 - \phi \lambda}{\phi \lambda} \right)^2 \quad (4.39)$$

Where the porosity,  $\lambda$ , of a woven screen of square mesh composed of wire strands of diameter,  $d$ , was given by:

$$\lambda = (1 - md)^2 \quad (4.40)$$

and the coefficient of contraction of the flow,  $\phi$ , was expressed as:

$$\phi = 1.09 - 0.35\lambda \quad (4.41)$$

The parameter  $K/K_{\infty}$ , in Equation 4.38, was dependent on the Reynolds number, and was found from an adaption of graphical data published by Ward-Smith (1980), as shown in Figure 4.9.

The Reynolds number used in Figure 4.9 was dependent on the wire diameter. Given the mean velocity of the flow approaching the screen,  $V$ , the Reynolds number,  $Re_d$ , was expressed by the following equation:

$$Re_d = \frac{Vd\rho}{\mu} \quad (4.42)$$

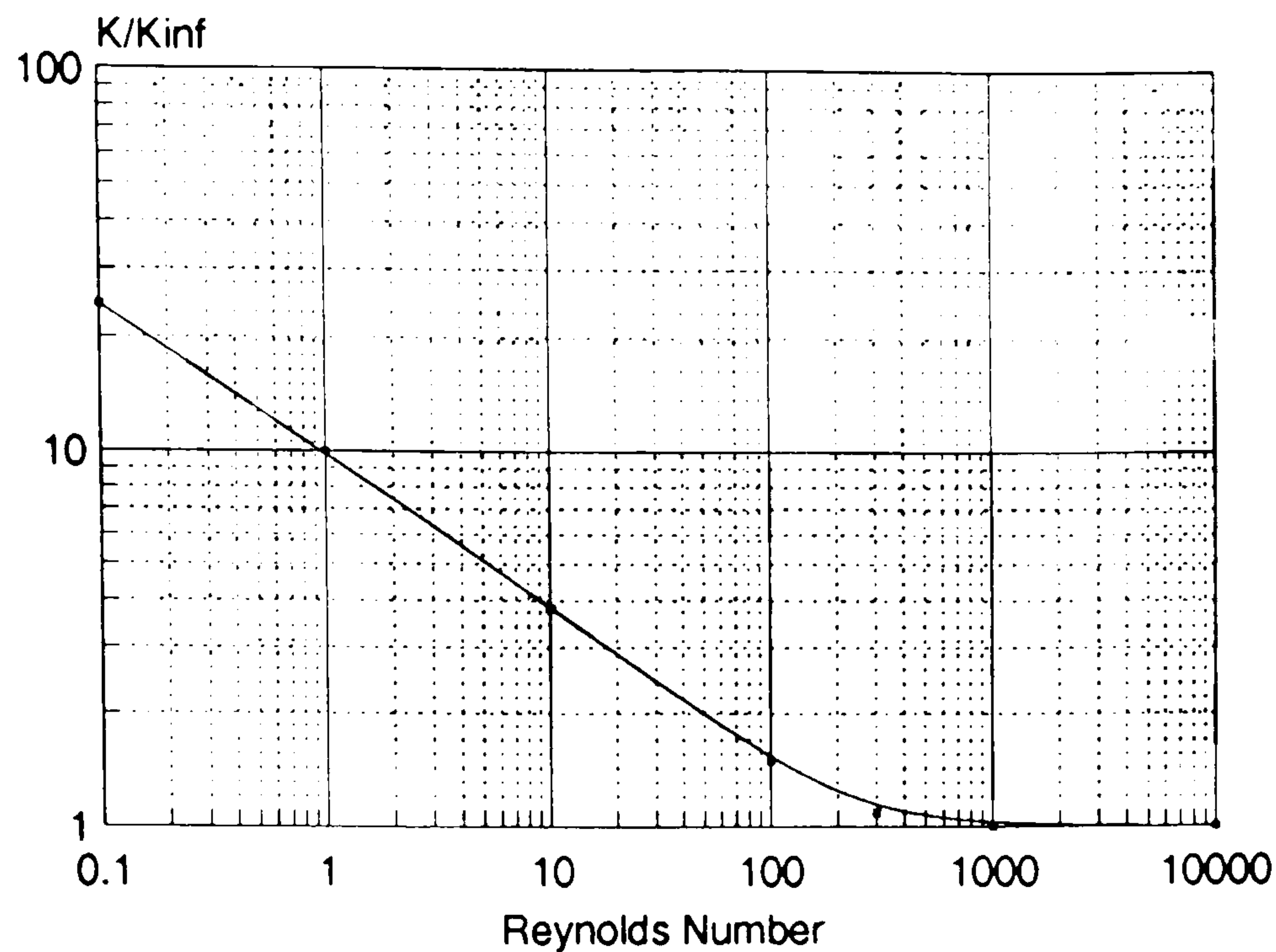


Figure 4.9. Influence of Reynolds number on pressure drop across a woven screen

## 4.6 Oil Filters

The equation used to represent the pressure loss v flow rate relationship through the oil filter was based on an equation derived by Jaisinghani and Sprenger (1981):

$$\frac{\Delta P}{L} = \frac{224 (1.07 - \epsilon)}{Re \log_{10} \left( \frac{10^6}{Re} \right)} \cdot \frac{1 - \epsilon}{\epsilon^2} \cdot \frac{\rho V^2}{D_f} \quad (4.43)$$

Where

$$Re = \frac{D_f V \rho}{\epsilon \mu} \quad \text{and} \quad V = \frac{Q}{A_f} \quad (4.44)$$

Therefore, by substitution, Equation 4.43 became:

$$P_1 - P_2 = \frac{224 L \mu (1.07 - \epsilon) (1 - \epsilon)}{D_f^2 A_f \epsilon \left( \log_{10} \left( \frac{1 \times 10^5 \epsilon A_f \mu}{D_f Q_{1,2} \rho} \right) \right)} \cdot Q_{1,2} = 0 \quad (4.45)$$

It had initially been assumed that the pressure loss v flow rate relationship of Equation 4.45 was of a non-linear form, because of the  $\text{Log}_{10} f(Q)$  term in the denominator. However, upon further investigation, it was found that the relationship was linear, not only at the operating oil flow rate of approximately  $2.0 \times 10^{-4} \text{ m}^3/\text{s}$ , but also over a wide range of flow rates. The results to show this linearity, for three ranges of oil flow rates, are shown in Appendix D.3.

As the relationship was linear, the pressure loss v flow rate characteristics for the filter were represented by the equation for a straight line,  $Y=MX+C$ . The model calculated two values of  $\Delta P$  ( $P_1-P_2$ ), for two arbitrary values of flow rate,  $Q_{1,2}$  ( $2.0 \times 10^{-4}$  and  $10.0 \times 10^{-4} \text{ m}^3/\text{s}$ ). This resulted in two simultaneous equations, from which the slope,  $M$ , and the constant,  $C$ , were calculated. This resulted in a single  $Y=MX+C$  equation which represented the pressure loss v flow rate relationship for the filter:

$$Y = 0 = P_1 - P_2 - MQ_{1,2} - C \quad (4.46)$$

The partial derivatives of Equation 4.46, which were used in the non-linear model, were of the form:

$$\frac{dY}{dP_1} = 1 \quad (4.47)$$

$$\frac{dY}{dP_2} = -1 \quad (4.48)$$

$$\frac{dY}{dQ_{1,2}} = -M \quad (4.49)$$

## 4.7 Journal Bearings

The primary purpose of any engine lubrication system is to provide a pressurised feed of oil to the various engine journal bearings. As such, the



journal bearings are usually the last component in each flow branch of the pressurised lubrication system. An accurate representation of the pressure loss and flow rate characteristics through the journal bearings is essential if an accurate simulation of the whole lubrication system is to be achieved.

Jaguar engines contained two types of journal bearings; partially grooved bearings, and non-grooved bearings. The equations which were initially used to represent the flow of oil through these types of bearings were derived from information contained in a Vandervell bearing design manual (1977). The equation for fully or partially grooved bearings was of the form:

$$Q_{1,2} = \left( \frac{C_r^3 (1 + 1.5 \epsilon^2)}{3\mu} \times \frac{2\pi R_1}{L} \right) P_1 = \frac{UC_r L \epsilon}{2} \quad (4.50)$$

and for non-grooved bearings:

$$Q_{1,2} = \left( \frac{C_r^3 (1 + 1.5 \epsilon^2)}{3\mu} \times \tan^{-1} \left( \frac{2\pi R_1}{L} \right) \right) P_1 = UC_r L \epsilon \quad (4.51)$$

Following a discussion with Glacier Vandervell, the bearing suppliers to Jaguar, it became clear that Equations 4.50 and 4.51 were subject to some error. It appeared that although Equation 4.50 provided flow predictions of the correct magnitude, Equation 4.51 over-estimated the flow and gave values greater than those predicted by Equation 4.50 for a bearing of comparable size. In fact, the flow through a non-grooved bearing should have been less than the flow through a grooved type of the same size. It was concluded that this error lay in the ' $\tan^{-1}$ ' term of Equation 4.51. This may have been a result of a typing error in the bearing design manual, or misinterpretation in the past when the equation was being formed.

Glacier Vandervell recommended the use of more 'up-to-date' equations, which are presented in the following sections. These equations were correlated by Martin and Lee (1982), for the prediction of the feed pressure flow (hydrostatic) of a journal bearing. As discussed in Section 2.5.1, these equations were reported to represent a good approximation to actual bearing oil flow rates.

#### 4.7.1 Partially Grooved Bearings

Jaguar engines contained several partially grooved bearings. Commonly, all the main bearings apart from the central main bearing were partially grooved. On the AJ6 engine the first bearing on each cam-shaft was also partially grooved. It was assumed that the groove extended for  $180^\circ$  around the circumference of the bearing, on the non-loaded side. The equation for a partially grooved bearing was of the form:

$$Y = 0 = Q_{1,2} - \left[ \left( \frac{1.25 - 0.25a/L}{6(L/a - 1)^{0.333}} \times f_1 \right) + \left( \frac{D/L}{6(1 - a/L)} \times f_2 \right) \right] \frac{C_r^3}{\mu} \cdot P_1 \quad (4.52)$$

The partial derivatives of Equation 4.52, which were used in the non-linear flow model, were of the form:

$$\frac{dY}{dP_1} = - \left[ \left( \frac{1.25 - 0.25a/L}{6(L/a - 1)^{0.333}} \times f_1 \right) + \left( \frac{D/L}{6(1 - a/L)} \times f_2 \right) \right] \frac{C_r^3}{\mu} \quad (4.53)$$

$$\frac{dY}{dP_2} = 0 \quad (4.54)$$

$$\frac{dY}{dQ_{1,2}} = 1 \quad (4.55)$$

The constants of feed groove geometry,  $f_1$  and  $f_2$  were dependent on groove extent and bearing eccentricity,  $\epsilon$ . The values of  $f_1$  and  $f_2$  were found

from graphical data (see Figure 4.10), published by Martin and Lee (1982)\*\*.

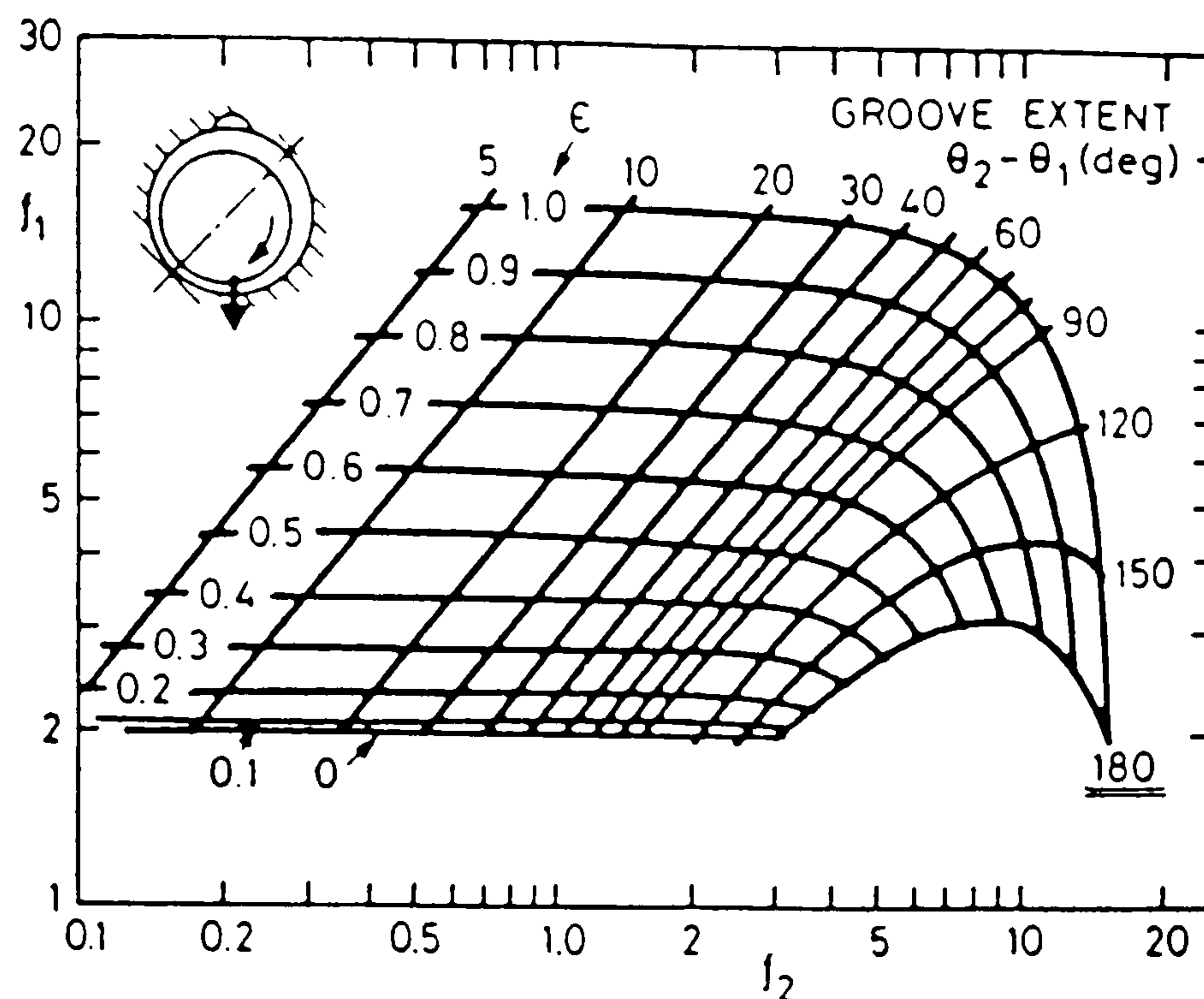


Figure 4.10. Groove functions for one groove in unloaded region

#### 4.7.2 Non-Grooved Bearings

The remaining bearings were usually of a simple feed hole geometry. These commonly included; the big-end bearings; all the cam bearings, apart from the first cam bearing on each cam-shaft in the AJ6 engine; the central main bearing; the timing chain bearing and the power steering pump bearing. The equation for a non-grooved bearing was of the form:

$$Y = 0 = Q_{1,2} - \left[ 0.675 \left( \frac{h_g}{C_r} \right)^3 \left( \frac{d_h}{L} + 0.4 \right)^{1.75} \right] \frac{C_r^3}{\mu} \cdot P_1 \quad (4.56)$$

The partial derivatives of Equation 4.56, which were used in the non-linear flow model, were of the form:

---

\*\*  $f_1$  and  $f_2$  were found using values of bearing eccentricity,  $\epsilon$ , supplied by Glacier Vandervell.



$$\frac{dY}{dP_1} = - \left[ 0.675 \left( \frac{h_g}{C_r} \right)^3 \left( \frac{d_h}{L} + 0.4 \right)^{1.75} \right] \frac{C_r^3}{\mu} \quad (4.57)$$

$$\frac{dY}{dP_2} = 0 \quad (4.58)$$

$$\frac{dY}{dQ_{1,2}} = 1 \quad (4.59)$$

The oil film thickness at the groove mid position,  $h_g$ , was estimated from journal centre orbit plots obtained from Glacier Vandervell (these plots are included in Appendix C.4). This was achieved by measuring the eccentricity of the bearing at various points in the engine cycle and averaging these values to obtain a general value for the oil film thickness at the groove position. The resulting relationship was found to be of the form:

$$h_g = (0.38056 \times \varepsilon \times C_r) + C_r \quad (4.60)$$

The equations for both grooved and non-grooved bearings were sensitive to the values of eccentricity ratio, radial clearance, and oil viscosity. Before the heat transfer model had been developed, the initial flow models assumed a constant oil temperature of 100°C throughout the system. It was concluded that this would yield imprecise results. Therefore, the bearing flow models incorporated a simple temperature rise model for the prediction of the working temperature, and therefore, the working viscosity of the oil. This temperature rise model is presented in section 5.3.1.

Following the completion of the full heat transfer model of the lubrication system, this simple temperature rise model was retained, for use in the first pass of the flow model. This provided more representative oil temperatures for use in the flow model, before more accurate oil temperatures were obtained from the heat transfer model in the following iterations.

## 4.8 Crank-Shaft Oil Transfer Holes

The equations used to represent the flow of oil through an oil transfer hole in a rotating crank-shaft were derived from a study by Meernik (1986). It was assumed that the main bearings were  $180^\circ$  partially grooved, and that there were two transfer holes,  $180^\circ$  apart, which connected to form a single transfer hole at approximately the centre of rotation of the crank-shaft. This eliminated the losses due to non-registry (see section 3.10.1), as almost constant oil feed would be maintained through the crank-shaft transfer holes to the big-end bearings.

The pressure losses were assumed to be the same as those for a pipe, but with the additional considerations of the centrifugal effects, and the losses due to the acceleration of the oil to near journal surface speed within the feed groove of the main bearing. Therefore:

$$\Delta P = \text{Frictional Losses} + \text{Acceleration Losses} + \text{Centrifugal Losses} \quad (4.61)$$

The centrifugal losses, however, were only within the section between the inlet of the transfer hole and the centreline of the crank-shaft. The remaining portion, the section between the centreline of the crank-shaft and the outlet from the transfer hole into the big-end bearing, resulted in a pressure gain. As the exit from the transfer hole was commonly at a larger radius to the centre of rotation than the entrance to the transfer hole, the centrifugal term resulted in a pressure gain rather than a pressure loss. Therefore, Equation 4.61 was re-written as:

$$\Delta P = \text{Frictional Losses} + \text{Acceleration Losses} - \text{Centrifugal Gain} \quad (4.62)$$

This resulted in a relationship of the form:

$$[P_1 - P_2] = \left[ \frac{128\mu L}{\pi D^4} Q_{1,2} \right] + \left[ \frac{1}{2} \varrho (\omega r)^2 \right] - \left[ \frac{1}{2} \varrho \omega^2 (R^2 - r^2) \right] \quad (4.63)$$

By re-arranging, Equation 4.63 became:

$$Y = 0 = P_1 - P_2 - \frac{128\mu L}{\pi D^4} Q_{1,2} - \varrho \left( (\omega r)^2 - \frac{(\omega R)^2}{2} \right) \quad (4.64)$$

The partial derivatives of Equation 4.64, which were used in the non-linear flow model, were of the form:

$$\frac{dY}{dP_1} = 1 \quad (4.65)$$

$$\frac{dY}{dP_2} = -1 \quad (4.66)$$

$$\frac{dY}{dQ_{1,2}} = - \frac{128\mu L}{\pi D^4} \quad (4.67)$$

## 4.9 Cam Bearing Oil Transfer Holes

The cam bearings on the AJ6 engine were supplied with oil through a transfer hole, from a gallery passing through the centre of the cam-shaft. The equations derived to represent the flow of oil within the cam bearing oil transfer holes, were similar to those used for the crank-shaft oil transfer holes. There were, however, two different types of oil transfer flow. In the first bearing on each cam-shaft, the oil flowed from the cam journal towards the centre of the cam-shaft. In the remaining cam bearings, the oil flowed away from the centre of the cam-shaft to the journal surfaces.



### 4.9.1 Flow Towards Cam-Shaft Centre

The equation derived to represent the flow of oil through the first cam bearing into the oil gallery at the centre of each cam-shaft, was of a similar form to Equation 4.61. As the oil flow was towards the centre of the rotating shaft, the centrifugal effects opposed the flow. Therefore:

$$\Delta P = \text{Frictional Losses} + \text{Acceleration Losses} + \text{Centrifugal losses} \quad (4.68)$$

This resulted in an equation of the form:

$$[P_1 - P_2] = \left[ \frac{128\mu L_T}{\pi D_T^4} Q_{1,2} \right] + \left[ \frac{1}{2} \rho (\omega R_c)^2 \right] + \left[ \frac{1}{2} \rho \omega^2 (R_c^2 - R_{in}^2) \right] \quad (4.69)$$

By re-arranging, Equation 4.69 became:

$$Y = 0 = P_1 - P_2 - \frac{128\mu (R_c - R_{in})}{\pi D_T^4} Q_{1,2} - \rho \left( (\omega R_c)^2 - \frac{(\omega R_{in})^2}{2} \right) \quad (4.70)$$

The partial derivatives of Equation 4.70, which were used in the non-linear flow model, were of the form:

$$\frac{dY}{dP_1} = 1 \quad (4.71)$$

$$\frac{dY}{dP_2} = -1 \quad (4.72)$$

$$\frac{dY}{dQ_{1,2}} = - \frac{128\mu (R_c - R_{in})}{\pi D_T^4} \quad (4.73)$$

### 4.9.2 Flow Away from Cam-Shaft Centre

The equation derived to represent the flow of oil from the oil gallery at the centre of the cam-shaft to the cam bearing journal surface, was similar in form to Equation 4.61. However, in this case, there were no acceleration losses as the oil was not being accelerated to journal speed within an oil feed groove. In addition, the oil flow was assisted by the centrifugal effects of the rotating transfer hole, resulting in a centrifugal pressure gain rather than a centrifugal loss. Thus:

$$\Delta P = \text{Frictional losses} - \text{Centrifugal gain} \quad (4.74)$$

This resulted in an equation of the form:

$$Y = 0 = P_1 - P_2 - \frac{128\mu(R_c - R_{in})}{\pi D_T^4} Q_{1,2} + \frac{1}{2} \rho \omega^2 (R_c^2 - R_{in}^2) \quad (4.75)$$

The partial derivatives of Equation 4.75 were the same as Equations 4.71, 4.72 and 4.73.

## 4.10 Oil Coolers

The pressure loss through an oil cooler was calculated using the same approach used for circular cross-sectional pipes, which were documented in section 4.3. For laminar flow, the flow characteristics through an oil cooler were represented by Equation 4.16 and the partial derivatives of this equation 4.17, 4.18 and 4.19. The pressure loss within the diverging and converging chambers at both ends of the oil cooler were considered to be negligible.

For turbulent flow, the flow characteristics were represented by Equation 4.26 and the partial derivatives 4.27, 4.28 and 4.29. The pressure

losses within the diverging and converging chambers at both ends of the oil cooler were accounted for by using loss coefficients obtained from Miller (1990). This was a similar approach taken for the losses through bends and other obstructions documented in section 4.3.2, for turbulent pipe flow.

The pressure loss due to friction within the oil cooler was considered to be represented by the pressure loss through one tube. In particular, this was equated to the pressure loss through one finned section within the tube. The cross-sectional shape of the finned section was represented by use of the hydraulic diameter concept,  $D_h$ . Therefore the diameter term,  $D$ , in Equations 4.16 and 4.26 were replaced by the hydraulic diameter,  $D_h$ . Figure 4.11 shows a cross-section through an oil tube of a typical Jaguar engine oil cooler.

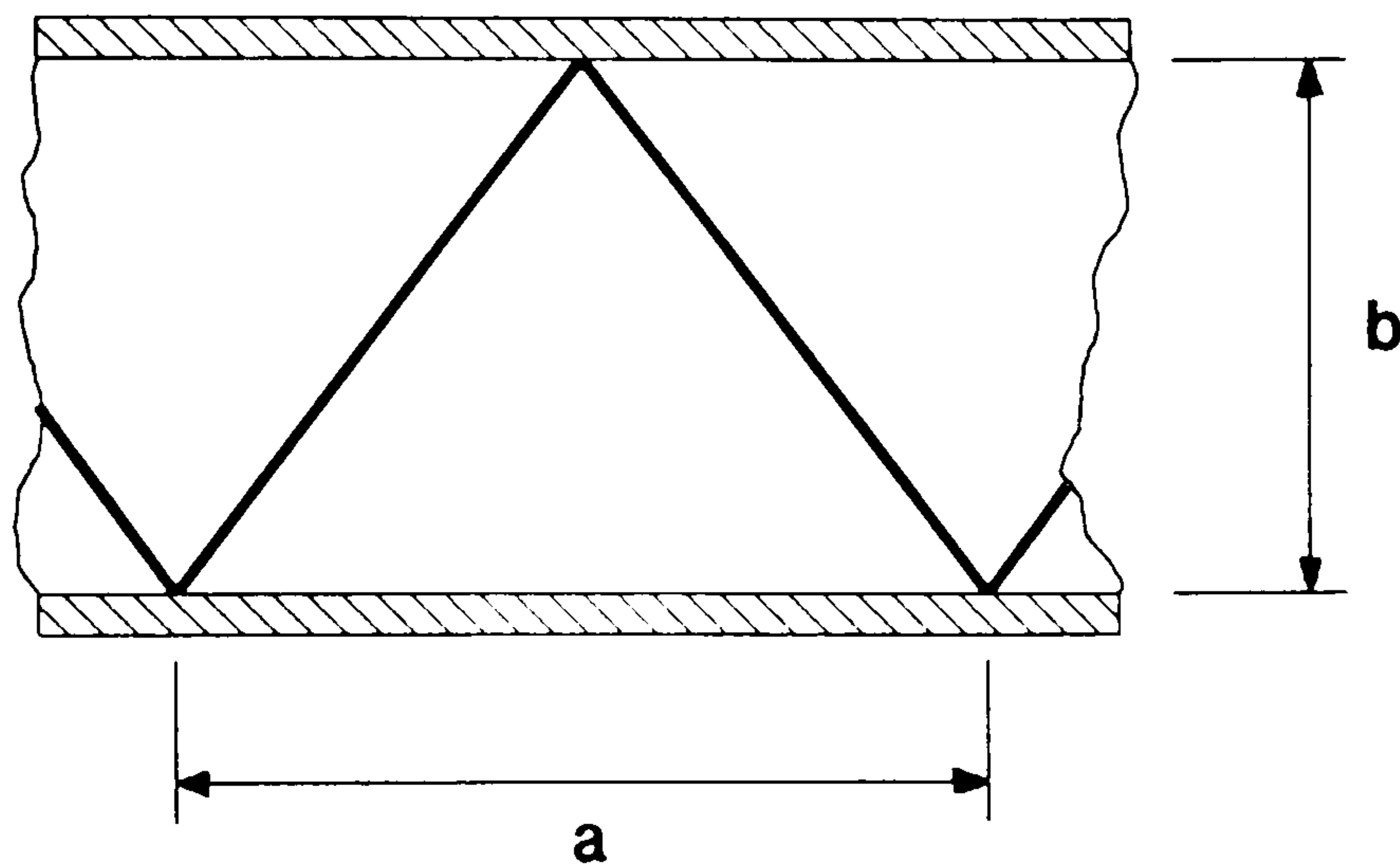


Figure 4.11. Cross-section through a finned oil tube in an oil cooler

The hydraulic diameter,  $D_h$ , for the triangular passage depicted in Figure 4.11 was represented as:

$$D_h = \frac{4 \times \text{flow area}}{\text{wetted perimeter}} \quad (4.76)$$



For an oil tube with a fin pitch,  $f_p$  per metre:

$$a = \frac{2}{f_p} \quad (4.77)$$

and Equation 4.76 became:

$$D_h = \frac{2ab}{\left( \left( \sqrt{\left( \frac{a}{2} \right)^2 + b^2} \times 2 \right) + a \right)} \quad (4.78)$$

## 4.11 Conclusions

The lubrication system flow network was represented by breaking the system down into a series of component elements joined at nodal points. The flow through each component element was represented by a pressure loss v flow rate equation. Flow continuity was maintained throughout the system by equating the sum of flows into each dividing node to zero.

In the linear flow model, the physical system was represented by six types of component elements; pumps, pipes, filters, journal bearings, crankshaft transfer holes, and cam bearing transfer holes. The characteristics of the linear flow model were:

- i, The pressure loss v flow rate equations for the elements were in a linear form.
- ii, It was assumed that the flow was laminar within the pipes and drillings. Pressure losses within bends and junctions were assumed to be negligible.
- iii, The oil pump characteristics were simplified to two linear regions.

- iv, It was assumed that the oil temperature was 100°C throughout the system. This was true for every component element apart from the journal bearing model, which included a simple temperature rise calculation to predict the working temperature of the oil.
- v, It was assumed that the pressures at entry and exit from the system were atmospheric. Oil gauge pressures were predicted simultaneously with oil flow rates.

The non-linear flow model utilised the same method of representing the physical system by breaking the system down into component elements joined at nodal points. However, due to the iterative solution method employed, the flow characteristics of the component elements could be represented by either a linear or a non-linear relationship. In addition to the component elements used in the linear model, the non-linear flow model incorporated; turbulent flow through pipes; laminar and turbulent flow through annular pipes; an oil strainer model, and an oil cooler model. The non-linear flow model was characterised by:

- i, The pressure loss v flow rate relationships were either in a linear or a non-linear form.
- ii, Turbulent flow losses could be modeled in pipe elements. The pressure losses included friction losses and losses due to bends and other disturbances.
- iii, Oil pump characteristics were represented by a piece-wise linear approach.
- iv, The simple oil temperature rise model for the bearings was retained for the flow calculation. The oil was assumed to be at a constant temperature throughout the rest of the system. This temperature was selected by the user. However, if the heat transfer model was included

in the simulation process, the predicted oil temperatures within each of the individual component elements could be used.

- v, The values for both the pressures and the flow rates were returned directly.

This chapter presented the relationships which were derived to represent the pressure loss v flow rate characteristics of each component element. Linear relationships were derived for the component elements used in the linear flow model. The non-linear flow model was constructed in such a manner as to allow the use of either the linear relationships derived for the linear model, or use the non-linear relationships derived to represent the flow through the individual components. Program flexibility was improved, with the addition of component elements with non-linear flow characteristics. The non-linear pressure loss v flow rate characteristics of these components were also presented.



## Chapter 5

# Mathematical Model of Heat Transfer Within the Lubrication System

### 5.1 Introduction

The full thermofluid simulation of an engine lubrication system was achieved by an interaction between an analysis of the flow conditions (using the models described in Chapter 4) and an analysis of the heat transfer within the system. The predictor/corrector modelling procedure which was developed is shown in the flow chart in Figure 5.1.

The heat transfer within the lubrication system was assumed to consist of two parts; heat transfer within the pressurised side of the system, and heat transfer to the oil splashed or sprayed onto the engine surfaces. The fundamentals of the heat transfer through these two paths was presented in Chapter 3. Two models were developed to represent both these heat transfer paths. The first heat transfer model developed accounted for the heat transfer within the pressurised side of the lubrication system. This model will hereafter be referred to as 'the heat transfer model'. As shown in Figure 5.1, the heat transfer model utilised data produced by the non-linear flow model (described in Chapter 4). This data represented both the physical layout of the system and the pressure losses and flow rates through each component element. The heat transfer within the system was modelled with the simultaneous calculation of the oil temperature within each individual component element in the system.

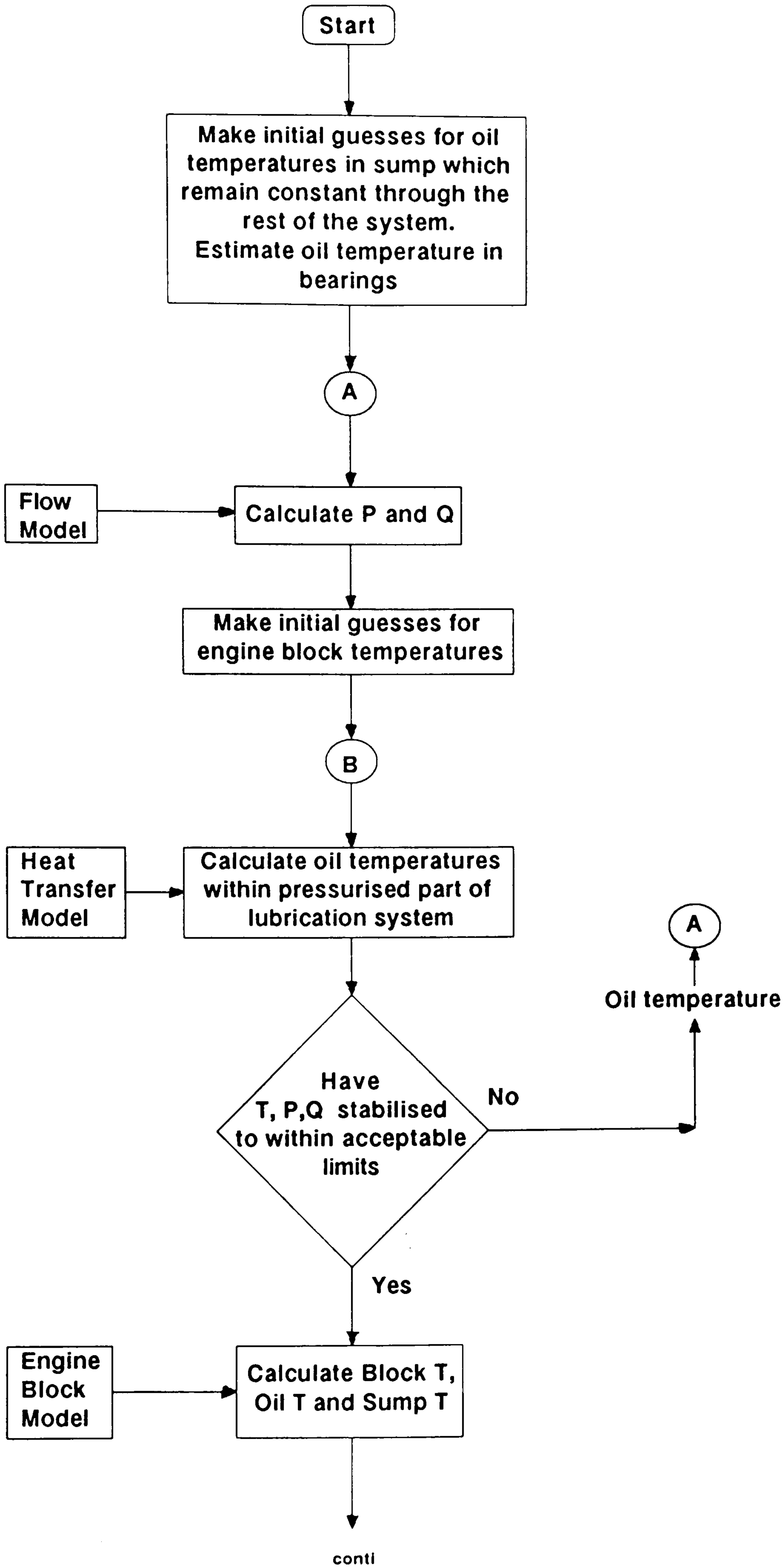


Figure 5.1. Thermofluid analysis procedure for an engine lubrication system

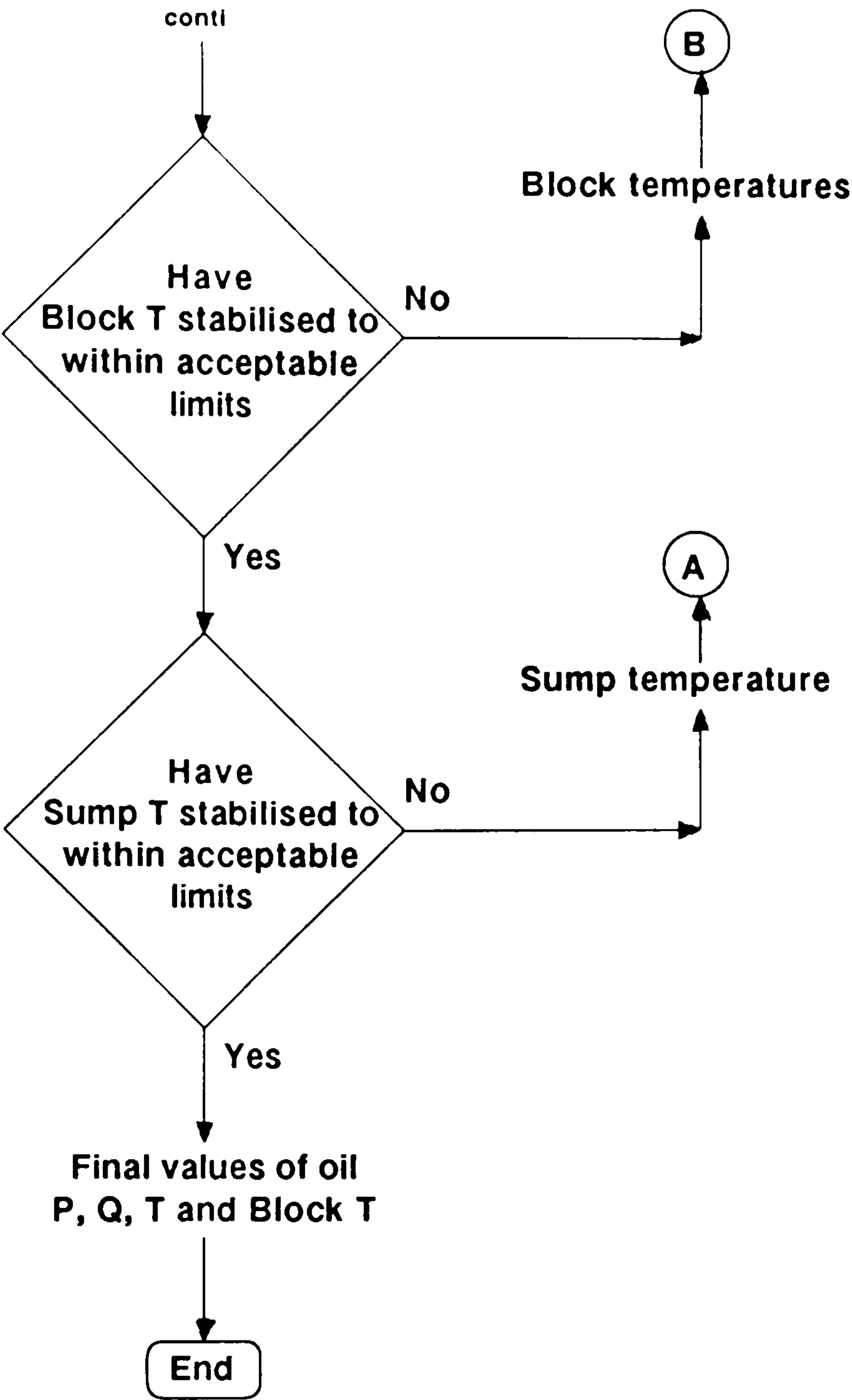


Figure 5.1. .... Continued



It was assumed that there was a negligible change in the oil temperature as it passed through what were considered to be non-heat generating components, such as the oil pump, the oil strainer and the oil filter. The heat transfer within the pipes, annular pipes, crankshaft transfer holes and cam bearing transfer holes, was represented by the expression for the heat transfer in a circular pipe, which is presented in section 5.2. Additional models were derived to represent the heat transfer within the journal bearings and the oil cooler.

The heat transfer model utilised the Levenberg-Marquardt non-linear routine (this routine is described in Appendix A.2.1). This was the same routine used in the non-linear flow model, the model with which it was intended to be integrated. The equations which were derived to represent the heat transfer within each component element, and the partial derivatives of these equations, are presented in this chapter. These equations were used in the Levenberg-Marquardt routine to calculate the oil temperatures at each node in the flow network.

The second heat transfer model accounted for the heat transfer to the oil which was splashed onto the various internal engine surfaces. This model will hereafter be referred to as 'the engine block model', which is presented in section 5.5. The approach taken, was to model the heat transfer processes of a representative piston/liner/block assembly. The physical layout of this assembly was represented by a series of block elements, which in turn, were represented by a nodal resistance network. The oil splash was modelled as a falling film of fluid on the internal surfaces of the engine. The falling oil film represented one of the boundary convective fluids in the engine block heat transfer model. The other boundary convective fluids were the combustion gases, the coolant and the air.

The engine block model used the Levenberg-Marquardt non-linear routine and predicted the engine metal temperatures and the temperatures of the oil film simultaneously. It was intended that the engine block model would eventually be integrated with the heat transfer model, for the prediction of the wall temperatures of the pipe elements. The equations which were derived to represent the various heat transfer paths within the engine block, are presented in this chapter.

### 5.1.1 Structure of the Heat Transfer and Engine Block Models

The heat transfer model utilised data provided by the non-linear flow model. This data represented the physical layout of the lubrication system by breaking the system down into component elements joined at nodal points. Each heat transfer element in the system (pipe, annular pipe, crank-shaft transfer hole, cam bearing transfer hole, bearing, oil cooler) was represented by a heat transfer equation, of the form shown in Equation 5.1.

$$Y = 0 = f(T_{bin}, T_{bo}) \quad (5.1)$$

Thus, the heat transfer through the whole lubrication system was represented by a set of simultaneous equations which represented the heat transfer characteristics of each of the appropriate component elements. The heat transfer within the pumps, strainers and filter elements was considered to be negligible. The exit temperature of the oil from these non-heat transfer components was assumed to be the same as at the inlet.

The set of simultaneous equations in the heat transfer model were solved by the Levenberg-Marquardt algorithm. This returned the temperatures at the entry and exit from each of the heat transfer elements. The standard deviation term,  $\sigma$ , was fixed at a value of 1.0 for each equation. Lubrication

systems of various sizes were modelled, no problems were encountered, and the value for  $\sigma$  appeared to be suitable for general use.

Each node,  $i$ , in the nodal resistance network with more than one thermal resistance connected to it was represented by an expression in the form of Equation 5.2:

$$Y = 0 = \sum_j f(t_j, t_i) \quad (5.2)$$

Thus, the whole nodal resistance network was represented by a set of simultaneous equations, which were solved by the Levenberg-Marquardt routine. This returned the temperatures at each of the these nodes. In the nodal resistance model  $\sigma$  was also fixed at a value of 1.0 for each equation.

In the oil splash model, which is presented in section 5.5.2, the oil flowing down the wetted internal surfaces of the engine was simplified to an oil flow network. This network was represented by a combination of two types of equations:

- i, An equation which represented the heat transfer to a falling oil film:

$$Y = 0 = f(T_{\text{entry}}, T_{\text{exit}}) \quad (5.3)$$

- ii, and an equation which linked the temperature of the oil film leaving one wetted surface with the temperature of the oil film entering the next wetted surface:

$$Y = 0 = f(T_{\text{entry}}, T_{\text{exit from previous surface}}, T_{\text{exit from other oil sources}}) \quad (5.4)$$



The 'other oil sources' shown in Equation 5.4 were considered to be the oil splashed onto the wetted surface from the various engine bearings.

Thus, the oil flow network, which represented the falling oil films within the engine, was in turn represented by a set of simultaneous equations. This set of equations were solved by the Levenberg-Marquardt routine to yield the inlet and exit temperatures of the oil for each wetted surface. A value of 1.0 was used for  $\sigma$  throughout the model, for both types of equations. The engine block model was tested for various sizes of systems, again no problems were encountered, and the value for  $\sigma$  appeared to be suitable for general use.

## 5.2 Pipe Model

The equation derived to represent the heat transfer within circular pipes was also used to represent annular pipes, crankshaft transfer holes, and cam bearing transfer holes. It was assumed that the wall temperature,  $t_s$ , remained constant throughout the calculation procedure (the values of  $t_s$  which were used to model the V8 engine were obtained from an FEA model of the V8 engine block by Chang et al (1992)). The resulting energy balance equation was of the form:

$$q = h\pi DL(t_s - t_b)_m = \dot{m}C_p(t_{bo} - t_{bin}) \quad (5.5)$$

$(t_s - t_b)_m$  was the mean of the temperature difference  $(t_s - t_b)$  over the length  $L$ . The mean value for  $(t_s - t_b)$  as it varied from  $(t_s - t_{bin})$  to  $(t_s - t_{bo})$  was represented by the log mean, as given in Equation 5.6.

$$(t_s - t_b)_m = \frac{(t_s - t_{bin}) - (t_s - t_{bo})}{\ln \left( \frac{t_s - t_{bin}}{t_s - t_{bo}} \right)} \quad (5.6)$$

Substituting Equation 5.6 into Equation 5.5 yielded the expression which was used to represent the heat transfer within a pipe element:

$$Y = 0 = h\pi DL \left( \frac{(t_s - t_{bin}) - (t_s - t_{bo})}{\ln \left( \frac{t_s - t_{bin}}{t_s - t_{bo}} \right)} \right) - \dot{m} C_p (t_{bo} - t_{bin}) \quad (5.7)$$

The partial derivatives of Equation 5.7 were:

$$\frac{dY}{dt_{bin}} = - \left( \frac{\left( h\pi DL \cdot \ln \left( \frac{t_s - t_{bin}}{t_s - t_{bo}} \right) \right) + \left( \frac{h\pi DL (t_{bo} - t_{bin})}{t_s - t_{bin}} \right)}{\left( \ln \left( \frac{t_s - t_{bin}}{t_s - t_{bo}} \right) \right)^2} \right) + \dot{m} C_p \quad (5.8)$$

$$\frac{dY}{dt_{bo}} = \left( \frac{\left( h\pi DL \cdot \ln \left( \frac{t_s - t_{bin}}{t_s - t_{bo}} \right) \right) - \left( \frac{h\pi DL (t_{bo} - t_{bin})}{t_s - t_{bo}} \right)}{\left( \ln \left( \frac{t_s - t_{bin}}{t_s - t_{bo}} \right) \right)^2} \right) - \dot{m} C_p \quad (5.9)$$

The variables,  $h$ ,  $\dot{m}$ , and  $C_p$  were found for the average bulk fluid temperature  $(t_{bin} + t_{bo})/2$ . The temperatures  $t_{bin}$  and  $t_{bo}$  were calculated during the previous iteration of the program. The heat transfer coefficient,  $h$ , was calculated from the expression:

$$h = Nu \frac{k}{D} \quad (5.10)$$

For fully developed **laminar** flow with a constant surface temperature, the Nusselt number,  $Nu$ , was given by Equation 5.11. This equation was used for 'long' pipes where the starting length was ignored. Pipes were considered to be long if  $(D/L)RePr < 10$ .

$$Nu = 3.66 \quad (5.11)$$

For  $(D/L)RePr \geq 10$ , the pipe was considered to be 'short', and the empirical relation of Sieder and Tate (1936) was used:

$$Nu = 1.86 \left[ \left( \frac{D}{L} \right) Re Pr \right]^{\frac{1}{3}} \left( \frac{\mu}{\mu_s} \right)^{0.14} \quad (5.12)$$

For **turbulent** flow conditions, the following empirical equation of Sieder and Tate (1936) was used to calculate the Nusselt number when the ratio  $L/D \geq 60$ .

$$Nu = 0.027 Re^{0.8} Pr^{\frac{1}{3}} \left( \frac{\mu}{\mu_s} \right)^{0.14} \quad (5.13)$$

For pipes with a ratio of  $L/D < 60$ , an equation derived by Nusselt (1931) was used:

$$Nu = 0.036 Re^{0.8} Pr^{\frac{1}{3}} \left( \frac{D}{L} \right)^{\frac{1}{18}} \quad (5.14)$$

The Reynolds number,  $Re$ , was found from Equation 4.13 and the Prandtl number,  $Pr$ , was found from the following general expression:



$$Pr = \frac{\mu C_p}{k} \quad (5.15)$$

### 5.3 Journal Bearing Model

The equations which represented the flow conditions through grooved and non-grooved bearings (see section 4.7) were sensitive to the value of oil viscosity. The linear flow model and the initial non-linear flow model assumed a constant oil temperature of 100°C throughout the system. It was concluded that this would lead to inaccurate results for the flow rates through the bearings. Therefore, the bearing flow model incorporated a simple temperature rise model for the prediction of the working temperature, and therefore the working viscosity of the oil.

#### 5.3.1 Simple Bearing Oil Temperature Rise Model

The simple oil temperature rise model was derived from a method published by Cameron (1981). The model initially calculated the parameter  $\Delta T/C_s$  from the expression:

$$\frac{\Delta T}{C_s} = 8.28 \times 10^{-9} \times \frac{\omega}{Q^*} \times \frac{R_1^2}{C_r^2} \quad (5.16)$$

While the effective flow factor,  $Q^*$ , was found from the relationship:

$$Q^* \approx 0.6 \left( 2 - \frac{L}{2R_1} \right) \quad (5.17)$$

Following the calculation of the parameter  $\Delta T/C_s$ , the temperature change  $\Delta T$  was estimated from graphical data published by Cameron, which was of the form shown in Figure 5.2. Once the working temperature of the oil within the bearing was known, the oil viscosity was found from temperature  $\nu$  viscosity data, which is presented in Appendix C.1.

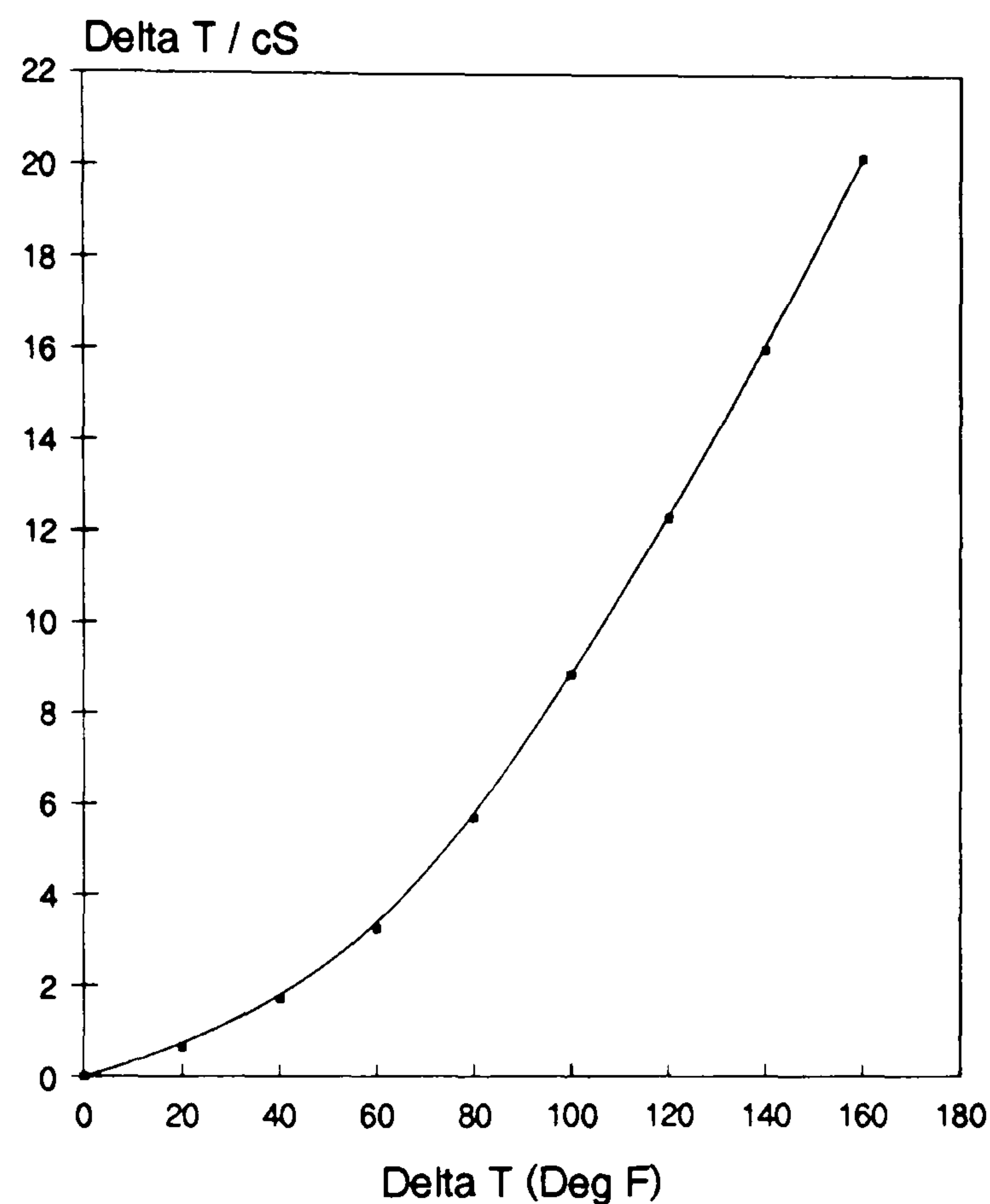


Figure 5.2. Bearing oil temperature rise

### 5.3.2 Enhanced Bearing Heat Transfer Model

It was intended that the heat transfer model of the lubrication system would predict accurate oil temperature values which would be used to estimate the working viscosity of the oil in each component element in the flow model. It was believed that the journal bearings were one of the key component elements and that they played a vital role in the heat transfer to the oil. However, it was considered that the development of an accurate oil temperature rise model for a dynamically loaded journal bearing was a major

research undertaking and was outside the scope of this study.

The oil temperature rise within a bearing was calculated from an adapted journal bearing mobility analysis model, which was developed for Jaguar by Lai (1993). Lai's model equated the oil temperature rise to the bearing cycle-average power loss, for a given speed, feed pressure, and inlet oil temperature. This model was adapted in two ways:

- i, The bearing model initially calculated the bearing power loss with the assumption of a fixed oil temperature within the bearing. The model was adapted to include an iterative loop whereby the working properties of the oil were changed on each iteration according to the power loss calculated on the previous iteration. The iterative procedure continued until a stabilised value for the oil temperature was obtained.
- ii, The bearing model was nested in a series of iterative loops. The adapted model calculated the oil temperature rise for a range of inlet oil temperatures and feed pressures. These results were stored in a data file for use in the heat transfer model. A full description of the adapted bearing program is given in section 7.2.1.

A typical bearing 'map' for a main bearing of the V8 engine is shown in Figure 5.3. The temperature rise characteristics of the bearing were represented by a piece-wise linear approach, where each data point was joined by a straight line. This was a similar approach taken for modelling the flow characteristics of the oil pump, as presented in section 4.2.2.

Using linear interpolation, a unique temperature characteristic curve was estimated for any given feed pressure. The linear region in which the



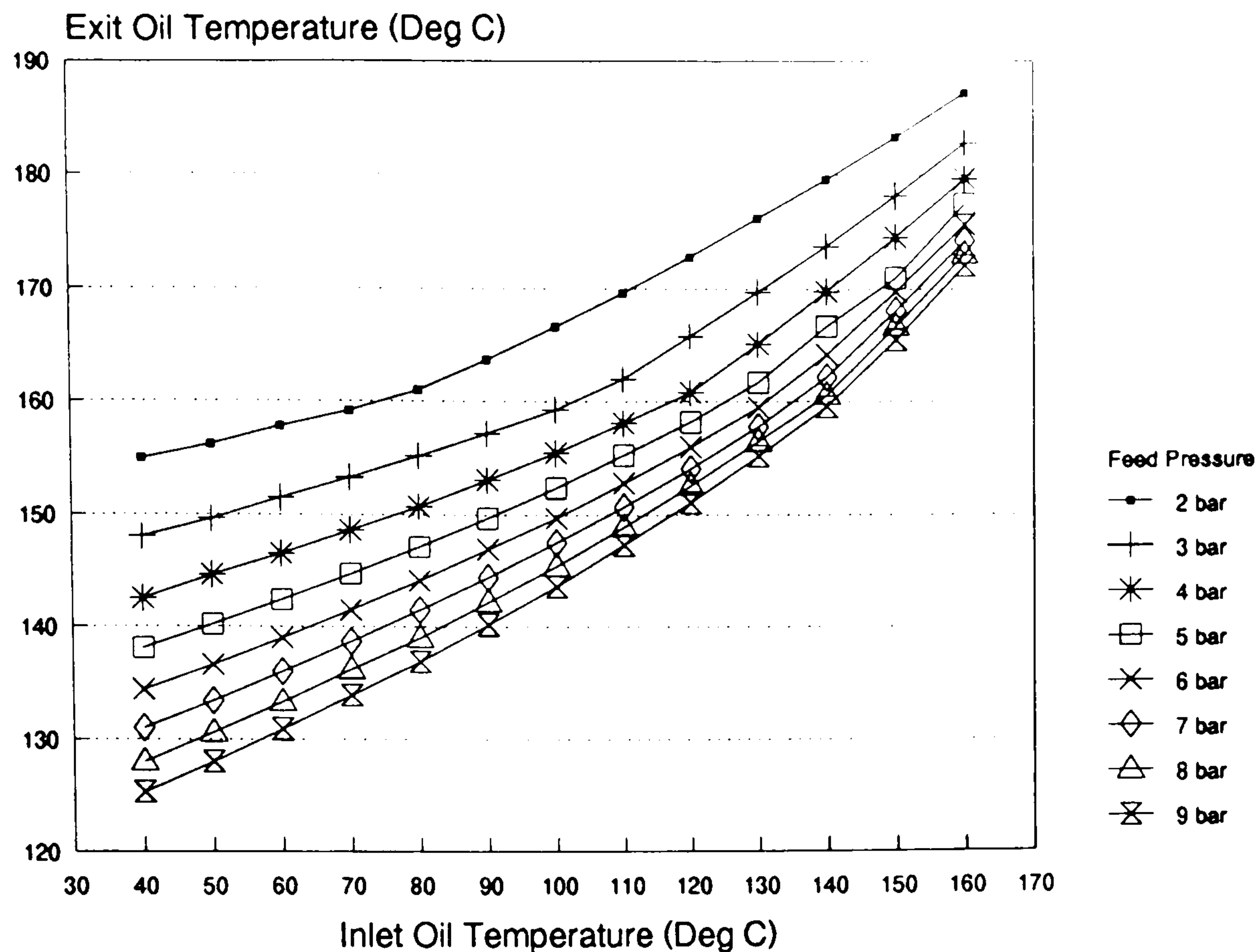


Figure 5.3. Oil temperature rise 'map' for the number 1 main bearing of the V8 engine

bearing was expected to be operating, was estimated from the inlet oil temperature, which was calculated during the previous iteration of the heat transfer model. The slope,  $M$ , and constant,  $C$ , were calculated by the method used for the oil pump model. This method is described in section 4.2.

The temperature rise characteristics for the bearing were represented by the general linear equation:

$$Y = 0 = Mt_{bin} + C - t_{bo} \quad (5.18)$$

The partial derivatives of Equation 5.18 were of the form:

$$\frac{dY}{dt_{bin}} = M \quad \text{and} \quad \frac{dY}{dt_{bo}} = -1 \quad (5.19)$$

## 5.4 Oil Cooler Model

The model derived to represent the heat transfer characteristics of an oil cooler utilised the 'effectiveness - NTU' method. The oil cooler model was based on the following assumptions:

- i, The two working fluids were oil and air. The oil was the 'hot' fluid, and the air was the 'cold' fluid.
- ii, The oil cooler was represented as a compact cross flow heat exchanger.
- iii, The basic construction of the heat exchanger was of a plate-fin type.
- iv, The surface of each plate was covered with an array of longitudinal fins. The fins were not louvred.
- v, The plates and the fins were manufactured from the same material.

The solution approach started with the selection of trial values for the air exit temperature,  $t_{co}$ , and the oil exit temperature,  $t_{ho}$ . The values selected for  $t_{ho}$  and  $t_{co}$  were the values predicted during the last iteration of the heat transfer model. However, for the first iteration of the heat transfer model, the initial guess for  $t_{co}$  was  $t_{cin} + 10^\circ\text{C}$ . The initial guesses for the oil inlet and exit temperatures are presented in section 7.2.3.

The average hot and cold temperatures,  $t_{hav}$  and  $t_{cav}$ , were calculated using the general expressions:

$$t_{cav} = \frac{t_{cin} + t_{co}}{2} \qquad t_{hav} = \frac{t_{hin} + t_{ho}}{2} \qquad (5.20)$$

The values of  $C_p$ , and  $\dot{m}$ , were found for the average temperatures, from the properties for oil and air which are presented in Appendix C.1 and C.2. A Refined estimate of  $t_{co}$  was then obtained using a basic heat balance approach.

The initial value for  $t_{ho}$  remained unchanged, but  $t_{co}$  was found from the following expression:

$$t_{co} = \frac{\dot{m}_h C_{Ph} (t_{hin} - t_{ho})}{\dot{m}_c C_{Pc}} + t_{cin} \quad (5.21)$$

The new value for  $t_{co}$  was substituted into Equation 5.20 and an iterative procedure commenced. It was found that three iterations were usually required to ensure convergence. Based on the assumed values of  $t_{cav}$  and  $t_{hav}$ , the Reynolds numbers for the two fluids were found from the general equation:

$$Re = \frac{D_h G}{\mu} \quad (5.22)$$

The hydraulic diameter,  $D_h$ , was found for both the hot and the cold finned surfaces, using the method presented in section 4.10 for the prediction of the pressure losses through the oil cooler.

Figure 5.4 presents the heat transfer correlation for the plate-fin geometry which closely matched the geometry of the heat exchangers used on Jaguar engines. The data presented in Figure 5.4 was extracted from Kays and London (1964), for two finned plate gaps of 6.35 mm and 2.54 mm. To enhance program flexibility, it was assumed that other plate gaps could be accounted for by interpolating or extrapolating between these curves. Thus, for the Reynolds numbers calculated in Equation 5.22, the parameter  $(h/GC_p)Pr^{2/3}$ , was found from Figure 5.4, for both the hot and the cold fluids. This yielded the heat transfer coefficients,  $h_c$  and  $h_h$ , when the mass velocity,  $G$ , of each stream was given by the expression:



$$G = \frac{\dot{m}}{A_x} \quad (5.23)$$

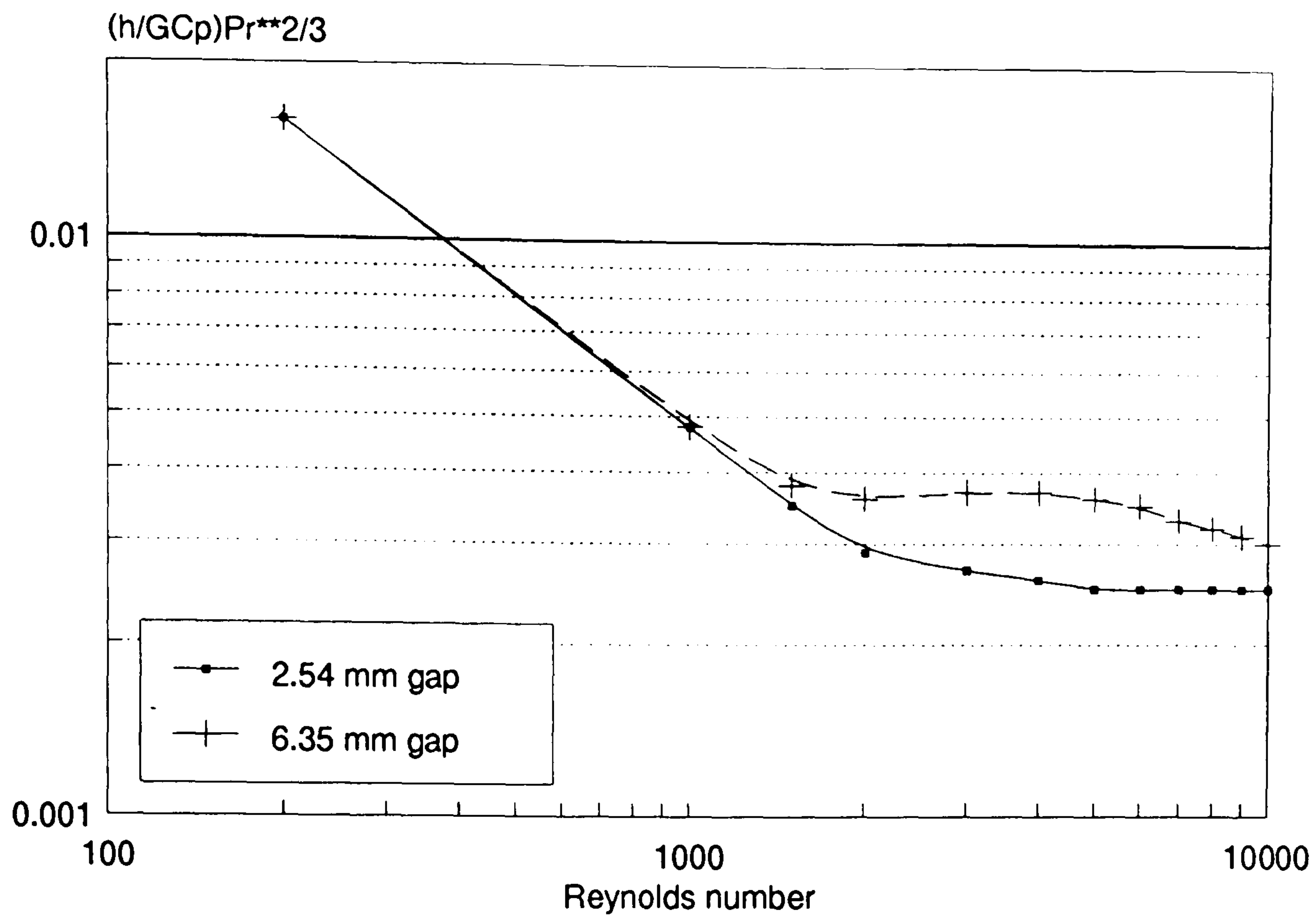


Figure 5.4. Heat transfer data for plate-fin heat exchanger surfaces

The calculation continued with the prediction of the effectiveness,  $\eta$ , of both surfaces, which was given by the expression:

$$\eta = 1 - \left( \frac{A_F}{A} \right) (1 - \kappa) \quad (5.24)$$

The fin efficiency,  $\kappa$ , in Equation 5.24, was calculated for each surface from the expression:

$$\kappa = \frac{\tanh mL}{mL} \quad (5.25)$$

Where

$$mL = L \sqrt{\frac{2h}{kw}} \quad (5.26)$$

and,  $L$ , represented half the length of the fins between the plates. With reference to the fin geometry presented in Figure 4.11, the length,  $L$ , for each finned surface, was given by:

$$L = \frac{\sqrt{\left(\frac{a}{2}\right)^2 + b^2}}{2} \quad (5.27)$$

The overall heat transfer coefficient for the heat exchanger,  $U$ , was calculated for both the hot side and the cold side surfaces. The overall  $U$  for both surfaces were given by the expressions:

$$U_c = \left[ \frac{A_c/A_h}{\eta_h h_h} + \left( \frac{A_c}{A_w} \right) \frac{\Delta x}{k} + \frac{1}{\eta_c h_c} \right]^{-1} \quad (5.28)$$

$$U_h = \left[ \frac{A_h/A_c}{\eta_c h_c} + \left( \frac{A_h}{A_w} \right) \frac{\Delta x}{k} + \frac{1}{\eta_h h_h} \right]^{-1} \quad (5.29)$$

The maximum heat which could be transferred was dependent on the fluid stream with the least capacity rate. If  $\dot{m}_h C_{Ph} < \dot{m}_c C_{Pc}$ , the capacity ratio  $C_R$ , and the Number of Transfer Units, NTU, were defined as:

$$C_R = \frac{\dot{m}_h C_{Ph}}{\dot{m}_c C_{Pc}} \quad \text{and} \quad NTU = \frac{U_h A_h}{\dot{m}_h C_{Ph}} \quad (5.30)$$

or if  $\dot{m}_h C_{Ph} > \dot{m}_c C_{Pc}$ ,  $C_R$  and NTU were defined as:

$$C_R = \frac{\dot{m}_c C_{Pc}}{\dot{m}_h C_{Ph}} \quad \text{and} \quad NTU = \frac{U_c A_c}{\dot{m}_c C_{Pc}} \quad (5.31)$$

The corresponding heat exchanger effectiveness,  $\epsilon$ , was found from graphical data extracted from Chapman (1987). This data is presented in Figure 5.5.

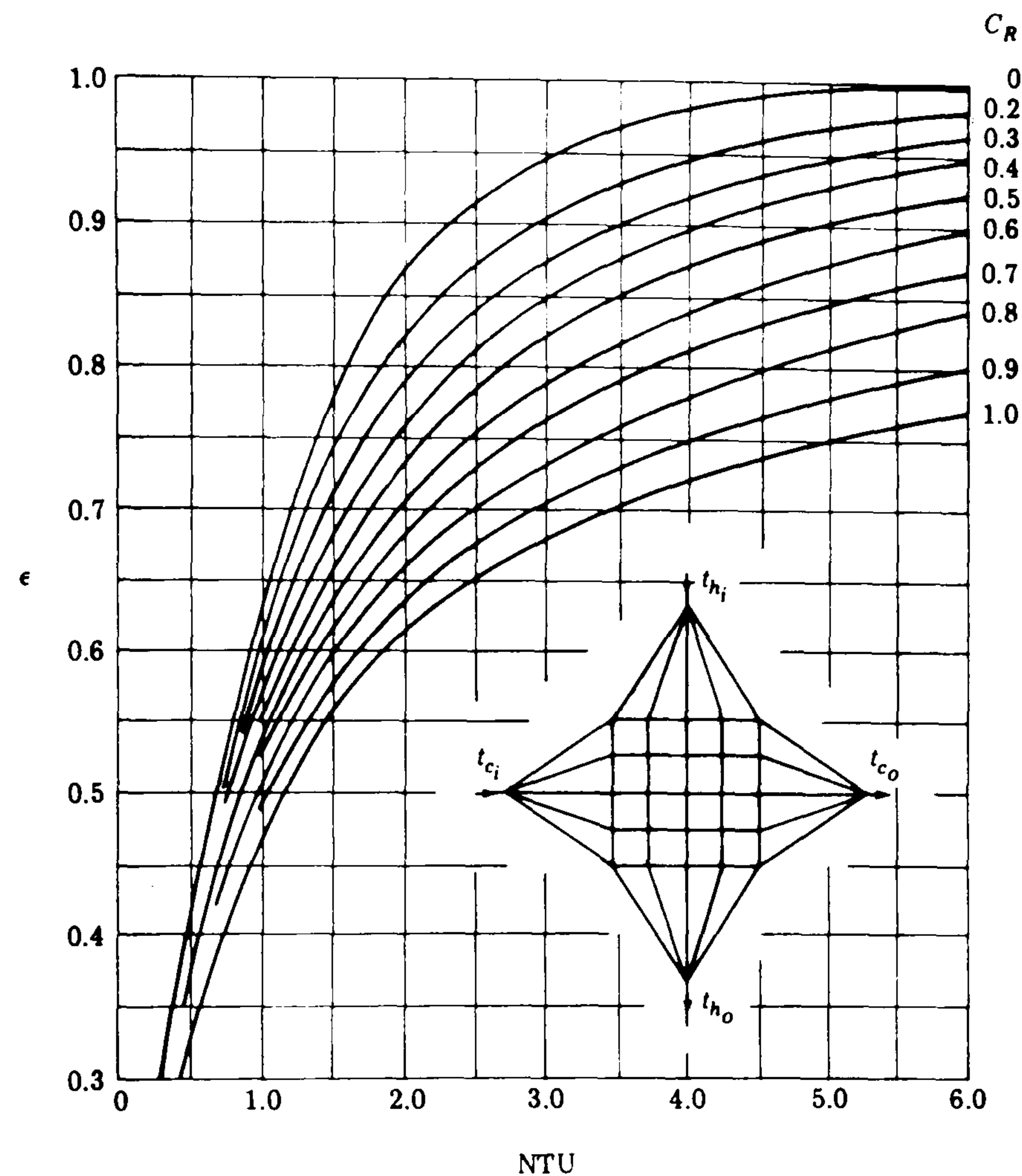


Figure 5.5. Effectiveness - NTU relationship for a cross-flow heat exchanger with both fluids unmixed

The equation selected to represent the temperature characteristics of an oil cooler was dependent on which fluid stream had the smaller capacity rate. If  $\dot{m}_h C_{Ph} < \dot{m}_c C_{Pc}$ , the exit temperature of the oil was calculated directly from the expression used to represent the temperature characteristics of the oil cooler:



$$Y = 0 = t_{hin} - t_{ho} - \varepsilon (t_{hin} - t_{cin}) \quad (5.32)$$

The partial derivatives of Equation 5.32 were:

$$\frac{dY}{dt_{hin}} = 1 - \varepsilon \quad \frac{dY}{dt_{ho}} = -1 \quad (5.33)$$

If  $\dot{m}_h C_{Ph} > \dot{m}_c C_{Pc}$ , the exit temperature of the air was initially calculated from the expression:

$$t_{co} = \varepsilon (t_{hin} - t_{cin}) + t_{cin} \quad (5.34)$$

Following the calculation of  $t_{co}$ , a new value of  $t^{cav}$  was calculated from Equation 5.20 and the corresponding value of  $C_{Pc}$  was found from Equation 5.21. The temperature characteristics of the oil cooler were then represented by an adaption of the basic heat balance equation:

$$Y = 0 = t_{hin} - \frac{\dot{m}_c C_{Pc} (t_{co} - t_{cin})}{\dot{m}_h C_{Ph}} - t_{ho} \quad (5.35)$$

The partial derivatives of Equation 5.35 were of the form:

$$\frac{dY}{dt_{hin}} = 1 \quad \frac{dY}{dt_{ho}} = -1 \quad (5.36)$$

## 5.5 Engine Block Model

The internal engine surfaces which were wetted by the oil spray had a much larger surface area than any of the pipes and drillings within the lubrication system. It was considered that the oil spray would have a significant effect on the temperature of the internal surfaces of the engine, and that the heat transfer by the oil spray could not be modelled by the method

used for the pipes and drillings. It was considered that the assumption of a fixed surface temperature, as used in the pipe model, would lead to inaccurate results.

The heat transfer paths within an engine were represented by taking a cross-section through a single piston/liner/block arrangement (the cross-section used to model the V8 engine is shown in Figure 9.6). The representative cross-section assumed the piston to be fixed at its mid-stroke position. The metal temperatures of the engine and the temperature of the oil sprayed on to the internal surfaces, were calculated simultaneously. The heat generated by friction between the piston and the liner was ignored.

As the heat transfer to the oil spray lay outside the pressurised side of the lubrication system, the engine block model was developed separately from the heat transfer model. The models were linked, however, as the engine block model used oil temperature data from the heat transfer model and pressure and flow rate data from the flow model. This data was used to estimate the quantity and temperature of the oil sprayed from the bearings onto the internal surfaces of the engine. The engine block model returned a value for the temperature of the oil in the sump, which was used as input to the flow model and the heat transfer model.

The engine geometry was represented by a series of block elements, which in turn, were represented by a nodal resistance network. As shown in Figure 5.6, each block element was represented by a central node connected by a heat transfer resistance to a node on each face. The boundary condition for each face incorporated a heat transfer resistance, which either represented conduction to another block element, or convection to a fluid. This modelling approach allowed one, two, or three dimensional models to be generated. The



representative block element arrangement which was developed to model the V8 engine is presented in Figure 9.6. The heat conduction from the piston through the connecting rod was ignored in the V8 engine model.

The four types of heat transfer resistances which were used in the engine block model were:

- i, Conduction through a solid.
- ii, Convection to a fluid mass of known temperature.
- iii, Convection to oil spray.
- iv, Convection to oil in the sump.

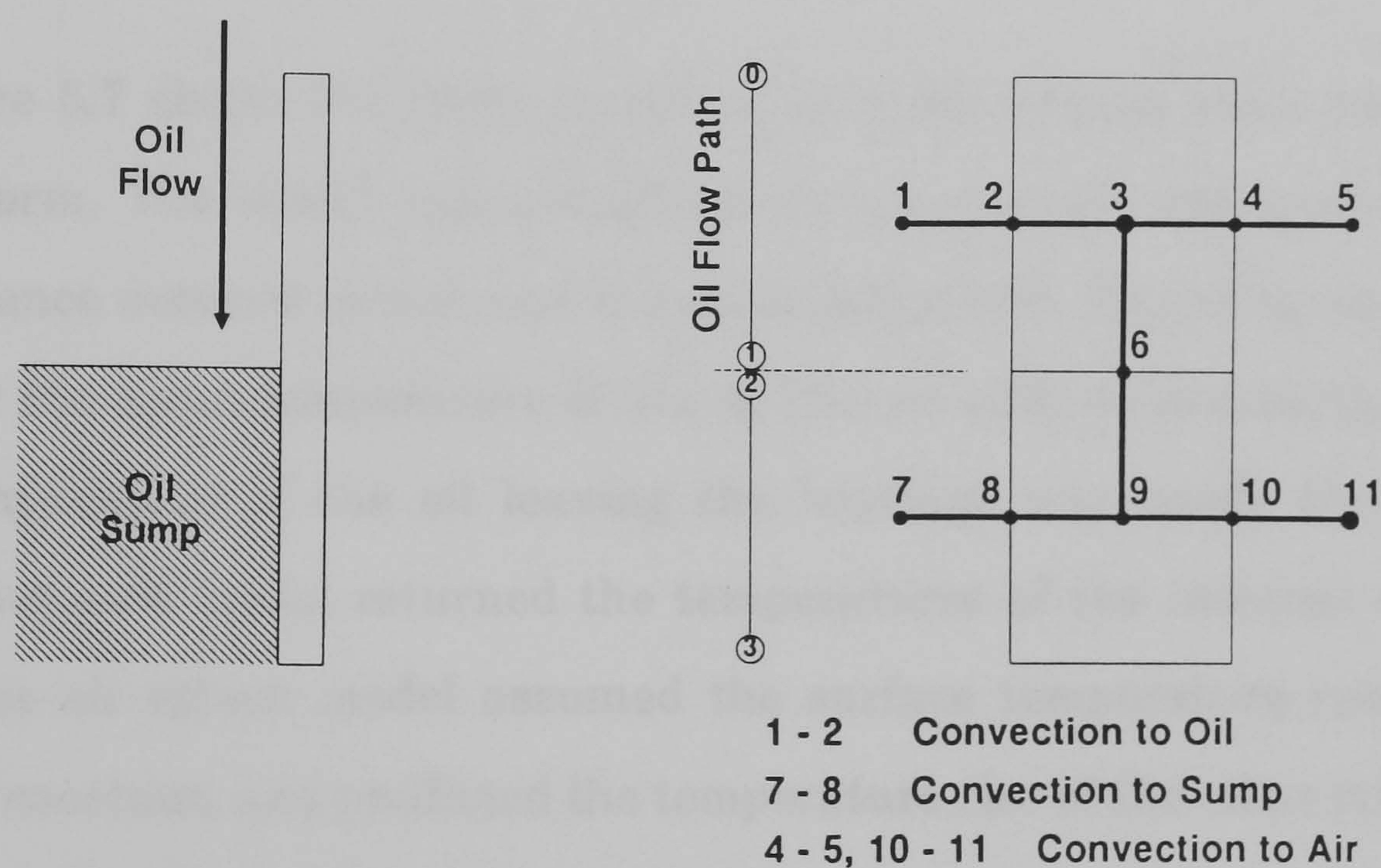


Figure 5.6. Block element and corresponding nodal resistance network for two dimensional conduction and convection.

In addition to the oil, the other fluid masses which were accounted for in the engine model were the combustion gases, the coolant, and the air. It was considered that the prediction of the cycle averaged temperature of the combustion gases and in-cylinder heat transfer coefficients could be obtained



from existing cycle simulation programs. The cycle averaged gas temperature for the V8 engine was estimated from data obtained from an engine simulation model at Jaguar (ref. Bingham (1987) and Barraclough (1991)), which was published in a report by Chang et al (1992). This data is presented in Appendix C.3. The cycle averaged heat transfer coefficient for the combustion chamber gas of the V8 engine was extracted from data published by Veshagh and Chen (1993). It was initially intended that the heat transfer coefficients of the coolant and the air would be calculated within the model. However, due to time constraints, this calculation was not included. The temperatures and heat transfer coefficients for the coolant and the air were extracted from data presented by Veshagh and Chen (1993) and remained constant throughout the calculation procedure.

Figure 5.7 shows the basic construction of the engine block model in schematic form. The model was comprised of two separate sub-models; the nodal resistance network model, and the oil splash model. Following an initial estimate for the mean temperature of the oil film on each wetted surface (the average temperature of the oil leaving the bearings was used), the nodal resistance network model returned the temperatures of the internal engine surfaces. The oil splash model assumed the surface temperature remained temporarily constant, and predicted the temperature rise of the oil as it flowed past each surface. New estimates for the mean oil temperature were returned, for input to the nodal resistance network model. The iterative procedure continued until convergence occurred. A description of the construction of the program for the engine block model is given in section 7.3.

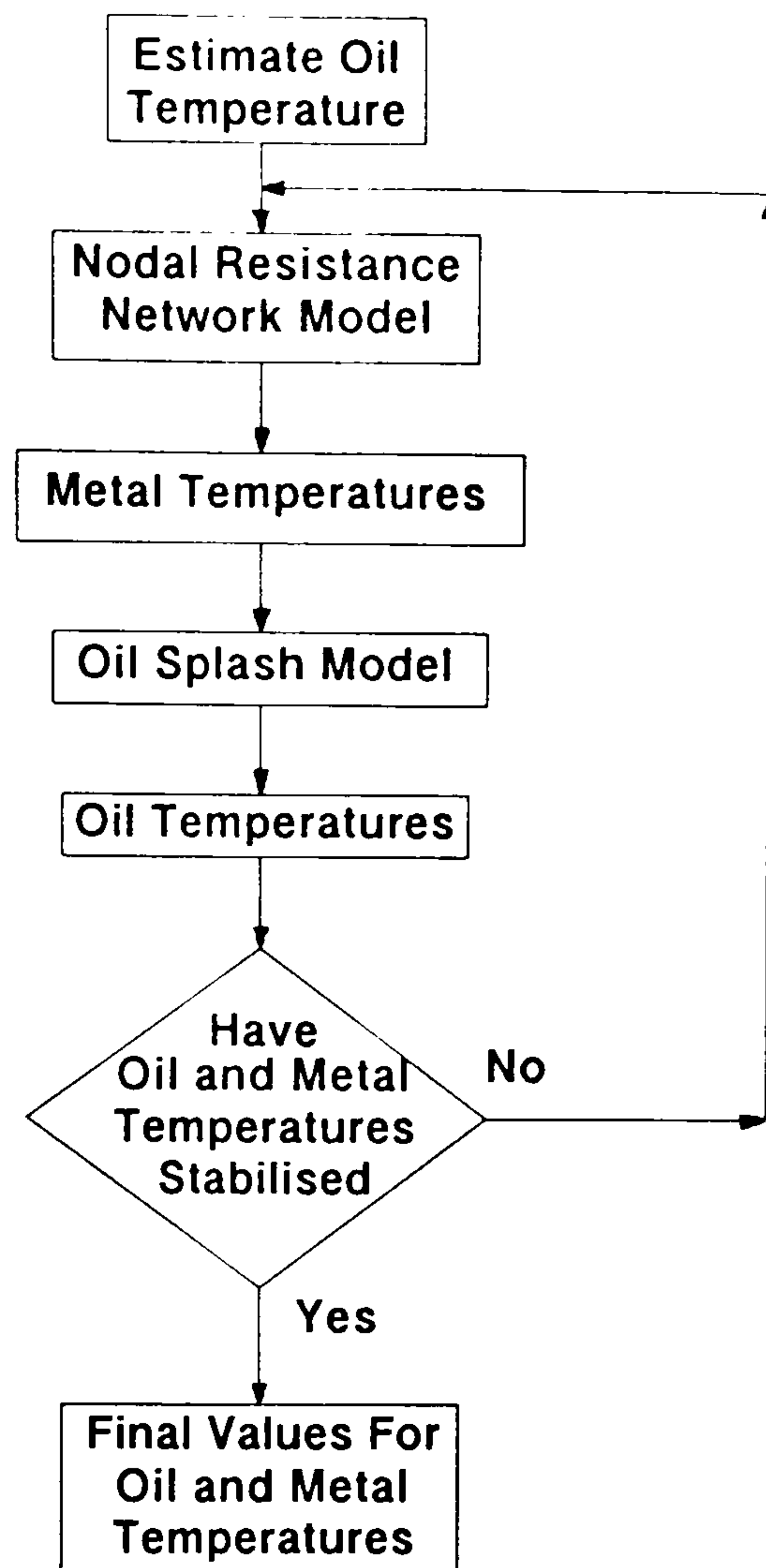


Figure 5.7. Basic construction of the engine block model.

### 5.5.1 Nodal Resistance Network Model

The nodal resistance network was modelled by representing each node, with more than one heat transfer resistance connected to it, by the following expression: At the node  $i$ ,

$$Y = 0 = \sum_j \frac{t_j - t_i}{R_{ij}} \quad (5.37)$$

The partial derivatives of Equation 5.37 were:

$$\frac{dY}{dt_i} = - \sum_j \frac{1}{R_{ij}} \quad \frac{dY}{dt_j} = \frac{1}{R_{ij}} \quad (5.38)$$

The subscript,  $j$ , in Equations 5.37 and 5.38, denoted all neighbouring nodes connected to node  $i$ . The total thermal resistance,  $R$ , was defined as:

$$R_{ij} = \begin{cases} \frac{\delta_{ij}}{kA_{kij}} & \text{for conduction} \\ \frac{1}{h_{ij}A_{cij}} & \text{for convection} \end{cases} \quad (5.39)$$

For the calculation of the conductive thermal resistance in Equation 5.39,  $\delta_{ij}$  represented the distance between nodes  $i$  and  $j$ ,  $k$  represented the thermal conductivity of the material, and  $A_{kij}$  represented the cross-sectional area of the conductive path. Similarly,  $A_{cij}$  represented the surface area of the element exposed to a convective fluid. The heat transfer coefficient,  $h$ , was supplied by the user for all convective fluids apart from the oil. The values of  $h$  which were used to model the convective fluids in the V8 engine are presented in Table 9.7. The value of  $h$  for the oil was provided by the oil splash model during the last iteration of the engine block model.

### 5.5.2 Oil Splash Model

The mechanism of the oil spray onto the engine internal surfaces was simplified to that of a falling oil film. The model which was developed was based upon the following assumptions:

- i, The oil sprayed onto each surface originated from either the main, the big-end, or the cam bearings, or any combination of the three.
- ii, The oil was assumed to flow down a vertical surface, the inlet position being the top edge of this surface.
- iii, The flow rate of the oil was the total flow rate of oil which was sprayed onto the whole surface of the element.



- iv, The fluid film flowed with constant velocity.
- v, The film thickness was constant over the whole surface.
- vi, The flow was laminar.
- vii, The engine was operating under steady-state conditions.

The oil flow down the wetted surfaces of the engine was represented by a flow network. This is demonstrated by the simple two element arrangement shown in Figure 5.8<sub>a</sub>. The resulting flow network is shown in Figure 5.8<sub>b</sub>. The oil inlet condition for the upper section, node 0, was calculated from the percentage of oil from the main, big-end, and cam bearings, which sprayed onto the surface of this section. The oil temperature at node 1, the exit condition for the upper section, was found for the heat transfer characteristics of this section. The inlet condition for the lower section, node 2, however, was dependent on the percentage of the flow from the upper section which continued to the lower, and the amount of 'new' oil splashed onto this surface from the bearings.

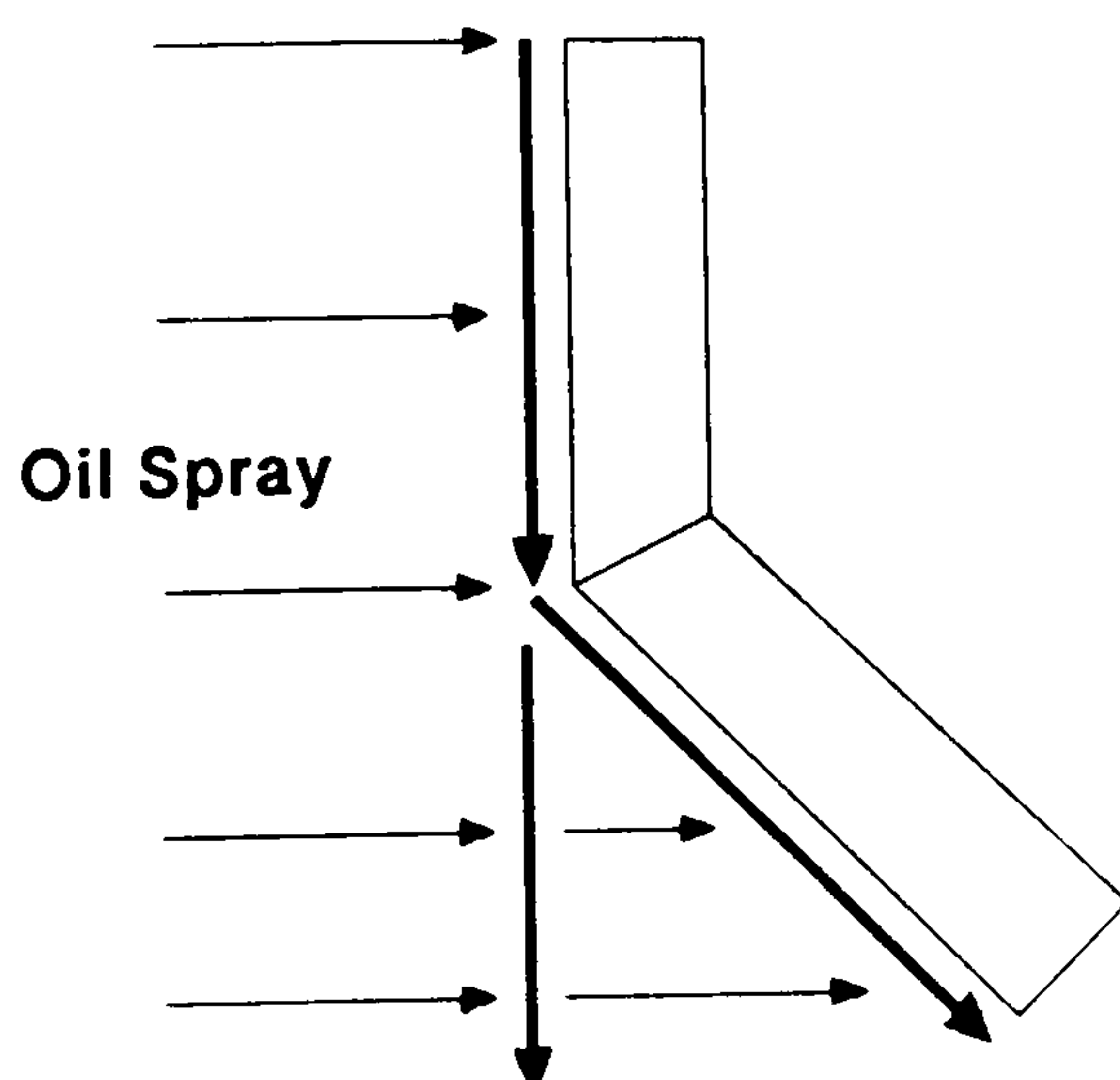


Figure 5.8<sub>a</sub>. Oil splash onto two elements.



Figure 5.8<sub>b</sub>. Oil flow network.

The flow network, therefore, was represented by two types of equations; equations which represented the heat transfer characteristics of the flow past each surface (nodes 0-1 and 2-3 in Figure 5.8<sub>p</sub>) and equations which linked the flow and temperature conditions of adjacent elements (nodes 1-2 in Figure 5.8<sub>p</sub>). The latter equation will hereafter be referred to as 'the continuity equation'. These two types of equations were used to represent the various arrangements of falling oil films within any engine cross-section.

The engine was modelled under steady-state conditions. Consequently, it was assumed that the heat transfer to the oil in the sump could be modelled by a similar method to that used for a falling oil film. The flow rate past the surface of an element wetted by the oil in the sump (sump element) was assumed to be the total oil flow rate through the lubrication system. The heat transfer equation was the same as for a falling oil film, while the continuity equation depended on the type of oil flow of the preceding element. Two different continuity equations were derived, one for the continuity between a falling oil film and a sump element, and the other for the continuity between sump elements.

#### 5.5.2.1 Heat Transfer Equation

The heat transfer to a falling oil film was represented by the equation developed for heat transfer within a pipe. This was presented as Equation 5.7, and the partial derivatives of this equation were presented as Equations 5.8 and 5.9. The heat transfer coefficient,  $h$ , which was used in Equation 5.7, was calculated from a falling liquid film theory developed by Nusselt (1923<sub>a</sub>). Thus, for an oil film falling down a surface of height,  $H$ , the heat transfer coefficient,  $h$ , was calculated from the expression:

$$h = \frac{\dot{W}' C_P}{H} \ln \left( \frac{1}{1 - \phi} \right) \quad (5.40)$$

The weight flow per unit time over unit length of the upper edge of the wetted surface,  $\dot{W}'$ , was given by:

$$\dot{W}' = \dot{m}' g \quad \text{and} \quad \dot{m}' = \frac{\dot{m}}{C_w} \quad (5.41)$$

where  $\dot{m}'$  represented the mass flow rate per unit length of the upper edge of a surface and  $C_w$  represented the width of the wetted surface. The mass flow rate,  $\dot{m}$ , for each wetted surface, was found from the relationship:

$$\dot{m} = \varrho (\psi_m Q_m + \psi_b Q_b + \psi_c Q_c + \psi_{ab} Q_{ab}) \quad (5.42)$$

The subscripts, m, b, and c represented the main, big-end and cam bearings respectively. The subscript, ab, represented the conditions from the element above. The percentage of the flow rate,  $Q$ , from each type of bearing which was splashed onto the surface, and the percentage of the flow from the previous element which continued on to the next, was represented by  $\psi$ .

The value of the temperature ratio,  $\phi$ , in Equation 5.40, was dependent on the value of the dimensionless quantity  $\xi$ .

$$\begin{aligned} \text{For } \xi < 0.05, & \quad \phi = 2.230 \xi^{0.656} \\ \text{For } \xi > 0.05, & \quad \phi = 1 - 0.9101 e^{-5.65 \xi} \end{aligned} \quad (5.43)$$

where

$$\xi = \frac{\mu k H}{\gamma^2 C_P s^4} \quad \text{and} \quad \gamma = \varrho g \quad (5.44)$$



The symbol,  $\gamma$ , represented the specific weight of the oil. The thickness of the falling oil film,  $s$ , was calculated from the following equation:

$$s = \sqrt[3]{\frac{3\mu\dot{m}'}{\rho^2 g}} \quad (5.45)$$

### 5.5.2.2 Continuity Equation

The continuity of flow equation which was derived for a falling oil film linked the temperature conditions at the exit from one element to the inlet conditions for the next. The continuity equation took into account the percentage of oil which flowed from one surface to the next (which was estimated by the user) and also accounted for any new oil which was sprayed from the bearings onto the succeeding element. The continuity equation which linked two falling oil films was of the form:

$$Y = 0 = \left[ \frac{\psi_m Q_m t_m + \psi_b Q_b t_b + \psi_c Q_c t_c + \psi_{ab} Q_{ab} t_{bin}}{\psi_m Q_m + \psi_b Q_b + \psi_c Q_c + \psi_{ab} Q_{ab}} \right] - t_{bo} \quad (5.46)$$

The partial derivatives of Equation 5.46 were of the form:

$$\frac{dY}{dt_{bin}} = \frac{\psi_{ab} Q_{ab}}{\psi_m Q_m + \psi_b Q_b + \psi_c Q_c + \psi_{ab} Q_{ab}} \quad (5.47)$$

and

$$\frac{dY}{dt_{bo}} = -1 \quad (5.48)$$

The engine was modelled by taking a representative section through a single piston/cylinder arrangement. Therefore, for a multiple cylinder engine, such as the V8, the oil temperature from the bearings,  $t$ , was the average oil

temperature from all the bearings of a same type.

The continuity equation which linked a falling oil film element with a sump element, was similar to Equation 5.46, but also accounted for the temperature effects of additional oil which entered the sump. The sources of this additional oil were commonly:

- i, The oil sprayed from the chain tensioners.
- ii, The oil ejected from other engine bearings and chain tensioners which didn't spray directly onto the internal engine surfaces being modelled.
- iii, The oil which dripped off the internal surfaces without flowing on to the surface of the next element.

The continuity equation which was derived for this situation was of the form:

$$Y = 0 = \left[ \frac{\psi_{Rm} Q_m t_m + \psi_{Rb} Q_b t_b + \psi_{Rc} Q_c t_c + Q_{ab} t_{bin} + \sum_j (1 - \psi_{abj}) Q_{abj} t_{abt} + \sum_n Q_n t_n}{Q_{tot}} \right] - t_{bo} \quad (5.49)$$

The partial derivatives of Equation 5.49 were of the form:

$$\frac{dY}{dt_{bin}} = \frac{Q_{ab}}{Q_{tot}} \quad \text{and} \quad \frac{dY}{dt_{bo}} = -1 \quad (5.50)$$

The  $\psi_R$  term, in Equation 5.49, represented the remaining percentage of oil from the bearings which didn't splash onto any of the wetted surfaces. The sum of the variables with the subscript, j, represented the sum of the oil from each of the wetted surfaces which didn't continue to flow down to the next wetted surface. It was assumed that this oil dripped directly into the sump at the temperature it left the wetted surface. The sum of the variables with the

subscript, n, represented the oil from all the additional oil sources, such as the chain tensioners and other engine bearings. This oil was assumed to enter the sump at the temperature it left the pressurised part of the lubrication system.

The continuity equation between sump elements was of a much simpler form. The temperature and flow conditions at the exit from the surface of one sump element were the inlet conditions for the next. The flow rate past each surface wetted by the oil in the sump, was taken to be the total flow rate of oil for the representative section of the engine. Thus, the continuity equation which linked two sump elements, was of the form:

$$Y = 0 = t_{bin} - t_{bo} \quad (5.51)$$

The partial derivatives of Equation 5.51 were:

$$\frac{dY}{dt_{bin}} = 1 \quad \text{and} \quad \frac{dY}{dt_{bo}} = -1 \quad (5.52)$$

## 5.6 Concluding Remarks

The heat transfer in the lubricating oil was analyzed with the development of two separate models; the heat transfer model and the engine block model. The first model analyzed the heat transfer within the pressurised side of the lubrication system. This model utilised data generated in the non-linear flow model which represented the physical layout of the system by breaking the system down into component elements joined at nodal points. The component elements which were accounted for in the heat transfer model were the pipes, annular pipes, crankshaft transfer holes, cam-bearing transfer holes, oil coolers and journal bearings. The heat transfer within the pumps, strainers



and filters was assumed to be negligible. Each heat transfer element was represented by a temperature change equation. This resulted in a set of simultaneous equations which were solved by the Levenberg-Marquardt algorithm.

The equation derived to represent the temperature change of the oil within the pipes was also used for the annular pipes, the crankshaft transfer holes and the cam bearing transfer holes. It was assumed that the wall temperature of these pipe elements would remain constant during the calculation procedure and that these temperatures would be provided by the user. The wall temperatures would either be estimated for the first pass of the heat transfer model, or they would be predicted by a previous run of the engine block model. The pipe model accounted for both turbulent and laminar flow in short and long pipes.

A simple oil temperature rise model was developed for the journal bearings, for use in the linear and non-linear flow model. This simple temperature rise model provided an estimate of the working temperature and viscosity of the oil within the journal bearings. This was used in the first pass of the flow model before more accurate values were obtained from the heat transfer model. The heat transfer model utilised bearing oil temperature rise 'maps', which were generated from an adapted bearing model developed by Lai (1993).

The oil cooler was simplified to a plate-fin type cross flow heat exchanger. The cold fluid was assumed to be the ambient air. The surface of each plate was assumed to be covered with an array of plane longitudinal fins. The heat transfer characteristics of this type of heat exchanger were calculated using an 'effectiveness - NTU' method. This solution method was based on

empirical data for plate-fin arrays published by Kays and London (1964). The oil cooler model used an iterative solution technique which yielded the exit temperatures of the oil and the air, given the inlet temperatures of these fluids and the velocity of the air flow.

The engine block model was developed to analyze the heat transfer role of the oil spray onto the internal engine surfaces. It was considered that the oil spray would have a significant effect on the temperatures of the wetted surfaces. For this reason, the engine block model simultaneously predicted the temperature of the engine block and the temperature of the oil which was sprayed onto the internal surfaces. It was assumed that the effect of the oil spray on the whole engine heat transfer would be adequately represented by analyzing a single piston/liner/block arrangement. This engine arrangement was simplified to a series of block elements, which in turn, were represented by a nodal resistance network.

The data which represented the physical layout of the lubrication system and the flow rates through the system, was obtained from the flow model. The temperature of the oil which was sprayed from the bearings onto the internal surfaces was obtained from the heat transfer model. The temperature and heat transfer coefficient data for the combustion gases, the coolant, and the ambient air, were supplied by the user. The heat convection to the oil, which was sprayed onto the internal surfaces of the engine, was modelled by simplifying the oil spray to that of a falling oil film. As the engine was modelled under steady-state conditions it was assumed that the oil in the sump could also be modelled by the same method used for a falling oil film.

The engine block model returned the temperatures at each node in the resistance network, and the temperature of the oil at the inlet and exit of the

surface of each of the wetted block elements. This oil data included the oil temperature in the sump. The engine block model represented the final step in the simulation of the flow and heat transfer conditions of the lubrication system. The oil temperature in the sump was used in the flow model and the heat transfer model, and the predicted metal temperatures could be used as wall temperature data for the pipe elements in the heat transfer model. This iteration procedure produced more refined results for the pressures, flow rates and temperatures throughout the engine lubrication system.



## Chapter 6

# Structure of Flow Model Computer Program

### 6.1 Introduction

This chapter presents the computer program which was written for the flow analysis of the lubrication system. Initial program development concentrated on the linear flow program, which includes a Gauss-Jordan linear matrix solving technique. This program is structured in a modular manner, utilising a subroutine format. It was intended that this format would allow easy formation of alternative programs by utilising the same subroutines.

When the initial linear flow program had been fully developed, a comprehensive comparison was made between the two linear matrix solving techniques, Gauss-Jordan elimination and LU decomposition. It was found that the LU decomposition method produced more accurate results and reduced the program run time (a description of this comparison is given in section 8.2). The Gauss-Jordan subroutine was simply replaced by an LU decomposition subroutine, to form what could be considered to be a second linear flow program. As both the linear programs are basically of the same construction, they will hereafter be referred to as 'the linear program'.

Following the completion of the linear program (see flow chart in Figure 6.1), the development of the non-linear flow program was undertaken. The aim of this program was to compute the pressures and flow rates by an iterative procedure using the Levenberg-Marquardt algorithm (this routine is described

in Appendix A.2.1). During the initial development stages, however, the majority of the non-linear program was comprised of subroutines which were developed for the linear program. Therefore, the methods used to represent the physical system, the input of data, the output of results and the majority of the user interface, were initially the same as those used in the linear program.

The non-linear flow program was developed further to incorporate additional component elements (these were discussed in Chapter 4), improve program flexibility, and improve the user interface. The decisions made at each stage in the development of the full non-linear flow program (see flow chart in Figure 6.2) are presented in this chapter.

### 6.1.1 Programming Language

In selecting a suitable programming language, consideration was made of the eventual user, who would be an engine design engineer at Jaguar with limited programming knowledge, rather than a professional software developer. The programming language selected was FORTRAN 77, for the following principal reasons:

- i, The eventual users at Jaguar were familiar with writing and using programs in FORTRAN.
  - ii, FORTRAN was a well established language and there were numerous numerical routines which were easily available (Press et al (1990)).
  - iii, It was intended to integrate the thermofluid analysis of the lubrication system with other vehicle thermodynamic simulation projects under development at the Advanced Technology Centre (Veshagh et al (1992)).
- These simulation programs were also being written in FORTRAN.

Program development was initially carried out on a 386 16 MHz PC. However, it was found that the developing programs soon reached the limits of the memory and processing speed for this host machine and programming was switched to a UNIX based workstation. The host machine had an influence on the programming methods which were employed and these influences are also discussed throughout this chapter.

A full listing of the FORTRAN programs which were developed for the simulation of the flow conditions within the lubrication system are given in Volume II. A user manual for the programs, which was supplied to Jaguar to supplement the program installation, is also included in Volume II. The user manual gives a full description of the required procedure for running the programs and illustrates the prompts which are displayed to the screen.



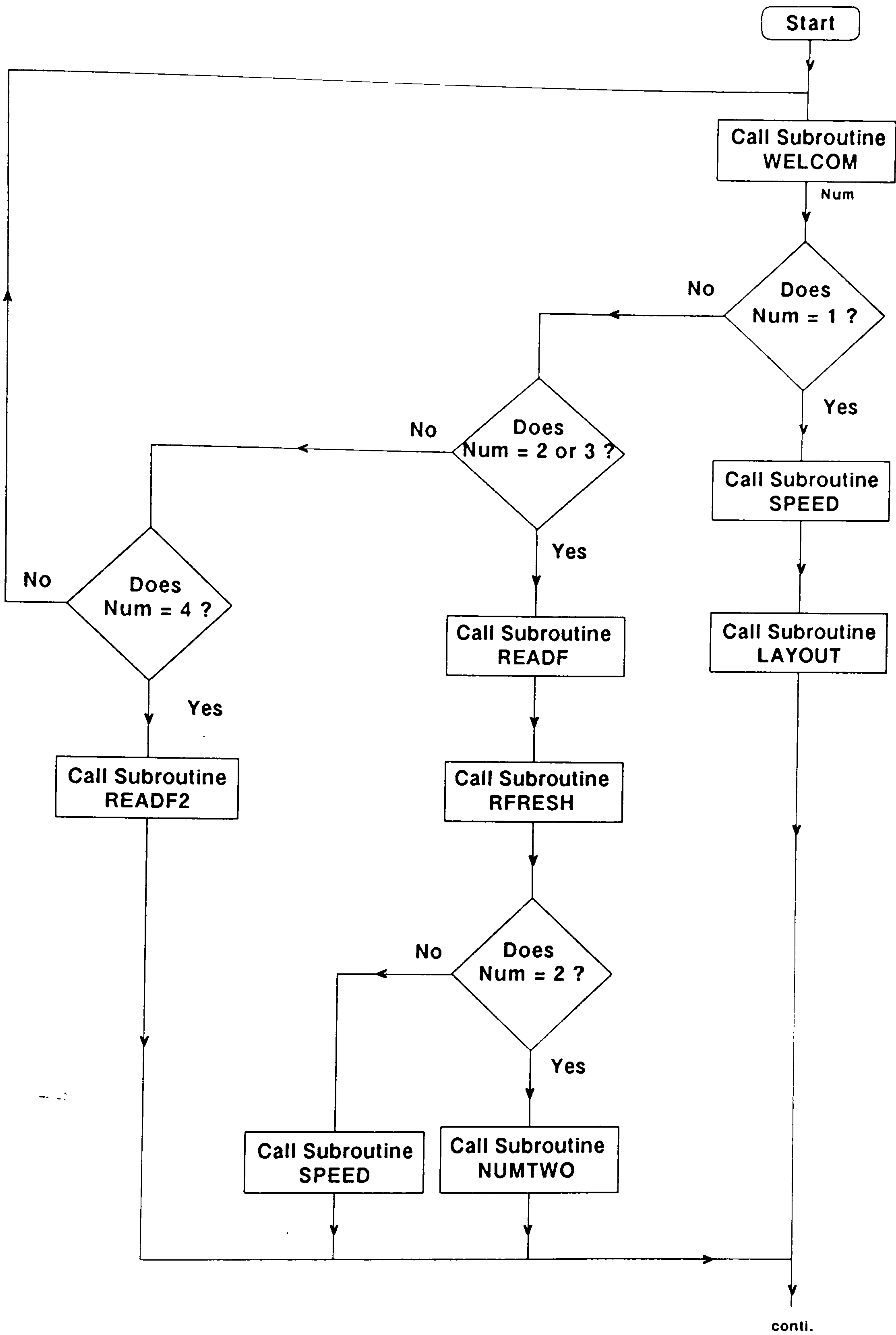


Figure 6.1. Flow chart of linear flow program

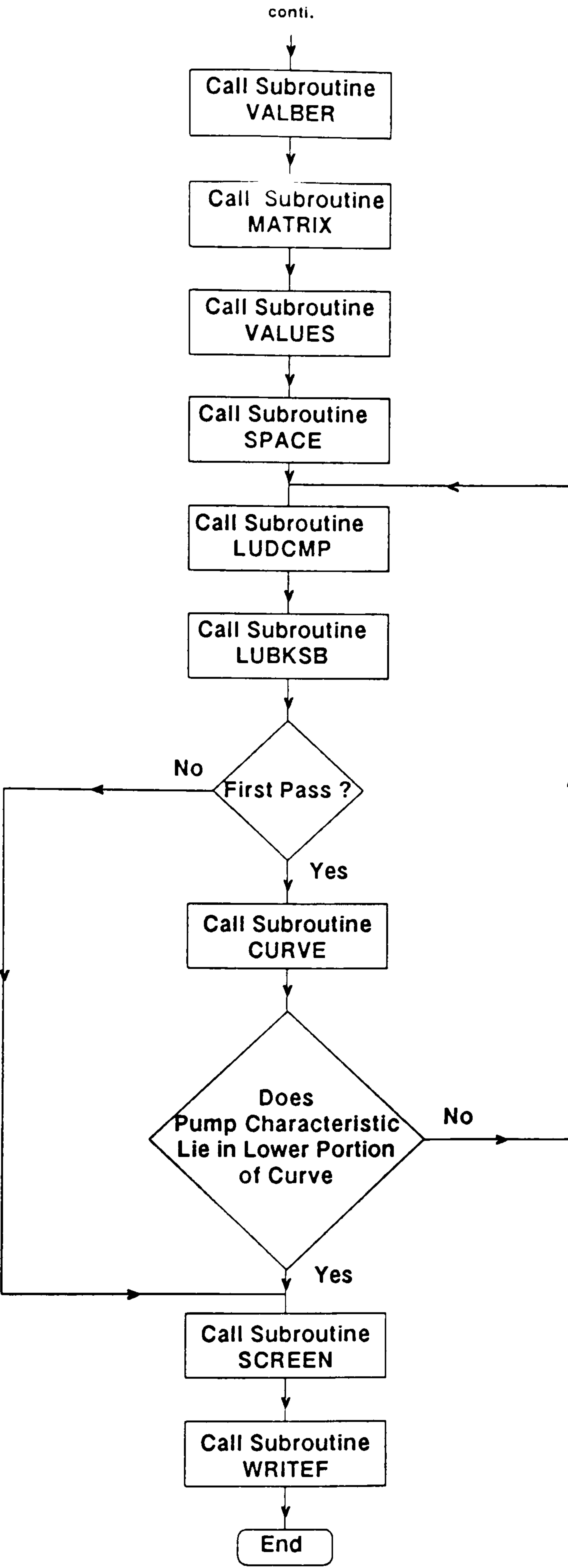


Figure 6.1. .... Continued

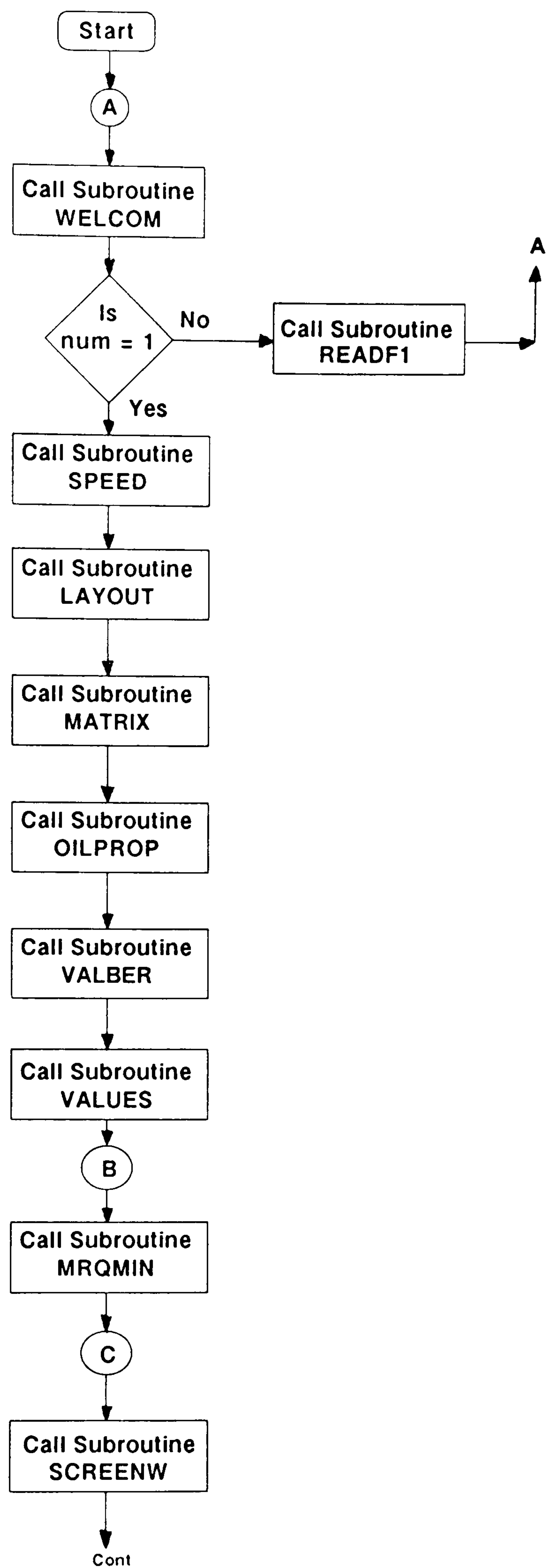


Figure 6.2. Flow chart of the non-linear flow program



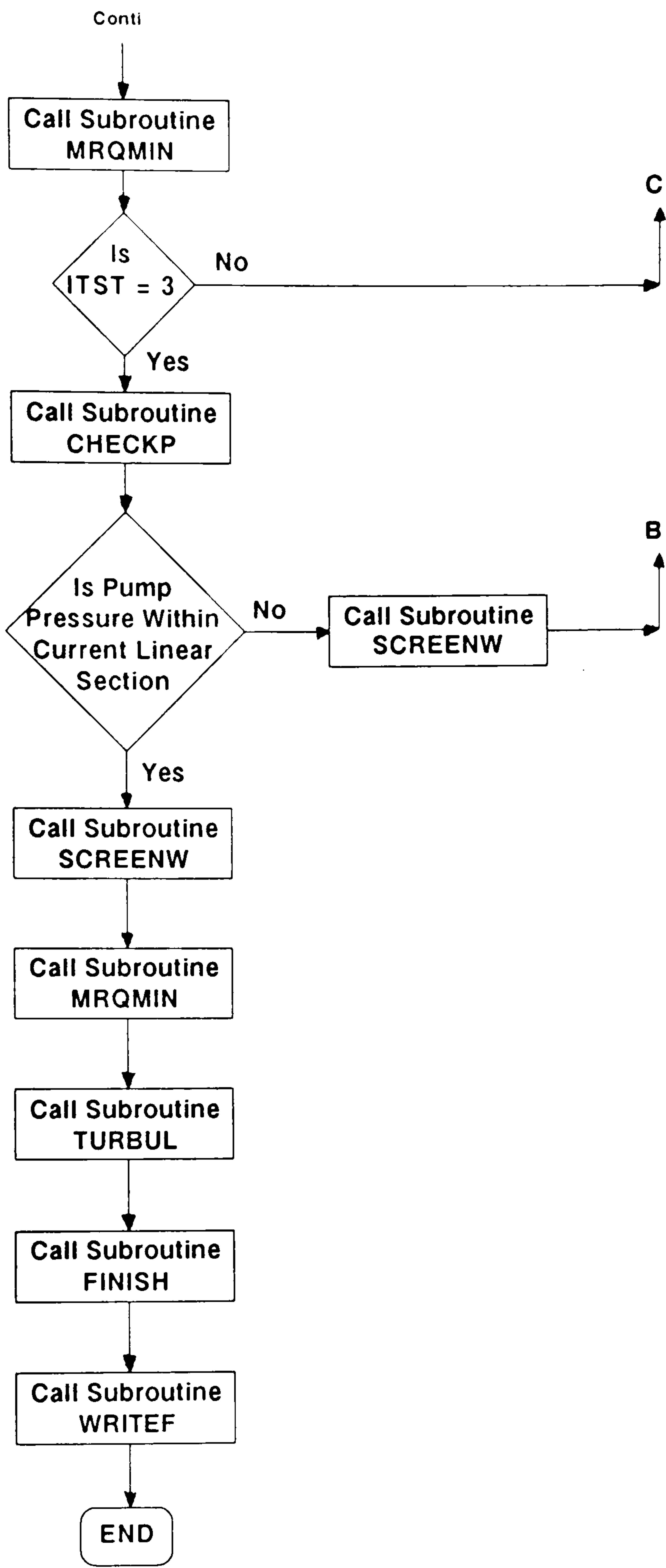


Figure 6.2. .... Continued

## 6.2 Initiating the Flow Program

The simulation model of the lubrication system consists of three programs; the flow program, the heat transfer program and the engine block program. These programs have to be run separately and in the correct order. The flow program is always run first, because the layout of the physical lubrication system is modelled in this program. The data which is generated to represent the physical layout of the system is stored in the data file PANDQ.OUT for use in the heat transfer program and the engine block program.

The flow program is run from the shell script named 'GO'. When this shell script is started, the flow program is initiated and the main program calls subroutine WELCOM, which gives the user several options for running the flow program. In the linear program these are:

- i,      Model a new system 'from scratch'.
- ii,     Use a pre-formed system stored on a data file.
- iii,    Use an 'echo file' as a user input device. This is described in more detail in section 6.7.

The non-linear program only gives the user the options, i, and iii.

As options, ii, and iii, can only be selected if the flow program has previously been run and the lubrication system layout has been previously modelled, the following sections assume the user selects option, i. This gives a clear insight into how the lubrication system is modelled and how the necessary data files are generated to allow the user to select options ii, and iii, in the future.

### 6.3 Representing the Physical System

The non-linear program prompts the user for the general operating conditions for the engine and its lubrication system. The main program calls subroutine SPEED, which prompts the user to input the engine speed and the temperature of the oil in the sump. The sump temperature is either selected as a trial value or is obtained from a previous run of the engine block program (this program is presented in section 7.3). The value for the oil temperature is checked against oil data stored in data file OILVIS.INP. If the selected oil temperature lies outside the range of oil temperatures contained in this file, an error message is displayed. At this stage in the program the oil temperature is assumed to be constant throughout the lubrication system, apart from in the bearings where a temperature rise calculation is included.

In the linear program, the sump temperature is assumed to be fixed at 100°C throughout the system and the engine speed is input during the data input stage for the oil pump.

To represent the physical system, the main program calls subroutine LAYOUT. This subroutine prompts the user to set up the model by stating the number of nodes in the proposed system, the number being stored as integer NODES. The number of component elements in the system is NODES - 1, this number is stored as integer LOOPS. As all the sections are linked at nodal points, the user is prompted to input the start node number, end node number, and type, for each element in the system. The layout of the proposed system is stored in memory, in the two-dimensional array BIN and the type of element between each node pair is stored in the one-dimensional array TYP.



A one-dimensional array is used for this task because a problem was encountered during the initial program development on the PC. The available memory was not sufficient for the storage of the various arrays. An attempt was made to solve this problem by replacing many of the two-dimensional arrays with one-dimensional types, using the format described above. However, this only allows lubrication systems with diverging nodes to be modelled, a system which contains one or more converging nodes can not be modelled.

After program development switched to the workstation, the memory constraints were lifted. However, the original one-dimensional array formats were not changed, as no problems were encountered with the modelling of the AJ6 or the V8 engine lubrication systems, which did not contain any converging nodes.

Arrays BIN and TYP are initially conditioned to contain only zero's. A '1' is placed at the i,j co-ordinate within BIN to represent that the nodes i and j are linked by a flow element. The first subscript, i, references the row and the second subscript, j, references the column. Array TYP stores an integer number (whole number with no fractional portion or decimal point) in location, j, to represent the type of element which exists between nodes i, and j. The integer number which is stored in array TYP depends on the type of flow element it represents:

#### Linear and initial non-linear program

1 = Pipe.

2 = Pump.

3 = Oil filter.

4 = Journal bearing.

5 = Crankshaft transfer hole.

#### Final non-linear program

1 = Laminar pipe.

2 = Pump.

3 = Oil filter.

4 = Journal bearing.

5 = Crankshaft transfer hole.

6 = Cam bearing transfer hole.

6 = Cam bearing transfer hole.

7 = Oil strainer.

8 = Turbulent pipe.

9 = Laminar annular pipe.

10 = Turbulent annular pipe.

11 = Oil cooler.

At this stage in the program, all the pipes and annular pipes are considered to be under laminar flow conditions. The pipes and annular pipes are represented in array TYP as numbers 1 and 9 respectively. These numbers are changed to 8 and 10 respectively if the user selects turbulent flow conditions at the data input stage (see section 6.4).

When all the elements in the proposed lubrication system are represented by their start node number, end node number, and type, subroutine 'MATRIX' is called by the main program to process the two-dimensional array BIN. The first task carried out by subroutine MATRIX is to calculate the sum of each row in the array BIN and place the result in the final column. Initially, the array BIN is allocated 110 columns and 110 rows, so the sum of each row is placed in the 110th column. The value of 110 was chosen as it was marginally greater than the maximum number of elements (89) that made up the AJ6 lubrication system (see Figure 8.2). When the program development switched to the workstation the arrays were increased in size from 110 to 350 rows and columns. The value of 350 was selected as it was comfortably larger than the largest lubrication system modelled to date. This was the full V8 engine lubrication system which was represented by 232 nodes.

The purpose of calculating the sum of each row is to keep a record of the types of linkages at each node. For example, a '0' in the 110th column of row

'i', would indicate no flow path out of node 'i'. A '1' would indicate one flow path, a '2' would indicate two flow paths, ... etc.

The process of representing the layout of a system is best illustrated with a simple example. Consider the simple lubrication system shown in Figure 6.3, which is comprised of one pump, one pipe, and two bearings.

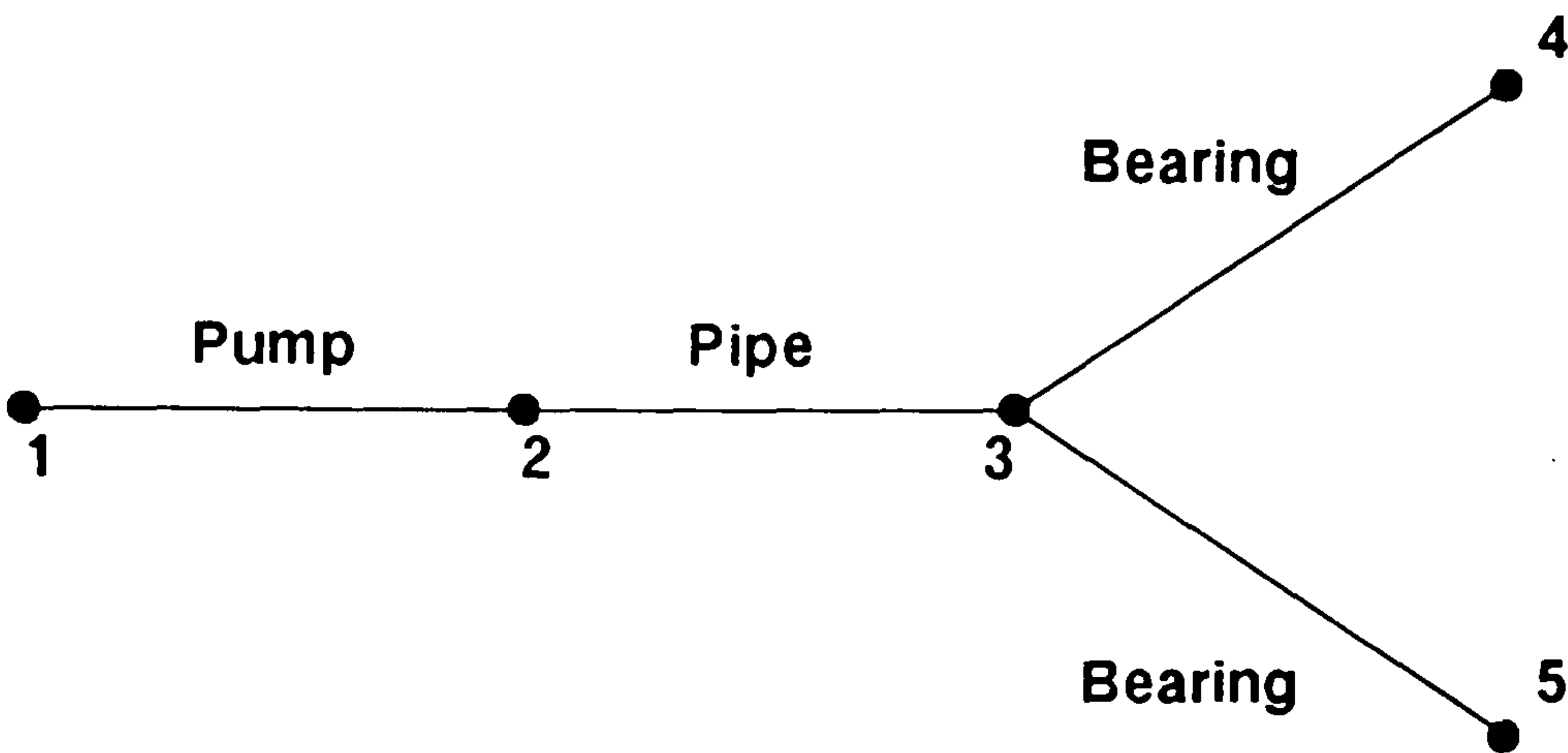


Figure 6.3. Simple four element lubrication system

The two-dimensional array BIN, which would be formed for this system in the linear program, would be of the form shown in Table 6.1.

		j							
		1	2	3	4	5	.	.	110
i	1	0	1	0	0	0	.	.	1
	2	0	0	1	0	0	.	.	1
	3	0	0	0	1	1	.	.	2
	4	0	0	0	0	0	.	.	0
	5	0	0	0	0	0	.	.	0

Table 6.1. Two-dimensional array BIN with sum of rows



The one-dimensional array TYP would be of the form:

	j				
	1	2	3	4	5
1	0	2	1	4	4

Table 6.2. Example of one-dimensional array TYP

It can be seen from Table 6.1 that the array BIN is predominantly sparse. A more concise method of storing this data was developed in the final non-linear flow program which only used two rows. The first row stores the integer 'i' in the 'j' column. The second row stores the sum of each row, i, which was previously stored in the last column of the array BIN (see Table 6.1). Thus, for the example shown in Figure 6.3 the condensed array BIN would be of the form:

		j				
		1	2	3	4	5
i	1	0	1	2	3	3
	2	1	1	2	0	0

Table 6.3. Array BIN generated in the fully developed non-linear flow program

The data stored in the array BIN is used by the subroutine MATRIX to allocate flow rate and pressure labels to the system. For example, for the simple system shown in Figure 6.3, the flow rate between nodes 1 and 2 will be the same as between nodes 2 and 3 and will be labelled  $Q_1$ . The flow divides at node 3, so the flow rate between nodes 3 and 4 will be labelled  $Q_2$ , and equally, the flow rate between nodes 3 and 5 will be labelled  $Q_3$ .

In the linear program, subroutine MATRIX performs the task of labelling the flow rates by scanning the 110th column of array BIN. If a '1' is encountered there is only one flow path out of node 'i', therefore the flow rate count remains at its present value. If a '0' is encountered, there is no flow element connected from node 'i', therefore the present flow path has reached its final destination and the flow rate count is increased by one. If a number larger than a '1' is encountered, node 'i' is a diverging node, therefore the flow rate count is incremented by one for each path out of node 'i'. A similar procedure is carried out in the non-linear flow program using the data stored in the second row of the condensed array BIN.

The flow rate count for each element is stored as an integer in the one-dimensional array QNUM, in the elements 'j' co-ordinate. In addition, the largest flow rate number for the system is recorded as an integer QMAX. For the example system shown above, QMAX will be '3', while the array QNUM will be of the form:

	j				
	1	2	3	4	5
1	0	1	1	2	3

Table 6.4. One-dimensional array QNUM

In addition to the requirement to know the flow rate label for each element, there is also a requirement to know for which node numbers within the system a pressure value is required to be calculated. Therefore, each node which is not at atmospheric pressure needs to be labelled as  $P_1$ ,  $P_2$ ,... etc. Subroutine MATRIX scans array BIN and finds the first node where a pressure is required to be calculated. The node number for this node is placed in the first location of the one-dimensional array PNUM. The scanning continues and

the node number of the second node, where a pressure is required to be calculated, is placed in the second location in PNUM, ..., etc. This process is repeated for the whole system.

For the example illustrated in Figure 6.3, the one-dimensional array PNUM would consequently be of the form:

PNUM					
	1	2	3	4	5
1	2	3	0	0	0

Table 6.5. One-dimensional array PNUM

The array PNUM in this example, shows that  $P_1$ , represents a pressure at node number 2, and  $P_2$  represents a pressure at node number 3.

The physical system is represented, therefore, by the arrays; BIN, TYP, QNUM, and PNUM, and the integer NODES. The linear program forms a data file which stores the above arrays and integers, so the physical system which had been modelled can be easily re-modelled at a later date. The non-linear program writes these arrays to the file PANDQ.OUT for use in the heat transfer and engine block programs.

## 6.4 Input of Data

When the physical system has been represented, the non-linear program calls subroutine OILPROP to ascertain if the oil temperature is to be assumed to be constant throughout the system (the sump oil temperature), or if more representative temperature data is available from a previous run of the heat transfer program. This data is stored in a data file named OIL-T.OUT. If the



latter option is selected by the user the program calculates the density and viscosity of the oil, for each component element in the system, from oil property data stored in the file OILVIS.INP. The density and viscosity values for each component element are stored in arrays RHO and NEU respectively, in their 'j' co-ordinate.

The program continues by calling subroutine VALBER to scan the arrays BIN and TYP, to check if the system contains any bearings. In the linear program, the arrays BIN and TYP can either have just been formed, as described in the above section, or they can be read from a data file which was formed on a previous run of the program. The user is given the choice at the beginning of the program which route he wishes to take.

As the primary task of any lubrication system is to supply a flow of oil to journal bearings, lubrication systems often contain a relatively large numbers of bearings (the V8 engine contained 33 journal bearings). Therefore, a large amount of data is required to be input by the user for the whole system (the mathematical relationship used to represent a bearing is discussed in more detail in section 4.7). In an attempt to reduce the modelling time for a system where only approximate results are required, default data for the various types of bearings is stored in the data file BEARING.INP. Subroutine VALBER allows the user to view and/or change the bearing default data values, which can be used later in the program. If the user selects to change the default data, subroutine BEARVA is called to prompt the user to input variable values for the partially grooved bearings and subroutine BEARVB is called for the simple feed hole types.

Subroutine 'VALUES' is called to prompt the user to input the desired variable values for each component element in the lubrication system. Arrays

BIN and TYP are scanned to find the location and type of each component element and the user is prompted to input the required variable values for each one.

If there is an oil pump in the system, the linear program prompts the user for the engine speed and pump drive ratio. The non-linear program simply prompts for the pump drive ratio. After a check is made to ensure that the resulting value for the oil pump speed lies within the limits of the data stored in data file PUMPDAT2.INP, subroutine VALUES calls subroutine PUMP2. This subroutine interpolates the oil pump data (using the interpolation subroutines INTERP and LOCATE) which is stored in the file PUMPDAT2.INP and returns a unique set of pressure and flow rate co-ordinates for the resulting characteristic curve. The gradient,  $M$ , and constant,  $C$ , for each linear region of this curve are stored in arrays GRAD and CONST respectively.

The user is given the option of modelling the pipe and annular pipe elements with laminar or turbulent flow conditions. The user is reminded that it is recommended that these components are initially modelled with laminar flow conditions. Under these flow conditions, the pressure losses within the bends and other flow restrictions are considered to be negligible. The user is prompted for the physical dimensions of the pipes or annular pipes and the program calculates the resulting frictional pressure loss. If turbulent flow conditions are chosen by the user, the integer number which represents the pipe or annular pipe in the array TYP, is changed from 1 to 8, or 9 to 10 respectively. In addition to prompting the user for the physical dimensions of the pipe or annular pipe element, the user is prompted for the loss coefficient,  $K_b$ , for any flow constriction within the component. If the pressure loss due to a bend or other flow constriction is to be ignored, the user is prompted to input a value of zero for the loss coefficient,  $K_b$ .



If there are any bearings within the system, the user is given the choice of either using the previously stored default variable values, or inputting new values. If the user selects to input new bearing values, either subroutine BEARVA or subroutine BEARVB is again called to perform this task, depending on the type of bearing being modelled (see above).

For partially grooved bearings, subroutine VALUES calls subroutine GROOVE, which interpolates the tabulated data stored on data file GROOVF.INP. This data file contains data from Figure 4.10, in a tabular form, for a bearing with a groove extent of  $180^\circ$ . Therefore, for a given value of bearing eccentricity, subroutine GROOVE returns the values for  $f_1$  and  $f_2$  (see section 4.7.1).

The simple bearing oil temperature rise model (see section 5.3.1) is contained in subroutine OILPRO, which is called for each bearing in the lubrication system. Subroutine OILPRO initially calculates the parameter  $\Delta T/C_s$ . The value of  $\Delta T$ , which corresponds to the value for parameter  $\Delta T/C_s$ , is estimated from interpolation of the data contained in the data file OILVIS.INP. This data file contains data from Figure 5.2, which is stored in a tabular form. Once the working temperature of the oil within the bearing is known, the oil viscosity is found from interpolation of temperature v viscosity data, which is also stored in data file OILVIS.INP.

If the system contains an oil cooler, the user is informed that the physical properties for the oil cooler are read from the data file OILCOOL.INP. The program extracts the data contained in this file and displays a summary of its contents to the screen.



## 6.5 Data Processing

In addition to prompting the user for the required input for each component element, subroutine VALUES also calculates all the constant terms in each pressure loss v flow rate relationship. It is at this point that the main differences occur between the construction of the linear and the non-linear programs.

### 6.5.1 Linear Program

The linear program constructs a set of linear equations which can be represented in the following form:

$$\begin{aligned}
 a_{11}x_1 + a_{12}x_2 + a_{13}x_3 + \dots + a_{1N}x_N &= b_1 \\
 a_{21}x_1 + a_{22}x_2 + a_{23}x_3 + \dots + a_{2N}x_N &= b_2 \\
 &\dots \\
 &\dots \\
 a_{M1}x_1 + a_{M2}x_2 + a_{M3}x_3 + \dots + a_{MN}x_N &= b_M
 \end{aligned} \tag{6.1}$$

or in matrix form:

$$A \cdot x = b \tag{6.2}$$

Subroutine LAYOUT prompts the user to input the required variable values for each element in the system. Therefore, the constants  $a_{i1}$ ,  $a_{i2}$ ,  $a_{i3}$ , ...,  $a_{iN}$ , and  $b_i$ , are calculated for each equation,  $i$ . The values for the  $a_{ij}$  constants are placed in a two-dimensional array 'A' and the  $b_i$  values are placed in a one-dimensional array 'B'. The manner in which this is achieved is best demonstrated with a simple example. For the simple four element system shown in Figure 6.3, there are five unknowns to be solved for: two pressures,  $P_1$  (at node 2) and  $P_2$  (at node 3) and three flow rates,  $Q_1$  (between nodes 1 and

3),  $Q_2$  (between nodes 3 and 4) and  $Q_3$  (between nodes 3 and 5). The nodes at which the two pressures labelled  $P_1$  and  $P_2$  are actually being solved for are obtained from array PNUM. Similarly, elements which are represented by the three flow rates  $Q_1$ ,  $Q_2$ , and  $Q_3$  are obtained from array QNUM.

As there are five unknowns there must also be five equations: one equation for each of the four elements, and one equation to represent flow continuity at the dividing node 3. Therefore, the program sets up array A as a 5 x 5 array (to represent a 5 x 5 matrix), and array B is set up as a 1 x 5 array (to represent a 1 x 5 matrix).

Each column in array A represents a constant  $a_i$  which is associated with an unknown,  $x_i$ , where  $i=1$  to 5. Therefore,  $x_1$  represents  $P_1$ ,  $x_2$  represents  $P_2$ ,  $x_3$  represents  $Q_1$ ,  $x_4$  represents  $Q_2$ , and  $x_5$  represents  $Q_3$ . The arrays A and B are initially conditioned to contain only zero's.

If we consider the moment where the program is prompting the user to input data for the pipe element between nodes 2 and 3. The pressure loss v flow rate equation for a laminar pipe (this relationship is discussed in more detail in section 4.3) is of the form:

$$P_{(node\ 2)} - P_{(node\ 3)} - con \cdot Q_{(between\ nodes\ 2\ and\ 3)} = 0 \quad (6.3)$$

where

$P_{(node\ 2)}$  = Pressure at node 2.

$P_{(node\ 3)}$  = Pressure at node 3.

con = Constant associated with  $Q_{(between\ nodes\ 2\ and\ 3)}$ .

$Q_{(between\ nodes\ 2\ and\ 3)}$  = Flow rate between nodes 2 and 3.

If we compare this equation to the general form for a linear equation:

$$a_1x_1 + a_2x_2 + a_3x_3 + a_4x_4 + a_5x_5 = b \quad (6.4)$$

Following the rules presented above:

- i,  $x_1$  represents  $P_1$ , in turn representing  $P_{(\text{node } 2)}$ , therefore  $a_1 = 1$ .
- ii,  $x_2$  represents  $P_2$ , in turn representing  $P_{(\text{node } 3)}$ , therefore  $a_2 = -1$ .
- iii,  $x_3$  represents  $Q_1$ , in turn representing  $Q_{(\text{between nodes 1 and 2})}$ , and  $Q_{(\text{between nodes 2 and 3})}$ . Therefore  $a_3 = \text{con.}$
- iv,  $x_4$  represents  $Q_2$ , in turn representing  $Q_{(\text{between nodes 3 and 4})}$ , as it does not appear in Equation 6.3,  $a_4$  is zero.
- v,  $x_5$  represents  $Q_3$ , in turn representing  $Q_{(\text{between nodes 3 and 5})}$ , as it does not appear in Equation 6.3,  $a_5$  is zero.
- vi,  $b$  represents the constant on the right-hand side, therefore  $b$  is zero.

As the pipe element is the second element in the example system, this corresponds to the second equation in the set of linear simultaneous equations, and also the second row of arrays A and B. Consequently subroutine VALUES would store the constants for this element with the following labels:

- i,  $a_1 = A(2,1)$  (second row, first column).
- ii,  $a_2 = A(2,2)$  (second row, second column).
- iii,  $a_3 = A(2,3)$  (second row, third column).
- iv,  $b = B(2)$  (second row)
- v, All the other values for A on the second row are zero.

When this process has been carried out for each of the elements in the system, the final task carried out by subroutine VALUES is to represent the continuity of flow at the dividing nodes. The array BIN is scanned and if a



dividing node is found a continuity of flow equation is constructed for that node.

For the simple example shown in Figure 6.3, the equation for the continuity of flow at node 3 would be of the form:

$$Q_{(\text{between nodes 1 and 3})} - Q_{(\text{between nodes 3 and 4})} - Q_{(\text{between nodes 3 and 5})} = 0 \quad (6.5)$$

If this equation is compared to the general form for a linear equation (Equation 6.3), then:

- i,  $x_1$  and  $x_2$  represent pressures at nodes 2 and 3. As there are no pressure terms in the above equation,  $a_1$  and  $a_2$  are zero.
- ii,  $x_3$  represents  $Q_1$ , in turn representing  $Q_{(\text{between nodes 1 and 2})}$  and  $Q_{(\text{between nodes 2 and 3})}$ . Therefore  $a_3 = 1$ .
- iii,  $x_4$  represents  $Q_2$ , in turn representing  $Q_{(\text{between nodes 3 and 4})}$ . Therefore  $a_4 = -1$ .
- iv,  $x_5$  represents  $Q_3$ , in turn representing  $Q_{(\text{between nodes 3 and 5})}$ . Therefore  $a_5 = -1$ .
- v,  $b$  represents the constant on the right-hand side, therefore  $b$  is zero.

Subroutine VALUES stores the values for these constants on the fifth row of arrays A and B:

- i,  $a_3 = A(5,3)$  (fifth row, third column).
- ii,  $a_4 = A(5,4)$  (fifth row, fourth column).
- iii,  $a_5 = A(5,5)$  (fifth row, fifth column).
- iv,  $b = B(5)$  (fifth row)
- v, All the other values for A on the fifth row are zero.

By following a similar procedure, subroutine LAYOUT can form the arrays A and B for any system layout. These arrays represent the matrices [A] and [b], which are solved by either the Gauss-Jordan or the LU decomposition linear matrix solving techniques. The first linear program utilised subroutine GAUSSJ, which contained a method for partial pivoting of matrix [A] and contained the Gauss-Jordan algorithm (a description of this routine is presented in Appendix A.1.2). Subroutine GAUSSJ returned the results for the required unknowns, x, in a one-dimensional array named 'X'.

In a similar way, the second linear program processes matrices [A] and [b], by calling the two subroutines LUDCMP and LUBKSB, which contains the LU decomposition algorithm (a description of this routine is presented in Appendix A.1.3). Subroutine LUDCMP conducts a partial pivoting process and additionally returns an LU decomposition of matrix [A]. This is input into the second subroutine LUBKSB which returns the results with the solution vector [X]. The subroutines GAUSSJ, LUDCMP, and LUBKSB, were obtained from Press et al (1989).

### 6.5.2 Non-Linear Program

Subroutine VALUES prompts the user to input the required variable values for each component element in the system. If we take the simple system shown in Figure 6.3 as an example, and again consider the moment when the user is being prompted to input data for the laminar pipe element between nodes 2 and 3. The equation which represents the pressure loss v flow rate characteristics for a pipe is of the form:

$$P_{(node\ 2)} - P_{(node\ 3)} - con \cdot Q_{(between\ nodes\ 2\ and\ 3)} = 0 \quad (6.6)$$

Subroutine VALUES calculates the value for the constant term 'con' and stores this value in a one-dimensional array named 'CON1'. The value of 'con' is stored in the elements 'j' co-ordinate, so for this example, with the pipe element between nodes 2 and 3, 'con' would be stored in location CON1(3). The value of the constant term is stored in memory because it remains constant throughout the non-linear iteration procedure, and as such, is not affected by different values for the unknowns at each iteration step.

The actual pressure loss v flow rate relationships which are used to represent each element in the system are discussed in more detail in Chapter 4. Some of these relationships have more than one constant term within them. For this reason, additional one-dimensional arrays are formed which are named 'CON2', 'CON3' and 'CON4'. These arrays are used to store the additional sets of constant terms.

When subroutine LAYOUT has prompted the user to input the required variable values for each element in the system, and all the constant terms have been stored in arrays CON1 to 4, subroutine MRQMIN is called, which contains the Levenberg-Marquardt algorithm (a description of this routine is presented in Appendix A.2.1). This routine was extracted from Press et al (1990). MRQMIN in turn, calls subroutine MRQCOF, at the heart of which is the LU decomposition linear matrix solver (for the solution of Equation A.34) and the subroutine FUNCS. The subroutine FUNCS contains the pressure loss v flow rate relationships and the partial derivatives of these relationships, for each type of component element.

For each iteration loop, MRQMIN calls MRQCOF to scan the system layout, stored in the array BIN, and check the type of each element in array TYP. MRQCOF calls subroutine FUNCS for each element in the system and



a calculation is made for the dependent variable ' $Y_{i,c}$ '. Each type of component element is represented by a unique pressure loss v flow rate relationship. Guessed values are made for the unknowns to be solved, and the relevant constant terms are extracted from arrays CON1 to 4.

On the first iteration, initial guesses for the unknowns,  $a_i$ , of  $1.0 \times 10^5 \text{ N/m}^2$  for all the pressures and  $1.0 \times 10^{-5} \text{ m}^3/\text{s}$  for all the flow rates are made. In the linear program, the oil pump is assumed to be operating in the lower of the two linear regions, while in the non-linear program, the oil pump is assumed to be operating in the linear region which is the closest to the centre of the performance curve. The slope,  $M$ , and constant,  $C$ , for this linear region, are extracted from arrays GRAD and CONST respectively. Using the guessed values for  $a_i$  and the constant values stored in arrays CON1 to 4, subroutine FUNCS returns the calculated new value of  $Y_{i,c}$ , and the partial derivatives  $dY_{i,c}/da$ . Each equation used to represent the pressure loss v flow rate relationship is manipulated into the form:

$$Y_i = 0 = f(\Delta P_i, Q_i) \quad (6.7)$$

The true value for  $Y_i$  ( $Y_{i,T}$ ), is known to be zero for each equation,  $i$ .

If, for example, we again take the pipe element for the simple system shown in Figure 6.3, the equation for the pipe element is stored in subroutine FUNCS in the form of Equation 6.6. In the non-linear program the unknowns are designated,  $a_i$ , rather than  $x_i$ . However, the same rules apply to the labelling of the unknowns to their respective system pressures and flow rates. By scanning arrays PNUM and QNUM it can be seen that:

- i,  $a_1$  represents  $P_1$ , which in turn represents pressure at node 2. Therefore  
 $a_1 = 1.0 \times 10^5 \text{ N/m}^2$ .

- ii,  $a_2$  represents  $P_2$ , which in turn represents pressure at node 3. Therefore  $a_2 = 1.0 \times 10^5 \text{ N/m}^2$ .
- iii,  $a_3$  represents  $Q_1$ , which in turn represents flow rate between nodes 1 and 2, and between 2 and 3. Therefore  $a_3 = 1.0 \times 10^{-5} \text{ m}^3/\text{s}$ .
- iv,  $a_4$  represents  $Q_2$ , which in turn represents flow rate between nodes 3 and 4. Therefore  $a_4 = 0$  for this equation.
- v,  $a_5$  represents  $Q_3$ , which in turn represents flow rate between nodes 3 and 5. Therefore  $a_5 = 0$  for this equation.

The partial derivatives for Equation 6.6 are:

- i,  $dY_{i,C}/da_1 = 1$ .
- ii,  $dY_{i,C}/da_2 = -1$ .
- iii,  $dY_{i,C}/da_3 = -\text{con} = -\text{CON1}(3)$ .
- iv,  $dY_{i,C}/da_4 = 0$ .
- v,  $dY_{i,C}/da_5 = 0$ .

Thus, subroutine FUNCS returns the values for  $Y_{i,C}$  and  $dY_{i,C}/da_i$  for the pipe element. When all the elements in the system have been represented in the above manner, the continuity of flow at each dividing node is represented by a simple equation of the form:

$$Q_{(\text{between nodes 1 and 3})} - Q_{(\text{between nodes 3 and 4})} - Q_{(\text{between nodes 3 and 5})} = 0 \quad (6.8)$$

Which again returns the values for  $Y_{i,C}$  and  $dY_{i,C}/da_i$ , in a similar manner to the pressure loss v flow rate equation shown above:

- i,  $a_1$  and  $a_2$  represent the pressures at nodes 2 and 3. Therefore  $a_1$  and  $a_2$  are zero with respect to this equation.
- ii,  $a_3$  represents  $Q_1$ , which in turn represents the flow rate between nodes

- 1 and 2, and between nodes 2 and 3. Therefore  $a_3 = 1.0 \times 10^{-5} \text{ m}^3/\text{s}$ .
- iii,  $a_4$  represents  $Q_2$ , which in turn represents the flow rate between nodes 3 and 4. Therefore  $a_4 = 1.0 \times 10^{-5} \text{ m}^3/\text{s}$ .
- iii,  $a_5$  represents  $Q_3$ , which in turn represents the flow rate between nodes 3 and 5. Therefore  $a_5 = 1.0 \times 10^{-5} \text{ m}^3/\text{s}$ .

The partial derivatives for Equation 6.8 are:

- i,  $dY_{i,C}/da_1 = 0$ .
- ii,  $dY_{i,C}/da_2 = 0$ .
- iii,  $dY_{i,C}/da_3 = 1$ .
- iv,  $dY_{i,C}/da_4 = -1$ .
- v,  $dY_{i,C}/da_5 = -1$ .

The Levenberg-Marquardt algorithm returns new values for the unknowns, for input into the next iteration. The above process is repeated until the  $\chi^2$  merit function decreases by less than 0.1. The number of iterations which are required is dependent on the size of the lubrication system. It was found that four iterations were usually sufficient for the AJ6 system, while the larger V8 system often required in excess of eight iterations. At this point convergence is assumed and the present values of the unknowns,  $a_i$ , ie, the pressures and flow rates through the system, are returned as the results.

The main program calls subroutine CHECKP to ascertain if the predicted output pressure from the pump lies within the confines of the linear region it is assumed to be operating in. The maximum and minimum pressures for each linear region are stored in array SWITCHP. If the pump output pressure lies outside the maximum and minimum pressures of the current linear region, it is assumed that the pump is operating in the neighbouring



linear region. The slope,  $M$ , and constant,  $C$ , are found for the new linear region from the arrays GRAD and CONST respectively. The program returns to the beginning of the Levenberg-Marquardt routine and the iteration process is repeated. This process is repeated until the pump output pressure lies within the confines of the linear region it is assumed to be operating in.

## 6.6 Output of Results

The results produced by both the linear and non-linear flow programs are stored in one-dimensional arrays. This array is named 'X' in the linear program and 'A' in the non-linear program. However, the order in which the results are stored is the same in both arrays. In the linear program, subroutine 'SCREEN' is called to display the results to the screen. The initial non-linear program displayed the current values for the unknowns to the screen after each iteration, enabling the user to observe how the results were converging to the stabilised values. However, it was found that when the V8 engine lubrication system was modelled, which was represented by 231 flow elements compared to 89 for the AJ6 engine, a very large amount of data was displayed to the screen (158 pressures and 142 flow rates). The amount of time between iterations, when the program was run on the workstation, was not adequate to study the information which was displayed. Therefore, the subroutine SCREENW was developed, which displays a summary of the programs progress after each iteration. The summary includes:

- i, The present iteration number
- ii, The value of 'ITST'. This demonstrates how close the program is to convergence for the linear portion of the pump curve in which it is assumed to be operating. Convergence is assumed when  $ITST = 3$  (see the description of the Levenberg-Marquardt algorithm in Appendix

A.2.1).

- iii, The value of  $\chi^2$  (see Appendix A.2.1)
- iv, The current linear portion of the oil pump curve the program assumes the pump is operating in.

When the non-linear program has finished its iteration procedure and the results have converged to their final values, the main program calls subroutine FINISH. This subroutine displays a message to the screen to inform the user that the flow program has finished running. The user is informed of the number of iterations carried out and the linear region in which the oil pump is finally found to be operating in. In addition, the user is informed that the results for the pressures and the flow rates are stored in the output file ANS.OUT.

The linear and the non-linear programs call subroutine WRITEF to store the final results in output files. The output files for the linear program are called RES.OUT and ANSWER.OUT. The file RES.OUT simply contains the results for the pressures and flow rates through the system, both in metric and in imperial units. However, the file ANSWER.OUT contains the various arrays (BIN, TYP, PNUM, QNUM, etc) which are formed to model the system. This gives the user the opportunity of checking for errors, by studying the arrays which represent the system.

The output file for the non-linear program is named 'ANS.OUT'. This file contains the results for the pressures and flow rates throughout the system in metric units. Additional information is included in the file to identify the modelling conditions for the system. This data is comprised of; the date, the program run-time, the system title, the name of the echo file (described in section 6.7) used to run the program (this remains blank if a system is



modelled from scratch), the engine speed, the sump oil temperature and the default values for the radial clearances for the main, big-end and cam bearings. An example of the output file ANS.OUT, which was generated for the V8 engine lubrication system, is given in Volume II.

Subroutines SCREEN and WRITEF scan the arrays PNUM and QNUM to ascertain which results correspond to which pressures and which flow rates. The results are then presented in the following form:

' Pressure at node \*\* = \*.\*\* N/m<sup>2</sup> '

or

' Flow rate between nodes \*\* and \*\* = \*.\*\* m<sup>3</sup>/s '

The flow rate results are presented as the flow rates between dividing nodes. For the simple example system shown in Figure 6.3, the flow rate for the oil flow through the pipe element is labelled  $Q_1$ , which in turn represents the flow rate between nodes 1 and 2, and also between nodes 2 and 3. This would be presented as 'the flow rate between nodes 1 and 3'.

The output file ANS.OUT is enhanced with the labelling of the pipe elements which are experiencing turbulent flow conditions. The main program calls subroutine TURBUL to calculate the Reynolds number,  $Re$ , for each pipe element. If the Reynolds number is found to be greater than 2100, turbulent conditions are assumed and the character string '\*T' is stored in the character array TRANS. The character array TRANS is written to the output file ANS.OUT, adjacent to the listing of the flow rates through the system. Consequently a '\*T' appears next to a flow rate section which is experiencing turbulent flow in one of its pipe sections. The relevant pipe section, and the Reynolds number for this pipe section, are listed at the end of the output file



ANS.OUT. This information allows the user to change the data for any of these pipe sections, which is stored in the echo file, from laminar flow to turbulent flow conditions. The system can then be re-modelled with these new flow conditions.

The process of labelling the turbulent pipe sections was chosen in preference to automatically changing them to turbulent flow within the program. It was considered that the latter method would introduce instability in the program. The pressure losses associated with turbulent flow were found to be greater than with laminar, especially when bend losses were included. Greater pressure losses in one part of the system can change the pressures and flow rates through the rest of the system. Therefore, pipe sections which were previously found to be turbulent, might revert back to being laminar under these new conditions. This would necessitate changing these pipe sections back to laminar and re-calculating the whole system ... etc. Labelling the turbulent pipe elements, instead of automatically calculating for them, allows the user to use his judgement in selecting the pipe elements which should be changed.

The linear program gives the user the opportunity of storing the system layout in a data file. The data file, the name of which is provided by the user, stores all the relevant arrays that the program has formed to model the system (arrays BIN, TYP, PNUM, QNUM, A, B, etc). This data file enables the rapid re-modelling of the same system at a later date.

In addition to generating the output file ANS.OUT, the non-linear flow program calls subroutine WRITEF, which generates a second output file named 'PANDQ.OUT'. This output file stores all the data necessary to represent the physical system (ie. arrays BIN, TYP, PNUM, QNUM, ... etc), and the results for the pressures and flow rates throughout the system. The data contained in

this data file is used in the heat transfer and engine block programs.

## 6.7 User Interface

Both the linear and the non-linear programs are written to be 'user friendly', prompting the user at every stage with clear instructions and providing many safety catches to prevent the accidental input of incorrect data. The safety catches are comprised of two types; checking the order of magnitude of the data and ensuring that it is of the correct type. A check is made on all the input data to prevent accidental input of negative values, which could result in a division by zero at a later stage of the program. The order of magnitude checks are only carried out on some of the critical data items. For example, a check is made to ensure that the characteristics for the engine speed and pump drive ratio chosen by the user, can be interpolated from the available data.

The second type of check performed by the program is of the data type, ie, whether it is a real number, an integer number, or a character. This eliminates the risk of accidentally 'crashing' the program at the input stage. If the program were crashed, all the data input by the user up to that point would be lost. To eliminate this problem, if an input error occurs, the program calls subroutine ERROR. This subroutine displays an error message to the screen and returns control to the user for another attempt at inputting the same piece of data.

Both the linear and the non-linear programs incorporate an 'echo file' system. Each variable value input by the user, and accepted by the program as being both of the correct type and of the correct magnitude, is stored sequentially in a data file. In the linear program this file is named 'ECHO.FIL'



and in the non-linear program it is named 'ECHONL.FIL'. Following the input of each item of data by the user, subroutine SHUT is called, which closes the echo file and immediately re-opens it. This approach was taken because the data written to a file was stored in a buffer within the computer until the program was completed, whereupon the file was closed. If the program was terminated before the file was closed, the buffer was emptied without writing to the file and the data was lost. Closing the echo file and immediately re-opening it, after each data input, ensures that the data is safely written to the echo file and the user can safely terminate the program at any time.

If a mistake is made by the user, in terms of the order of magnitude of an item of data, the program can be terminated by the user and the data edited in the echo file. The program can be re-started with the echo file as a data input device, returning the control back to the user at the point in the program where it was previously terminated. This alleviates the problem of having to laboriously input all the data again, up to the point where the mistake was made.

When the option of modelling a system from an echo file is selected from the opening screen, which is displayed by the subroutine WELCOM, the main program calls subroutine READF1 to prompt the user for the name of the echo file which is to be used. The user is given the option of providing the name of the echo file, or using the default echo file, which was automatically formed during the last successful run of the program. The default echo file is named SHADOW.FIL.

The flow program is run from a shell script called 'GO', which incorporates a routine which copies the contents of the echo file ECHONL.FIL to the default file SHADOW.FIL. This is only achieved when the flow program



has run successfully to the end. If the program is terminated by the user, the echo file ECHONL.FIL has to be re-named or copied to a new file by the user, before the contents of the file can be used as input for the program. This procedure is necessary because the program can not read from, and write to, the same file simultaneously.

When a complete system had been modelled, the echo file, which can be re-named by the user, allows the stored values to be checked and/or changed at a later date. The program can be re-run using this, and any other echo file, as a user input device. This eliminates the laborious task of re-modelling the whole system 'from scratch' if only a few values need to be changed from a previously formed system. Consequently, the addition of the echo file system enhances the design analysis capabilities of the program. Thus, the user is given four options of modelling a lubrication system when the linear program is initiated:

- i, Construct a new system 'from scratch'. If this option is taken, the user can either model the system using a 'rapid' method which uses default values for the bearings, or the user can input every variable value for the system. The latter method, although time consuming when modelling the system for the first time, forms a comprehensive echo file which contains every variable value. This enables variable values to be changed for any component element in the system and the program re-run using the echo file as a data input device.
- ii, Use a pre-formed system stored on a data file, but not changing the values for any of the variables. This allows the rapid re-modelling of an identical system, if the original results are lost or are accidentally overwritten by a following run of the program.

- iii, Use a pre-formed system stored on a data file, but inputting new values for all the variables. This allows systems with identical layouts to be rapidly re-modelled, but the user has to supply new values for the component variables on each run.
- iv, Restart, using an echo file as a data input device. As discussed above, this allows either an entire system to be re-modelled with minor changes, or a previous modelling attempt can be re-started after a mistake was made.

The non-linear program only gives the user the options, i, and iv. It was found that for large systems, such as the V8 engine lubrication system, option, iii, was rarely used because it required a large amount of input data from the user. It was found that once a system had been modelled using option, i, the echo file was used for all subsequent modelling runs for that system. The echo file system provides greater flexibility than option, ii, and allows the user to carry out parametric studies with ease.

## 6.8 Summary of Chapter 6

This chapter has presented a description of the FORTRAN programs which were developed to simulate the flow conditions within the pressurised side of the lubrication system. The construction of the programs was influenced by the type of computer used to carry out the development work. Program development followed an 'evolutionary' path as it moved from the PC to the workstation. The final, fully developed, non-linear flow program inherited many of the programming techniques which were developed to enable the initial linear program to be run on the smaller memory capacity and slower PC. Consequently, this only allowed lubrication systems with diverging nodes to be



modelled.

The linear flow program was developed to a stage where the physical system is represented by a combination of six types of component elements; laminar pipes, pumps, filters, journal bearings, crank-shaft transfer holes and cam bearing transfer holes. The resulting set of simultaneous equations, which represent the flow conditions through the system, are solved in the final linear flow program by an LU decomposition routine. The program was developed in a modular manner, utilising a subroutine format. Many of these subroutines were used to construct the initial non-linear flow program. Consequently, the initial non-linear flow program was of a similar construction to the linear program, except the set of simultaneous equation were solved by an iterative process using the Levenberg-Marquardt routine. This allowed a true comparison to be made between the linear and non-linear solution methods. A description of the differences in the accuracy of results and the computer run times are given in section 8.3.

The non-linear flow program was developed further to include additional component elements, some of which are represented by non-linear pressure loss v flow rate relationships. These components elements include; turbulent pipes with bend losses, annular pipes (turbulent or laminar), oil strainers and oil coolers. This program has a greatly refined user interface. The user is prompted, with clear instructions, for all the required data. A comprehensive series of checks are automatically carried out on the information supplied. This ensures that the data is of the correct 'type' and order of magnitude.

The fully developed non-linear flow program, however, maintains the same basic structure to that developed for the early programs. The subroutine format breaks the program down into four distinct stages; representation of the



physical system; input of variable values; solving for the unknowns and the output of the results.

The physical system is represented by a series of component elements joined at nodal points. This system is stored in memory by the start node number, end node number, and type, for each component element in the system. This data is analyzed, firstly, to ascertain for which nodes a pressure is to be calculated and, secondly, to find the component elements which lie between dividing nodes, which share the same flow rates.

When the layout of the physical system has been represented, the program prompts the user to input the required variable values for each component element in the system. A check is made on the type and order of magnitude of the values which are supplied. This reduces the risk of accidentally 'crashing' the program with the input of incorrect data. The linear program assumes a constant oil temperature of 100°C throughout the system, except for the bearings, where a simple oil temperature rise calculation is included. In the non-linear program the oil temperature is either selected by the user or extracted from a data file which was automatically generated during a previous run of the heat transfer program.

When all the variable values have been input by the user, for every component element in the system, the program begins the data processing stage. In the linear flow program, a set of simultaneous equations are generated from the equations which represent the linear pressure loss v flow rate relationship for each component element and the flow continuity at each dividing node. The constant terms in the set of simultaneous equations are stored in the arrays 'A' and 'B'. These arrays are passed to the LU decomposition routine which returns the results for the pressures and flow

rates in a one-dimensional array 'X'.

In the non-linear flow program, the solution of the set of simultaneous equations is carried out by an iterative technique, using the Levenberg-Marquardt routine. On the first iteration, initial guesses are made of  $1.0 \times 10^5$  N/m<sup>2</sup> for all the pressures and  $1.0 \times 10^{-5}$  m<sup>3</sup>/s for all the flow rates. At the heart of the Levenberg-Marquardt routine lies the subroutine 'FUNCS'. Using the values for the unknowns which were predicted during the last iteration of the program (or the guesses values on the first iteration), this subroutine returns the new values for  $Y_i$  and the partial derivatives  $dY_i/da_i$  for each pressure loss v flow rate relationship and flow continuity equation. These values are passed to the Levenberg-Marquardt routine which returns new values for the unknowns when every component element and dividing node in the system has been represented in such a manner. The iterative process continues until convergence occurs and the final results are returned in a one-dimensional array 'A'.

The linear flow program displays the results to the screen and automatically generates two output files named 'RES.OUT' and 'ANSWER.OUT'. The output file RES.OUT stores the pressure and flow rate results in metric and imperial units, while the file ANSWER.OUT stores the various arrays which are formed to model the system. The non-linear program displays a summary of the programs progress to the screen between each iteration. The user is informed when the program has converged and the output files 'ANS.OUT' and 'PANDQ.OUT' are automatically formed. The file ANS.OUT stores the results for the pressures and flow rates in metric units, in a format which is easy to read by the user. The pipe elements which are experiencing turbulent flow conditions are marked with a '\*T' symbol. The output file PANDQ.OUT stores both the results and the arrays which represent

the system. This file is generated for use in the heat transfer and engine block programs.

The flow programs flexibility and robustness is greatly enhanced with the development of the 'echo file' system. The program automatically stores each variable value, which has been input by the user, in a data file. This process allows the program to be terminated at any time and the information provided by the user up to that point will be saved in the echo file. This file can be edited by the user and used as a data input device to run the program again. The program will run up to the point where it was previously terminated and the control will be returned to the user. The echo file is automatically labelled to inform the user which section of data refers to which program prompt. This aides the editing of the echo file for conducting parametric studies on the system.



## **Chapter 7**

# **Structure of Heat Transfer Model and Engine Block Model Computer Programs**

### **7.1 Introduction**

This chapter presents the computer programs which were written for the simulation of the heat transfer by the lubricating oil within the engine. Attention initially focused on the development of the 'heat transfer program' (see flow chart in Figure 7.1), which simulates the heat transfer in the pressurised side of the lubrication system. The program uses geometric and flow data, stored in a data file which is generated by the non-linear flow program. This data represents the physical layout of the lubrication system and provides the pressures and flow rates of the oil at the exit from each bearing and chain tensioner.

The simulation of the heat transfer by the oil splashed on to the internal surfaces of the engine was achieved with the development of the 'engine block program' (see flow chart in Figure 7.2). This program utilises oil flow rate and pressure data produced by the non-linear flow program, and oil temperature data from the heat transfer program. This data is stored in data files which are automatically generated by the flow and heat transfer programs.

One of the greatest priorities in the development of the heat transfer programs was to retain as much commonality as possible between all the

different programs. The heat transfer program and the engine block program utilise the Levenberg-Marquardt routine for solving for the sets of simultaneous equations which are generated to model the system. Commonality is also retained in the user interface and in the method of storing input data in 'echo files' for future use. This technique was developed to reduce the risk of 'crashing' the program at the input stage and allows the user to re-run the program using previously stored data. This programming technique was described in detail in section 6.7.

For commonality with the flow program, and for the principal reasons presented in section 6.1.1, the heat transfer programs are also written in FORTRAN 77. Program development was carried out on a UNIX based workstation, which removed many of the programming restraints imposed on the non-linear flow program, which were documented in Chapter 6. Thus, the program construction was not based on the 'evolution' process, as the program development moved from a PC to a workstation. This led to a simpler programming technique, where large two-dimensional arrays (eg. 350 x 350 arrays) were often generated for the storage of data which was required to model the system.

A full listing of the FORTRAN programs which were developed for the simulation of the heat transfer within the lubrication system are given in Volume II. A user manual for the programs, which was supplied to Jaguar to supplement the program installation, is also included in Volume II. The user manual gives a full description of the required procedure for running the programs, and illustrates the prompts which are displayed to the screen.

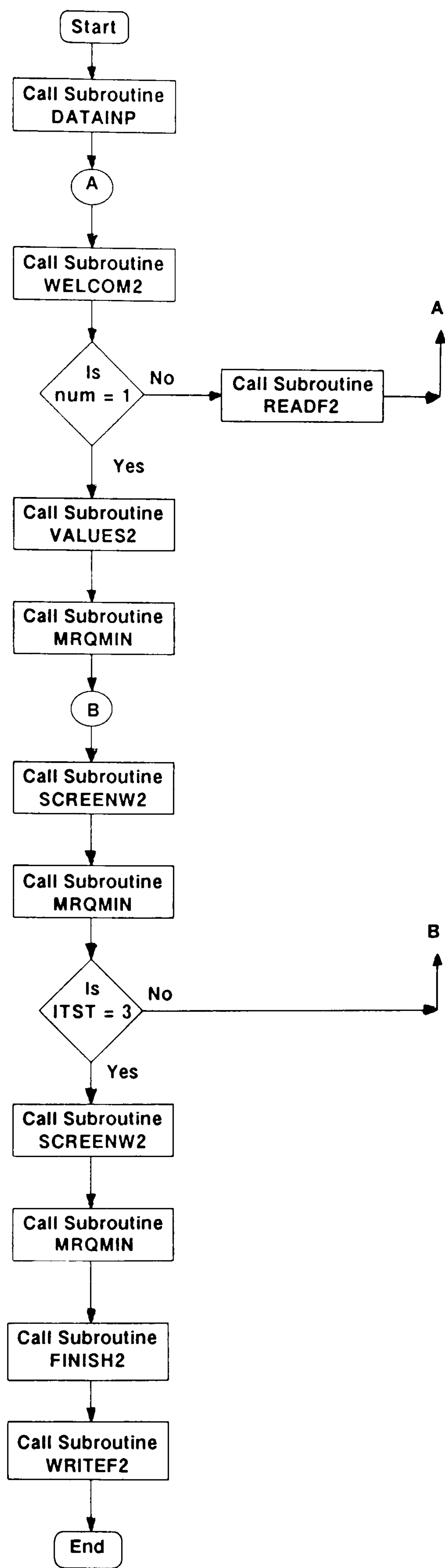


Figure 7.1. Flow chart of the heat transfer program



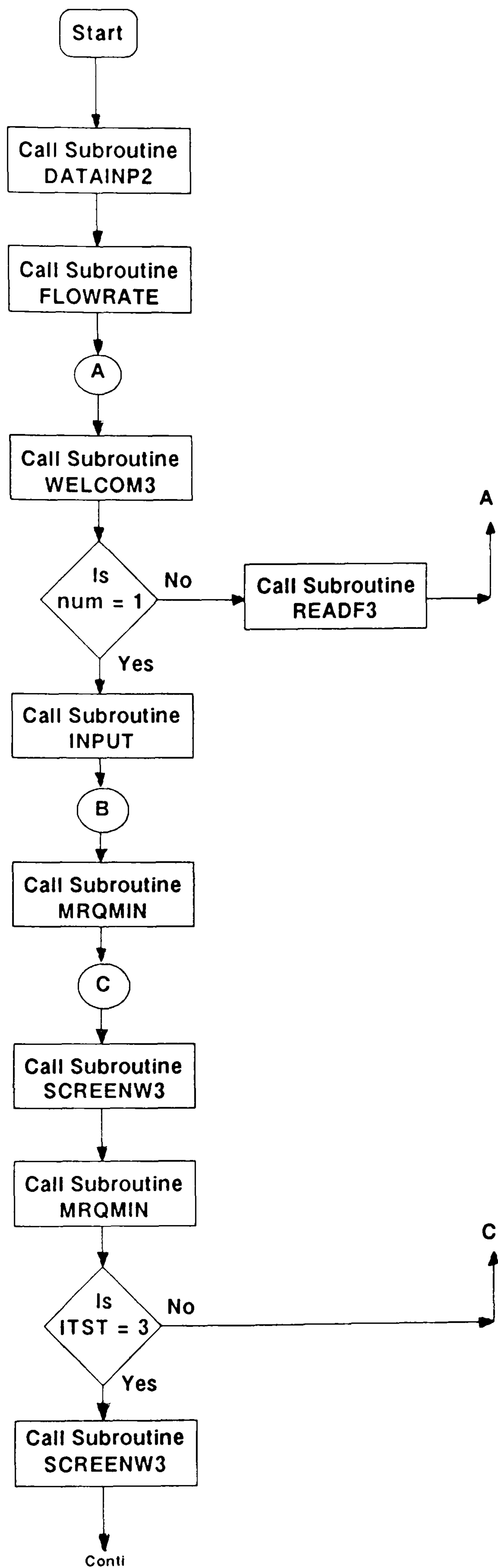


Figure 7.2. Flow chart of the engine block program

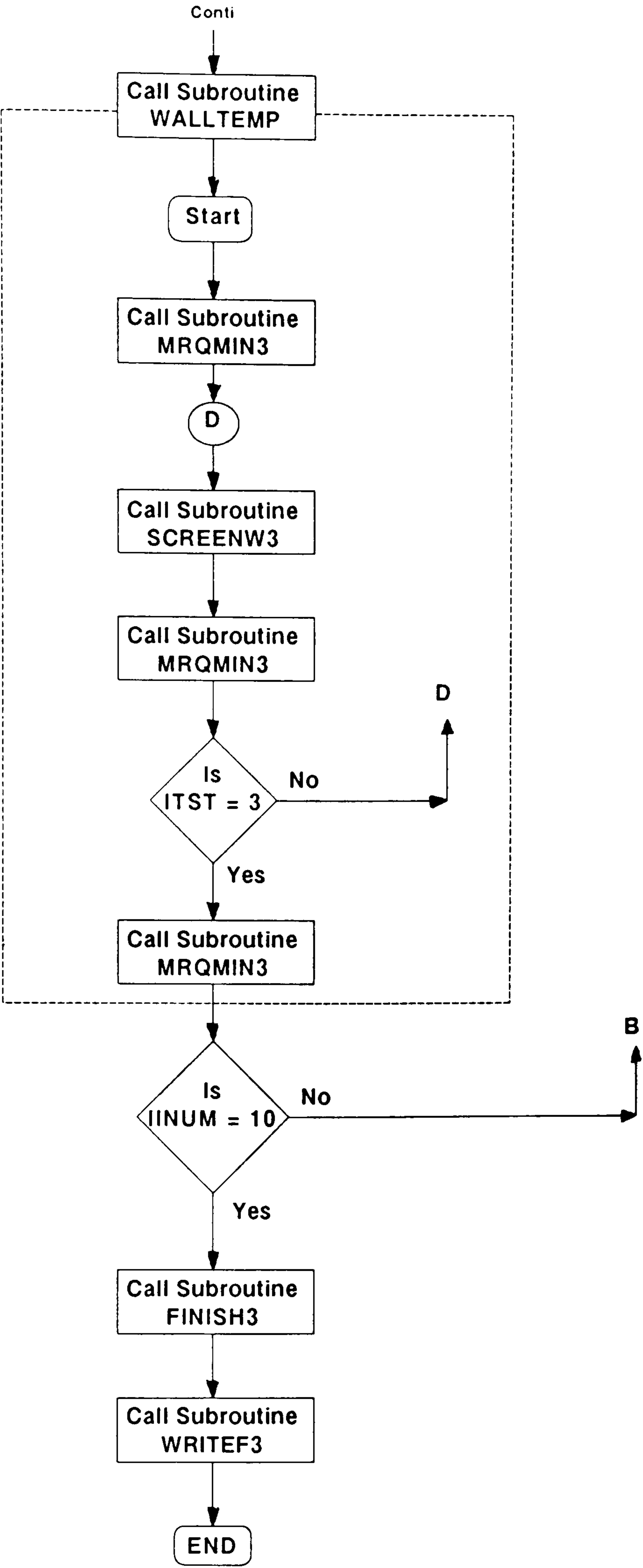


Figure 7.2.... Continued

## 7.2 Heat Transfer Program

The heat transfer program was developed with a structure similar to the non-linear flow program. As this program is run in conjunction with the flow program, the heat transfer program does not contain any method of representing the physical system. Instead, when the program is initiated, the main program calls subroutine DATAINP which extracts the arrays BIN, TYP, PNUM ..etc, from the data file PANDQ.OUT. This data file is formed during the previous run of the non-linear flow program.

The main program sequentially scans the data stored in the array TYP. If a heat transfer component element (eg. a pipe) is found, the variables ICOUNT and MA are incremented by one. The new value of ICOUNT is stored in the array TEMVAL, in the elements 'j' co-ordinate. If a non-heat transfer component element is found (eg. a pump), the present value of ICOUNT is stored in the array TEMVAL, in the elements 'j' co-ordinate. When this process is complete, the final value for MA represents the number of equations and the number of unknowns to be solved. The array TEMVAL is used to label the positions of the unknowns,  $a_i$ , in the Levenberg-Marquardt routine. For example, for a component element between the nodes  $i$  and  $j$ , the oil temperature at inlet to the component will be labelled  $a(\text{TEMVAL}(i))$ , and the temperature at exit will be  $a(\text{TEMVAL}(j))$ .

When the heat transfer program is initiated, the first screen seen by the user is very similar to that of the non-linear flow program. This screen is displayed by the subroutine WELCOM2. The user is given the option of inputting the required variable values 'from scratch', or using an echo file as a data input device. The echo file system used in the heat transfer program is similar in construction to the one used in the flow program. The echo file which



is automatically generated during each run of the heat transfer program is named ECHONL2.FIL.

If the option of using an echo file is selected by the user, the main program calls subroutine READF2 to prompt the user for the name of the file. This is a similar procedure to that described in section 6.7, for the flow program. However, as the option of using an echo file can only be selected if the program has previously been run and the lubrication system layout has previously been modelled, the following program description assumes the user is modelling the heat transfer within the system for the first time.

### 7.2.1 Preparation of Bearing Data

The heat transfer characteristics of the journal bearings are modelled using data stored in data 'maps' (these were discussed in more detail in section 5.3.2). Each bearing in the lubrication system requires an individual map. These maps are generated before the heat transfer program is initiated, using an adapted journal bearing program which was originally developed by Lai (1993). A listing of the adapted bearing program, which is named 'BEARING', is included in Volume II.

The bearing program requires two input files, a bearing geometry data file and a bearing polar load data file. The bearing geometry data file contains the geometry data for the journal bearing and the engine operating conditions. The bearing load file contains a list of the bearing loads for every  $10^\circ$  of rotation. A bearing load file for each bearing in the V8 engine was obtained from a bearing mobility analysis program developed at Jaguar (Smith (1990)).

The program BEARING is run for each bearing in the system. When the V8 engine lubrication system was modelled, each of the five main bearings were modelled individually. However, only one cam bearing and one big-end bearing was modelled. It was assumed that the loading variation would be minimal between the individual cam bearings and similarly, be minimal between the individual big-end bearings. When the bearing program is initiated, the user is prompted for a description of the bearing, the names of the bearing data files and the extent of the oil feed groove. The extent of the oil feed groove is represented by its start and end angular locations. These locations are relative to the positive x-axis (see Figure 7.3).

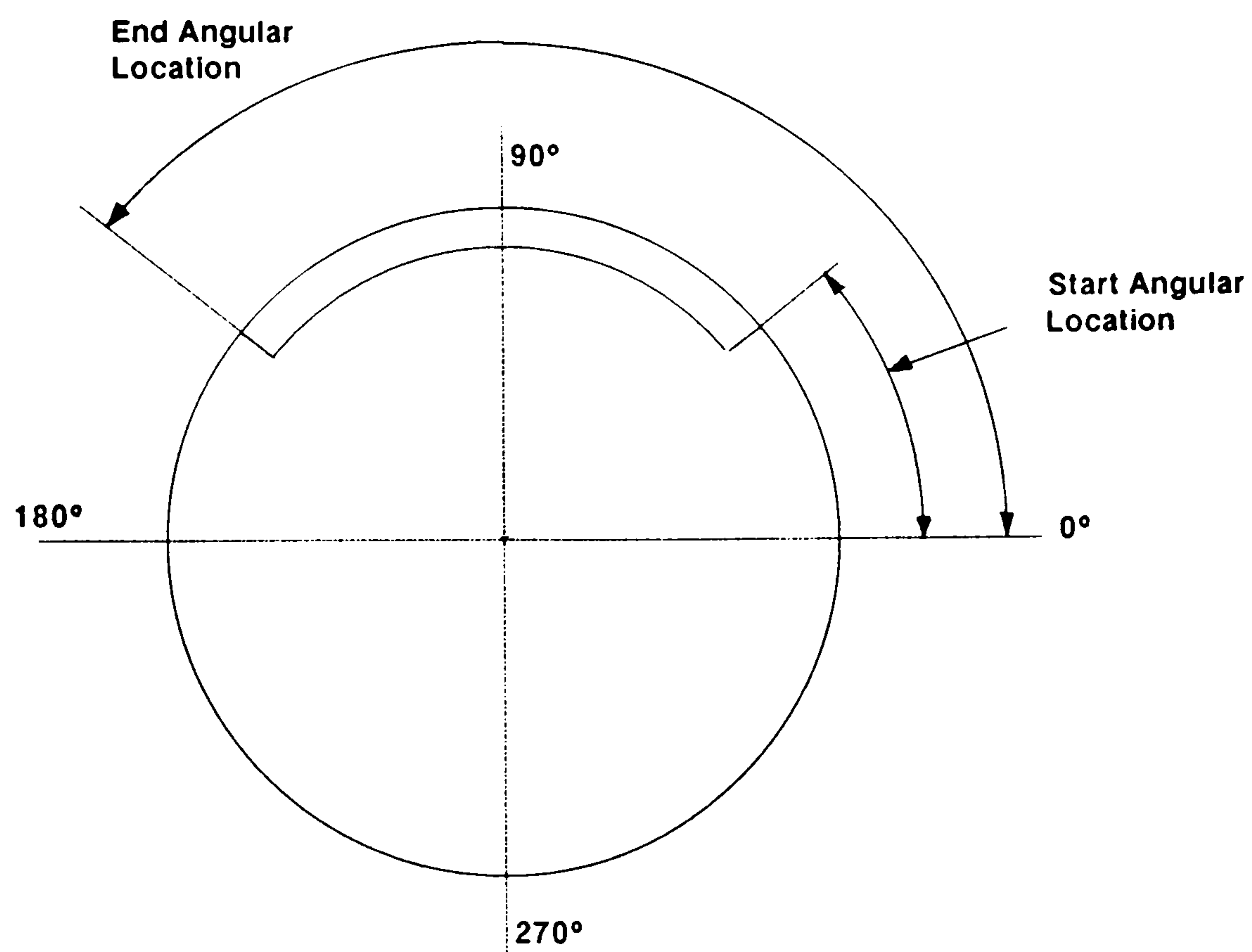


Figure 7.3. Journal bearing oil feed groove extent

All the journal bearings of the V8 engine were modelled as partially grooved bearings. The partially grooved bearings were modelled with a groove start location of  $0^\circ$  and an end location of  $+180^\circ$ . The bearings with simple oil feed holes geometry were modelled as grooved bearings, but with a small

groove extent. This was usually about  $2 - 3^\circ$ , depending on the diameter of the journal and the diameter of the oil feed hole. The start and end angular positions were dependent on the geometry of the bearing being modelled.

The bearing program developed by Lai was re-named as subroutine FRED2. This subroutine returns a value for the oil temperature rise within the bearing, given the input oil temperature and oil feed pressure. The subroutine FRED2 is nested inside a series of iterative loops within the program BEARING. Thus, the oil temperature rise is calculated for oil feed pressures ranging from  $1 \times 10^5 \text{ N/m}^2$  to  $7 \times 10^5 \text{ N/m}^2$  (in increments of  $1 \times 10^5 \text{ N/m}^2$ ), and inlet oil temperatures ranging from  $40^\circ\text{C}$  to  $160^\circ\text{C}$  (in increments of  $10^\circ\text{C}$ ). This data is stored in a file, the name of which is supplied by the user.

### 7.2.2 Input of Data

The main program calls subroutine VALUES2 to prompt the user for the data which is required to model the heat transfer within the lubrication system. The layout of the system is represented in arrays BIN, TYP, PNUM, QNUM, etc., which are extracted from data file PANDQ.OUT (generated by the flow program). The heat transfer program prompts the user for the temperature of the oil in the sump. This is stored as variable TEMPIN. This oil temperature is either estimated by the user (eg. the temperature of the oil for which the pump characteristics were obtained) or predicted during a previous run of the engine block program (see section 7.3).

If the system contains any pipes, annular pipes, crank-shaft transfer holes or cam bearing transfer holes, the user is prompted for the wall temperature for these components. These temperatures are stored in array CON3, in the elements 'j' co-ordinate. The dimensional data for the pipe



elements is extracted from additional data stored in the file PANDQ.OUT.

The program scans array TYP to find the location of the bearings in the lubrication system. The user is prompted, for each bearing in the system, for the name of the data file which contains the temperature map for the bearing. The temperature map for each bearing is generated previously, by the program BEARING, as described in section 7.2.1. The name of the data file for each bearing is stored in the character array BDFILE, in the bearing element's 'j' co-ordinate.

If the lubrication system contains an oil cooler, the user is prompted for the temperature and velocity of the air at the inlet. These are stored as variables AIRIN and AIRSPEED respectively. The user is reminded that an air velocity in the region of 20% of the vehicle velocity is considered to be a suitable figure. The remaining data, which represents the physical dimensions of the oil cooler, is stored in the data file OILCOOL.INP. The physical dimensions of the oil cooler are stored in a data file as it was considered to be the easiest way of conducting parametric studies on this type of component. It was considered that one of the primary uses of the heat transfer program would be to size the oil cooler in a lubrication system. It was assumed that editing the data stored in a well labelled data file would be easier than having to search and edit the relevant data in a relatively large echo file.

### 7.2.3 Data Processing

The heat transfer program utilises the Levenberg-Marquardt routine, the same routine used in the non-linear flow program. Initial guesses are made for the unknowns,  $a_i$ , (oil temperatures) throughout the lubrication system. When the program was first developed, the oil temperature in the sump was

used for the initial guess for the temperature at each node. However, it was found that using the same temperature at each node resulted in a division by zero in Equation 5.7, the equation used for the pipe elements. A similar problem was encountered when the initial guess for the exit temperature from a pipe element was assumed to be lower than the inlet, when in fact the oil was being heated. This was also true for the opposite case, when the initial guess for the exit temperature was assumed to be higher than at the inlet, when in fact the oil was being cooled.

To overcome the instability problems in the models for the pipe elements, unique initial guesses are made for the oil temperature at each node in the system. The inlet oil temperature into the system is known to be the sump oil temperature. The main program sequentially scans the array TYP to ascertain the type of component elements in the system. For each pipe element (pipe, annular pipe, crankshaft transfer hole or cam bearing transfer hole) the initial guess for the exit oil temperature,  $t_{bo}$ , is dependent on the relationship between the inlet oil temperature,  $t_{bin}$ , and the wall temperature,  $t_s$ :

- i,      If  $t_s > t_{bin}$ ,      then  $t_{bo} = t_{bin} + 0.1^\circ\text{C}$ .      ie.  $a(\text{TEMVAL}(j)) = a(\text{TEMVAL}(i)) + 0.1$ .
- ii,      If  $t_s < t_{bin}$ ,      then  $t_{bo} = t_{bin} - 0.1^\circ\text{C}$ .      ie.  $a(\text{TEMVAL}(j)) = a(\text{TEMVAL}(i)) - 0.1$ .

It is assumed that the exit temperature of the oil from an oil cooler will always be less than the inlet. Therefore, condition, ii, is assumed for all oil coolers. Equally, it is assumed that the exit oil temperature from each journal bearing will be greater than the inlet. Consequently condition, i, is assumed for all journal bearings.



The solution method is very similar to that documented for the non-linear flow program (see section 6.5.2). The Levenberg-Marquardt routine is contained in subroutine MRQMIN. This subroutine is called for each heat transfer equation to be solved for in the system. Subroutine MRQMIN calls subroutine MRQCOF, at the heart of which is the subroutine FUNCS. Using the guessed values for the oil temperatures throughout the system, the subroutine FUNCS returns the calculated new value of  $Y_{i,c}$  and the partial derivatives  $dY_{i,c}/da$ .

Each type of heat transfer element is represented in subroutine FUNCS by a unique oil temperature change equation and the partial derivatives of this equation. The actual relationships which are used to represent each heat transfer element in the system were presented in Chapter 5.

When a journal bearing is being modelled, subroutine FUNCS calls subroutine BDATAF. This subroutine extracts the temperature change data stored in the relevant bearing 'map'. The name of the data file which contains this data is stored in the bearing elements 'j' co-ordinate in the character array BDFILE. Given the oil feed pressure, subroutine BDATAF estimates by interpolation (using the interpolation subroutines INTERP and LOCATE) the unique temperature characteristic curve for the bearing. The relevant linear portion of this curve is estimated from the inlet oil temperature. The slope,  $M$ , and constant,  $C$ , are calculated for this linear region. These two constants are used to calculate the new value of  $Y_{i,c}$  and the partial derivatives  $dY_{i,c}/da$ .

When the temperature characteristics through an oil cooler are being modelled, subroutine FUNCS calls the subroutine COOLER. This subroutine contains the oil cooler model which was presented in section 5.4. The subroutine COOLER extracts the dimensional data for the oil cooler from the



data file OILCOOL.INP, extracts the oil properties from data file OILVIS.INP and the air properties from data file AIRPROP.INP. The new value for  $Y_{i,c}$  and the partial derivatives  $dY_{i,c}/da$ , are returned.

When all the heat transfer elements in the lubrication system have been represented by their temperature characteristics and partial derivatives of these equations, the Levenberg-Marquardt routine returns new values for the oil temperatures at each node. These new temperatures are used as the guessed values for the unknowns in the next iteration. The iterative procedure continues, in a similar way to that described for the non-linear flow program (see section 6.5.2), until convergence is assumed. At this point the present values of the unknowns,  $a_i$ , ie. the oil temperatures through the system, are returned as the results.

#### 7.2.4 Output of Results

The results for the temperatures at each node in the system are stored by the program in the one-dimensional array 'A'. Thus, any unknown,  $a(\text{TEMVAL}(i))$ , represents the temperature at the node,  $i$ . The method of displaying the results to the user is very similar to that employed in the non-linear flow program. The main program calls subroutine SCREENW2 after each iteration, which displays a summary of the programs progress. This summary includes:

- i,      The present iteration number.
- ii,     The value of 'ITST' (see Appendix A.2.1).
- ii,     The value of  $\chi^2$ .

When the program has finished its iteration procedure and the results have converged to their final values, the main program calls subroutine FINISH2. This subroutine informs the user that the program has finished running and how many iterations the program has made. The user is reminded that the results for the oil temperatures are stored in the output file TEMPER.OUT. The main program calls subroutine WRITEF2 to write the results to this output file, which contains the results for the oil temperature at each node in the lubrication system. The results are presented in the form:

'The value of the oil temperature at node \*\* = \*\*\*.\*\*\* °C'

The header of the output file includes additional information which identifies the modelling conditions for the system. This data is comprised of:

- i, The system title (extracted from the data file PANDQ.OUT).
- ii, The name of the echo file which was used to model the system in the non-linear flow program. This remains blank if the system was modelled 'from scratch'.
- iii, The name of the echo file which was used to run the heat transfer program. Again, this remains blank if the oil temperatures were input 'from scratch'.
- iv, The engine speed.
- v, The temperature of the oil in the sump.
- vi, If an oil cooler is included in the lubrication system, the air velocity and the air inlet and exit temperatures through the oil cooler are also displayed.

An example of the output file TEMPER.OUT, which was generated for the V8 engine, is given in Volume II.

The second output file OIL-T.OUT is also generated by subroutine WRITEF2, which stores the oil temperatures at each node in the system. This data file is generated for use in the non-linear flow program and the engine block program. This enables the non-linear flow program to be re-run, using the oil temperatures stored in this data file. These new oil temperatures will replace the oil temperatures which were assumed to remain constant throughout the whole system, during the first pass of the flow program. In addition, the oil temperatures at the exit from each branch in the system (usually the exit temperature from the bearings) are extracted from the data file OIL-T.OUT by the engine block program. This data is used in the engine block program to estimate the temperature of the oil which is sprayed onto the internal surfaces of the engine (see section 7.3.2).

### 7.2.5 User Interface

The heat transfer program utilises many of the methods developed in the non-linear flow program for the improvement of the user interface. These were described in more detail in section 6.7. Similar checks are made on the input data to ensure the data is of the correct order of magnitude and of the correct type. The heat transfer program also incorporates an echo file system. The echo file, which is re-written during each run of the program, is named 'ECHONL2.FIL'.

If the option of modelling the system using an echo file is selected at the opening screen, the main program calls subroutine READF2. The user is given the option of providing the name of the echo file, or using the default echo file which was formed during the last successful run of the program. In this case, the default echo file name is 'SHADOW2.FIL'. The heat transfer program is run from a shell script called 'GO2', which incorporates a routine



which copies the contents of the echo file ECHONL2.FIL to the default file SHADOW2.FIL. As described in section 6.7, this is only achieved when the program has run successfully to the end. If the program is terminated by the user, the echo file ECHONL2.FIL has to be re-named, if the data it contains is to be retained. The new echo file can then be used as a data input device. The program will run up to the point where it was previously terminated, whereupon the control will be returned to the user.

### 7.3 Engine Block Program

The engine block program utilises a similar program construction to the non-linear flow program and the heat transfer program. Consequently, only the programming aspects which are unique to this program will be described in this section. The engine block program is comprised of two sub-programs; the nodal resistance network program and the oil splash program. The nodal resistance network program is built into the main program ENGINE, while the oil splash program is included in a sub-program named WALLTEMP. Both programs use the Levenberg-Marquardt non-linear routine to solve for the unknowns.

The engine block program ENGINE can only be run when the non-linear flow program and the heat transfer program have both been run previously. The flow program and the heat transfer program generate the data files PANDQ.OUT and OIL-T.OUT respectively, which are essential for the operation of the engine block program. These data files contain the oil flow rate and oil temperature data which is used to estimate the oil spray conditions within the engine.

When the engine block program is initiated, the main program calls subroutine WELCOM3. The user is given the option of modelling a new engine arrangement 'from scratch', or using an echo file as an input device. If the user selects the latter option, the main program calls subroutine READF3, which prompts the user for the name of the echo file. The user is given the option of using the default echo file, or naming the echo file which is to be used. The shadow file system used in the engine block program is similar in construction to the system documented for the non-linear flow program in section 6.7, the only differences being in the names of the files. The engine block program is run from the shell script 'GO3'. This includes a routine which generates the default echo file SHADOW3.FIL from the echo file ECHONL3.FIL. The latter echo file is automatically generated during the operation of the main program.

### 7.3.1 Representing the Engine Arrangement

The engine arrangement, which is comprised of series of block elements, is represented by a nodal resistance network (see section 5.5). The main program calls subroutine INPUT to prompt the user to model the layout of the resistance network. It is assumed that a single piston/liner/block section will be modelled, which will adequately represent the heat transfer within a complete engine arrangement. If the chosen piston/liner/block section is considered to be a unit, the user is prompted for the number of such units there are in the whole engine. The user is further prompted for the number of main, big-end and cam bearings there are in the unit being modelled. This information is used at a later stage in the program to calculate the oil flow rates splashed onto the wetted surfaces of the engine. These bearing numbers are normally the total number of each type of bearing in the whole engine, divided by the number of units. Consequently the numbers of each type of bearing do not necessarily have to be whole numbers.



The process of representing the layout of the nodal resistance network is initiated with the prompt for the maximum number of thermal resistances in the network, the number being stored in memory as variable NRESISTANCES. The user is then requested to define the start node number, end node number, and type of resistance, for each resistance in the network. The network is constructed with a combination of four types of thermal resistances:

- 1 = Conduction through a solid.
- 2 = Convection to a fluid of known temperature.
- 3 = Convection to oil spray.
- 4 = Convection to the oil in the sump.

The layout of the network is stored in memory, in a two-dimensional array IBIN. The integer number corresponding to the type of thermal resistance, shown in the list above, is placed in both the  $ij$  co-ordinate and the  $ji$  co-ordinate within array IBIN. When all the resistances in the network are represented in this way, the program scans each row,  $i$ , of the array IBIN and places the sum of the resistances connected to each node,  $i$ , in the last column. The array IBIN is allocated 350 columns and rows, so the sum of resistances at each node are placed in the 350th column. This data is used at a later stage in the program to ascertain which of the nodes have more than one thermal resistance connected to them.

The process of representing the layout of the thermal resistance network is best illustrated with a simple example. Consider the simple two element block arrangement, with its representative thermal resistance network, which is shown in Figure 7.4. The upper left-hand surface is wetted by oil spray, while the lower left-hand surface is wetted by the oil in the sump. The right-



hand surfaces are subject to convection to the ambient air. The two-dimensional array IBIN which would be formed to represent the resistance network for the upper element of this system (nodes 1 to 6), is shown in Table 7.1.

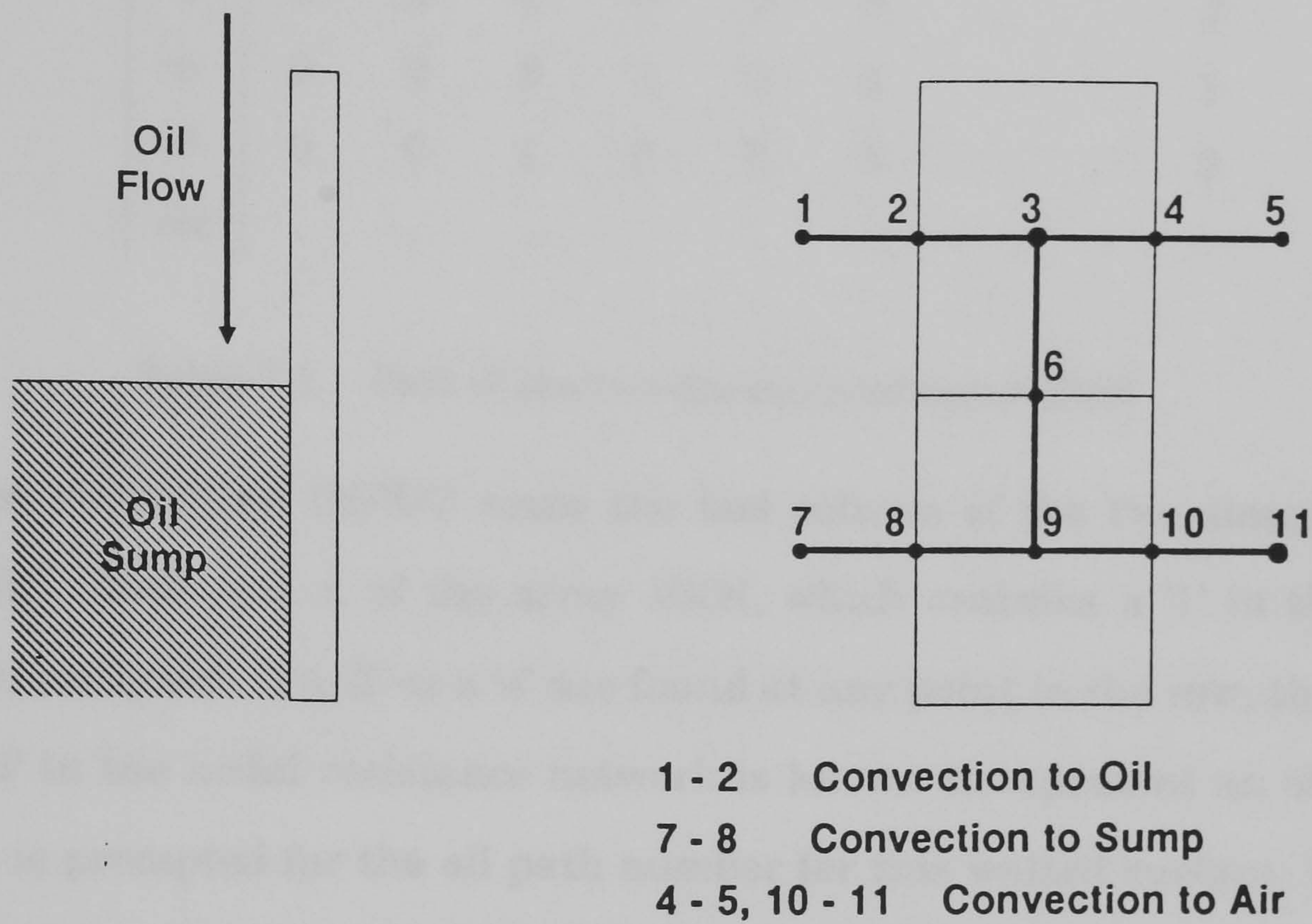


Figure 7.4. Simple two block element arrangement with thermal resistance network

When the physical layout of the nodal resistance network has been represented in this way, the program switches attention to the modelling of the oil spray. The flow of oil down the wetted surfaces of the engine is represented by a flow network. The flow network is comprised of two types of equations; an equation to represent the heat transfer to a falling oil film, which includes the heat transfer to the oil in the sump, and a continuity equation between surfaces (see section 5.5.2).



	j								
	1	2	3	4	5	6	etc	.	350
i	1	0	3	0	0	0	0	.	1
	2	3	0	1	0	0	0	.	2
	3	0	1	0	1	0	1	.	3
	4	0	0	1	0	2	0	.	2
	5	0	0	0	2	0	0	.	1
	6	0	0	1	0	0	0	.	2
	etc	.	.	.	.	.	.	.	.

Table 7.1. Part of the two-dimensional array IBIN

The subroutine INPUT scans the last column of the two-dimensional array IBIN. Each row, *i*, of the array IBIN, which contains a '1' in the last column, is analyzed. If a '3' or a '4' are found at any point in the row, the node number '*i*' in the nodal resistance network is known to represent an oil film. The user is prompted for the oil path number for this wetted surface. This is represented by the variable NUMOIL. The oil path number indicates the direction of the oil flow, from surface to surface, within the engine. The node, *i*, is stored in memory in the one-dimensional array IOILPATH, in the arrays 'NUMOIL' co-ordinate. The inlet and exit node numbers, for each section in the representative flow network, are generated automatically. These node numbers are stored in the arrays NINLET and NOUTLET, respectively, in the arrays '*i*' co-ordinate.

For the simple example shown in Figure 7.4, the representative oil flow network would be of the form shown in Figure 7.5. The arrays IOILPATH, NINLET and NOUTLET would be of the form shown in Tables 7.2, 7.3 and 7.4 respectively.

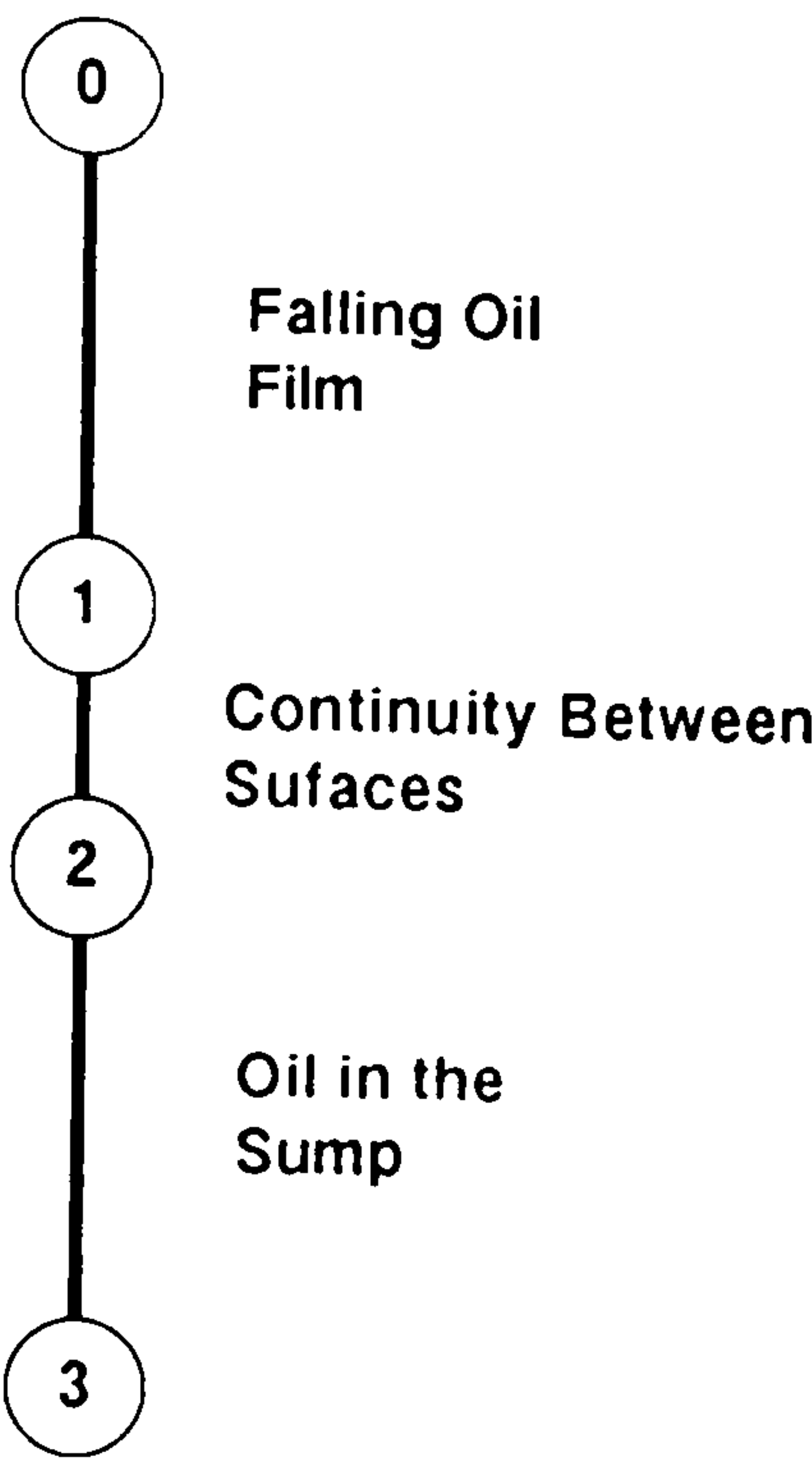


Figure 7.5. Representative flow network for the two block element arrangement shown in Figure 7.4.

		NUMOIL			
		1	2	.	etc
j	1	1	7	.	.

Table 7.2. Part of the one-dimensional array IOILPATH

		j								
		1	2	3	4	5	6	7	.	etc
1		0	0	0	0	0	0	2	.	.

Table 7.3. Part of the one-dimensional array NINLET

7.3.2 Input of Data

When the main program is initiated, subroutine DATAINP2 extracts the data contained in the data files PANDQ.OUT and OIL-T.OUT. These data files were automatically generated by the non-linear flow program and the heat



	j								
	1	2	3	4	5	6	7	.	etc
1	1	0	0	0	0	0	3	.	.

Table 7.4. Part of the one-dimensional array NOUTLET

transfer program. These files contain the pressures, flow rates and temperatures for the oil throughout the whole lubrication system. The main program calls subroutine FLOWRATE to process this data. The array BIN is scanned to ascertain which elements are at the end of each flow branch in the lubrication system. As these elements are usually journal bearings, the sum of the oil flow rates out of each of the three types of bearings (main, cam and big-end) are calculated. Thus, given the number of bearings of the same type there are in the system, subroutine FLOWRATE calculates the average oil flow rate and oil exit temperature for each bearing type. A similar calculation is made to find the total oil flow rate from the remaining component elements which deposit oil into the engine. These component elements are commonly the automatic chain tensioners, the tappet guides and any additional journal bearings. The oil from these components is classified as 'additional oil'. The average oil flow rate and oil temperature of this additional oil is calculated, given the number of representative piston/liner/block arrangements there are in the whole engine. This number is previously provided by the user (see section 7.3.1) and stored as variable NSECTIONS.

In addition to representing the physical layout of the engine, the subroutine INPUT also prompts the user to provide the required variable values. This process initially concentrates on modelling the nodal resistance network. The user is prompted for the data for each thermal resistance in the network. A summary of the data which is required by the program for each thermal resistance is presented in Table 7.5.

Type of Thermal Resistance	Input Data Required				
	Cross-sectional area between nodes i and j	Distance between nodes i and j	Thermal conductivity of the material	Heat transfer film coefficient	Fluid bulk temperature
(1) Conduction	✓	✓	✓		
(2) Convection to a fluid of known temperature	✓			✓	✓
(3) Convection to a falling oil film	✓				
(4) Convection to the oil in the sump	✓				

Table 7.5. Summary of the input data required to model the heat transfer within the engine block

When all the data for the nodal resistance network has been provided by the user, the subroutine INPUT prompts the user for the data which is necessary to model the heat transfer to the oil. This process commences with the prompt for the distance between the oil inlet and the oil exit for each wetted surface (node i). The user is then asked to estimate the percentage of the oil from each type of bearing which is splashed onto each wetted surface. This data is stored in the one-dimensional arrays PERCENTMAIN, PERCENTCAM, and PERCENTBIG, for the main, cam and big-end bearings respectively, in the arrays 'i' co-ordinate.

The user is also prompted for an estimate of the percentage of the oil which flows down the previous wetted surface, which continues onto the

present surface. This data is stored in the one-dimensional array PERCENTFLOW, again being stored in the arrays 'i' co-ordinate. The previous wetted surface in this case, is considered to be represented by the node with an 'oil path number' which is one less than the present node's oil path number. This data is extracted from the array IOILPATH, which is described in section 7.3.1.

The percentages of oil flow rates, obtained during the above procedure, are used to calculate the oil flow rate for each wetted surface of the engine arrangement being modelled. This data is also used to calculate the inlet oil temperature for each falling oil film. The averaged oil flow rates and temperatures sprayed from each type of bearing were calculated previously, as described at the beginning of this section.

### 7.3.3 Data Processing

The main program initially solves for all the unknown temperatures within the nodal resistance network. The Levenberg-Marquardt routine is used, which is contained in the subroutine MRQMIN. This subroutine, in turn, calls subroutines MRQCOF and FUNCS3.

Initial guesses are made for the unknown temperatures at each node in the system. The program scans the two-dimensional array IBIN to identify the nodes in the thermal resistance network which require these initial guesses. The temperature at the nodes which represent a convective fluid (combustion gas, coolant, air), are provided by the user (see section 7.3.2). The initial guesses for the temperatures at the nodes which represent the oil film or oil sump are the average temperatures of the oil which is splashed onto these surfaces from the bearings. An initial guess of 100°C is made for the first of the



remaining unknown temperatures in the nodal resistance network, which is incremented by 1°C for each of the other unknowns.

On each iteration, the Levenberg-Marquardt routine calls subroutine FUNCS3 to represent each equation, in the set of simultaneous equations which model the nodal resistance network. The subroutine FUNCS3 scans the last column of the array IBIN to ascertain which node has more than one thermal resistance connected to it. The subroutine FUNCS3 returns the value of the dependent variable  $Y_{i,c}$  and the partial derivatives  $dY_{i,c}/da$ , for the equation which represents each of these nodes (see section 5.5.1 for a description of the nodal resistance network model). The node temperatures obtained from the last iteration (or the guessed values on the first iteration) are used to calculate these values.

When all the nodes with more than one thermal resistance connected to them have been represented in the above manner, the Levenberg-Marquardt routine returns new values for the temperatures at these nodes, for input into the next iteration. This procedure continues for approximately six iterations until the  $\chi^2$  merit function decreases by less than 0.1 (see the description of the Levenberg-Marquardt routine in Appendix A.2.1). At this point convergence is assumed and the present values of the unknowns,  $a_i$ , are returned as the results for the temperatures throughout the thermal resistance network.

The above procedure calculates the metal temperatures throughout the representative engine arrangement. These temperatures are calculated with initial guesses for the temperatures of the oil films on each of the wetted internal surfaces. The program now switches attention to the calculation of more representative oil temperatures. The main program calls subroutine WALLTEMP to calculate the inlet and exit oil temperatures for each falling oil

film and the temperature of the oil in the sump. The wall temperatures, calculated in the nodal resistance network calculation above, are assumed to remain constant during the calculation of the temperatures of the oil films and the oil in the sump.

Initial guesses are made for the inlet and exit oil temperature for each falling oil film. These temperatures are selected through a similar procedure documented for the component elements in the heat transfer program (see section 7.2.3). The inlet oil temperature for the first wetted surface is known to be the average temperature of the oil splashed onto this surface from the bearings. For each node,  $i$ , in the nodal resistance network which represents a falling oil film or the oil in the sump, the initial guess for the exit oil temperature,  $t_{bo}$ , is dependent on the relationship between the inlet oil temperature,  $t_{bin}$ , and the wall temperature,  $t_s$ :

- i,      If  $t_s > t_{bin}$ ,      then  $t_{bo} = t_{bin} + 0.1^\circ\text{C}$ .      ie.  $a(\text{NOUTLET}(i)) = a(\text{NINLET}(i)) + 0.1$ .
- ii,      If  $t_s < t_{bin}$ ,      then  $t_{bo} = t_{bin} - 0.1^\circ\text{C}$ .      ie.  $a(\text{NOUTLET}(i)) = a(\text{NINLET}(i)) - 0.1$ .

Following the selection of the initial guesses for the unknowns, the subroutine MRQMIN3 is called, which contains the Levenberg-Marquardt routine. The subroutine, in turn, calls subroutine MRQCOF3, at the heart of which is the subroutine FUNCS4. Subroutine FUNCS4 is called to provide the solution for each heat transfer and continuity equation which model the representative oil flow network (see section 5.5.2 for a description of the representative oil flow network model). This subroutine returns the value of the dependent variable  $Y_{i,c}$  and the partial derivatives  $dY_{i,c}/da$ , for each of these equations. The inlet and exit oil temperatures obtained from the last iteration



(or the guessed values on the first iteration) are used to calculate these values.

When all the equations have been represented in the above manner, the Levenberg-Marquardt routine returns new values for the inlet and exit oil temperatures for each wetted surface. These new temperatures are used as the new guessed values for the next iteration. This procedure continues for approximately six iterations until the  $\chi^2$  merit function decreases by less than 0.1. At this point convergence is assumed and the present values of the unknowns,  $a_i$ , are returned as the oil temperatures throughout the representative flow network.

The new values for the oil temperatures at the inlet and exit from each of the wetted surfaces are used to calculate the average oil temperature for each falling oil film. The main program returns to the nodal resistance network model and uses these averaged oil temperatures as the new guesses for the temperatures at the nodes which represent the oil film or oil sump. The nodal resistance network model is re-run with these new initial guesses for the oil temperatures, but with the same initial guesses for the other node temperatures which were documented above. This returns the corresponding values for the engine surface temperatures which, in turn, are assumed to remain constant for the calculation of new inlet and exit oil temperatures for each wetted surface. This process is repeated for ten iterations, at which point, it is assumed that the surface and oil film temperatures have reached an equilibrium condition.

#### 7.3.4 Output of Data

When the results for the temperatures throughout the nodal network and the temperatures of the oil film are assumed to have stabilised to their



final values, the results are written to output files. The results for the oil temperatures, which are generated in the subroutine WALLTEMP, are stored in array 'A'. However, when these results are returned to the main program they are transferred to the array OILTEMP. The array 'A' is reserved in the main program for the results for the temperatures throughout the nodal resistance network.

The user is informed of the programs progress after each iteration. Both the main program and subroutine WALLTEMP call subroutine SCREENW2 to display a progress summary after each iteration of the nodal resistance network model and the oil film model. This summary includes:

- i, The present iteration number. This is the total number of iterations carried out to date, which includes the iterations within the nodal resistance network model and the oil film model.
- ii, The present 'pass' number. This is the number of times the nodal resistance network model has passed the nodal temperature results to the oil film model. Convergence is assumed on the tenth pass.
- iii, The value of 'ITST'.
- iv, The value of  $\chi^2$ .

When the program has finished its iteration procedure and the results had converged to their final values, the main program calls subroutine FINISH3. This subroutine informs the user that the program has finished running and displays how many iterations the program has made. The user is reminded that the results for the engine block temperatures, the temperatures of the oil films and the temperature of the oil in the sump, are stored in the output file BLOCK-T.OUT. This output file is generated by the subroutine WRITEF3. The results are presented in the form:

- i, For each node,  $i$ , in the nodal resistance network:  
'The value of the block temperature at node,  $i = \text{***.*** } ^\circ\text{C}$ '
- ii, For each node,  $i$ , in the nodal resistance network which represents an oil film or oil in the sump:  
'Oil temperature entering node,  $i, = \text{***.*** } ^\circ\text{C}$ '  
'Oil temperature exiting node,  $i, = \text{***.*** } ^\circ\text{C}$ '
- ii, For each node,  $i$ , in the nodal resistance network which represents an oil film or oil in the sump:  
'Heat transfer coefficient at node,  $i, = \text{*****.} \text{ W/m}^2\text{ } ^\circ\text{C}$ '

The header of the output file includes additional information which identifies the modelling conditions for the engine block arrangement. This data is comprised of:

- i, The system title (extracted from the data file PANDQ.OUT).
- ii, The name of the echo file which was used to model the system in the non-linear flow program (extracted from the data file PANDQ.OUT). This remains blank if the system was modelled 'from scratch' in the flow program.
- iii, The name of the echo file which was used to run the heat transfer program (extracted from the data file OIL-T.OUT). Similarly, this remains blank if the oil temperatures were input 'from scratch' in the heat transfer program.
- iv, The name of the echo file which was used to run the engine block program. Again, this remains blank if the engine block was modelled 'from scratch'.
- v, The engine speed.

An example of the output file BLOCK-T, which was generated for the V8 engine representative piston/cylinder/block arrangement, is given in Volume II. The representative engine block arrangement and nodal resistance network, which was used to model the V8 engine, is presented in Figure 9.6.

### 7.3.5 User Interface

The engine block program utilises many of the 'user friendly' techniques which were developed in the non-linear flow program. The user is prompted at every stage with clear instructions, and the program makes a check on the 'type' and order of magnitude of each item of input data. These checks are documented in more detail in section 6.7.

The program also includes an echo file system, similar to that documented in the non-linear flow program. The engine block program is initiated from the shell script 'GO3'. The opening screen gives the user the option of either modelling a new engine arrangement 'from scratch', or using an echo file as a data input device. If the user selects to use an echo file, the main program calls subroutine READF3, which prompts the user for either the name of the echo file which is to be used, or if the user wishes to use the default echo file, named 'SHADOW3.FIL', which was generated on the previous run of the program.

Upon completion of the program, the shell script GO3 copies the echo file 'ECHONL3.FIL', which is automatically generated during each run of the engine block program, to the default echo file SHADOW3.FIL. This is only achieved when the program has run successfully. If the program is terminated by the user, the echo file ECHONL3.fil has to be re-named, if the data it contains is to be used to re-run the program. If the re-named echo file is used



to run the program, the program will run up to the point where it was previously terminated and the control will be returned to the user.

## 7.4 Summary of Chapter 7

This chapter described the construction of the computer programs which were developed to model the heat transfer of the lubrication oil within an engine lubrication system. Two computer programs were developed, which were both written in the programming language FORTRAN 77. The first program, referred to as 'the heat transfer program', analyzes the heat transfer processes within the pressurised side of the lubrication system. The second program models the heat transfer to the oil which is sprayed onto the internal surfaces of the engine. This program is referred to as 'the engine block program'.

The heat transfer program models the heat transfer to the oil within the pressurised side of the lubrication system. The layout of the lubrication system is extracted from the data file 'PANDQ.OUT', which was formed during the last run of the non-linear flow program. The heat transfer to the oil was modelled within the pipe elements (pipes, annular pipes, crank-shaft transfer holes and cam bearing transfer holes), the journal bearings and the oil cooler. The program requires as input; the wall temperatures of the pipe elements (which are assumed to remain constant); the geometry of the oil cooler (stored in data file 'OLLCOOL.INP') and the file name of the temperature 'map' for each of the journal bearings. The bearing temperature maps are generated from an adapted journal bearing program which was originally developed by Lai (1993).

The heat transfer program utilises the non-linear Levenberg-Marquardt routine, to solve for the unknown temperatures in the lubrication system, using an iterative procedure. This routine is contained in subroutines MRQMIN and

MRQCOF, which in turn, call subroutine FUNCS to represent the heat transfer characteristics for each heat transfer element in the system. Following initial guesses for the unknowns, this subroutine returns the calculated new value for the dependent variable  $Y_{i,c}$  and the partial derivatives  $dY_{i,c}/da$ , for each element. After each iteration, the Levenberg-Marquardt routine returns new estimates for the unknown temperatures at each node. This continues until convergence is assumed and the present values for the unknown temperatures are assumed to represent the final results.

The final results for the oil temperatures throughout the lubrication system are stored in an output file named 'TEMPER.OUT'. A second output file 'OIL-T.OUT' is also generated, which stores the oil temperature results for each node in the system. This data is used to calculate more realistic oil properties in the non-linear flow program and is used to estimate the temperature of the oil which was sprayed on to the engine internal surfaces in the engine block program.

The engine block program provides the ability to model the heat transfer to the oil splashed on to the internal surfaces of an engine. The engine geometry is represented by a series of block elements, which in turn, are represented by a nodal thermal resistance network. The user models this network by stating the start node number, end node number and type, for each thermal resistance in the network. The network is represented by a combination of four types of thermal resistances; conduction through a solid; convection to a fluid of known temperature; convection to oil spray and convection to the oil in the sump.

The heat transfer to the oil spray and the heat transfer to the oil in the sump are both modelled by the method. The oil on each wetted surface is



represented as a falling film of oil. The flow of oil down each wetted surface in the engine forms a representative flow network. The user defines the flow network by stating the oil path number for each wetted surface. The falling oil film is assumed to pass from one wetted surface to the next. The percentage of oil which continues from one surface to the next, and the percentage of the oil thrown from each type of engine bearing, which is splashed on to each wetted surface, are defined by the user. The average oil flow rates and oil temperatures, thrown from each type of bearing, are calculated from data stored in data files PANDQ.OUT and OIL-T.OUT. These data files are generated in previous runs of the non-linear flow program and heat transfer program.

The engine block program calculates the engine block temperatures and the oil film temperatures, using an iterative procedure. Following the input of the bulk temperatures and heat transfer coefficients for the combustion gas, coolant and air, the program makes initial guesses for the temperature of each of the falling oil films and calculates the temperatures at every node of the nodal resistance network. The temperatures are calculated using the Levenberg-Marquardt non-linear iterative routine.

The engine block temperatures are assumed to remain constant during the second calculation phase, the calculation of the oil film temperatures. Following initial guesses for the oil temperatures at the inlet and exit from each wetted surface, new values for these oil temperatures within the representative flow network are calculated, in a second Levenberg-Marquardt non-linear iterative routine. These oil temperatures are passed back to the first calculation phase and new block temperatures are calculated in the nodal resistance network. This procedure continues for ten iterations, at which point temperature stability is assumed and the present values for the block



temperatures at each node in the thermal resistance network and the oil temperatures at the inlet and exit from each wetted surface, are assumed to be the final results. The results are written to the output file 'BLOCK-T.OUT'.

Commonality is maintained between the non-linear flow program, the heat transfer program and the engine block program. The heat transfer program and the engine block program are constructed in a modular manner, utilising a subroutine format. Many of the programming techniques which were developed in the non-linear flow program are integrated into these programs. This aided the development of the heat transfer and engine block programs and provides a user interface which is common to all three programs. The user is clearly and precisely prompted for all the required input data, and a comprehensive series of checks are made on this data to ensure it is of the correct type and order of magnitude. All the programs utilise the echo file system, which prevents the loss of data if the program is terminated before completion. This greatly improves the programs flexibility by allowing parametric studies to be carried out with ease.

## Chapter 8

# Flow Analysis of AJ6 Engine Lubrication System

### 8.1 Introduction

This chapter presents the results from the non-linear flow program. The first sections discuss the differences between the two linear solution methods, LU decomposition and Gauss-Jordan, which were analyzed during the development of the linear flow model. The discussion includes the differences in the accuracy of the results and the overall run times of the program. This is followed by a similar comparison, which is made between the linear and the non-linear solution techniques.

The principal objective of this chapter, however, is to compare the predicted results with measured values, for the purpose of validating the modelling approach. The AJ6 engine lubrication system was used throughout the development stages of the non-linear flow program. The fully developed non-linear flow program was used to model the full AJ6 engine lubrication system layout. The results from this model were compared to both measured pressure and flow rate results from engine tests, and predicted flow rate results provided by Glacier Vandervell, the bearing suppliers to Jaguar.

It was found that several enhancements were necessary to improve the accuracy of the predicted results. Each enhancement was investigated further

to see if the final modelling conditions were of a realistic nature. The lessons which were learned during the development of the non-linear flow program and during the modelling runs of the AJ6 engine are presented in this chapter. The lessons which were learned during the modelling of the AJ6 engine were incorporated in the model of the Jaguar V8 engine. The results from the thermofluid analysis of the V8 engine lubrication system are presented in Chapter 10.

## 8.2 Comparison Between the Two Linear Flow Programs

A comparison was made between two exact linear methods, Gauss-Jordan elimination and LU decomposition, at the early stages of the linear program development. Little difference could be found between the two methods with regard to the run times and accuracy, for small to medium sized systems (<30 elements). Consequently, the initial linear flow program was developed with a Gauss-Jordan exact linear algorithm, as it was regarded as being a robust and reliable routine (Chapra and Canale (1985)).

To investigate the differences between the two linear solution techniques for larger sized systems, a second linear model was developed by simply replacing the Gauss-Jordan routine with the LU decomposition routine. A comparison was made between the two linear programs for modelling the lubrication system of the AJ6 engine, which contained 89 component elements. A schematic diagram of this lubrication system is shown in Figure 8.2 and the predicted results for the pressures and flow rates are discussed in section 8.4.3.3. The LU decomposition method proved to be much faster, reducing the run time for the 89 element system, on a 16MHz 386PC, from 11 minutes 45 seconds using the Gauss-Jordan method, to 5 minutes 40 seconds. Taking the results for the sum of flows through the dividing nodes as a guide, the LU



decomposition method also proved to be more accurate than the Gauss-Jordan method.

The difference in the accuracy of the two programs, for the calculation of the sum of flows at each dividing node, is demonstrated in Table 8.1. Table 8.1 presents the predicted results for the oil flow rates into and out of node number 85 (chosen arbitrarily), for the AJ6 engine lubrication system shown in Figure 8.2. The system was modelled with big-end and main bearing radial clearances of 0.0125 mm, cam bearing radial clearances of 0.03 mm, and an engine speed of 2000 rpm (similar to the conditions for which the results later shown in Table 8.5 were obtained). A comparison was made between the two programs using single precision for all real numbers.

Method	Node Numbers	Flow Rate (m <sup>3</sup> /s)	Accuracy	Run Time
Gauss-Jordan	85 - 90	5.293471 x 10 <sup>-7</sup>	-	11 minutes 45 seconds
	85 - 87	5.294785 x 10 <sup>-7</sup>	-	
	82 - 85	1.055597 x 10 <sup>-6</sup>	99.6%	
	True sum of flows 85-90 & 85-87			
LU decomposition	85 - 90	5.291188 x 10 <sup>-7</sup>	-	5 minutes 40 seconds
	85 - 87	5.291280 x 10 <sup>-7</sup>	-	
	82 - 85	1.058247 x 10 <sup>-6</sup>	100%	
	True sum of flows 85-90 & 85-87			
Gauss-Jordan	1 - 7	2.525810 x 10 <sup>-5</sup>	95.2%	-
LU decomposition	1 - 7	2.651602 x 10 <sup>-5</sup>		-

Table 8.1      Comparison of oil flow rates predicted by Gauss-Jordan and LU decomposition exact linear methods (AJ6 engine)

The value for the flow rate between nodes 82-85 should equal the sum of flows 85-90 and 85-87. It can be seen that the Gauss-Jordan method returned a sum which was slightly inaccurate (99.6% accurate), while the LU decomposition method returned an exact result. As each dividing node in the system had a similar continuity of flow sum, this resulted in an accumulation of the individual inaccuracies further down-stream in the system. This is demonstrated in Table 8.1 by comparing the two values for the flow rates between nodes 1-7, which was the flow rate through the pump. The predicted value obtained by the Gauss-Jordan method reduced to 92.5% of the value obtained by the LU decomposition routine.

A possible cause for the imprecision in the Gauss-Jordan method can be attributed to numerical errors such as round-off errors, which this type of numerical method were known to be prone to (Press et al (1989)), especially under a PC environment. It was concluded that a 89 element system was approaching the maximum number of elements which could be solved by the Gauss-Jordan model. When consideration was made of the improvements in the run times and the accuracy of the results, it was decided that the LU decomposition linear model would be used for all further linear program development.

### **8.3 Comparison Between Linear and Non-Linear Flow Programs**

The non-linear flow model was initially developed with a Gauss-Jordan elimination linear matrix solver at the heart of the Levenberg-Marquardt algorithm. However, following the comparison between the two linear solution techniques for the linear flow model, the Gauss-Jordan elimination algorithm was replaced with the LU decomposition method. Although no difference was



found in the accuracy of the results, with respect to the sum of flows through the dividing nodes, a large reduction in the program run time was achieved. A comparison between the run times for the two types of non-linear flow models, for the full AJ6 lubrication systems, is shown in Table 8.2. It can be seen that the non-linear program which incorporated the LU decomposition routine was 2.5 times faster than the Gauss-Jordan version.

Host Machine	Linear matrix solving technique used in the Levenberg-Marquardt algorithm	
	Gauss-Jordan	LU Decomposition
16MHz 386 PC	38 minutes 24 seconds	14 minutes 56 seconds

Table 8.2. Comparison of run times for two non-linear modelling routines

Table 8.3 shows a comparison between the results obtained by the linear and the non-linear flow programs, for the AJ6 engine lubrication system. These results were obtained using the same engine speed and bearing clearances as those used in Table 8.1 above.

It can be seen from Table 8.3 that the non-linear flow program, which utilised a LU decomposition linear matrix solver within the Levenberg-Marquardt algorithm, returned results which matched to within six decimal places those obtained from the LU decomposition linear flow program. The high accuracy of these results, in comparison with the linear flow program, indicated that the values for the standard deviation term,  $\sigma_i$ , which were used in the calculation of the  $\chi^2$  merit function (see Appendix A.2.1), were suitable for modelling a typical engine lubrication system configuration. The values of  $\sigma_i$  used in the flow program, were 10000 for the pressure v flow rate equations and 0.00001 for the flow continuity equations.



System Size & Engine Speed	Bearing Radial Clearances	Node Numbers	Results from <u>Linear</u> Model	Results from <u>Non-Linear</u> Model
Full AJ6 Engine Lubrication System  Engine Speed 2000 rpm	Main and Big-End $1.25 \times 10^{-5}$ m  Cam $3.0 \times 10^{-5}$ m	Pressure 4	$4.715408 \times 10^5$ N/m <sup>2</sup>	$4.715409 \times 10^5$ N/m <sup>2</sup>
		Pressure 69	$4.711356 \times 10^5$ N/m <sup>2</sup>	$4.711356 \times 10^5$ N/m <sup>2</sup>
		Q 1 - 7	$2.651602 \times 10^{-5}$ m <sup>3</sup> /s	$2.651602 \times 10^{-5}$ m <sup>3</sup> /s
		Q 40 - 70	$7.499628 \times 10^{-6}$ m <sup>3</sup> /s	$7.499629 \times 10^{-6}$ m <sup>3</sup> /s
		Q 82 - 85	$1.058247 \times 10^{-6}$ m <sup>3</sup> /s	$1.058248 \times 10^{-6}$ m <sup>3</sup> /s
		Q 85 - 87	$5.291286 \times 10^{-7}$ m <sup>3</sup> /s	$5.291287 \times 10^{-7}$ m <sup>3</sup> /s
		Q 85 - 90	$5.291188 \times 10^{-7}$ m <sup>3</sup> /s	$5.291189 \times 10^{-7}$ m <sup>3</sup> /s

Table 8.3      Comparison of results from the LU linear flow program and non-linear flow program (with LU linear matrix solver)

A further test was carried out for a simple two element system shown in Figure 8.1, which comprised of a pump and pipe arrangement. Two modelling runs were made, the first with a large pipe diameter which resulted in large oil flow rates but small pressures, and the second with a small pipe diameter which resulted in small oil flow rates but large pressures. The results from this test are shown in Table 8.4.

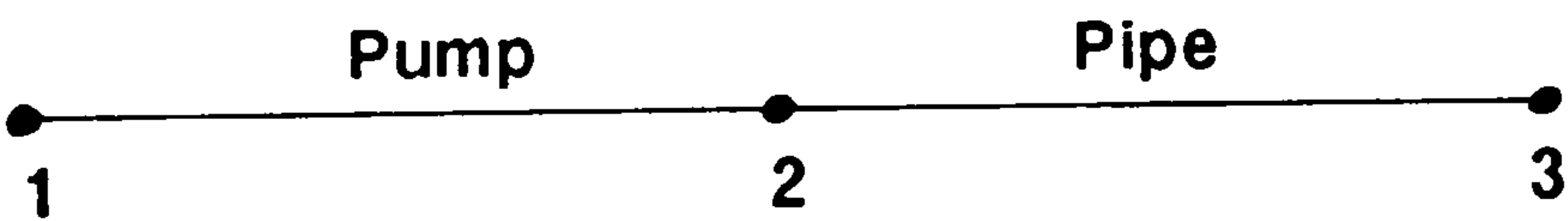


Figure 8.1.    Simple two element test system

It can be seen from Table 8.4 that the results matched exactly over a wide range of order of magnitude. This confirmed that the non-linear program was truly flexible and that the values which were derived for the standard deviation term,  $\sigma_i$ , were suitable for any system size, with any order of magnitude for the pressures and flow rates.

Test Conditions	Node Numbers	Results	
		Linear Flow Program	Non-Linear Flow Program
Pipe Diam. 0.1 m Pipe Length 1 m Engine Speed 2000 rpm	Pressure 2	2.219582 N/m <sup>2</sup>	2.219582 N/m <sup>2</sup>
	Q 1 - 3	5.319993x10 <sup>-4</sup> m <sup>3</sup> /s	5.319993x10 <sup>-4</sup> m <sup>3</sup> /s
Pipe Diam. 0.0001 m Pipe Length 1 m Engine Speed 2000 rpm	Pressure 2	4.757384x10 <sup>5</sup> N/m <sup>2</sup>	4.757384x10 <sup>5</sup> N/m <sup>2</sup>
	Q 1 - 3	1.140271x10 <sup>-10</sup> m <sup>3</sup> /s	1.140271x10 <sup>-10</sup> m <sup>3</sup> /s

Table 8.4      Comparison of results from linear and non-linear flow programs for simple test system

8.4    Modelling the AJ6 Engine Lubrication System

The Jaguar AJ6 engine lubrication system was the first lubrication system modelled by the flow program. Although this system was modelled throughout the development stages of the linear and non-linear flow programs, the results presented in this section were obtained from the final, fully developed non-linear flow program. The AJ6 lubrication system was used for the initial validation of the flow program results.

No attempt was made to simulate the heat transfer within the AJ6 engine lubrication system, or model the AJ6 engine block. The principal reason for this was that no temperature or heat transfer data was available for this engine during the development of the heat transfer and engine block programs. It was considered that these programs would be adequately validated with the V8 engine, as more temperature data would become available for this engine during its development at Jaguar. The results obtained for the V8 engine lubrication system are presented in Chapter 9.

The results obtained from the flow program were validated in two stages. The first stage was to estimate the accuracy of the order of magnitude of the results by studying the 'trends' of the pressures and flow rates through the system, and comparing the predicted flow rate results with those provided by Glacier Vandervell, the bearing suppliers to Jaguar. The second stage consisted of a more comprehensive validation, by carrying out a series of engine tests on a 4.0 litre AJ6 engine and obtaining measurements of the pressures and flow rates throughout the lubrication system. The results obtained during the two-stage validation procedure are presented in the following sections.

#### 8.4.1 Pressure and Flow Rate Trends

The first check carried out on the predicted results was to ensure that the system 'behaved' as expected. It was found that the pressure and flow rate results did change as expected, under varying system environment changes. For example:

- i, The flow rates and the pressures increased with increasing engine speed.
- ii, Increased oil pressures were predicted up-stream of a flow restriction in the system, with decreased pressures and flow rates down-stream (see Table 8.4).
- iii, The sum of the flow rates exiting a node always equated to the flow rate entering the node.

Although the above observations did not validate the order of magnitude of the results, they did show that flow continuity was maintained through the system. Therefore, if the order of magnitude of some of the results could be verified, the 'trend' indicated that the other results would also be correct.



### 8.4.2 Comparison Between Predicted Results and those Provided by Glacier Vandervell

The flow rate results for the main and big-end bearings were compared to the calculated hydrostatic flow rates which were provided by Glacier Vandervell from their 'rapid' bearing model (this is discussed in more detail in Chapter 2). A comparison between the Glacier Vandervell results and those obtained from the non-linear flow program is shown in Table 8.5. These results were obtained for an engine speed of 2000 rpm and a pump drive ratio of 0.636:1 (the drive ratio currently used on the AJ6 engine). The main and big-end bearings were modelled with radial clearances of 0.0125 mm. The values for the bearing eccentricity ratios were provided by Glacier Vandervell.

It can be seen from Table 8.5 that the results for the non-grooved bearings (big-end 1, and main 4) compared reasonably favourably. The results for the remaining 180° partially grooved bearings tended to be approximately 30-45% larger than those provided by Glacier Vandervell. This suggested a discrepancy in the equation which was used to represent the pressure loss v flow rate relationship through these types of bearings. With reference to Equation 4.52, there appeared to be little indication of where this discrepancy arose. Apart from the variable values which represented the physical dimensions of the bearings, the only other variables in the equation were:

- i, The oil dynamic viscosity,  $\mu$ .
- ii, The constants of feed groove geometry,  $f_1$  and  $f_2$ .
- iii, The oil feed pressure,  $P_f$ .

The oil dynamic viscosity,  $\mu$ , was related to the oil temperature. However, it can be clearly seen from Table 8.5 that the predicted oil

2000 rpm. Main and Big-End Bearing Radial Clearance 0.0125 mm. (Cam Bearing Radial Clearance 0.03 mm)						
Bearing	Node Number	Mean Eccentricity Ratio	Glacier Vandervell		Non-Linear Flow Model	
			Oil Temp °C	Hydrostatic Flow Rate l/s	Oil Temp °C	Hydrostatic Flow Rate l/s
Big-end 1	36-39	0.7553	152.8	0.000146	155.3 (2% large)	0.000183 (25% large)
Main 1	36-37	0.6871	157.4	0.000975	151.6 (4% small)	0.001402 (44% large)
Main 2	31-32	0.6734	150.2	0.001066	151.6 (1% large)	0.001372 (28% large)
Main 3	26-27	0.7020	152.9	0.001047	151.6 (1% small)	0.001438 (37% large)
Main 4	7-9	0.5165	154.1	0.000765	153.1 (1% small)	0.000841 (10% large)
Main 5	11-12	0.7012	152.9	0.001048	151.6 (1% small)	0.001435 (37% large)
Main 6	16-17	0.6731	150.3	0.001067	151.6 (1% large)	0.001371 (28% large)
Main 7	21-22	0.6940	157.5	0.001008	151.6 (4% small)	0.001418 (41% large)

Table 8.5 Comparison of bearing hydrostatic flow rates (AJ6 engine)

temperatures were always within 4% of those provided by Glacier Vandervell, which suggested that the corresponding viscosities were also very similar.

The constants of feed groove geometry  $f_1$  and  $f_2$  were extracted from graphical data published by Martin and Lee (1982). This graphical data was derived for use with Equation 4.52, which was extracted from the same source. The values of  $f_1$  and  $f_2$  were dependent on the eccentricity ratio,  $\epsilon$ . However, the value of the eccentricity ratio for each bearing was also supplied by Glacier Vandervell, and used in the non-linear flow model. Therefore, it was assumed that the discrepancy in the results did not lie in the calculation of the constants  $f_1$  and  $f_2$ .



It was concluded that the error lay in the value for the feed pressure,  $P_f$ . The bearing flow rates were calculated by Glacier Vandervell using data stored for the AJ6 engine, but there was no indication of the order of magnitude of the oil pressures which were used. However, Glacier Vandervell did calculate the oil pressure rise through the crank-shaft oil transfer hole, which was found to be 0.72 bar. The Flow program calculated an oil pressure rise of approximately 0.55 bar through each crank-shaft oil transfer hole.

The linear and non-linear flow programs solved for all pressures and flow rates simultaneously. A change to one part of the system would have repercussions throughout the rest of the system. Therefore, if the pressure rise through the crank-shaft oil transfer hole was actually larger than presently predicted, the oil flow rate through the big-end bearing would be greater, while the flow rate through the main bearing would be less.

If the discrepancy of the oil pressure rise through the crank-shaft oil transfer holes was combined with an overall pressure loss in the rest of the system, this could account for the slight differences in the results. It was considered that the difference in the feed pressure to the main gallery (node 8 in Figure 8.2) could be due to an increased flow rate through the cam bearings, or a simply discrepancy in the oil pump data. The increased flow rate through the cam bearings could be caused by large cam bearing radial clearances. The cam-bearing radial clearances used in the LU decomposition model were 0.03 mm. Glacier Vandervell gave no indication of the radial clearances of the cam-bearings or the oil feed pressures taken from the AJ6 engine, which were used for their calculations.

The AJ6 engine lubrication system was re-modelled with larger cam bearing radial clearances to investigate the effects on the feed pressure to the



main gallery and the resulting effects on the flow rates through the main and big-end bearings. Table 8.6 presents the oil flow rate results when the system was re-modelled with cam bearing radial clearances of 0.09 mm.

2000 rpm. Main and Big-End Bearing Radial Clearance 0.0125 mm. (Cam Bearing Radial Clearance 0.09 mm)						
Bearing	Node Number	Mean Eccentricity	Glacier Vandervell		Non-Linear Flow Model	
			Oil Temp °C	Hydrostatic Flow Rate l/s	Oil Temp °C	Hydrostatic Flow Rate l/s
Big-end 1	36-39	0.7553	152.8	0.000146	155.3 (1% large)	0.000144 (2% small)
Main 1	36-37	0.6871	157.4	0.000975	151.6 (4% small)	0.001067 (9% large)
Main 2	31-32	0.6734	150.2	0.001066	151.6 (1% large)	0.001044 (2% small)
Main 3	26-27	0.7020	152.9	0.001047	151.6 (1% small)	0.001095 (4% large)
Main 4	7-9	0.5165	154.1	0.000765	153.1 (1% small)	0.000640 (15% small)
Main 5	11-12	0.7012	152.9	0.001048	151.6 (1% small)	0.001093 (4% large)
Main 6	16-17	0.6731	150.3	0.001067	151.6 (1% large)	0.001044 (2% small)
Main 7	21-22	0.6940	157.5	0.001008	151.6 (4% small)	0.001079 (7% large)

Table 8.6. Comparison of bearing hydrostatic flow rates with cam bearing radial clearance of 0.09 mm

It was found that changing the cam bearing radial clearances from 0.03mm to 0.09mm reduced the feed pressure to the main gallery (node 35) from 4.49 bar to 3.49 bar. It can be clearly seen from Table 8.6, that when the system pressures were artificially reduced in this way, the values for the flow rates through the main and big-end bearings were in much closer agreement. The results predicted for the big-end bearings were in very close agreement, with only a 2% difference between the two values. The results for the main

bearings were within 9%, apart from the oil flow rate through the central main bearing (main 4), which reduced to within 15% of the value provided by Glacier Vandervell.

### 8.4.3 Discussion of Engine Test Results for the AJ6 Engine

A series of engine tests were carried out on the Jaguar AJ6 4 litre engine, at the engine test facility of the Jaguar Engineering Centre, Coventry. The primary objective of these tests was to obtain temperature, pressure and flow rate measurements for the main bearings of the AJ6 engine, for the validation of the bearing model being developed by Lai (1993). However, additional pressure, temperature and flow measurements were taken on the engine, for the purpose of this study. These additional measurements concentrated on the part of the lubrication system which fed the cylinder head and cam bearings. A description of the modifications made to the engine for the purpose of the test and a description of the test schedule, are given in Appendix E.

The lubrication system was modified to allow the oil flow rates into two of the main bearings to be measured. The engine tests were comprised of two phases. During the first phase, the oil flow rate entering the central main bearing and the oil flow rate entering the head were measured. The oil pressure was measured at the entry to the main gallery (node 8) and at the ends of both the cam-shafts (nodes 76 and 98). A schematic diagram of the modified lubrication system (named 'Layout1'), which was modelled by the non-linear flow program, is presented in Figure 8.2. During the second phase, the oil flow rates into the first and seventh main bearings were measured. Oil pressures were measured at the same points as in Layout 1, but with two additional pressure measurements in the main gallery at nodes 27 and 43. A



schematic diagram of this modified lubrication system, which was named 'Layout 2', is presented in Figure 8.3.

Both modified lubrication systems were modelled using the non-linear flow program. The results were compared to the measured data from the engine tests. A full discussion of the comparison between the measured and predicted results is made in sections 8.4.3.2 and 8.4.3.3.

#### **8.4.3.1 Oil Temperature Observations**

The engine tests were carried out over an engine speed range of 2000 to 5000 rpm, and  $\frac{1}{4}$ ,  $\frac{1}{2}$  and  $\frac{3}{4}$  full loads. The results showed that the rise in oil temperature, as expected, was more greatly influenced by higher engine speeds than by an increase in load. These trends are shown graphically in Figure 8.4 and Figure 8.5. Similar results were found by Hayashi (1969) and Andrews et al (1989). Both authors attributed the influence of the engine speed on the overall oil temperature to be primarily due to the increase in oil temperature within the bearings. The rise in temperature of the oil film in the bearings was a result of the increase in oil film shear at high rotational speeds. This had a larger effect on the bearing oil film temperature than an increase in oil film pressure at large engine loads.

#### **8.4.3.2 Oil Pump Characteristics**

Results from the engine tests showed that the oil pressure reached a maximum of 6.11 bar at the centre of the oil gallery (node 8 in Figure 8.2 and Figure 8.3). However, according to the available oil pump data, the maximum oil pressure which could be attained was 5.24 bar at 5000 rpm. This demonstrated that the oil pump characteristics used in the model were



Layout 1

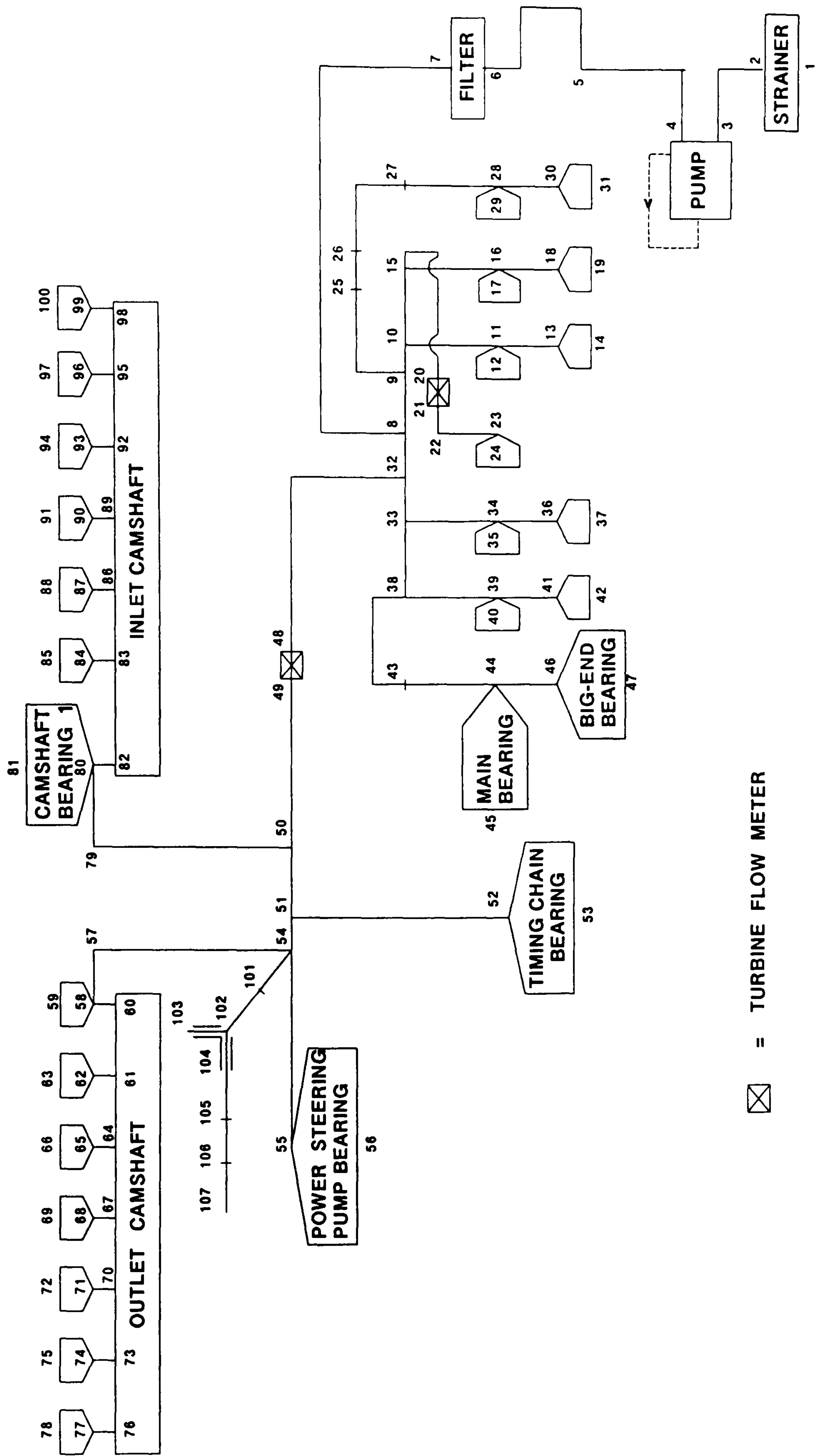
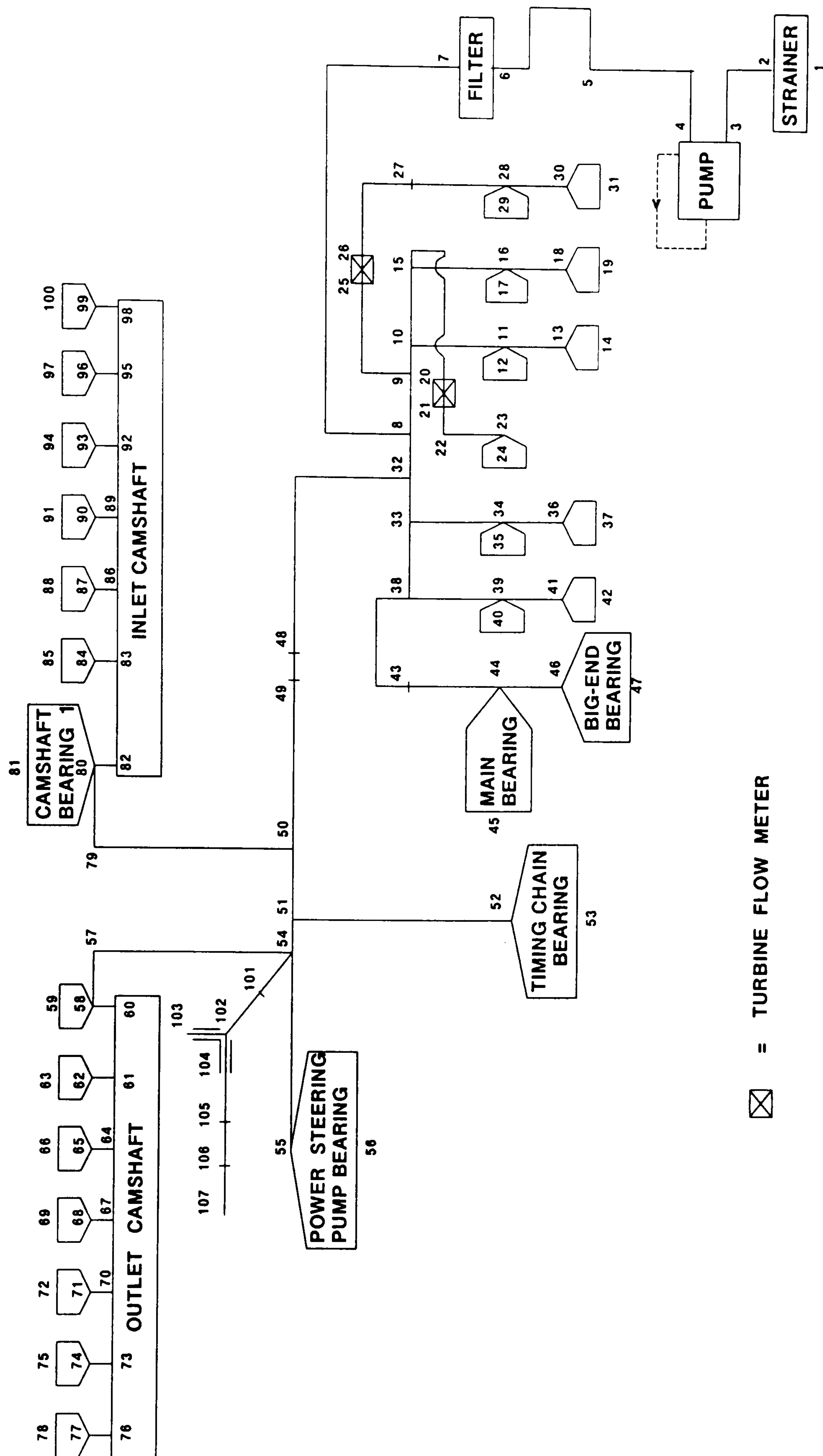


Figure 8.2. Schematic diagram of the modified AJ6 engine lubrication system - 'Layout1'

## Layout 2



**Figure 8.3. Schematic diagram of the modified AJ6 engine lubrication system - 'Layout2'**

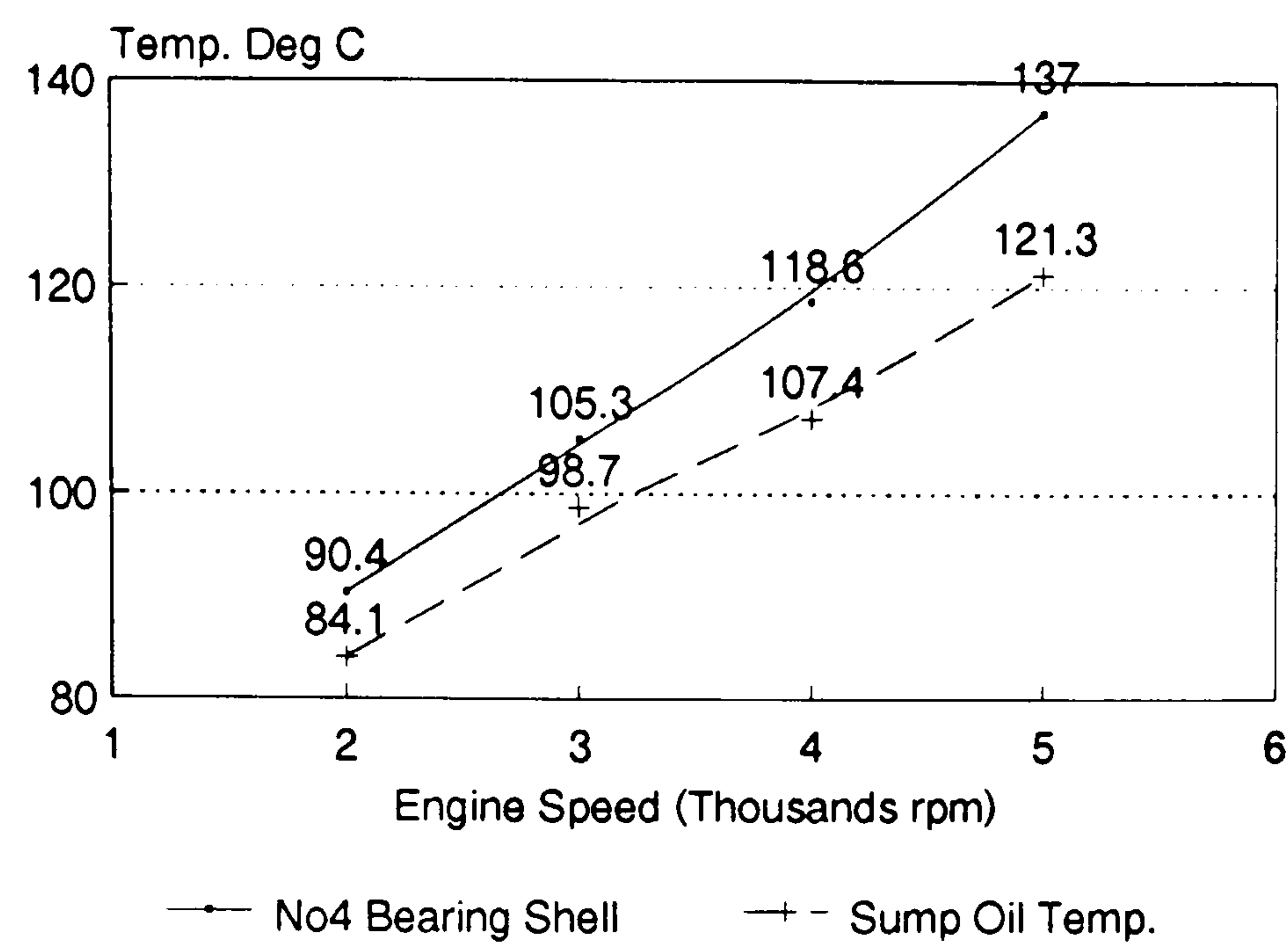


Figure 8.4. Engine speed influence on oil temperature (1/2 load)

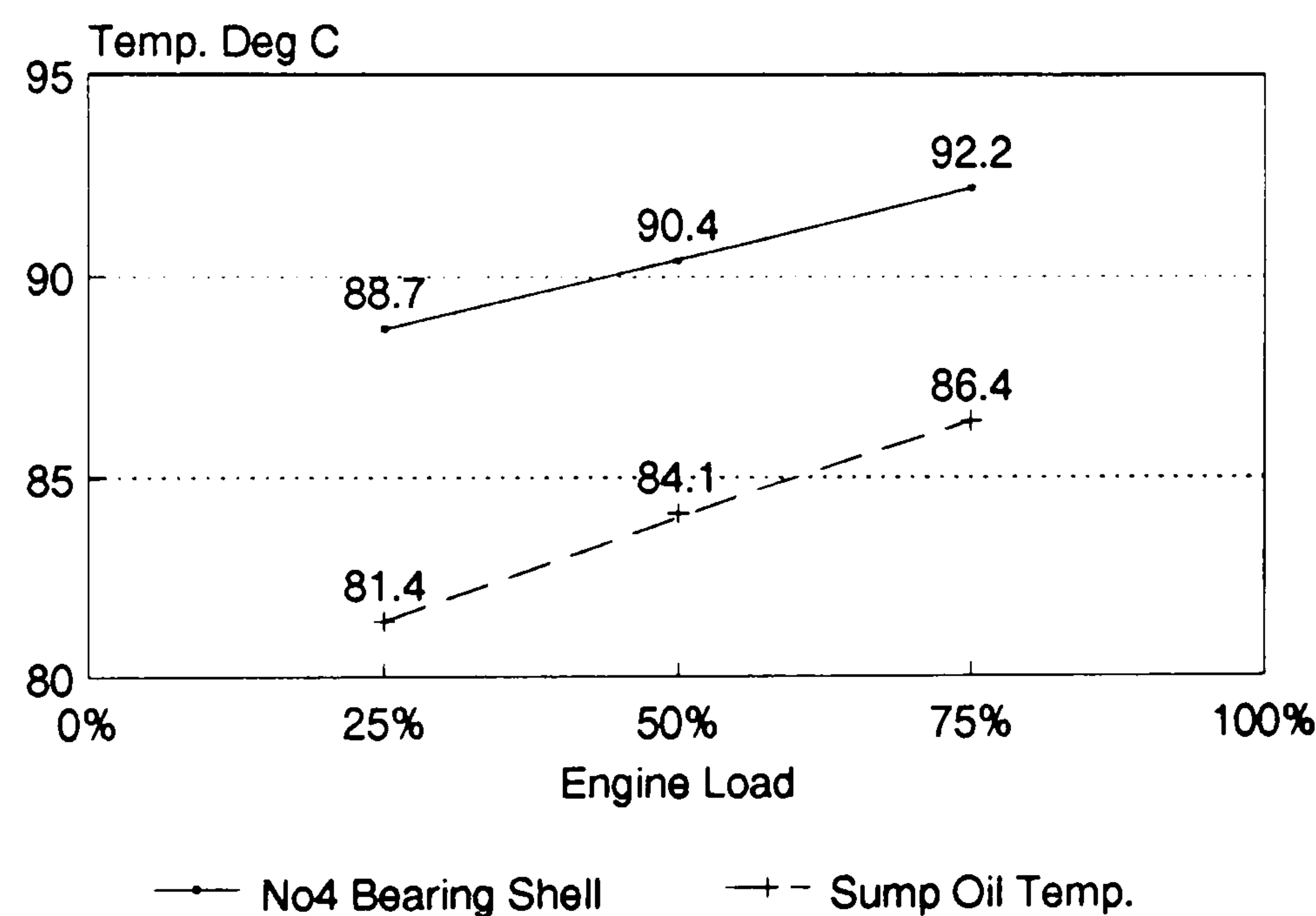


Figure 8.5. Engine load influence on oil temperature (2000 rpm)

inaccurate. Upon further investigation, it became clear that the oil pump characteristics which were being used in the model were obsolete and that the oil pump being used on the present day AJ6 engines had been up-graded. In an attempt to model the flow characteristics through the whole AJ6 engine lubrication system, the oil pump characteristics were temporarily changed to the form shown in Figure 8.6.



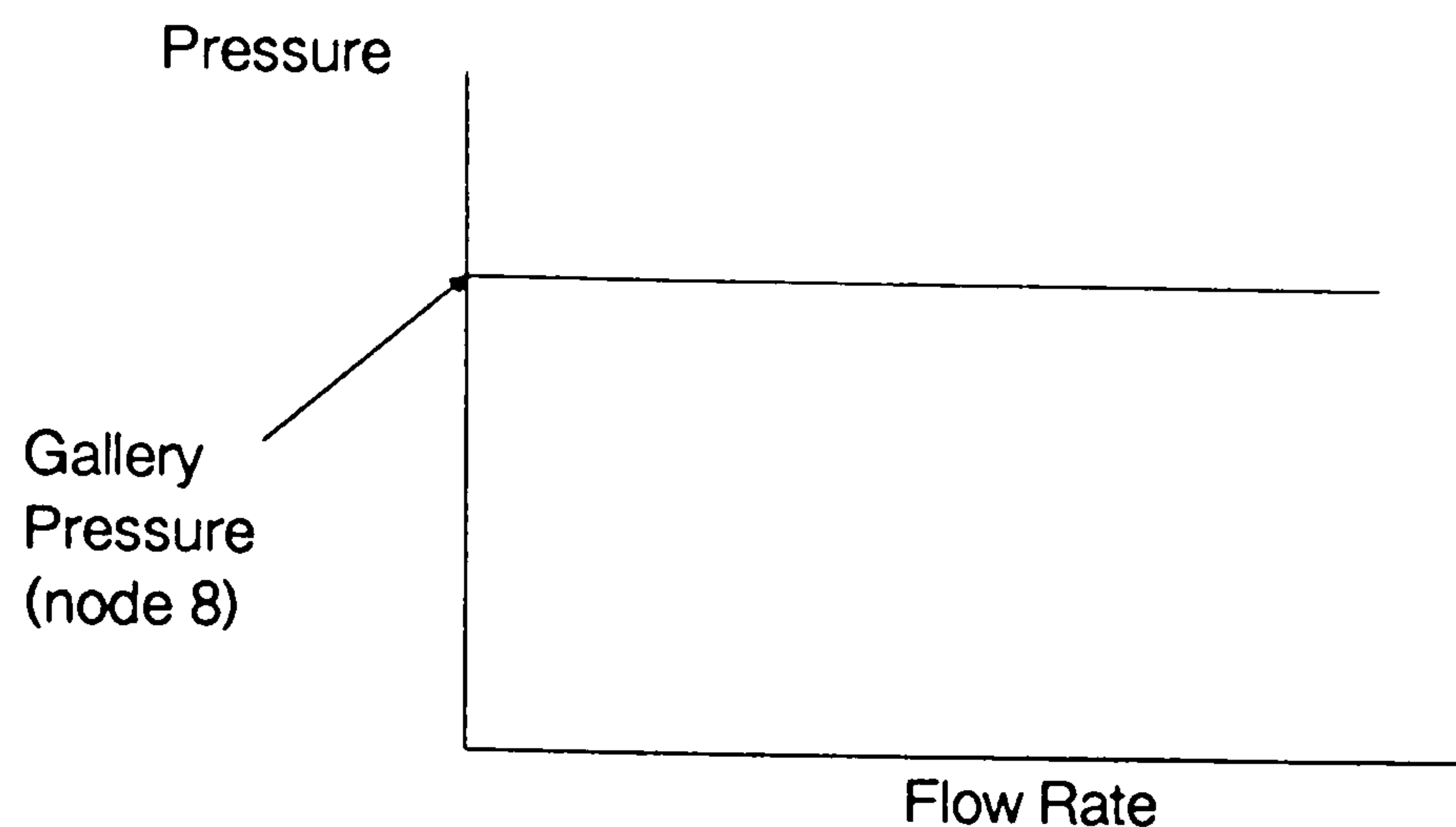


Figure 8.6. Simplified oil pump characteristics, used to model the AJ6 engine lubrication system

The oil pump characteristics shown in Figure 8.6 were adjusted for each run of the non-linear flow program to match the measured oil pressure within the main gallery of the engine (node 8 in Layout 1 and Layout 2). The results presented in section 8.4.3.3 were obtained using this simplified oil pump model.

#### 8.4.3.3 Comparison Between Predicted and Measured Values

The oil temperatures in the non-linear flow model were assumed to be 100°C throughout the lubrication system, under all speed and load conditions, apart from in the bearings where a simple oil temperature rise calculation was performed. The results from the engine tests showed that the oil temperature in the sump stabilised at approximately 100°C, at an engine speed of 3000 rpm. Thus, the measured and predicted results were compared at this engine speed.

The diametral tolerances for the main, big-end and cam bearings of the AJ6 engine are shown in Table 8.7. The corresponding minimum, maximum and average radial clearances for each type of bearing are also presented. The bearings in the AJ6 engine lubrication system were initially modelled using the

average bearing radial clearances.

Bearing Type	Shaft Diameter (mm)	Housing Diameter (mm)	Shell Thickness (mm)	Radial Clearance (mm)	Average Radial Clearance (mm)
Main Bearings	min. 76.224 max. 76.230	min. 80.429 max. 80.442	min. 2.078 max. 2.087	min. 0.0125 max. 0.0310	0.0218
Big-End Bearings	min. 52.974 max. 52.987	min. 56.718 max. 56.731	min. 1.844 max. 1.853	min. 0.0125 max. 0.0345	0.0235
Cam Bearings	min. 26.937 max. 26.950	min. 26.987 max. 27.000	-	min. 0.0185 max. 0.0315	0.0250

Table 8.7. AJ6 engine bearing dimensions and radial clearances

Table 8.8 shows a comparison between the measured and the predicted pressures and flow rates for Layout 1. The upper half of Table 8.8 (rows 1 to 3) shows the results from three natural oil temperature tests (see test schedule in Appendix E.3). The averaged values from the three tests, the values which were used for comparison purposes, are shown in the shaded portion (row 4). It was found that the pressure measurements at nodes 76 and 98 were very similar throughout the engine tests. Therefore, the pressure measurement at node 98 was considered to be representative of the two pressures and is used in the following comparison.

It was initially assumed that there was a negligible flow of oil through the chain tensioners. Therefore, the component elements between nodes 54 and 107, which were subsequently added to Figures 8.2 and 8.3 to represent the chain tensioner, were initially ignored. The predicted results for this simplified layout, using average bearing clearances, are shown in row 5 of Table 8.8. It can be seen that the predicted flow rates to the head and to the centre main bearing were only 20% - 21% of the measured values. The predicted pressure



Layout 1						
Measured Values (3000 rpm, ½ load)						
Row No.	Test No.	Bearing Radial Clearances (m)	Pressure node 98 (bar)	Pressure node 8 (bar)	Flow Rate 32 - 50 (m³/s)	Flow Rate 15 - 24 (m³/s)
1	4	-	4.90	6.11	1.050 x 10 <sup>-4</sup>	3.202 x 10 <sup>-5</sup>
2	6	-	4.90	6.10	1.032 x 10 <sup>-4</sup>	3.665 x 10 <sup>-5</sup>
3	11	-	4.85	6.06	1.041 x 10 <sup>-4</sup>	2.938 x 10 <sup>-5</sup>
4	Average	-	4.88	6.09	1.041 x 10 <sup>-4</sup>	3.268 x 10 <sup>-5</sup>
Predicted Values						
Row No.	Test No.	Bearing Radial Clearances (m)	Pressure node 98 (bar)	Pressure node 8 (bar)	Flow Rate 32 - 50 (m³/s)	Flow Rate 15 - 24 (m³/s)
5	-	Main 2.18x10 <sup>-5</sup> C. Main 2.18x10 <sup>-5</sup> Big-End 2.35x10 <sup>-5</sup> Cam 2.50x10 <sup>-5</sup>	5.98	6.09	2.148 x 10 <sup>-5</sup>	6.925 x 10 <sup>-6</sup>
6	-	Main 2.18x10 <sup>-5</sup> C. Main 2.18x10 <sup>-5</sup> Big-End 2.35x10 <sup>-5</sup> Cam 2.50x10 <sup>-5</sup> + Chain Tensioner	5.89	6.09	4.026 x 10 <sup>-5</sup>	6.926 x 10 <sup>-6</sup>
7	-	Main 3.70x10 <sup>-5</sup> C. Main 4.19x10 <sup>-5</sup> Big-End 3.70x10 <sup>-5</sup> Cam 4.71x10 <sup>-5</sup> + Chain Tensioner	4.90	6.09	1.042 x 10 <sup>-4</sup>	3.266 x 10 <sup>-5</sup>

Table 8.8. Comparison between measured and predicted values for Layout 1

loss between the main gallery and the end of each cam-shaft was only 9% of the measured pressure loss. However, it was anticipated that this predicted pressure loss would improve if more representative flow rates could be achieved.



Upon further examination of the AJ6 engine lubrication system, it became apparent that a significant amount of oil would flow through the chain tensioner. The annular pipe model was developed for use in modelling a chain tensioner device (the annular pipe model is described in section 3.5). Layout 1 and Layout 2 were modified to incorporate the chain tensioner, which was represented by a series of circular and annular pipes (nodes 54 to 107 in Figure 8.2 and Figure 8.3). The results for the pressures and flow rates through the full Layout 1 are shown in row 6 of Table 8.8. The addition of the chain tensioner doubled the predicted flow rate to the head, but only improved the predicted pressure drop between the main gallery and the end of the camshafts to 16% of the measured value.

It became clear that the predicted flow rates through the bearings were the principal reason for the large differences between the predicted and measured results. It was known that the bearing models were sensitive to the bearing clearances, ie. the flow rate was proportional to the cube of radial clearance. The measured radial clearances of the No. 4 and No. 7 main bearings in the test engine were  $2.3 \times 10^{-5}$  m, which was very similar to the average bearing clearance of  $2.35 \times 10^{-5}$  m, used in the model. It was concluded that the bearing clearances at operating temperature (generally between 75°C and 135°C) were significantly larger than the clearances measured at ambient temperature (20°C). The radial clearances at operating and ambient temperatures will hereafter be referred to as 'hot' and 'cold' clearances respectively.

The lubrication system of Layout 1 was re-modelled with larger engine clearances. A discussion of the effects of thermal expansion on the radial clearances of the bearings is given in section 8.4.3.4. The bearing clearances were adjusted by trial and error until the desired flow rates were achieved.

These predicted results are shown in the lower shaded portion of Table 8.8 (row 7). Once the desired flow rates had been achieved, the pressure loss attributed to the inclusion of the flow meters could be matched. The measured results showed a pressure drop of 1.2 bar between the main gallery and the end of each cam-shaft, when a turbine flow meter was incorporated in the flow path (nodes 48 to 49 in Figure 8.2 (Layout 1)). However, with reference to the results shown in Table 8.9, when the flow meter measuring the flow to the head was removed (see Figure 8.3 (Layout 2)), the pressure drop reduced to 0.75 bar. This suggested that the flow meter was responsible for 0.45 bar of the total pressure drop to the head, under the flow rate conditions experienced in the test. The pressure drop of 0.45 bar was matched between nodes 48 and 49 (Figure 8.2) by representing the flow meter as a pipe element, the dimensions of which were found from a trial and error procedure. The pressure drop was eventually achieved by representing the flow meter as a turbulent pipe, 1.0 m in length and  $6.0 \times 10^{-4}$  m in diameter.

All the pipe elements in the system were initially modelled under laminar flow conditions. However, with the flow rates experienced in the system with the hot bearing clearances, it was found that the pipe elements feeding each cam-shaft (nodes 57 to 58, and 79 to 80) experienced turbulent flow conditions. When these pipe elements were re-modelled with turbulent flow, the pressure and flow rate conditions shown in row 7 of Table 8.8 were achieved.

It can be seen from Table 8.8 that the pressure loss to the head and the flow rates to the head and to the centre main bearing compare very favourably. To validate the modelling conditions which were used to achieve these results, the same conditions were used to model Layout 2, shown in schematic form in Figure 8.3. Layout 2 was modelled as Layout 1, but with the component



elements 25 to 26 and 48 to 49, simply swapped over. A comparison between the predicted and the measured results for Layout 2 is given in Table 8.9.

Layout 2								
Measured Values (3000 rpm, ½ load)								
Row No.	Test No.	Bearing Radial Clearances (m)	Pressure node 98 (bar)	Pressure node 8 (bar)	Flow Rate 9 - 28 (m³/s)	Flow Rate 15 - 24 (m³/s)	Pressure node 27 (bar)	Pressure node 43 (bar)
1	12	-	5.19	5.97	3.952x10 <sup>-6</sup>	3.132x10 <sup>-6</sup>	5.85	5.9
2	14	-	4.87**	5.91	3.755x10 <sup>-6</sup>	2.843x10 <sup>-6</sup>	5.79	5.85
Predicted Values								
Row No.	Test No.	Bearing Radial Clearances (m)	Pressure node 98 (bar)	Pressure node 8 (bar)	Flow Rate 9 - 28 (m³/s)	Flow Rate 15 - 24 (m³/s)	Pressure node 27 (bar)	Pressure node 43 (bar)
3	-	Main 2.18x10 <sup>-6</sup> C. Main 2.18x10 <sup>-6</sup> B-End 2.35x10 <sup>-6</sup> Cam 2.50x10 <sup>-6</sup>	5.89	5.97	1.154x10 <sup>-6</sup>	6.792x10 <sup>-6</sup>	5.95	5.97
4	-	Main 2.18x10 <sup>-6</sup> C. Main 2.18x10 <sup>-6</sup> B-End 2.35x10 <sup>-6</sup> Cam 2.50x10 <sup>-6</sup> + Chain Tensioner	5.84	5.97	1.153x10 <sup>-6</sup>	6.786x10 <sup>-6</sup>	5.95	5.96
5	-	Main 3.70x10 <sup>-6</sup> C. Main 4.19x10 <sup>-6</sup> B-End 3.70x10 <sup>-6</sup> Cam 4.71x10 <sup>-6</sup> + Chain Tensioner	5.16	5.97	3.951x10 <sup>-6</sup>	3.190x10 <sup>-6</sup>	5.85	5.94

\*\* Low pressure reading due to failure of oil seal at end of inlet cam-shaft

Table 8.9. Comparison between measured and predicted values for Layout 2

The results from two natural oil temperature tests for Layout 2 are shown in upper half of Table 8.9. However, it was found that the results obtained from test No. 14 (row 2 in Table 8.9) were subject to errors, due to the failure of an oil seal at the end of the exhaust cam-shaft. Therefore, the results



from test No. 12 (shaded row 1) were used for comparison purposes. The lower half of Table 8.9 shows the predicted results for this system. The results presented on rows 3 and 4 were obtained under similar modelling conditions to those shown on rows 5 and 6 of Table 8.8, for Layout 1. The results shown in the lower shaded portion of Table 8.9 (row 5) were obtained with the modelling conditions which were used to obtain the final results for Layout 1.

It can be seen from Table 8.9 that the predicted and measured results match very closely. The predicted results were obtained after the pressure losses through the system were significantly affected by moving the flow meter from between nodes 48 - 49, to between nodes 25 - 26. The consistency of these results demonstrates the accuracy of the non-linear flow model. The predicted results shown in Table 8.9 were not 'tuned' by adjusting the modelling conditions, but were calculated with the modelling conditions obtained from the simulation of Layout 1. However, the predicted flow rates for Layout 1 and Layout 2 were obtained using bearing radial clearances which were significantly larger than the maximum allowable cold bearing clearances which were shown in Table 8.7. It was concluded that the increased temperature of an operating engine bearing created thermal expansion effects within the bearing, which had a significant effect on the bearing clearance.

#### **8.4.3.4 Influence of Thermal Expansion on Radial Clearance**

The key to the accurate simulation of the AJ6 engine lubrication system was in the selection of the hot bearing clearances used in the model. A check was made to ascertain if the hot bearing clearances used to obtain the final predicted results in Tables 8.8 and 8.9 were of the correct order of magnitude. It was recognized that the geometry of the engine block, the bearing shells and bearing caps, and the effect of bolting, all had an effect on the thermal

expansion of the bearings. In addition, the circularity of the bearing would also be effected by the thermal stresses. However, an analysis of all these effects was considered to be outside the scope of this study.

Since a detailed analysis of the thermal expansion within an engine was extremely complex, an attempt was made using a much simpler approach to account for the thermal expansion effect. This was simply to consider a free linear expansion of the shaft and housing for each engine bearing. However, the calculation of the linear expansion of the main and big-end bearings was complicated with the presence of bearing shells within the assembly. This was further complicated by the bearing caps being manufactured out of a different material (cast iron) than the other half of the housing (aluminium). In addition, it was not known what temperature variation was experienced through the engine block surrounding the main bearings and within the crank-shaft and connecting rod which influenced the big-end bearings. It was assumed that these bearing assemblies were cooled to some extent by the oil mist and oil spray which was present within the engine.

It was concluded that the order of magnitude of the hot bearing clearances used in the model of the AJ6 engine, could be compared to the calculated hot clearances of the cam bearings. The cam bearings were of a simpler construction to the main and big-end bearings, being comprised of only a shaft and a housing. The thermal properties of the shaft and housing are shown in Table 8.10. It was assumed that the cam-shaft and cam bearing assembly was subjected to less oil cooling effects than the main and big-end bearings. It was assumed that cam bearing temperature would be at the same temperature of the oil leaving the bearing. The linear expansion was calculated between ambient temperature (20°C) and the mean temperature of the bearing.

Component	Material	Coefficient of Linear Expansion (K <sup>-1</sup> )
Cam-Shaft	Alloy Steel	10.0 x 10 <sup>-6</sup>
Cylinder Head and Bearing Cap	Aluminium Alloy	23.5 x 10 <sup>-6</sup>

Table 8.10. Thermal properties of cam bearing materials

The free linear expansion of the cam-shaft and housing was calculated from the expression:

$$x_2 = x_1 + (x_1 \alpha \Delta T) \tag{8.1}$$

- where:
- $x_1$  = Original dimension (m).
  - $x_2$  = New dimension (m).
  - $\alpha$  = Coefficient of thermal expansion (K<sup>-1</sup>).
  - $\Delta T$  = Difference between ambient and working temperature (K).

The estimated hot bearing dimensions and resulting radial clearances for the cam bearings of the AJ6 engine are shown in Table 8.11. The values shown in Table 8.11 were calculated with an assumed bearing working temperature of 120°C.



Shaft Diameter (mm)	Housing Diameter (mm)	Radial Clearance (mm)	Average Radial Clearance (mm)
min. 26.964 max. 26.977	min. 27.050 max. 27.063	min. 0.03673 max. 0.04975	0.04324

Table 8.11.     Calculated hot (120°C) radial clearances for the AJ6 engine cam-shaft bearings

It can be seen that the value used for cam bearing radial clearance in Layout 1 and Layout 2 (0.047 mm) lay within the range of hot bearing clearances shown in Table 8.11. Although the value of 0.047 mm was greater than the average calculated hot bearing clearance (0.043 mm) it was still less than the theoretical maximum value of 0.050 mm. This indicated that the hot bearing radial clearances used to model the lubrication system of the AJ6 engine were of realistic order of magnitude.

A true comparison of the results was difficult at this stage because of the uncertainty of the other temperature effects on the oil within the lubrication system. The flow model assumed a constant oil temperature of 100°C throughout the system, apart from in the bearings where a simple oil temperature rise calculation was performed. If the oil in the pipes and drillings which fed the cam-shafts was heated to a temperature greater than 100°C, the working temperature of the oil within the bearings would be greater than predicted. This would result in greater oil flow rates for a given bearing radial clearance. A full thermal analysis of the AJ6 engine was not attempted because of the lack of data which was required for the heat transfer and engine block programs. It was concluded that the results from the AJ6 engine indicated the accuracy and flexibility of the non-linear flow model. The validation of the heat transfer and engine block models was reserved for the analysis of the V8

engine.

## 8.5 Summary of Chapter 8

Two linear flow models were developed, one using the Gauss-Jordan algorithm, and the other using an LU decomposition routine. After a comprehensive comparison between the two linear solution methods, it was concluded that the linear flow model, which incorporated an LU decomposition routine, produced more accurate results and reduced the run time for the flow analysis of a lubrication system by over 50%.

Using the lessons learned from the linear model, the non-linear flow model was developed with an LU decomposition linear matrix solver at the heart of the Levenberg-Marquardt iteration algorithm. The results produced by the non-linear flow program matched exactly those obtained from the LU decomposition linear program. A range of lubrication system sizes, oil pressures, and oil flow rates were modelled, and the results matched exactly in every case. Having gained confidence in the robustness and flexibility of the Levenberg-Marquardt solution method in the flow program, the same routine was utilised for the solution of the unknowns in the heat transfer and engine block programs.

The AJ6 engine lubrication system was used as base system during the development of the non-linear flow model and for the initial validation of the pressure and flow rate results. Many lessons were learned during the early stages of modelling the AJ6 engine lubrication system. These lessons enabled the model to be set-up more accurately, to simulate the operating conditions of a hot running engine, and predict realistic pressure and flow rate values under hot operating conditions.



During initial model development, the pressure and flow rate results were verified by studying the 'trends' of the results through the system. The trends of the results showed that the system 'behaved' as expected, flow continuity was maintained throughout the system and oil pressures increased or decreased with inverse proportionality to the changing oil flow rates (see Table 8.4). In addition, the values for the oil flow rates through the main bearings of the AJ6 engine were compared to values provided by Glacier Vandervell, from their own 'rapid' bearing oil flow model. These values compared very favourably, but some uncertainty remained as to the modelling conditions used by Glacier Vandervell, in particular, the values which were used for the oil feed pressures into each bearing.

The results from the non-linear flow program were compared to results from test-bed measurements on the AJ6 engine. These engine tests showed that several adjustments had to be made to the modelling conditions before the predicted pressures and flow rates matched the measured values. The observations from the engine tests and subsequent adjustments to the model were:

- i, The results from the engine tests showed that the oil pump characteristics which were being used were obsolete. The oil pump characteristics were changed to a simplified linear form, which returned the measured oil gallery pressure independent of the oil flow rate.
- ii, The oil flow rate through the chain tensioners was initially assumed to be negligible, therefore, the chain tensioners were not included in the first model of the AJ6 engine lubrication system. However, the engine tests showed that approximately 20% of the flow to the head passed through the chain tensioner. This necessitated the development of the



annular pipe model (presented in section 3.5) and the addition of the chain tensioner device to the model of the AJ6 engine lubrication system. The chain tensioner was modelled as an arrangement of turbulent circular and annular pipes.

- iii, To accurately model the pressure drop within the lubrication system of an engine, which was instrumented to measure the flow rate within the oil passages, the pressure drop through the flow meter had to be accounted for. The flow meter used in the AJ6 engine test was represented by a turbulent pipe section, 1.0 m long and  $6.0 \times 10^{-4}$  m in diameter.
- iii, The oil flow rate through the engine journal bearings was found to be very sensitive to the bearing radial clearances. It was found that the bearing clearances of a hot running engine were significantly larger than the clearances measured at ambient temperature. It was found that the hot clearances could be estimated from a simple calculation of the free linear expansion of the bearing shaft and housing. Using this method, it was found that the hot bearing clearances, which were selected to match the measured flow rate results, were of a realistic order of magnitude.

The lessons which were learned during the modelling stages of the AJ6 engine were applied to the model of the V8 engine lubrication system. The thermofluid analysis of the V8 engine lubrication system is presented in Chapter 10.

## Chapter 9

# Modelling the V8 Engine Lubrication System

### 9.1 Introduction

The V8 engine proved to be a more suitable engine than the AJ6 for the validation of the lubrication system simulation model, especially the heat transfer and engine block models. Firstly, data was available for this engine which allowed the generation of the bearing temperature maps, which were used to model the oil temperature rise within the journal bearings. These temperature maps were generated by the bearing program, which in turn used bearing load data files generated by a bearing mobility analysis program developed at Jaguar (Smith (1990)). Secondly, the combustion gas temperatures were available for the V8 engine. These were provided by an engine simulation model at Jaguar (Bingham (1987) and Barraclough (1991)). Finally, predicted engine block temperatures were available from an FEA model of the V8 engine block (Chang et al (1992)), which could be used as input data in the first pass of the heat transfer program and also used for comparison purposes with the predicted metal temperatures from the engine block program.

The schematic diagram of the lubrication system of the V8 engine is shown in Figure 9.1. Three sources of data were available for the purpose of validating the results for the V8 engine. These were:

- i, Pressure and flow rate measurements from a series of rig tests on one of the heads of the V8 engine.

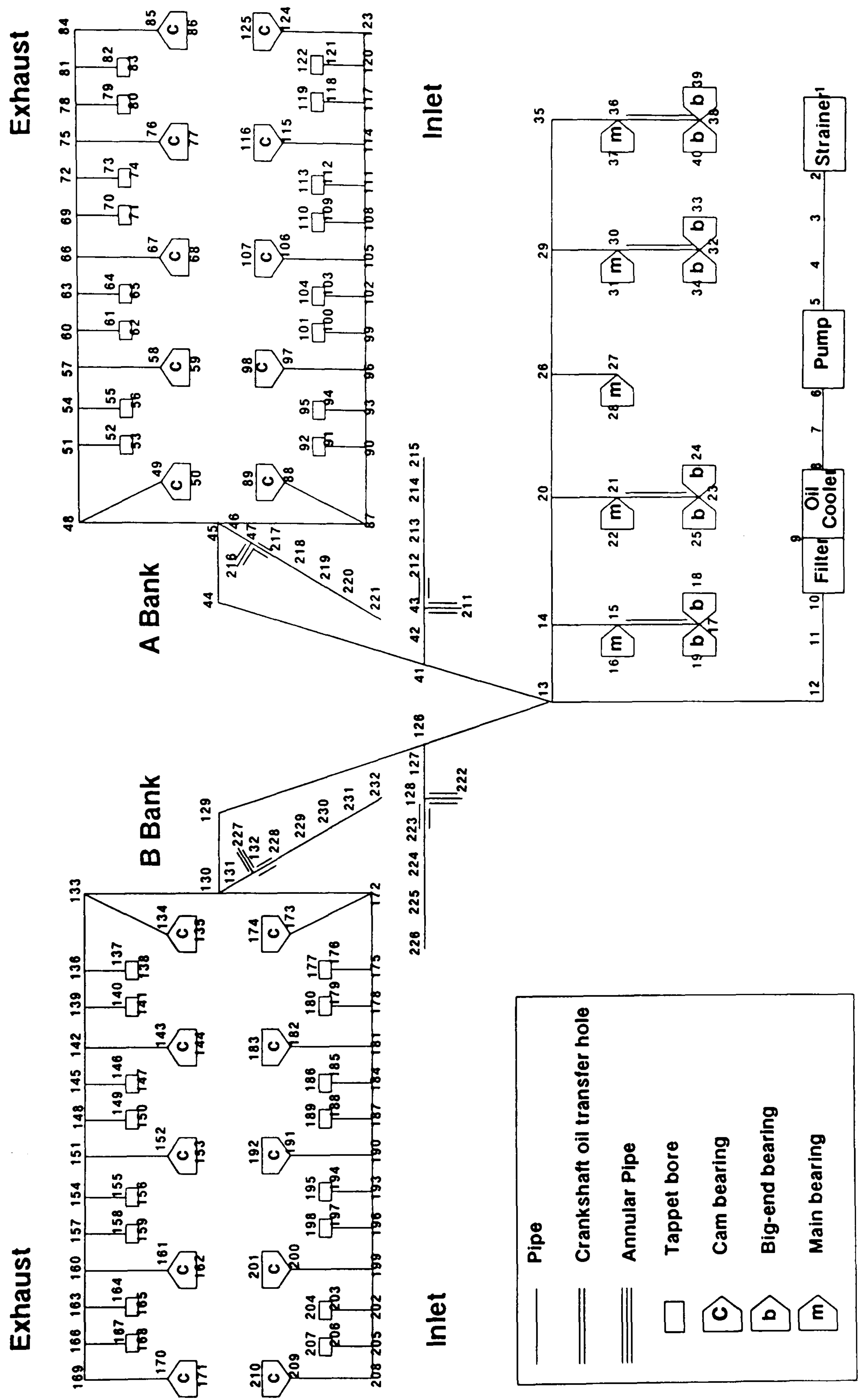


Figure 9.1. Schematic diagram of V8 engine lubrication system



- ii, Pressure, flow rate and temperature measurements, from a series of engine tests which were carried out on a V8 4 litre engine at Jaguar.
- iii, Predicted engine block temperatures from an FEA model of the V8 engine (Chang et al (1992)).

## **9.2 Comparison with Results from V8 Valve Train Rig Tests**

A comparison was made between the predicted results obtained from the non-linear flow program and measured results from a V8 engine valve train rig test at Jaguar. The valve train rig was comprised of one bank of cylinder heads of a Jaguar V8 engine. The assembly included one chain tensioner and two oil galleries which fed the tappets and cam bearings. This arrangement was represented in the flow program by modelling one of the heads shown in Figure 9.1 ('A' bank, nodes 41 to 125). The pipe element between nodes 41 and 44 was replaced by a pump element. The pipe and annular pipe elements between the nodes 45 and 221 represented the oil flow path through the chain tensioner.

The tappets were modelled as non-grooved bearings. These bearings were labelled as cam bearings during the modelling of the system layout, for the benefit of the engine block program. The engine block program would later extract the layout of the system from the data file created by the flow program and use this data to calculate average flow rate and temperatures for each type of engine bearing. Labelling the tappets as cam bearings allowed the oil conditions at the exit from these components to be included in the calculation of the average flow rate and temperature of the oil splashed on to the head.

The bearings which represented the tappets were modelled with zero eccentricity and a low rotational speed (bearing speed/engine speed ratio of

0.2). The axial length of the bearing was selected as twice the shortest flow path through the tappet, which was the distance between the top of the feed hole and the top of the tappet guide when the tappet was fully depressed. This gave a bearing axial length of 20 mm.

### 9.2.1 Constant Oil Feed Pressure and Temperature

Figure 9.2 presents a comparison between the predicted and measured results for the V8 engine head, with a constant feed pressure of 3 bar and oil temperature of 110°C. The flow rate labelled 'inlet cam' in Figure 9.2 represents the flow into the oil gallery which fed the tappets and cam bearings on the inlet valve side of the head (nodes 45 to 86).

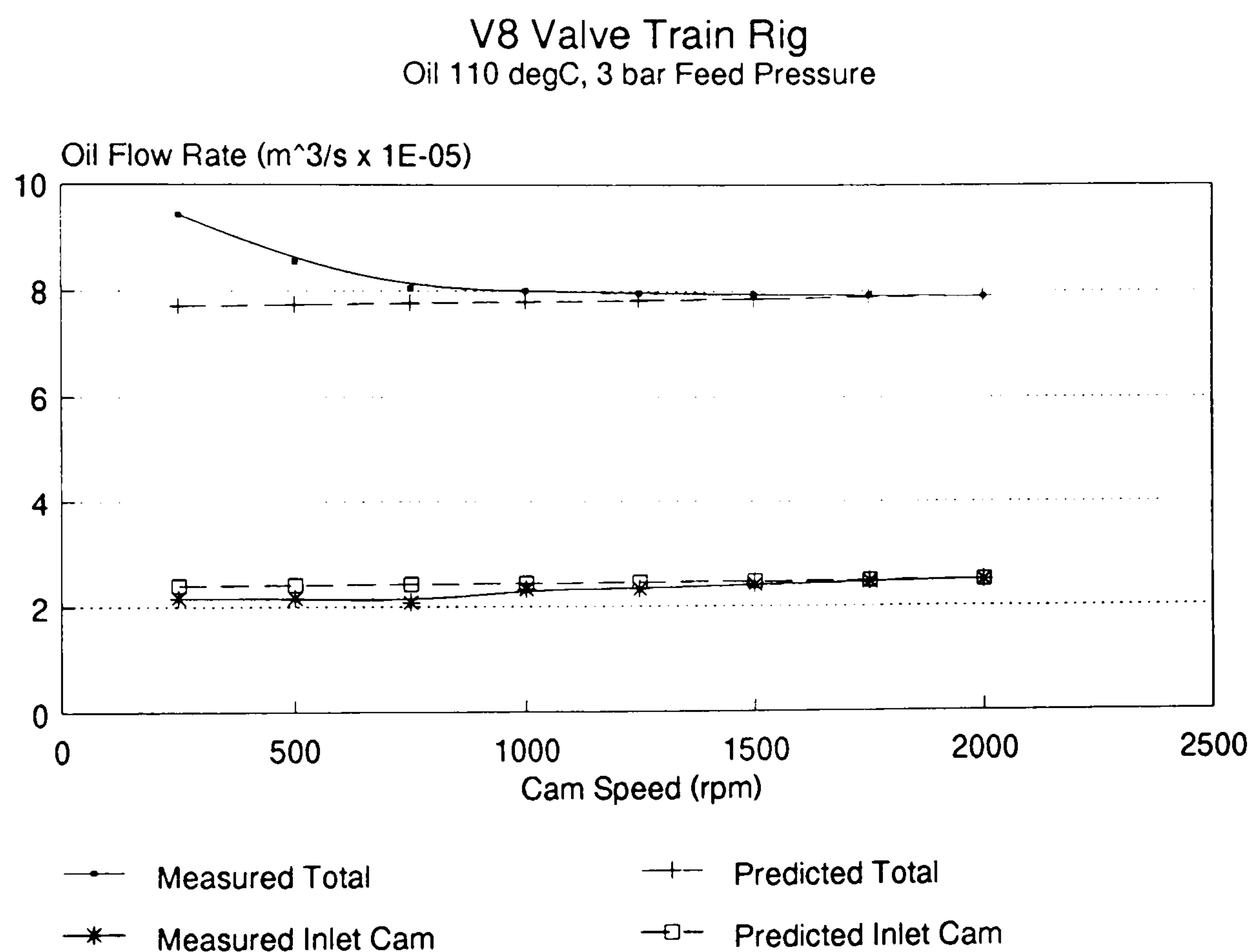


Figure 9.2. Comparison between predicted and measured flow rates for V8 head

The radial clearances for the cam bearings and the tappets were adjusted by trial and error, to match the measured results at a cam speed of

2000 rpm (engine speed of 4000 rpm). The oil pump characteristics were changed to provide a constant feed pressure to the head of 3 bar, independent of the oil flow rate. The results shown in Figure 9.2 were obtained with the 'hot' cam bearing and tappet dimensions shown in Table 9.1.

Variable	Cam	Tappet
Radial Clearance	$4.35 \times 10^{-5} \text{ m}$	$4.35 \times 10^{-5} \text{ m}$
Eccentricity Ratio	0.85	0

Table 9.1. Initial modelling conditions used for the cam bearings and tappets of the V8 head

Table 9.2 shows the theoretical hot bearing clearances for the cams and tappets, which were calculated using the method described in section 8.4.3.4. It can be seen that the radial clearances used to model the V8 engine head were within the range of hot clearances shown in Table 9.2.

Bearing Type	Cold Radial Clearances (mm)	Hot Radial Clearances (mm)	Average Hot Radial Clearance (mm)
Cam Bearing	min. 0.015 max. 0.026	min. 0.0353 max. 0.0463	0.0408
Tappet	min. 0.019 max. 0.023	min. 0.0413 max. 0.0453	0.0433

Table 9.2. Calculated hot (120°C) radial clearances for the V8 engine cam-shaft bearings and tappets

The predicted results shown in Figure 9.2 are in close agreement with the measured values, especially between the cam speed range of 1000 and 2000 rpm (engine speeds of 2000 and 4000 rpm). The close agreement between the



results for the flow rate to the inlet valve side of the head was a result of the adjustment of the cam and tappet clearances. However, assuming that the oil flow rate to the exhaust valve side of the head was very similar to the flow rate to the inlet valve side, the very close agreement between the results for the total flow rate to the head validated the modelling method employed for the chain tensioner. The chain tensioner was represented by a series of circular and annular pipes, the majority of which were modelled with turbulent flow conditions. The flow rate through the chain tensioner was found to be  $3.3 \times 10^{-5} \text{ m}^3/\text{s}$ , which was approximately 40% of the total flow rate to the head.

The increase in the measured total flow rate at cam speeds of 1000 rpm or less, was attributed to either measurement error or a flow abnormality through the chain tensioners. Although the results for the flow rate to the inlet valve side of the head deviated slightly at these low speeds, the difference between the values did not echo the larger difference seen for the total flow rate to the head.

### 9.2.2 Varying Oil Feed Pressures

Figure 9.3 shows the predicted and measured results for the flow rate to the oil gallery on the inlet valve side, with the same oil temperature ( $110^\circ\text{C}$ ) used to obtain the results shown in Figure 9.2, but under varying feed pressures. The varying feed pressures were obtained by changing the oil pump characteristics to provide the desired pressure, independent of the oil flow rate.

As expected, the predicted and measured results were in close agreement when the feed pressure was 3 bar, as these were the same operating conditions used to obtain the results shown in Figure 9.2. However, the results at feed pressures of 2 bar and 4 bar differed by a large margin. The pressure

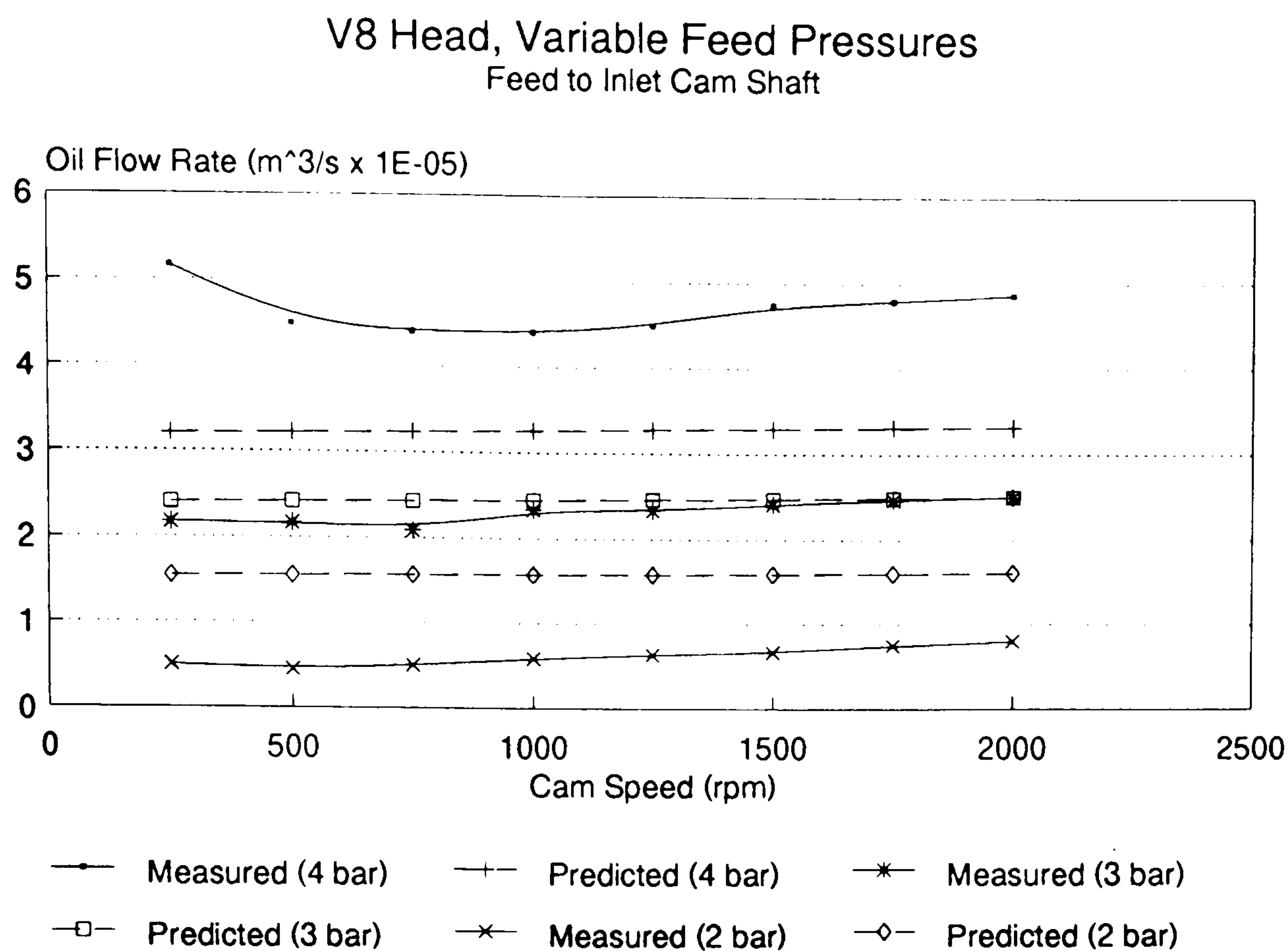


**Figure 9.3.** Comparison of results for the flow rate to the inlet valve side of the V8 engine head. Varying feed pressures.

the flow rate relationships used in the flow model to represent the pipes and bearings were linear, and therefore, the predicted flow rate was directly proportional to the pressure. It can be seen from Figure 9.3 that when the feed pressure increased by 33%, the predicted flow rate also increased by 33%. The measured data, however, showed that when the feed pressure increased by 33%, the flow rate increased by almost 100%. Similarly, when the feed pressure decreased by 33%, the measured flow rate decreased by 66%.

The differences in the behaviour of the predicted and measured results are shown in Figure 9.4. This chart shows the flow rate results which were previously shown in Figure 9.3 at a cam speed of 2000 rpm. An additional set of results are shown on this chart, for an oil feed pressure of 1 bar. It can be seen that the predicted results followed a linear trend, whereas, the slope of the line for the measured results increased with increasing feed pressure. It was concluded that a possible reason for this discrepancy was that the feed

pressure to the cam bearings and tappets had an effect on the eccentricity of these components. A high feed pressure could have led to increased axial flow near the feed hole of the bearing.

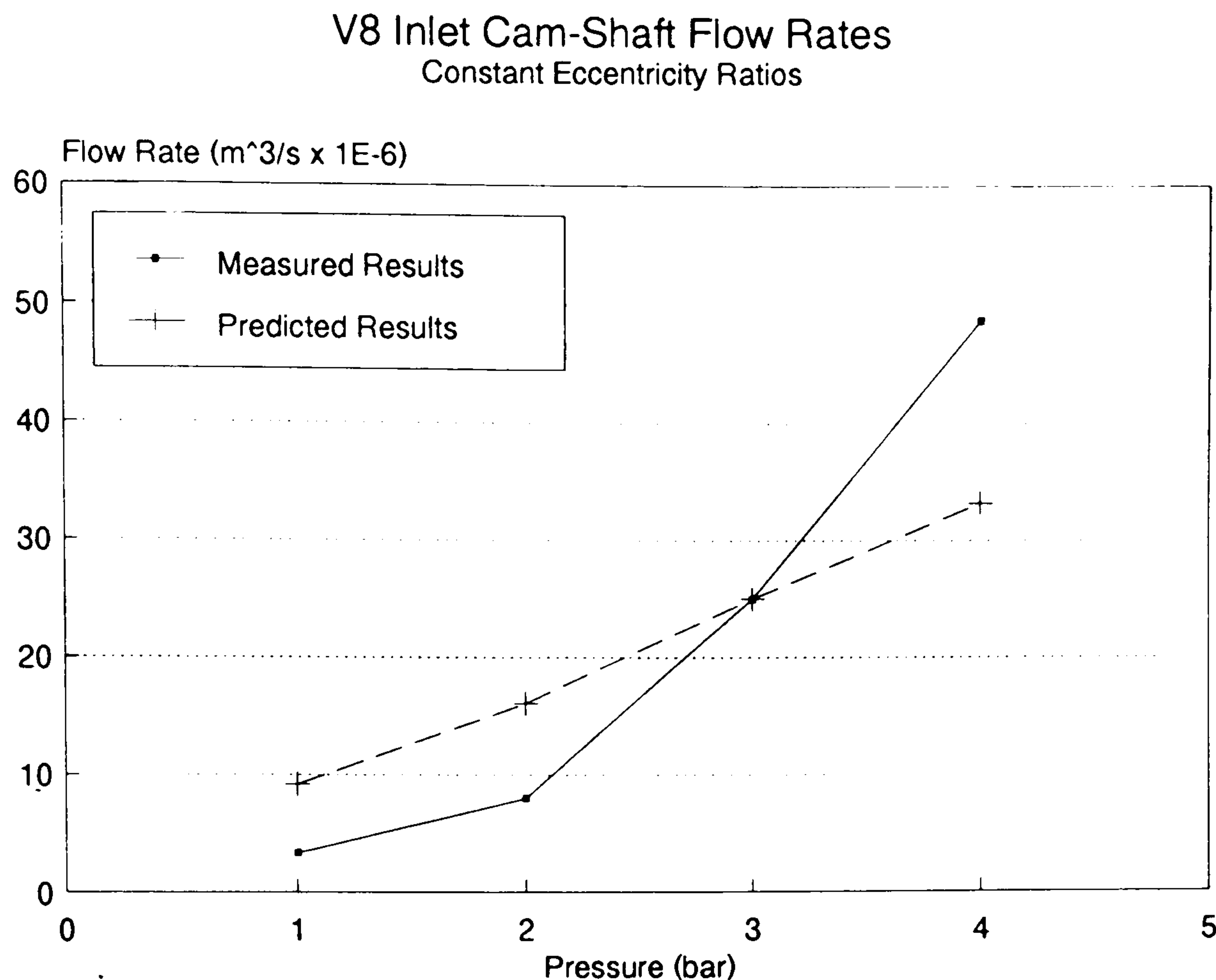


Figure 9.4. Comparison between predicted and measured result trends at cam speed of 2000 rpm. Fixed cam and tappet eccentricity ratios.

A further study was made to investigate the effect of the bearings eccentricity ratios on the oil flow through the cam bearings and tappets. The flow rate to the inlet valve side of the head was again matched, at a cam speed of 2000 rpm, with an oil at 110°C and a feed pressure of 3 bar. The cam and tappet radial clearances were the same as those used in the above study, but an arbitrary value of 0.4 was selected for the tappet eccentricity ratio. The cam bearing eccentricity ratio was reduced in a trial and error procedure until the results were matched. The eccentricity ratios of the cams and tappets at the remaining feed pressures were estimated, to investigate the effect on the overall oil flow rate. The values which were selected are shown in Table 9.3, and a comparison between the predicted and measured results under these



modelling conditions is shown in Figure 9.5.

Oil Feed Pressure (bar)	Eccentricity Ratio (dimensionless)	
	Cam Bearing ( $C_R = 4.35 \times 10^{-5}$ m)	Tappet ( $C_R = 4.35 \times 10^{-5}$ m)
1	0.35	0
2	0.50	0.2
3	0.65	0.4
4	0.90	0.9

Table 9.3. Estimated eccentricity ratios for the cam bearings and tappets with varying oil feed pressures

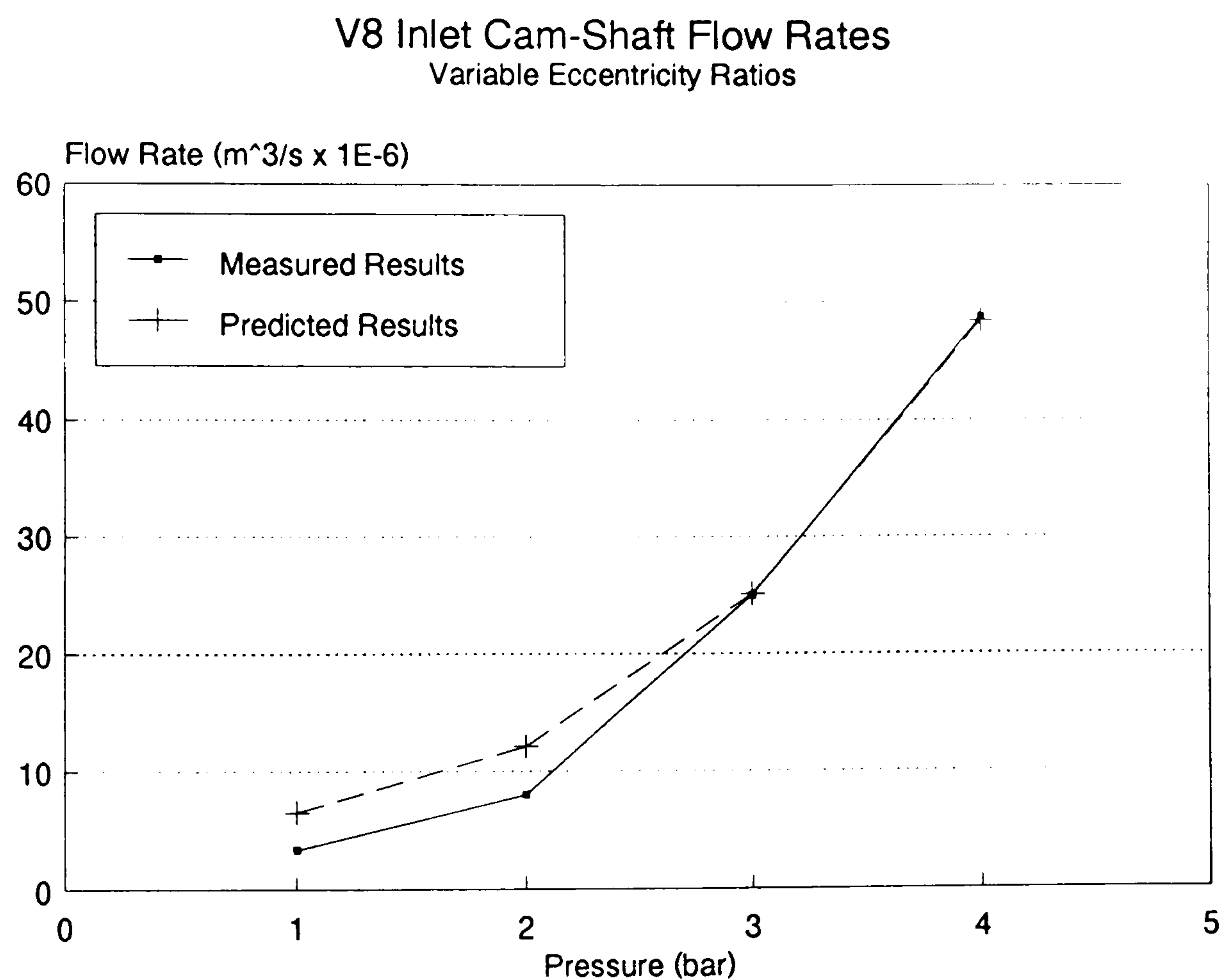


Figure 9.5. Comparison between predicted and measured result trends at cam speed of 2000 rpm. Varying cam and tappet eccentricity ratios.

It can be seen from Figure 9.5 that the predicted results now lie in closer agreement with the measured values. This indicated that the feed

pressures may have had an effect on the eccentricity of the cam bearings and tappets, which may have been the cause of the discrepancy between the results shown in Figures 9.3 and 9.4. The findings of this study highlighted the difficulty in modelling the flow through dynamic components such as the bearings and tappets. It became clear that careful consideration of the possible feed pressure to these components must be made, in addition to the consideration of the working temperature of these components, before a selection of the operating variables is made in the future.

### 9.3 Comparison with Results from V8 Engine Tests

A series of engine tests were carried out on a four litre V8 engine at Jaguar. The results from these tests were the only measured results which were available for validation of the predicted results from the flow model, and more importantly, the heat transfer and engine block models. The engine tests were conducted to investigate the oil temperatures and pressures at various points in the lubrication system, with varying oil inlet temperatures and oil pump operating conditions. The oil temperature at the entrance to the main gallery (node 13 in Figure 9.1) was maintained at either 70°C, 100°C, or 130°C. Tests were also conducted with the oil pump operating with its pressure relief valve open and closed.

The results of most interest to this study were those obtained with the oil pump relief valve open (normal operating condition) and a controlled oil gallery temperature of 100°C. This oil temperature was considered to be the closest to the actual operating temperature of the oil, at the chosen test speed of 6000 rpm. In addition, 100°C was close to the oil temperature under which the oil pump performance characteristics were obtained (110°C). The test speed of 6000 rpm was selected because it was the engine speed at which the

majority of the FEA analysis results (Chang et al (1992)), were obtained. The high engine speed was also expected to produce the largest temperature variations through the engine block and in the oil within the lubrication system.

### 9.3.1 Pressure and Flow Rate Results

The V8 lubrication system was modelled with the hot cam and tappet dimensions which were presented in Table 9.3, with an oil feed pressure of 3 bar. The main and big-end bearings were assumed to be operating under similar temperature conditions to those of the AJ6 engine. Therefore, the hot clearances used for these bearings were those used to model the AJ6 engine lubrication system, which was described in section 8.4.3.3. The pressure loss through the turbine flow meter was accounted for by representing the flow meter (placed between nodes 7 and 8 in Figure 9.1) by a turbulent pipe section. The dimensions of this pipe section were the same as those used in the model of the AJ6 engine, described in section 8.4.3.3. The dimensions of the bearings, the tappets and the pipe section used to represent the flow meter, are summarised in Table 9.4.

Table 9.5 shows a comparison between the measured results and the predicted pressure and flow rate results from the non-linear flow program. The upper half of Table 9.5 shows the results from two oil system tests (see test schedule in Appendix F). The averaged values from the two tests, the values which were used for comparison purposes, are shown in the upper shaded row.

The predicted results are shown in the lower shaded portion of Table 9.5. These results were obtained with the component dimensions shown in Table 9.4, with no further adjustments or dimensional corrections made to the



Component	Hot Radial Clearance (m)	Eccentricity Ratio (dimensionless)	Represented in the model as:
Cam Bearing	4.35x10 <sup>-5</sup>	0.65	-
Main Bearing	3.70x10 <sup>-5</sup>	0.84	-
Big-End Bearing	3.70x10 <sup>-5</sup>	0.75	-
Tappet	4.35x10 <sup>-5</sup>	0.40	Non-Grooved Bearing
Flow Meter	-	-	Turbulent Pipe Section Length 1.0 m Diameter 6.0x10 <sup>-4</sup> m

Table 9.4. Component dimensions which were used to model the V8 engine lubrication system

Source	Test No.	Oil Pressure (bar)								Oil Flow Rate (l/s)
		Node 9	Node 10	Node 35	Node 13	Node 45	Node 130	Node 169	Node 84	Node 1-13
Measured Values	12	3.7	3.5	3.4	3.4	3.2	3.2	3.2	*	*
	3	*	*	3.3	3.3	3.1	3.2	3.1	3.2	0.51
	Av.	3.7	3.5	3.35	3.35	3.15	3.2	3.15	3.2	0.51
Predicted Values	-	3.56	3.46	3.45	3.45	3.39	3.39	3.39	3.39	0.49

\* Not recorded

Table 9.5. Comparison between measured and predicted pressure and flow rate results for the V8 engine

model of the system. The flow, heat transfer and engine block programs were run approximately three times (see the flow chart of the simulation process in section 5.1), at which point, the flow and temperature results were assumed to have stabilised to their equilibrium condition. The measured and predicted oil pressure at node 208 was found to be same as at node 169 and the oil pressure at node 123 was the same as at node 84. Consequently, a comparison of the oil pressure results at nodes 208 and 123 have been omitted from Table 9.5.



It can be seen from Table 9.5 that the measured and predicted pressures and flow rates through the V8 engine lubrication system compare very favourably. In addition, the predicted pressure results also echo the measured pressure result trends very closely. The very small discrepancies between the results were attributed to the differences between the measured and predicted oil temperatures, which are discussed in the following section.

9.3.2 Oil Temperature Results

On the first pass of the heat transfer program, the wall temperature for each pipe section in the lubrication system was estimated from the results from the FEA model by Chang et al (1992). This allowed the results from the heat transfer program to be used in the engine block program. In the subsequent runs of the heat transfer program, the wall temperatures were estimated from the results for the block temperatures predicted by the engine block program (see section 9.4). A comparison between the measured and predicted oil temperature results is given in Table 9.6.

Source	Test No.	Oil Temperature (°C)								
		Node 35	Node 13	Node 45	Node 130	Node 169	Node 208	Node 123	Node 84	Sump Temp.
Measured Values	12	102.1	**	99	96.6	110.8	95.8	85.8	92.8	116.6
	3	101.1	**	101.3	99.6	102.5	93.5	84.7	87.5	114.3
	Av.	101.6	-	100.2	98.1	106.7	94.7	85.3	90.2	115.5
Predicted Values	-	102.6	100.9	101.2	101.2	99.3	98.7	98.7	99.3	121.6

\*\* Measurement error

Table 9.6. Comparison between measured and predicted oil temperature results for the V8 engine



The oil temperature entering the main oil gallery (node 13) was adjusted in the model to match the experimentally controlled temperature of 100°C. This was achieved by adjusting the inlet air temperature and air speed through the oil cooler. This was considered to be a good representation of the method used to control the oil temperature in the engine test cell.

It can be seen from Table 9.6 that the measured and predicted results are of a similar order of magnitude throughout the lubrication system. It was found that the measured oil temperatures were lower in the oil galleries in the 'A' bank head of the engine (nodes 123 and 84), in comparison to 'B' bank (nodes 169 and 208). It was considered that this may be due to non-uniform oil distribution between the heads, or possibly, non-uniform heat transfer with the coolant. However, the lubrication system was modelled with the same block temperatures in each head, which resulted in the predicted oil temperature at node 84 being the same as at node 169, and the oil temperature at node 123 was the same as at node 208.

The measured results showed a significant temperature difference between the inlet and exhaust valve oil galleries. If we take the oil temperatures in the 'A' bank head as an example, the oil temperature at node 84 (exhaust) was between 3 and 7°C higher than at node 123 (inlet). Unfortunately, the temperature effects of the exhaust gasses passing through the exhaust ports were not accounted for in the engine block model (see section 9.4). The results from the engine block model exhibited an almost constant temperature profile across the cylinder head. The slight variation in the predicted oil temperatures at nodes 123 and 84 were a result of the small temperature differences in the head, which were attributed to engine geometry effects.



The predicted oil sump temperature, presented in Table 9.6, was obtained from the engine block program. The predicted oil temperature was approximately 6°C higher than the measured value. This was considered to be a very reasonable result, considering the complex geometry of the V8 engine block, with the numerous engine internal surfaces which influence the temperature of the oil splashed on to them. The nodal resistance network which was used to model the V8 engine block and the modelling conditions which were used to predict the block and sump temperatures, are presented in section 9.4.

#### **9.4 Modelling the V8 Engine Block. Comparison of Engine Block Temperature Results with Results from an FEA Model**

The heat transfer through the engine block was represented by taking a cross section through a single piston/liner/head/sump assembly. The piston was assumed to be fixed at its mid-stroke position and the heat transfer effects through the con-rod were not included. The block element arrangement and representative nodal resistance network, which were used to model the V8 engine geometry, are presented in Figure 9.6 (block elements are not drawn to scale).

The cross-section through a single cylinder of the V8 engine was represented by 58 block elements. The heat transfer through these block elements was, in turn, represented by 274 thermal resistances, which were connected to 263 nodes to form a two-dimensional nodal resistance network. It was considered that the heat transfer through the chosen engine section was adequately represented by a two-dimensional network. The temperature difference between adjoining cylinders was considered to be minimal, and

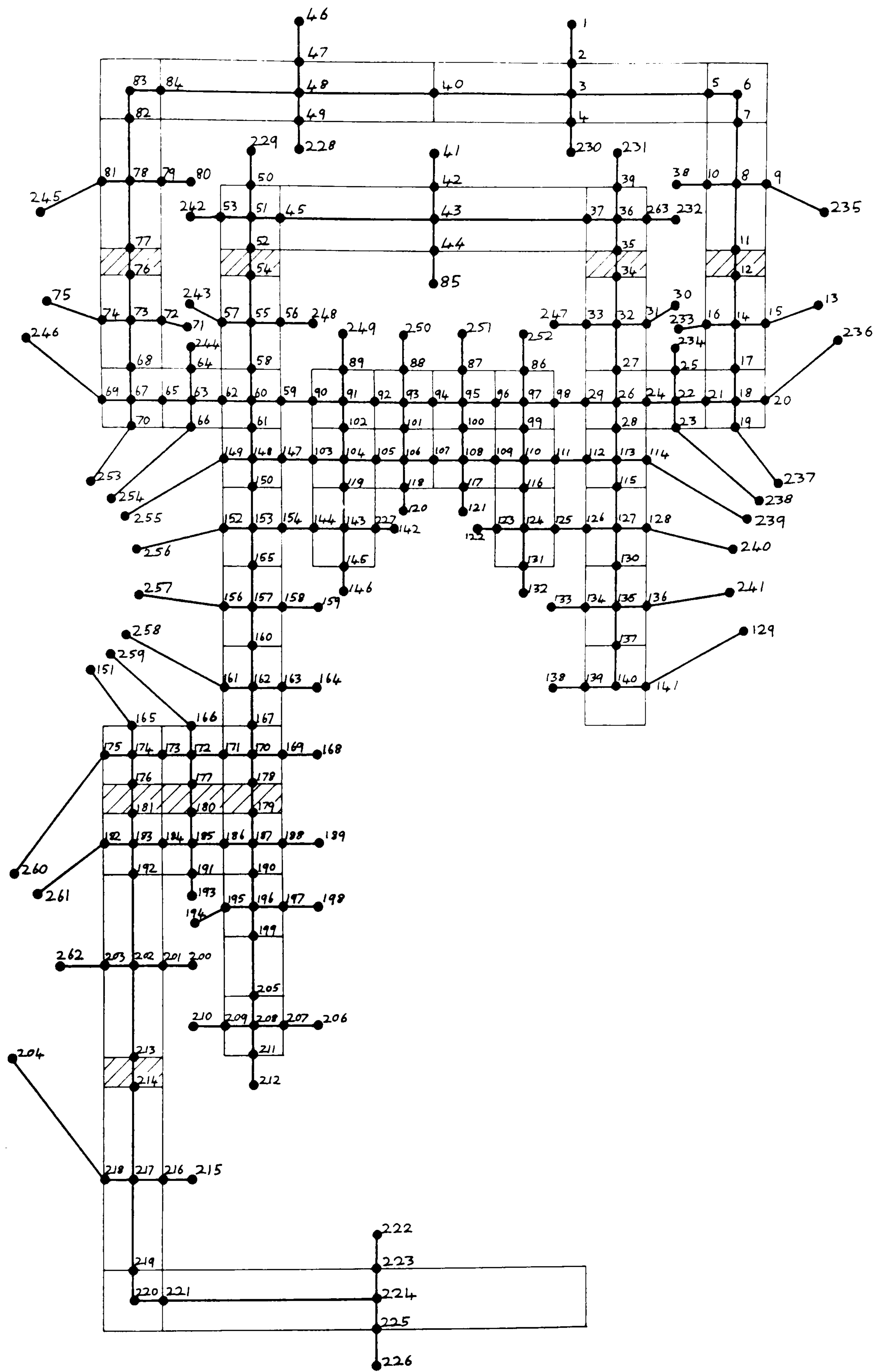


Figure 9.6. Block element arrangement and nodal resistance network of V8 engine block

consequently, the heat transfer between adjoining cylinders was ignored. The modelling conditions which were used for the V8 engine are summarised in Table 9.7.

A sample of the predicted block temperatures are shown in Figure 9.7. The mean oil temperature, for each node in the nodal resistance network which represented a falling oil film, is also presented in Figure 9.7 (these numbers are underlined with a single line). The numbers shown with both an underline and an overline designate the mean oil temperature at a node which represents the oil in the sump.

Although measured data was not available for the validation of the predicted block and oil film temperature results, an estimation of the accuracy of the predicted temperature profile through the engine block was obtained by comparing the predicted results with the results from an FEA model (Chang et al (1992)). The FEA model of the V8 engine analyzed thermal properties of the complete engine assembly, but did not include the engine sump. The engine block was run in one assembly, containing the cylinder block, pistons and piston rings. The analysis accounted for the heat transfer from the combustion gas and from heat generated between the piston and bore. The engine block was represented by 53,060 elements, while each piston was represented by 2,700 elements. The ANSYS finite element code was used in the thermal analysis of the head and block.

The FEA analysis included a separate coolant flow model which represented the coolant passages in the block and the head. The model was developed for the STAR-CD fluid dynamic code and contained 360,000 cells. The coolant flow model returned the local velocity vectors throughout the coolant jacket. These velocities were used in the calculation of the film



Mode	Medium	Thermal Conductivity (W/mC)	Fluid Temperature (°C)	Heat Transfer Film Coefficient (W/m²C)	Notes
Conduction	Aluminium	150	-	-	Used for majority of elements
	Paper	0.18	-	-	Used for engine gaskets
	Steel	50	-	-	Used for piston rings
Convection	Air (nodes 13, 235, 236, 237, 238, 239, 240, 241, 129, 245, 75, 246, 253, 254, 255, 256, 257, 258, 259, 151, 260, 261, 262, 204, 226, 194, 193)	-	20	33	Air flow of 7 m/s
	Coolant (nodes 71, 244, 243, 242, 80, 229, 228, 41, 230, 231, 38, 232, 30, 233, 234)	-	80	330	Ref. Veshagh and Chen (1993)
	Combustion Gas (nodes 85, 247, 248, 249, 250, 251, 252)	-	750 (see Appendix **)	406 (Veshagh and Chen (1993))	-
	Oil Film (nodes 1, 46, 120, 121, 122, 132, 133, 138, 142, 146, 159, 164, 168, 189, 198, 200, 206, 210, 212)	-	Calculated in the engine block program		85% of oil from main & b-end bearings hit internal surfaces.
	Oil Sump (nodes 215, 222)	-			100% of oil from cam bearing hit top of head

Table 9.7. Modelling conditions used in the nodal resistance network model of the V8 engine block

coefficients, which were applied to the coolant jacket in the thermal analyses. The FEA results were obtained with the modelling conditions presented in Table 9.8. A sample of the results from the FEA model of the V8 engine, are shown in Figures 9.8 through to 9.11.

Mode	Medium		Modelling Conditions
Conduction	Block		$k = 125 \text{ W/mC}$
	Piston		$k = 117 \text{ W/mC}$
	Rings		$k = 55 \text{ W/mC}$
Convection	Air		Data not provided
	Coolant		T and h calculated in separate sub-model
	Combustion Gas	to Piston	$T = \text{Variable}$ $h = 385 \text{ Wm}^2\text{C}$
		to Block	$T = \text{Variable}$ $h = 137 \text{ to } 343 \text{ W/m}^2\text{C}$
	Oil Spray	to Piston	$T = 140^\circ\text{C}$ $h = 1000 \text{ to } 4000 \text{ W/m}^2\text{C}$
		to Block	$T = 130 \text{ to } 140^\circ\text{C}$ $h = 300 \text{ W/m}^2\text{C}$

Table 9.8      Summary of the modelling conditions used in the FEA model of the V8 engine (Chang et al (1992))

A summary of the comparison between the results is given in Table 9.9. The results shown in Table 9.9 were selected to give a comparison for the block temperatures in the regions which were both effected by, and have an effect on, the oil temperature.

It can be seen from Table 9.9 that there is a discrepancy between the FEA and predicted results for the temperature profile in the engine block in the region around the liner. The FEA results show that the highest liner

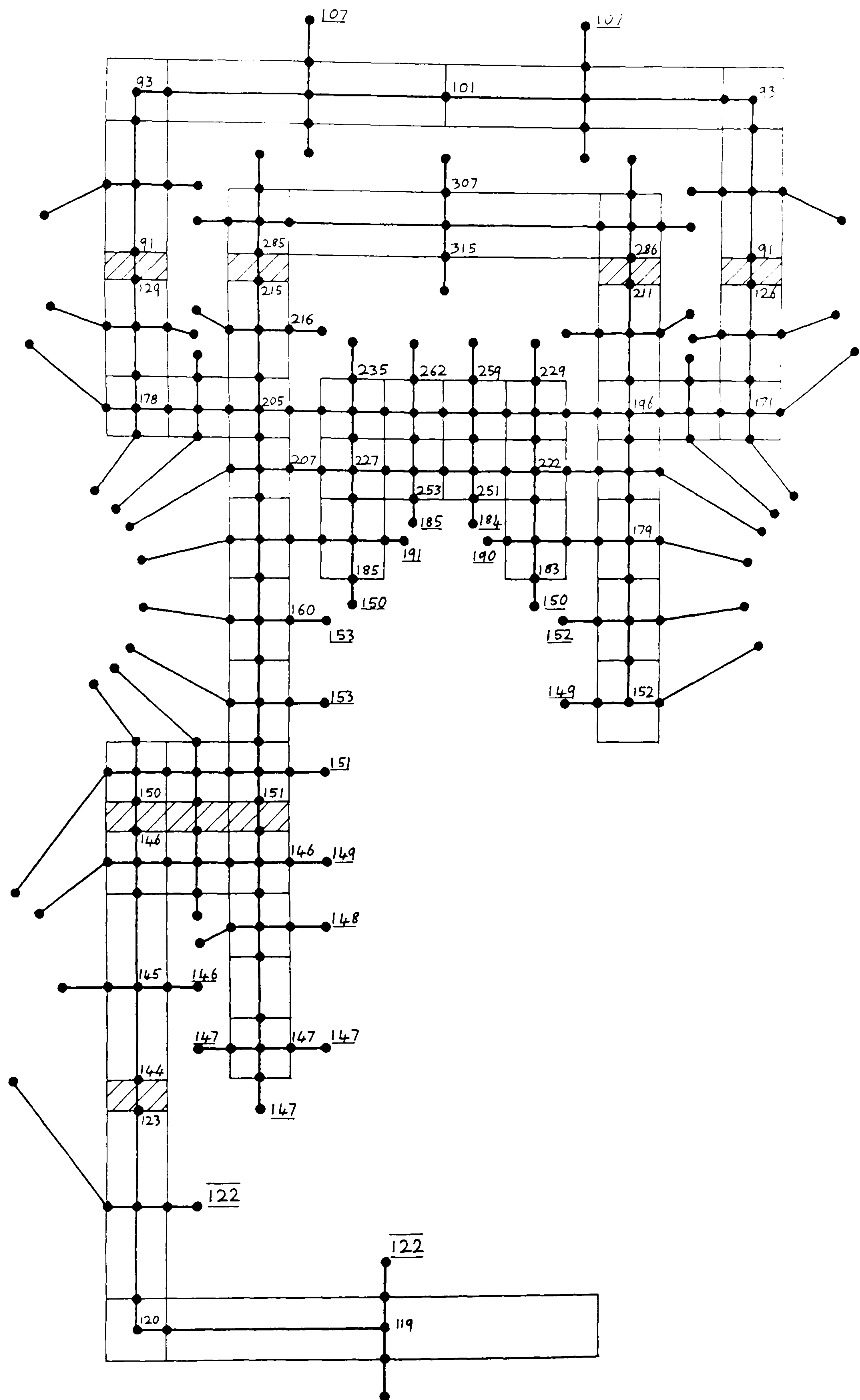


Figure 9.7. V8 engine block temperatures and mean oil film temperatures returned by the engine block program (°C)



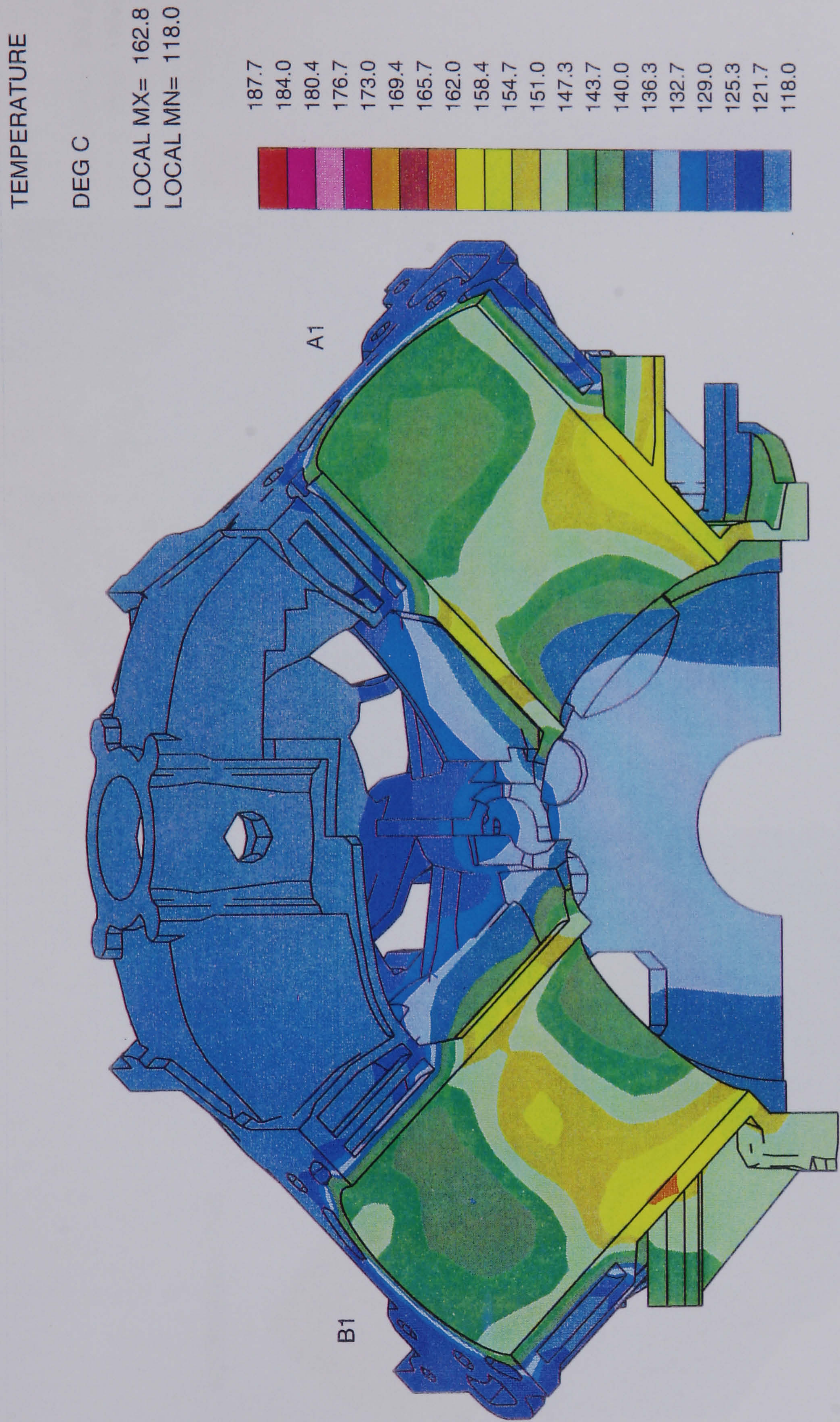


Figure 9.8. FEA temperature results for the V8 engine block at 6000 rpm (cylinder 1)



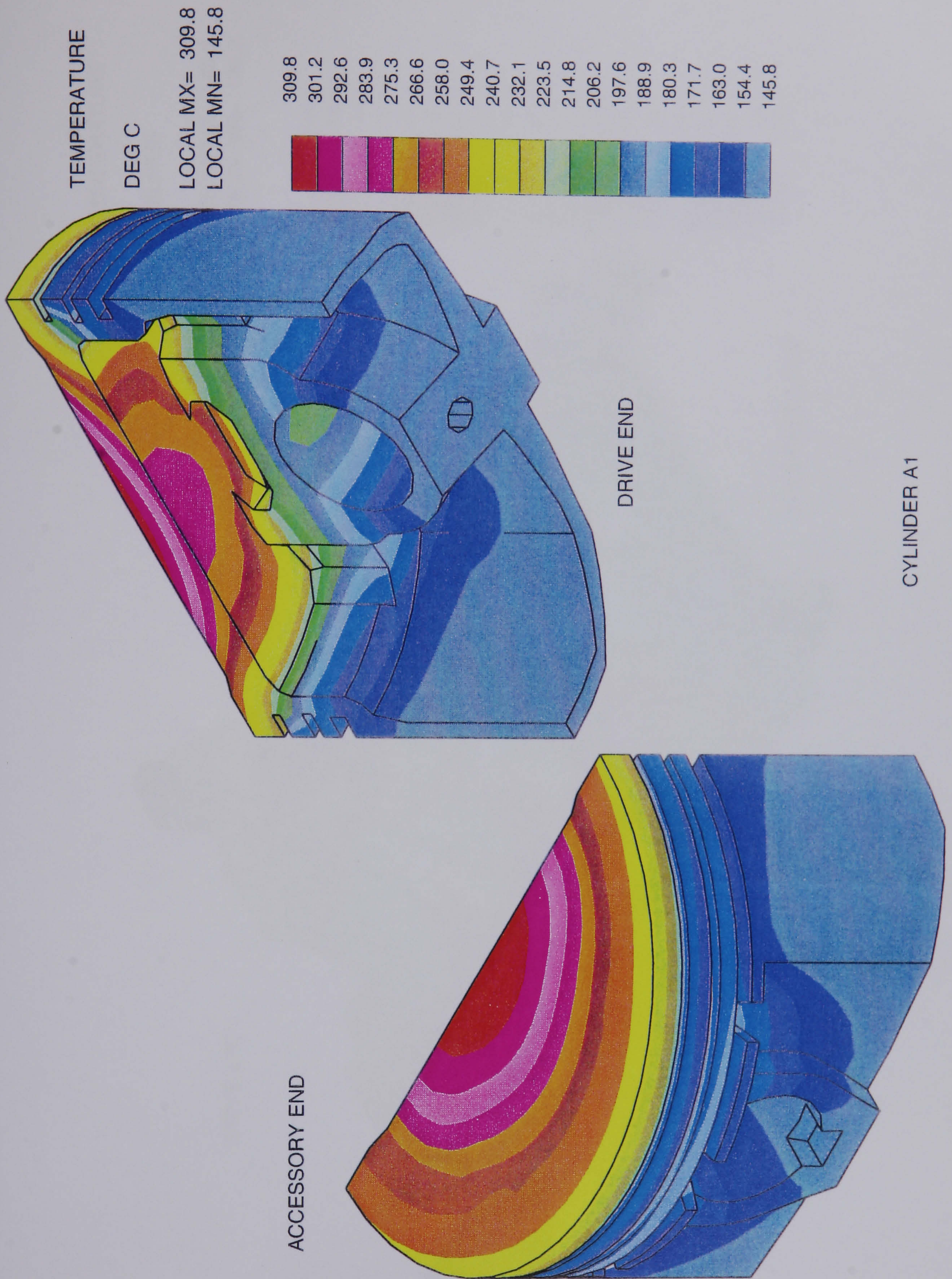


Figure 9.9. FEA temperature results for the V8 engine piston at 6000 rpm (cylinder 1, 'A' bank)



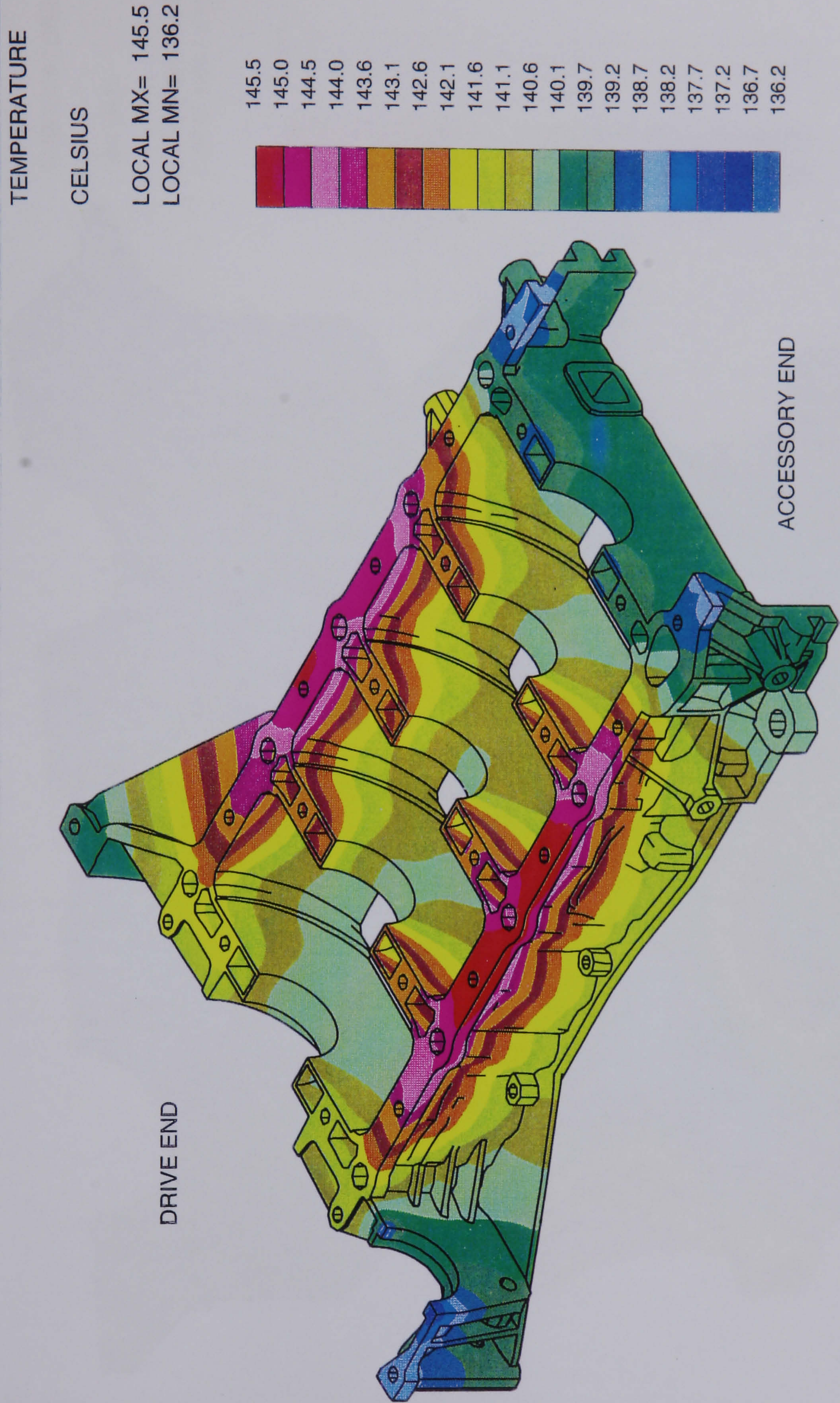


Figure 9.10. FEA temperature results for the V8 engine bedplate at 6000 rpm



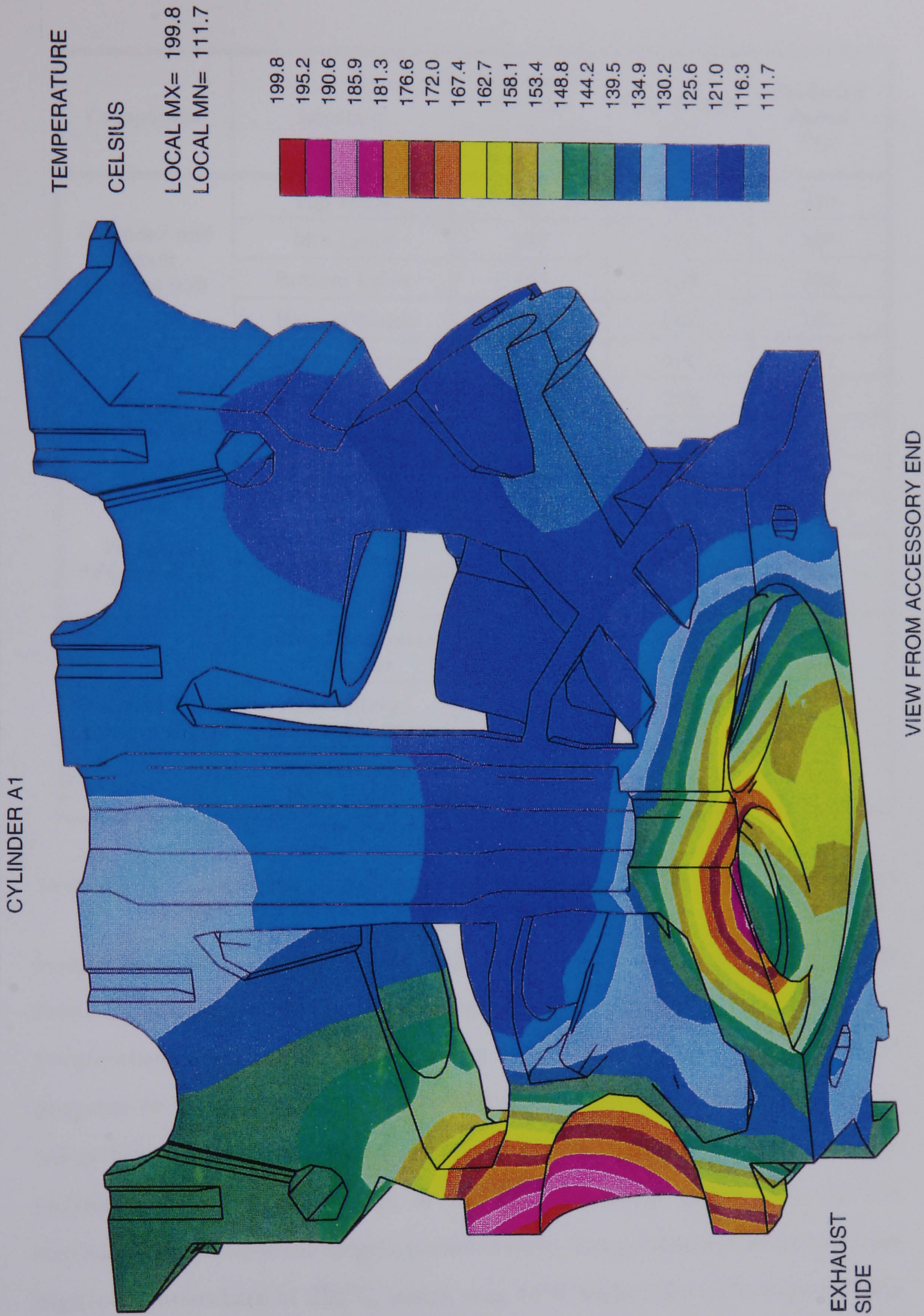


Figure 9.11. FEA temperature results for the V8 engine cylinder head at 6000 rpm (cylinder 1, 'A' bank)



Component	Location	Resistance Network Node Number (Fig. 9.7)	FEA Result (°C)	Predicted Result (°C)
Cylinder and Block (Figure 9.8)	Top Liner	56	147	216
	Mid-Liner	147	162	207
	Bottom Liner	158	154	160
	Base of Block	178	147	151
Piston (Figure 9.9)	Crown Centre	88	292	262
	Crown Edge	89	249	235
	Under Crown	118	258	253
	Bottom Skirt	145	145	185
Bedplate (Figure 9.10)	Top	188	143	146
	Outer Base	213	141	144
	Inner Skirt	207	141	147
Cylinder Head (Figure 9.11)	Centre Combustion Chamber	44	199	315
	Oil Gallery, Exhaust Valves	83	140	93
	Oil Gallery, Inlet Valves	6	125	93

Table 9.9 Comparison of predicted block temperature results and results obtained from an FEA model of the V8 engine

temperature occurs at the piston mid-position, with the lowest temperature found in the region of the liner cooled by the water jacket. The predicted temperature results echo the modelling approach taken in the engine block program of fixing the piston in its mid-stroke position. This approach was taken because it was expected to represent the operating condition of the engine, with the upper region of the cylinder being exposed to the hot combustion gasses for the largest period of time. The predicted results show the highest temperature of 216°C, which was 44°C higher than the highest FEA result, occurred at the top of the liner. The higher temperatures in the region of the water jacket were considered to be a result of the simplification of the

engine geometry in this area. The heat transfer routes within the engine were simplified and ignored the heat transfer 'bridges' between the hot liner and the cooler outer wall of the water jacket.

The simplified approach to modelling the geometry of the engine was also considered to be the primary reason for the difference in the temperature results for the engine head. The highest predicted temperature of  $315^{\circ}\text{C}$  at the centre of the combustion chamber crown was significantly larger (by  $116^{\circ}\text{C}$ ) than the temperature predicted by the FEA model. Similarly, the predicted block temperatures in the regions of the inlet and exhaust valve oil galleries were  $32$  to  $47^{\circ}\text{C}$  lower than the FEA results. It was considered that if the regions on either side of the water jacket were bridged, as they are in the actual geometry of the head, the temperature of the lower region of the head would stabilise at a lower value, with the upper region at a higher level.

The heat transfer by the exhaust gasses passing through the exhaust port was ignored in the engine block model. This was considered to be the primary reason for the discrepancy in the block temperatures between the inlet and exhaust valve oil galleries. The difference in these block temperatures was the reason for the discrepancy between the oil temperature in these oil galleries, which was discussed in section 9.3.2.

The predicted temperatures within the piston were of a similar order of magnitude to the FEA temperature results, especially at the under-crown surface which was sprayed with oil. The temperatures for the piston skirt differed slightly, but this was attributed to the value of the heat transfer film coefficient of the oil spray which was used in the FEA model. The FEA model assumed a constant value for  $h$  of  $4000\text{ W/m}^2\text{C}$ , for the oil on the piston skirt, while the engine block model used a value which was approximately  $1000$



W/m<sup>2</sup>C. It was considered that the higher value of  $h$  used in the FEA model would artificially control the piston skirt temperature to a value which was closer to the temperature of the oil sprayed onto it (140°C). The predicted mean oil temperature for these surfaces in the engine block model was 190°C, which was calculated to be in thermal equilibrium with the piston temperature.

The FEA and predicted temperature results at the bottom of the liner and at the base of the engine block were in very close agreement, as were the temperatures throughout the engine bedplate. The small discrepancies between the results echoed the differences between the oil temperatures which were sprayed on these surfaces. The FEA model assumed a constant temperature for the oil spray of 140°C, while the engine block program calculated that the mean temperature of the oil sprayed onto these surfaces varied between 147 and 153°C.

## 9.5 Summary of Chapter 9

The analysis of the V8 engine initially concentrated on the simulation of the flow conditions within the oil passageways of one of the engine heads. Measured results were available, for the validation of the predicted results, from a V8 engine valve train rig test at Jaguar. As a dedicated tappet flow model had not been developed, the tappets were modelled as non-grooved journal bearings with zero eccentricity and a low rotational speed.

It was found that the predicted pressures and flow rates were in close agreement with the measured values, when the oil feed pressure to the head was 3 bar. However, when the system was re-modelled using the same modelling conditions, but with different oil feed pressures, it was found that larger discrepancies between the results occurred. It was concluded that the oil

feed pressure had an effect on the eccentricity of the cam bearings and the tappet guides. When the V8 head was re-modelled with different estimated values for the eccentricity ratio for each feed pressure, the predicted and measured flow rate results were found to be in closer agreement. This highlighted the requirement to account for the effect of the oil feed pressure to each engine bearing, in the selection of the modelling conditions used to represent the bearing.

A series of engine tests were carried out on a complete four litre V8 engine. The measured results from these tests were used to validate the predicted pressure and flow rate results from the flow program. More importantly, these were the only results available for the validation of the oil temperatures predicted by the heat transfer program and the engine block program. The cam and tappet dimensions used in the model of the V8 engine head were used in the flow model of the full V8 engine lubrication system. The hot clearances used for the main and big-end bearings and the dimensions of the turbulent pipe section used to represent the flow meter, were taken directly from the model of the AJ6 engine, documented in Chapter 9. No further adjustments or dimensional corrections were made to the model of the system.

The flow, heat transfer and engine block programs were run approximately three times, at which point, the flow and temperature results were assumed to have stabilised to their equilibrium conditions. The measured and predicted pressures and flow rates through the system compared very favourably. The predicted pressures were all within 7% of the measured values and the overall flow rate through the system was within 4% of the measured value.



The small discrepancies between the pressure and flow rate results were attributed to the differences between the measured and predicted oil temperatures. The predicted oil temperatures in the main oil gallery and feeds to the heads were within 3% of the measured value. However, a larger discrepancy between the results was found for the oil temperatures at the ends of each oil gallery which fed the valves and cams in each head. The predicted oil temperatures at these locations were within 4 to 14% of the measured values.

It was not understood why the measured oil temperatures were lower in the oil galleries in the 'A' bank head, in comparison to 'B' bank head. However, it was found that the oil temperature was between 3 and 7° higher in the exhaust valve oil gallery than in the inlet valve gallery. The difference between the predicted and measured oil temperatures between inlet and exhaust oil galleries was attributed to the simplified model used to represent the engine head geometry in the engine block program. The exhaust ports were not accounted for in this model, which resulted in the engine block model exhibiting an almost constant temperature profile across the head.

The V8 engine geometry was modelled in the engine block program by taking a cross-section through a single piston/liner/head/sump assembly. This cross-section was represented by 58 block elements, which in turn, was represented by a nodal resistance network comprising of 274 thermal resistances. The predicted oil temperature in the engine sump, which was returned from the engine block program, compared very favourably with a measured value. The predicted temperature was within 5% of the measured sump oil temperature from the V8 engine tests.



Although measured data was not available for the validation of the block and oil film temperatures which were returned from the engine block program, the predicted block temperatures were compared to results from an FEA model of the complete V8 engine assembly. The results were found to be very similar for the block elements which were directly affected by the oil spray. The small deviations between the results in these areas were attributed to the differences in the oil temperatures and heat transfer coefficients for the oil spray. The engine block program calculated the block temperature, oil temperature and heat transfer coefficient simultaneously, while the FEA model assumed fixed values of oil temperature and heat transfer film coefficients throughout the modelling procedure.

Larger differences between the temperature results were experienced in the engine head. It was concluded that the model of the engine head, used in the engine block program, was over simplified. The model omitted the heat transfer 'bridges' between the hot cylinder liner and head, and the cooler outer walls of the water jacket. This simplification led to higher temperature predictions at the top of the liner and in the part of the head exposed to the combustion gas, and lower temperature predictions on the outer surface of the water jacket. The simplified model also omitted the effects of the heat transfer from the exhaust gasses passing through the exhaust port. The results from the engine block program were used to estimate the wall temperatures of the pipe elements in the heat transfer program. It was concluded that the simplifications in the model of the engine geometry were responsible for the small discrepancies in the predicted oil temperatures in the oil galleries of the head.

## Chapter 10

# Conclusions and Suggestions for Future Work

### 10.1 Overall Conclusions

An extensive investigation has been undertaken of the thermofluid behaviour of an engine lubrication system. The existing detailed knowledge of the flow and heat transfer characteristics of the individual component elements which are found within an engine lubrication system, were correlated into a single design analysis package. A comprehensive, robust and flexible design analysis tool has been developed for the simulation of the flow and heat transfer conditions within any lubrication system configuration. The lubrication system simulation package, written in FORTRAN, represents a unique stand-alone design analysis tool which will predict the oil pressures, flow rates, temperatures and engine block temperatures, for any desired engine block and lubrication system arrangement.

The study included a comprehensive literature review and an examination of the flow and heat transfer characteristics of the components commonly found within a lubrication system. Mathematical models of the thermofluid behaviour of the lubrication system components were developed and these models were implemented in a suite of computer programs which formed the design analysis package. The flow and heat transfer characteristics of Jaguar AJ6 and V8 engine lubrication systems were analyzed and the results from these studies were compared to measured values from engine tests.

The three year study followed a systematic development approach. The first objective of this study was to develop a steady-state flow model of a lubrication system. This objective was achieved in two phases:

- i,     The objective of the first phase was to construct a simple flow model which would be used as a design analysis tool for the rapid prediction of oil pressures and oil flow rates through a lubrication system. This objective was satisfied with the development of the LU decomposition linear flow program. Although the linear program provided a rapid analysis tool, the accuracy of the results were limited by the simplified pressure loss v flow rate relationships which were used for some of the component elements.

The development of the linear model allowed a comparison to be made between two of the most popular linear matrix solving techniques, the Gauss-Jordan and the LU decomposition methods. It was concluded that the LU decomposition method was the most suitable technique for use in both the linear and non-linear models. It was shown to be twice as fast as the Gauss-Jordan method and achieved higher accuracies for the calculation of the sum of flows through the dividing nodes.

- ii,    The objective of constructing a more comprehensive flow model was approached during the second phase, with the development of the non-linear flow program. Each component element in the system was represented by its true pressure loss v flow rate relationship. As this relationship was sometimes of a non-linear nature, the program solved for the unknowns with an iterative technique using the Levenberg-Marquardt routine. Although the run times for the non-linear flow program were almost three times greater than the LU decomposition



linear program, the results matched exactly those produced by the linear solution method. It was concluded that program flexibility and accuracy of results had a higher priority than program run times. Consequently, program development concentrated on the non-linear flow program.

The physical system was represented in both flow models by being broken down into a series of component flow elements, comprising of either, pumps, pipes, annular pipes, filters, strainers, oil coolers, journal bearings, crank-shaft transfer holes, or cam bearing transfer holes. Any lubrication system configuration, which can be broken down into these component elements, can be simulated. However, the final fully-developed non-linear flow model inherited some of the programming constraints which were imposed on the earlier linear programs. These constraints prevented lubrication systems with converging flow paths to be modelled. Although this restricted the overall flexibility of the program, no problems were encountered when modelling the full AJ6 and V8 engine lubrication systems and no problems can be foreseen with the modelling of Jaguar engines in the visible future.

The second objective of this study was to develop a model of the heat transfer to the oil within the engine. This objective was again achieved in two phases:

- i, The heat transfer characteristics of the pressurised part of the lubrication system were analyzed during the first phase. This led to the development of the 'heat transfer program', which simulated the heat transfer to the oil within the lubrication system, previously modelled in the non-linear flow program. This was achieved with the completion of the heat transfer program. The heat transfer program required, as input, the wall temperature for each pipe element (circular pipe,

annular pipe, or transfer hole). As the pipe elements had relatively small surface areas, compared to the cross-sectional area of the engine block, the wall temperatures were assumed to remain constant throughout the calculation procedure. The wall temperatures were estimated from predicted block temperature results from the engine block program. However, the heat transfer program retained the capability to allow the user to use his experience and judgement in the selection of suitable wall temperature values. This gave the design package a larger degree of flexibility, and allowed a rapid thermal analysis of the lubrication system to be undertaken, without the need to model the engine geometry.

- ii, The heat transfer to the oil splashed on to the internal surfaces of the engine was approached during the second phase. The oil splashed onto each wetted surface was simplified to a falling film of oil. Due to the relatively large surface areas in question, the wall surface temperature was not considered to remain constant. Thus, the block and oil film temperatures were required to be calculated simultaneously. This objective was satisfied with the development of the engine block program. In addition to providing a method of calculating the oil film temperatures and the temperature of the oil in the sump, the engine block program returned the metal temperatures throughout the engine block. These temperatures were used to make more refined estimates of the wall temperatures for the various pipe elements, which were returned to the heat transfer program.

The third objective of the study was to validate the thermofluid model with measured results from engine tests. This objective was essentially satisfied with the test bed measurements of the Jaguar AJ6 and V8 engine



lubrication systems. Results from the V8 engine tests showed that the predicted pressures were within 7% of the measured values and the predicted flow rates were within 4% of the measured values. The predicted oil temperatures were found to be within 3% of the measured values in the main oil gallery and the feeds to the main bearings. However, the predicted values were found to fall to within 4 to 14% of the measured values in the pipes and drillings which fed oil to the cam bearings and tappets in the engine head. This small discrepancy was attributed to an error in the prediction of the block temperatures within the engine head. This was a result of an oversimplification of the model of the engine head geometry, used in the engine block program.

Unfortunately, there was no measured data available for the validation of the predicted engine block temperature results from the engine block program. However, the predicted results were compared to results from an FEA model of the V8 engine. The block temperatures compared very favourably in the regions wetted by the oil splash, but temperature discrepancies were highlighted in the region around the head. It was concluded that the block element arrangement and subsequent nodal resistance network, derived to represent the cross-section through the engine block, was over-simplified. The block element arrangement neglected the bridges between the head and the outer wall of the water jacket. This led to high predicted block temperatures in the head exposed to the combustion gasses and low temperatures in the part of the head where the oil galleries feeding the cam bearings and tappets were located. This was responsible for the discrepancies in the oil temperatures in these oil galleries.

The lubrication system of the Jaguar AJ6 engine was used throughout the development stages of the flow model. The lessons which were learned

during the early stages of modelling the AJ6 engine lubrication system proved invaluable for the accurate simulation of the V8 engine system. The principle conclusions drawn from the modelling work are as follows:

- i, Accurate oil pump performance data was essential for the realistic simulation of existing engine lubrication systems. The pressure losses through the entire lubrication system balanced themselves against the pressure v flow rate relationship of the oil pump. Therefore, representative pump characteristics are essential if the predicted pressures and flow rates through a system are to compare to measured values from engine tests. However, The model retains the capability to use theoretical pump characteristics to provide an insight into the flow behaviour of a prototype system at the design stages.
- ii, The oil flow rate through the oil fed chain tensioners was found to be much greater than expected. The AJ6 engine tests showed that 20% of the oil flow to the head passed through the chain tensioner. An accurate model of the flow characteristics through an oil fed chain tensioner was essential for the simulation of lubrication systems which contained these devices.

The discovery of the high flow rate through the chain tensioners opens the question of why these components are designed in this way. It is understood that some of the oil may be required to lubricate the timing chains, but the degree of oil ejected from the chain tensioners appears to be far in excess of the required amount. In addition, the design of the chain tensioner assembly in the AJ6 engine actually prevents the majority of the oil coming into contact with the chain any way.



- iii, The pressure drop through a turbine flow meter had to be accounted for, to accurately simulate the flow conditions through a lubrication system which had been instrumented to measure the flow rate within the oil passages. The flow meters incorporated in the lubrication systems of the AJ6 and V8 test engines were represented by a turbulent pipe section. This provided a predicted pressure drop through the flow meter which was in close agreement with the measured value.
- iv, It was found that in any lubrication system model, there were two principal component elements which were responsible for the control of the pressure and flow rate through the whole system. The first of these key components was the oil pump, which was discussed in part i above, and the second was the journal bearings which were commonly found at the end of each flow branch in the system. An accurate model of the flow conditions through the journal bearings was essential for the simulation of the lubrication system.

The predicted flow rates through the main and big-end bearings of the AJ6 engine, modelled with the manufacturers nominal clearances, compared very favourably with the values provided by Glacier Vandervell. This gave a high degree of confidence in the accuracy of the pressure loss v flow rate equations which represented the flow characteristics of the journal bearings. However, the bearing clearances of a hot running engine were found to be significantly larger than the clearances measured at ambient temperature. The 'hot' bearing clearances were estimated from a simple calculation of the free linear expansion of the bearing. Such estimates were essential for the accurate representation of the flow conditions within the engines journal bearings.

- v, It was concluded that the oil feed pressure had an effect on the eccentricity of the engine bearings and tappets. This highlighted the requirement to estimate the feed pressure to each bearing and account for the effect of the feed pressure in the selection of the eccentricity ratios when modelling the bearings.

To achieve the objective of providing a design analysis tool, the FORTRAN programs were structured for ease of use. The programs were written to be used by a design engineer with some knowledge of the lubrication system, but with no specialised knowledge of computer programming. It was acknowledged that the user would be a busy design engineer who required a fast, stable, easy to use simulation tool. As such, the user is guided through the programs with clear instructions and prompts. The programs incorporate many safety catches to eliminate the risk of the incorrect data being input by mistake and causing the program to 'crash'.

The development of the echo file, which records all the data input by the user, was found to be of great value. The echo file allowed the user to exit from the program at any stage, change a past mistake in the data, and return to the point in the program where it had been previously terminated. The echo file system also allowed a system which had been previously modelled, to be re-run with small changes in the operating conditions. This provided a rapid means of conducting parametric studies on a lubrication system.

In summary, the main objectives of the study were achieved. The lubrication system simulation package represents a user friendly and flexible design analysis tool. This is a unique self-contained simulation package which contains three individual programs which can rapidly predict the oil flow and temperature conditions within almost any lubrication system configuration.



Although other researchers have attempted to simulate a lubrication system with a flow analysis approach in the past (eg. Trapy and Damiral (1990)), or made a detailed investigation of the heat transfer conditions within an engine block (eg. Veshagh and Chen (1993)), no attempt has been made in the past to integrate the flow analysis, heat transfer analysis of the oil and the heat transfer within the whole engine block in a single simulation package.

The flow program and the heat transfer program provide a means of carrying out a detailed analysis of the pressurised side of any lubrication system configuration. The engine block program provides a rapid method of predicting the block temperatures within the engine. The predicted metal temperatures can be used as input data for the heat transfer program, but in addition, the engine block program provides a means of analyzing the heat transfer to the oil splashed on to the internal surfaces of the engine. No evidence was found that this had been attempted by any other researcher in the past.

The highly detailed FEA model of the V8 engine contained approximately 75,000 elements for the block and pistons alone, ignoring the elements used to represent the engine heads and bedplate. It took approximately six months between the commission of the work and the delivery of results. In comparison, the V8 engine geometry was represented in the engine block program by 58 block elements, which in turn, were represented by a nodal resistance network containing 274 thermal resistances. It took approximately one day to construct the model of the V8 engine and obtain an estimate of the temperature profile through the block. This comparison shows that the engine block program provides a simple and rapid means of modelling any engine geometry, for the prediction of the temperature trends through the block.

The simulation package remains a steady-state design analysis tool. The final objective of the study was to evaluate the feasibility of extending the model into a transient model for the simulation of engine warm-up. No attempt was made to begin the development of such a transient design analysis tool. However, it is considered that the steady-state model forms an excellent nucleus for the development of a full transient model. By linking the three analysis programs together, to run with a single command, the flow and temperature characteristics of the lubrication system could be analyzed with a quasi-steady approach at discrete time intervals. Such an approach would allow the analysis of an engine lubrication system under cold start and engine warm-up conditions. For example, the transient model could be used to conduct parametric studies of the lubrication system and engine block design for the optimisation of the oil warm-up, or for the calculation of minimum oil requirements. This work would form an excellent additional study and remains one of the suggestions for future work.

## 10.2 Suggestions for Future Work

Due to the complex nature of the study, the investigation covered many different fields of expertise. The relevant knowledge from each field was extracted and drawn together to form a single package. It was inevitable with such a study, that some assumptions and simplifications were found to be necessary and these were documented in the dissertation. The study revealed areas which would be suitable for further investigation, either as an enhancement to the existing design analysis package, or as a separate study. This section suggests the areas which emerged from the study which would be suitable for further work. The suggestions are listed in the order of complexity of the task.



- i, The flexibility of the flow program can be enhanced by allowing systems which contain both converging as well as diverging nodes to be modelled. This would be achieved by changing the method that the layout of the physical system is represented and stored. This could be achieved by simply changing the present one-dimensional arrays which represent the layout of the system with two-dimensional arrays.
- ii, The measured oil pump characteristic curve was represented by a linear piece-wise approach. The accuracy of the model depended on the number of linear elements were used to represent the curve, a large number of sections resulted in the best representation of the curve. However, the disadvantage of using a large number of linear sections was that the program run-time increased. A further investigation should be carried out to find a method of representing the curve through the measured data points but without a detrimental effect on the program run-time. The ideal solution would be to represent the performance curve with a single equation.
- iii, The tappets of the V8 engine were modelled as non-grooved journal bearings. Although this method resulted in reasonably accurate oil flow rate results, it was considered that the development of a dedicated tappet model would be of benefit to both the flow and heat transfer programs. This would eliminate the present requirement of simulating the tappet working conditions by estimating an equivalent operating condition for a journal bearing. A dedicated tappet model would allow parametric studies of the tappet design to be undertaken.
- iv, The investigation of the lubrication system of the V8 engine head revealed that the oil feed pressure had an effect on the eccentricity of

the cam bearings and tappets. To accurately predict the oil flow rates through the cam bearings and tappets, it was found that careful consideration had to be made of the oil feed pressure in the selection of suitable eccentricity ratios. A more detailed study of the effects of oil feed pressure would be worthwhile. The investigation would analyze the feasibility of developing the flow program to automatically calculate the change in the eccentricity ratios at different oil feed pressures.

- v, To predict accurate oil pressures and flow rates through an instrumented lubrication system, it was found that the pressure loss through the turbine flow meters had to be accounted for. In the models of the instrumented Jaguar AJ6 and V8 engine lubrication systems, each turbine flow meter was represented as a turbulent pipe section. The dimensions of the pipe section were obtained by a trial and error procedure until the predicted pressure loss matched the measured value. The flow program can be enhanced with the development of a dedicated model of a turbine flow meter. To cover the possibly large range of different flow meter designs and sizes, the pressure drop through the meter could be accounted for by using measured pressure loss v flow rate relationships.
- vi, It has been shown that the flow rate through a journal bearing is very sensitive to the bearings radial clearance. A major consideration in the modelling of any lubrication system is the effect of thermal expansion within the bearing on the bearings radial clearance. A suitable extension to the present research work is a thermal analysis of an operating journal bearing. A method needs to be developed for predicting the hot radial clearance of any journal bearing. This could be carried out as a separate calculation from the main program, or ideally, be incorporated



within the program. A possible solution is to obtain measured data from a series of rig tests and use this empirical data within the thermofluid model.

- vii, Due to time constraints, the models of the heat transfer to the air and coolant were not incorporated in the engine block program as desired. The program retained the capability of accounting for heat transfer to the air and coolant, but relied on the user to supply the bulk temperature and heat transfer film coefficient. This method maintained a high degree of flexibility in the program, as the heat transfer conditions can easily vary from surface to surface as the local velocity of the fluid changes. However, it is advantageous if the calculation of the heat transfer coefficient from each surface exposed to the air or the coolant were incorporated. This would improve modelling speed and reduce the design cycle time. The program flexibility can be enhanced by giving the user the option of either stating the heat transfer conditions for each surface or having them calculated within the program.
- viii, The heat transfer to the combustion gasses is presently accounted for in the engine block program by the user selecting a suitable cycle averaged gas temperature and heat transfer film coefficient. This process can be enhanced by integrating an existing cycle simulation program (eg. Chen (1990)) with the engine block program and automatically calculating the cycle averaged temperature and heat transfer coefficient values.
- ix, The results from the engine block program were found to compare favourably with the results from an FEA study of the V8 engine block. However, measured data is still required for the true validation of the

predicted results. A series of tests is required on the V8 engine to measure the temperature distribution throughout the engine block, head and liner, under a range of operating speeds and loads.

- x, The literature search revealed that little research has been carried out into the heat transfer between the engine internal surfaces and the oil splash. This heat transfer route was accounted for in the engine block program by simplifying the oil splash to a falling film of oil. This method proved to work very satisfactorily and produced oil sump temperature results which were in close agreement with measured values. However, considering the little available knowledge in this field, a further detailed examination of the heat transfer through oil splash would be an interesting and rewarding additional study. A greater understanding of this heat transfer route will be of benefit to engine designers in obtaining the optimum heat transfer capabilities of the lubricating oil. This would lead to optimised engine geometry design, in respect to engine thermal management, especially under cold start and warm-up operating conditions.
- xi, The present analysis package is a steady-state simulation tool. The package contains three separate analysis programs which although linked by common data files, are initiated and run separately by the user. This gives the user the flexibility of running any one of the programs as frequently as desired, for conducting parametric studies on any particular flow or heat transfer element. If the package is developed further to analyze transient response it will be beneficial to give the user the option of running all three programs from a single command. It will be necessary to link all three programs so that the data files are passed between them and the programs are run in the correct order and



for the correct number of loops. Having modelled the lubrication system layout and the geometry of the engine block on the first pass, the analysis package will have to run automatically on subsequent passes, using an echo file as a user input device. A method will have to be found to link the metal temperature results from the engine block program with the required wall temperature values for the heat transfer program.

- xii, If the programs are linked together, as described in section xi above, the analysis capabilities can be enhanced by incorporating a method of automatically analyzing a lubrication system over a range of engine speeds. The program could generate a Postscript file which can be printed out to present the pressure, flow rate and temperature distribution throughout the lubrication system in a graphical manner.
- xiii, Although the programs were written to be user friendly, the human user interface was restricted to the presentation available with FORTRAN. A beneficial additional study would be to investigate methods of enhancing the user interface. A possible solution would be to form and graphically display the layout of the lubrication system and the engine block geometry on the screen. In addition, the whole program could be menu driven, possibly using software such as MATLAB, which would allow the input data to be viewed and/or changed more rapidly. However, the greatest priority in such an investigation is to maintain the transportability of the program. The benefit of using FORTRAN as a programming language is that the software is widely distributed and very common in industry. A similar consideration would have to be made if additional software were used for the improvement of the user interface.

The above suggestions represent methods of enhancing and developing the lubrication system analysis package. The majority of the suggestions identify aspects of the existing analysis package which can be improved, usually through the development of dedicated component models or the automation of the calculation of operating conditions. However, some of the above suggestions identify areas which call for extensive additional investigations. For example, the development of graphical user interface, the study of the thermal aspects of a bearing, or the linking of the individual programs to form a single command initiated package, will form excellent MSc research projects. The study of the heat transfer to the oil splashed onto the internal surfaces of the engine could form a separate detailed long term project, possibly being undertaken as a new PhD study.



## References

- Alcock, J.F.** (1962), 'Heat Transfer in Diesel Engines,' Proc. Int. Heat Transfer Conf., Boulder, IMechE., Vol. 174.
- Andre, M.** (1989), 'Experimental Study on the Uses of Cars (EUREV),' SAE paper 890874.
- Andrews, G.E., J.R. Harris., and A. Ouzain.** (1989), 'SI Engine Warm-Up. Water and Lubricating Oil Temperature Influences,' SAE paper 892103.
- Annand, W.J.D.** (1953), 'The Resistance to Air Flow of Wire Gauzes,' J. Roy. Aeronaut. Soc., Vol. 57, p 141-5.
- Annand, W.J.D.** (1963), 'Heat Transfer in the Cylinders of Reciprocating Internal Combustion Engines,' Proc. IMechE., Vol. 177, p 973.
- Annand, W.J.D., and T.H. Ma.** (1971), 'Instantaneous Heat Transfer Rates to the Cylinder Head Surfaces of a Small Compression Ignition Engine,' Proc. IMechE., Vol 185, p 936.
- Barraclough, S.** (1991), 'Jaguar Report: V8 Engine Cycle Data Generated by the NEL Simulation Model for the adapco Thermal Analysis Survey,' Report No. AE691001, 16 January.
- Bearing Design Manual*, Technical Documentation, Vandervell Products Ltd., Annex 05.11.01, July 1977, Section 2.
- Bingham, J.F.** (1987), 'Intake System Design Using a Validated IC Engine Computer Model,' Proc. IMechE. Conf. on Computers in Engine Technology.
- Booker, J.F.** (1965), 'Dynamically Loaded Journal Bearings: Mobility Method of Solution,' Trans. ASME, J. Basic Eng., Vol. 187, p 537-546.
- Booker, J.F.** (1971), 'Dynamically-Loaded Journal Bearings: Numerical Application of the Mobility Method,' Trans. ASME, J. Lub. Tech., Vol. 93, January, p 168. (Also Errata: April 1971, p 315, - referring to H. Moes).
- Booker, J.F., P.K. Goenka., and H.L. Van Leeuwen.** (1982), 'Dynamic Analysis of Rocking Journal Bearings with Multiple Offset Segments,' J. Lub. Tech., Trans. ASME, Vol. 104, p 478-480.
- Borgnakke, C., V.S. Aparci, and R.J. Tabaczynski.** (1980), 'A Model for the Instantaneous Heat Transfer and Turbulence in a Spark Ignition

Engine,' SAE paper 800287.

**Bush, I.F.** (1980), 'AJ6 Oil Pump Performance,' Engineering Experimental Dept. Jaguar Cars, 6th June, Report No. Ed 2590/IFB.

**Bush, J.E., and A.L. London.** (1965), 'Design Data for "Cocktail Shaker" Cooled Pistons and Valves,' SAE paper 650727.

**Cameron, A.** (1981), *Basic Lubrication Theory. Third Edition*, Ellis Horwood.

**Campbell, J., P.P. Love, F.A. Martin, and S.O. Ratique.** (1967), 'Bearings for Reciprocating Machinery: A Review of the Present State of Theoretical, Experimental and Service Knowledge,' Proc. IMechE., Vol. 182, No. 3A, p 51.

**Chang, C.C., T.S. KU, J. Mannisto, and P.S. MacDonald.** (1992), 'Jaguar V8 Engine Cylinder Block Thermal Analysis Summary Report,' adapco Analysis and Design Application Co. Ltd. Report No. 68-04-008, 13 November.

**Chapman, A.J.** (1987), *Fundamentals of Heat Transfer*, Macmillan.

**Chapra, S.C., and R.P. Canale.** (1985), *Numerical Methods for Engineers*, McGraw-Hill Book Co.

**Chen, C.** (1990), 'SCIENS (Spark/Compression Ignition Engine Simulation) User Manual,' A.T.C. Technical Notes, University of Warwick.

**Chen, C., and A. Veshagh.** (1992), 'A One-Dimensional Model for In-Cylinder Heat Convection Based on the Boundary Layer Theory,' SAE paper 921733.

**Chen, J.C.** (1966), 'A Correlation for Boiling Heat Transfer to Saturated Fluids in Convective Flow,' Ind. and Engng. Chem., Process Design and Development, Vol. 5, p 322.

**Chiang, E.C., J.H. Johnson, and Z. Xu.** (1984), 'A Simulation Study of a Computer Controlled Cooling System for a Diesel Powered Truck,' SAE paper 841711.

**Chiang, E.C., V.J. Ursini, and J.H. Johnson.** (1982<sub>a</sub>), 'Development and Evaluation of a Diesel Powered Truck Cooling System, Computer Simulation Program,' SAE paper 821048.



- Chiang, E.C., V.J. Ursini, and J.H. Johnson.** (1982), 'A Computer Cooling System Study of a Diesel Powered Truck for Control of Transient Coolant, Oil and Cab Temperatures,' SAE paper 821049.
- Cinque, A.A., and H.C. Sheridan.** (1968), 'Sizing Piping Networks for Incompressible Flow With a Digital Computer,' J. of Engineering for Industry, ASME, February.
- Colebrook, C.F.** (1939), 'Turbulent Flow in Pipes, with Particular Reference to the Transient Region Between the Smooth and Rough Pipe Laws,' J. Inst. Civil Engrs. (London), February.
- Conway-Jones, J.M., F.A. Martin, and R. Gojon.** (1990), 'Refinement of Engine Bearing Design Techniques,' T&N Handbook, Paper No. 1.
- Cornforth, J.W.** (1985), 'Finite Element Analysis of Engines,' Materials and Design, Vol. 5, No. 6, December/January.
- Couëtouse, H., and D. Gentile.** (1992), 'Cooling System Control in Automotive Engines,' SAE paper 920788.
- Das, P.K., and S.B. Dancer.** (1982), 'An Analysis of Flow and Friction in Diesel Engine Bearings,' ASME paper 82-DGEP-7.
- de Vahl Davis, G.** (1964), 'The Flow of Air Through Wire Screens,' Proc. First Australasian Conference on Hydraulics and Fluid Mechanics, p 191-212.
- Dittus, F.W., and L.M.K. Boelter.** (1930), Univ. Calif. Berkeley. Publ. Eng. Vol. 2, p 443.
- Dukler, A.E., and O.P. Bergelin.** (1952), Chem. Eng. Progress, Vol. 48, p 557.
- Eccleston, B.H., and R.W. Hurn.** (1978), 'Ambient Temperatures and Trip Length. Influences on Automotive Fuel Economy and Emissions,' SAE paper 780613.
- Eichelberg, G.** (1923), 'Temperaturverlauf und Wärmespannung in Verbrennungsmotoren,' Forsch. Ing. Wes. p 263.
- Ellinas, A.** (1988), 'A Fundamental Computer Simulation Model of Heat Transfer Processes in the Lubrication System of an Automotive Engine,' MSc Thesis, University of Warwick.

Exxon Publication: *Tables of Useful Information*, Publication No. DG-400.

Fenton, J. (1984), 'Design of Engine Lubrication Systems,' *Automotive Engineer*, Feb/Mar, p 24.

Finley, I.C. (1991), 'Alternative Fuels for Road Transport,' Course Notes, IDGS Thermal Systems Design Lecture, University of Warwick, 30th September.

Finley, I.C., R.J. Boyle, J.P. Pirault, and T. Biddulph. (1987), 'Nucleate and Film Boiling of Engine Coolants Flowing in a Uniformly Heated Duct of Small Cross Section,' SAE paper 870032.

Flynn, G., and A.F. Underwood. (1945), 'Adequate Piston Cooling - Oil Cooling as a Means of Piston Temperature Control,' SAE J. Trans. Vol. 53, No. 2, February.

Haddock, A.K. (1991), 'Computer Analysis of the Engine Lubricating System,' Proc. IMechE., Presented at Autotech 91, C427/7/062.

Hayashi. H. (1969), 'Heat Dissipating Capacity of Automotive IC Engine Lubricating Oil System,' SAE paper 690470.

Heywood, J.B. (1989), *Internal Combustion Engine Fundamentals*. McGraw-Hill Book Co.

Hirano, F., and N. Shodai. (1958), 'Oil Flow Coefficient of Pressure Fed Journal Bearing,' Bull. JSME., Vol. 1, No. 2, p 184-188.

Hovin, L.E., E.C. Chiang, and J.H. Johnson. (1988), 'Design and Computer Simulation of Microprocessor Controlled Lubricating Oil Cooling System for Truck Diesel Engine,' SAE paper 880488.

Huebner, K.H. (1975), 'A Simplified Approach to Flow Network Analysis: Application to Engine Lubrication Systems,' SAE paper 750080.

Jakob, M. (1963), *Heat Transfer. Volume II*, John Wiley and Sons Inc.

Jaisinghani, R.A., and G.S. Sprenger. (1981), 'Resistance to Flow of Liquids in Fibrous Beds, Applied to Cartridge Filtration,' *Filtration and Separation*, March/April.

Jennings, M.J., and T. Morel. (1990), 'An Improved Near Wall Heat Transfer Model for Multi-Dimensional Engine Flow Calculations,' SAE paper 900251.



**Johren, P.W., and B.A. Newman.** (1988), 'Evaluating the Oil Consumption Behaviour of Reciprocating Engines in Transient Operation,' SAE paper 880098.

**Jones, G.J., C.S. Lee, and F.A. Martin.** (1982), 'Crankshaft Bearings: Advances in Predictive Techniques Incorporating the Effects of Oil Holes and Grooving,' AE Symposium, April, Paper No. 1.

**Kaplan, J.A., and J.B. Heywood.** (1991), 'Modelling the Spark Ignition Engine Warm-Up Process to Predict Component Temperatures and Hydrocarbon Emissions,' SAE paper 910302.

**Kays, W.M.** (1989), 'Heat Transmission from the Engine to the Atmosphere,' Heat and Mass Transfer in Gasoline and Diesel Engines, Proc. of the Int. Centre for Heat and Mass Transfer, p 333.

**Kays, W.M., and A.L. London.** (1964), *Compact Heat Exchangers, Second Edition*, McGraw-Hill Book Co, New York.

**Kluck, C.E., and P.W. Olsen.** (1986), 'Lubrication System Design Considerations for Heavy-Duty Diesel Engines,' SAE paper 861224.

**Kyto, M.** (1989), 'Engine Lubrication in Cold Start-Up,' SAE paper 890033.

**Lai, C.K.K.** (1993), 'A Study of Partial Central Circumferential Groove Engine Bearings,' PhD Thesis, University of Leeds.

**Li, D.F., S.M. Rohde, and H.A. Ezzat.** (1982), 'An Automotive Lubrication Model,' ASLE Preprint No. 82-AM-2E-3.

**Lo, R.S.** (1971), 'Digital Simulation of Engine Lubrication Systems,' SAE paper 710205.

**Maeda, Y., T. Inoue, M. Nakada, and Y. Hamada.** (1986), 'Investigation of the Transient Oil Consumption of Engine by the Newly Developed Oil Consumption Meter,' SAE paper 860544.

**Manganielle, E.J., and D. Bogart.** (1945), 'Piston Heat Transfer Coefficient Across an Oil Film in a Smooth-Walled Piston Reciprocating-Sleeve Apparatus,' NACA A.R.Report No. ESK08.

**Martin, F.A.** (1983), 'Feed Pressure Flow in Plain Journal Bearings,' Technical Note, Tribology International, April, Vol. 16, No. 2, p 64-65.

**Martin, F.A.** (1985), 'Friction in Internal Combustion Engine Bearings,'

Proc. Inst. Mech. Engrs. Conf. on Reduction of Friction and Wear in Combustion Engines, paper C67/85, p 1-17.

**Martin, F.A., and C.S. Lee.** (1982), 'Feed-Pressure Flow in Plain Journal Bearings,' Trans. ASLE, Vol. 26, No. 3, p 381-392.

**Martin, F.A., P.M. Lo, and J.F. Booker.** (1987), 'Power Loss in Connecting Rod Bearings,' IMechE. Conference on Tribology Friction and Wear, London, July, Paper C167.

**Marquardt, D.W.** (1963), J. Soc. Ind. Appl. Math., Vol. 11, p 431-441.

**McAdams, W.H.** (1954), *Heat Transmission, 3rd Edition*, McGraw-Hill Book Co, New York.

**Meernik, P.R.** (1986), 'Lubricant Flow to Connecting Rod Bearings Through a Rotating Crankshaft,' SAE paper 860229.

**Metais, B., and E.R.G. Eckert.** (1964), 'Forced, Mixed, and Free Convection Regimes,' J. Heat Transfer, Vol. 86, p 295.

**Miller, D.S.** (1990), *Internal Flow Systems. Second Edition*, BHRA.

**Naber, J.D., and P.V. Farrell.** (1993), 'Hydrodynamics of Droplet Impingement on a Heated Surface,' SAE paper 930919.

**Neu, E.A., J.A. Wade, and A.C. Chu.** (1977), 'Simulating the Lubrication System of a Diesel Engine,' SAE paper 770032.

**Ninoyu, M., J. Kameyama, H. Doi, and H. Oka.** (1993), 'Prediction Method of Cooling System Performance,' SAE paper 930146.

**Nostrand, W.G.** (1975), 'Engine Lubrication Oil Filtration: A Paradox of Variable Constants,' SAE paper 740518.

**Nusselt, W.** (1923<sub>a</sub>), Z. Ver. Dtsch. Ing. Vol. 67, p 206.

**Nusselt, W.** (1923<sub>b</sub>), 'Die Wärmeübergang in den Verbrennungskraftmaschinen,' Z. Ver. Dtsch. Ing., Vol. 67, p 692-708.

**Nusselt, W.** (1931), 'Der Wärmeaustausch zwischen Wand und Wasser im Rohr,' Forsch Geb. Ingenieurwes. Vol. 2, p 309.

**Pachernegg, S.J.** (1971), 'The Hydraulics of Oil Scraping,' SAE paper 710816.



**Pais, M.R., L.C. Chow, and E.T. Mahefkey.** (1992), 'Surface Roughness and its Effects on the Heat Transfer Mechanism in Spray Cooling,' Trans. ASME, J. of Heat Transfer, Vol. 114, p 211, February.

**Parker, D.A.** (1989), 'The Tribology of Automotive Components: Development of Verified Predictive Design Techniques,' Fourth BP/IMechE Tribology Lecture, Autotech 89.

**Patton, K.J., R.G. Nitschke, and J.B. Heywood.** (1989), 'Development and Evaluation of a Performance and Efficiency Model for Spark-Ignited Engines,' SAE paper 890836.

**Petukhov, B.S.** (1970), 'Heat Transfer and Friction in Turbulent Pipe Flow with Variable Physical Properties,' Advances in Heat Transfer, Vol. 6, New York Academic Press, p 504.

**Poulos, S.G.** (1982), 'The Effect of Combustion Chamber Geometry on SI Engine Combustion Rates - A Modelling Study,' S.M. Thesis, Massachusetts Institute of Technology.

**Poulos, S.G., and J.B. Heywood.** (1980), 'The Effect of Chamber Geometry on Spark Ignition Engine Combustion,' SAE paper 800457.

**Press, W.H., B.P. Flannery, S.A. Teukolsky, and W.T. Vetterling.** (1990), *Numerical Recipes, The Art of Scientific Computing (Fortran Version)*. Cambridge University Press.

**Quayle, J.P.** (1987), *Kempe's Engineers Year-Book 1987*, 92nd Edition, Morgan-Grampian Book Publishing Co. Ltd.

**Rao, V.K., and M.F. Bardon.** (1985), 'Convective Heat Transfer in Reciprocating Engines,' Proc. IMechE., Vol. 199. No. D3.

**Rosenbrock, H.H.** (1960), 'An Automatic Method for Finding the Greatest or Least Value of a Function,' Computer J., Vol. 3, No. 3.

**Saito, K., T. Igashira, and M. Nakada.** (1989), 'Analysis of Oil Consumption by Observing Oil Behaviour Around Piston Ring Using a Glass Cylinder Engine,' SAE paper 892107.

**Seale, W.J., and D.H.C. Taylor.** (1970), 'Spatial Variation of Heat Transfer to Pistons and Liners of Some Medium Speed Diesel Engines,' Proc. Inst. Mech. Engrs. Vol. 185, p 203.

**Seth. B.B., and N.L. Field.** (1984), 'Oil Pressure Signatures for Engine

Lubrication System Monitoring,' SAE paper 840063.

**Sieder, E.N., and E.G. Tate.** (1936), 'Heat Transfer and Pressure Drop of Liquids in Tubes,' Ind. Eng. Chem., Vol. 28, p 1429.

**Sitkei, G.** (1962), 'Beitrag zur Theorie des Wärmeübergangs im Motor,' Konstruktion, Vol. 15, p 67.

**Shayler, P.J., S.J. Christian, and T. Ma.** (1993), 'A Model for the Investigation of Temperature, Heat Flow and Friction Characteristics During Engine Warm-Up,' SAE paper 931153.

**Smith, R.D.R.** (1990), 'Plotting and Handling Bearing Tribology Data,' Jaguar Internal Report.

'Steady-State Flow Analysis (SSFAN) Computer Program Technical Description,' Wright-Patterson Aeronautical Laboratories AFAPL-TR-76-43, Vol. 6, April 1980.

**Stotter, A.** (1966), 'Heat Transfer in Piston Cooling,' SAE paper 660757.

**Swamee, P.K., and A.K. Jain.** (1976), 'Explicit Equations for Pipe-Flow Problems,' Proc. ASCE, J. Hydraul. Div., Vol. 102 (HY5), May, p 657-664.

**Taylor, C.F., and Tau-Yi Toong.** (1957), 'Heat Transfer in Internal Combustion Engines,' ASME paper 57-HT-17.

**Tenkel, F.G.** (1974), 'Computer Simulation of Automotive Cooling Systems,' SAE paper 740087.

**Tio, K.K., and S.S. Sadhal.** (1992), 'Thermal Analysis of Droplet Spray Evaporation from a Heated Solid Surface,' Trans. ASME, J. of Heat Transfer, Vol. 114, p 220, February.

**Tran, P., T. Yamamoto, Y. Baba, and M. Hoshi.** (1987), 'An Analysis of Lubricating System of Automobile Gasoline Engine,' SAE paper 871659.

**Trapy, J.D., and P. Damiral.** (1990), 'An Investigation of Lubricating System Warm-Up for the Improvement of Cold Start Efficiency and Emissions of SI Automotive Engines,' SAE paper 902089.

**Veshagh, A., and C. Chen.** (1993), 'A Computer Model for Thermofluid Analysis of Engine Warm-Up Process,' SAE paper 931156.

**Veshagh, A., and R. Moffatt.** (1992), 'Computer Aided Analysis of Heat



Flows in Vehicle Cooling Systems,' SAE paper 920010.

**Wong, V.W., and D.P. Hoult.** (1991), 'Experimental Survey of Lubricant-Film Characteristics and Oil Consumption in a Small Diesel Engine,' SAE paper 910741.

**Woschni, G.** (1967), 'Universally Applicable Equation for the Instantaneous Heat Transfer Coefficient in the Internal Combustion Engine,' SAE paper 670931.

**Yang, J., and J.K. Martin.** (1989), 'Approximate Solution - One-Dimensional Energy Equation for Transient, Compressible, Low Mach Number Turbulent Boundary Layer Flows,' Trans. ASME. J. of Heat Transfer, Vol. 111.

## Bibliography

**Benedict, R.P.** (1980), *Fundamentals of Pipe Flow*, John Wiley and Sons.

**Carnahan, B., H.A. Luther, and J.O. Wilkes.** (1969), *Applied Numerical Methods*, John Wiley and Sons.

**Chapman, A.J.** (1967), *Heat Transfer. Second Edition*, Macmillan Publishing Co.

**Chapman, A.J.** (1987), *Fundamentals of Heat Transfer*, Macmillan Publishing Co.

**Chapra, S.C., and R.P. Canale.** (1985), *Numerical Methods for Engineers*, McGraw-Hill Book Co.

**Etter, D.M.** (1987), *Structured Fortran 77 for Engineers and Scientists. Second Edition*, Benjamin/Cummins.

**Holman, J.P.** (1986), *Heat Transfer. Sixth Edition*, McGraw-Hill Book Co.

**Jakob, M.** (1963), *Heat Transfer. Volume II*, John Wiley and Sons.

**LaFara, R.** (1973), *Computer Methods for Science and Engineering*, International Textbook Co. Ltd.

**Press, W.H., B.P. Flannery, S.A. Teukolsky, and W.T. Vetterling.** (1989), *Numerical Recipes, The art of Scientific Computing (FORTRAN version)*, Cambridge University Press.

**Shoup, T.E.** (1984), *Applied Numerical Methods for the Micro-Computer*, Prentice Hall.

**Stoecker, W.F.** (1989), *Design of Thermal Systems. Third Edition*, McGraw-Hill.

**Ward-Smith, A.J.** (1980), *Internal Fluid Flow*, Oxford University Press.



## **Appendix A**

### **Numerical Solution Methods**

## A.1 Linear Modelling

A linear equation is one whose dependent variable,  $b_i$ , is dependent on a linear relationship of the unknowns,  $x_i$ . The unknowns exist in the first order, in multiplicative combination only with constants,  $a_i$ , and in additive combination only with similar terms or constants. A general form for a set of linear equations is:

$$\begin{aligned}
 a_{11}x_1 + a_{12}x_2 + a_{13}x_3 + \dots + a_{1N}x_N &= b_1 & (a) \\
 a_{21}x_1 + a_{22}x_2 + a_{23}x_3 + \dots + a_{2N}x_N &= b_2 & (b) \\
 &\dots & \\
 a_{M1}x_1 + a_{M2}x_2 + a_{M3}x_3 + \dots + a_{MN}x_N &= b_M & (c)
 \end{aligned}
 \tag{A.1}$$

Or in matrix form:

$$A = \begin{bmatrix} a_{11} & a_{12} & a_{13} & \dots & a_{1N} \\ a_{21} & a_{22} & a_{23} & \dots & a_{2N} \\ & & & \dots & \\ a_{M1} & a_{M2} & a_{M3} & \dots & a_{MN} \end{bmatrix} \quad x = \begin{bmatrix} x_1 \\ x_2 \\ \dots \\ x_N \end{bmatrix} \quad b = \begin{bmatrix} b_1 \\ b_2 \\ \dots \\ b_M \end{bmatrix} \tag{A.2}$$

In order to obtain a unique solution, the number of unknowns,  $N$ , must be equal to the number of equations,  $M$ . If  $M < N$ , the system is under-determined, and a unique solution for all the unknowns is not possible. If  $M > N$  the system is over-determined, and a solution may or may not exist, and if it does exist, it can be unique.

If any equation of Equation A.1 can be represented exactly by a linear combination of any other equations in the set, then the equations are dependent. In this case, the set can be reduced to an under-determined set that cannot be solved for all the unknowns. As it is not always obvious that a set of equations are dependent, the linear equation solving packages available in Press et al (1990), contain a method of detection and correction, of dependency.



### A.1.1 Basic Principles for Solving Sets of Equations

Three linear methods; Graphical, Cramers rule and Algebraic manipulation, are limited to small ( $\leq 3$ ) numbers of equations, and are therefore of little use to this application.

The elimination of unknowns is an algebraic approach of solving for a set of two or more simultaneous equations. The basic approach of elimination of unknowns can be extended to larger sets of equations by developing an algorithm to eliminate unknowns and to back substitute. Gauss elimination is the most common of these. The solution technique consists of two phases: elimination of unknowns and solution through back substitution. By successive multiplication and elimination, this procedure can eliminate all the  $x_1$  terms from all the equations apart from Equation A.1(a).  $a_{11}$  is called the pivot element, and Equation A.1(a) is the pivot equation.

This process is continued for the remaining equations, and repeated for the remaining pivot equations. The final manipulation in the sequence is to use the (N-1)th equation to eliminate the  $x_{N-1}$  term from the Nth equation, leading to:

$$\begin{aligned}
 a_{11}x_1 + a_{12}x_2 + a_{13}x_3 + \dots + a_{1N}x_N &= b_1 & (a) \\
 a'_{22}x_2 + a'_{23}x_3 + \dots + a'_{2N}x_N &= b'_2 & (b) \\
 a''_{33}x_3 + \dots + a''_{3N}x_N &= b''_3 & (c) \\
 &\vdots & \\
 &\vdots & \\
 a^{(N-1)}_{NN}x_N &= b^{(N-1)}_N & (d)
 \end{aligned} \tag{A.3}$$

Equation A.3(d) can now be solved for  $x_N$ , and this result can be back substituted into the (N-1)th equation to solve for  $x_{N-1}$ . The procedure, which is repeated to evaluate the remaining  $x$ 's, can be represented by the following formula:

$$x_i = \frac{b_i^{(i-1)} - \sum_{j=i+1}^N a_{ij}^{(i-1)} x_j}{a_{ii}^{(i-1)}} \quad (\text{A.4})$$

For  $i = N-1, N-2, \dots, 1$ .

As computers carry only a limited number of significant figures (eight significant figures when using single precision), round-off errors can occur and must be considered when evaluating the results. The problem of round-off error can become particularly important when large numbers of equations are being solved. This is due to the fact that every result is dependent on previous results. Consequently, an error in the early steps will tend to propagate. A rule of thumb accepted by authors such as Chapra and Canale (1985), is that round-off errors may be important when dealing with 100 or more equations. It is recommended that double precision (16 significant figures) is used for more than 100 equations.

The adequacy of the solution also depends on the condition of the system. A well-conditioned system is one where a small change in one or more of the coefficients results in a similar small change in the solution. Ill-conditioned systems are those where small changes in coefficients result in large changes in the solution. Generally an ill-conditioned system is one with a determinant close to zero. In fact, if the determinant is exactly zero, the two slopes are identical, which denotes either no solution or an infinite number of solutions.

The foregoing technique is called 'naive' gauss elimination, because if a pivot element is zero, a division by zero would occur during the calculations. Similarly, if the pivot element is close to zero, then round-off errors can be introduced. For this reason most software packages include the technique of



pivoting to avoid these problems (Ref. Press et al (1990)).

Before each row is normalized, the largest available coefficient is determined. The rows can then be switched so that the largest element is the pivot element. This is called partial pivoting. Aside from avoiding division by zero, pivoting also minimises round-off error and is a remedy for ill-conditioning.

### A.1.2 Gauss-Jordan Elimination

The Gauss-Jordan method is a variation of Gauss-elimination. The major difference is that when an unknown is eliminated in the Gauss-Jordan method, it is eliminated from all other equations rather than just the subsequent ones. In addition, all rows are normalised by dividing them with their pivot elements. Thus the elimination step results in an identity matrix [I] rather than a triangular matrix. Consequently, it is not necessary to employ back-substitution to obtain the solution.

The Gauss-Jordan method relies on the concept that if a matrix [A] is square, there is another matrix,  $[A]^{-1}$ , which can be used to solve a set of simultaneous equations thus:

$$x = A^{-1} \cdot b \quad (\text{A.5})$$

The first linear flow model was developed utilising the Gauss-Jordan method for solving a square set of linear simultaneous equations. The Gauss-Jordan routine, which employs partial pivoting, was extracted from Press et al (1990). The coefficient matrix, [A], is augmented with an identity matrix [I], and then reduced to an identity matrix itself. When this is accomplished, the right-hand side of the augmented matrix contains the inverse. The inverse is then multiplied by the right-hand side vector, [b], to determine the solution.

Although the Gauss-Jordan technique and Gauss elimination appear almost identical, the former requires approximately 50% more operations and therefore is slower in raw operation count. The reason why this method was chosen for initial program development, was that it was considered to be straightforward, understandable and robust. In addition, the routine was easily obtainable from Press et al (1990).

### A.1.3 LU Decomposition

The primary appeal of LU decomposition is that the time-consuming elimination step can be formulated so that it only involves operations on the matrix of coefficients [A]. Thus, as with the Gauss-Jordan approach, it is well suited for those situations where many right-hand vectors [b], must be evaluated for a single value of [A]. It is actually preferable for such applications because it attains these solutions much more efficiently than the Gauss-Jordan approach, and it can be modified to determine the inverse  $[A]^{-1}$ .

If the equations to be solved are expressed in matrix notation as:

$$A \cdot x = b \quad (A.6)$$

Which can be rearranged to give:

$$A \cdot x - b = 0 \quad (A.7)$$

Suppose that Equation A.7 could be re-expressed as an upper triangular system with 1's on the diagonal:



$$\begin{bmatrix} 1 & u_{12} & u_{13} & u_{14} \\ 0 & 1 & u_{23} & u_{24} \\ 0 & 0 & 1 & u_{34} \\ 0 & 0 & 0 & 1 \end{bmatrix} \begin{Bmatrix} x_1 \\ x_2 \\ x_3 \\ x_4 \end{Bmatrix} = \begin{Bmatrix} d_1 \\ d_2 \\ d_3 \\ d_4 \end{Bmatrix} \quad (\text{A.8})$$

This is similar to the manipulation that occurs in the first step of Gauss elimination. It can also be expressed in matrix notation and rearranged to give:

$$U \cdot x - d = 0 \quad (\text{A.9})$$

If we also assume that there is a lower diagonal matrix:

$$L = \begin{bmatrix} l_{11} & 0 & 0 & 0 \\ l_{21} & l_{22} & 0 & 0 \\ l_{31} & l_{32} & l_{33} & 0 \\ l_{41} & l_{42} & l_{43} & l_{44} \end{bmatrix} \quad (\text{A.10})$$

that has the property that when Equation A.9 is pre-multiplied by it, Equation A.7 is the result. That is:

$$L \cdot \{U \cdot x - d\} = A \cdot x - b \quad (\text{A.11})$$

It follows from the rules of matrix multiplication that

$$L \cdot U = A \quad (\text{A.12})$$

and

$$L \cdot d = b \quad (\text{A.13})$$

Equation A.12 is referred to as the LU decomposition of [A]. One of the most efficient algorithms for decomposing [A] into [L] and [U] is called Crout decomposition. As such it lies at the heart of the LU decomposition method. The method can be implemented by the following concise formulas:

$$l_{i1} = a_{i1} \quad \text{for } i = 1, 2, \dots, N \quad (\text{A.14})$$

$$u_{1j} = \frac{a_{1j}}{l_{11}} \quad \text{for } j = 2, 3, \dots, N \quad (\text{A.15})$$

For  $j = 2, 3, \dots, N-1$ ,

$$l_{ij} = a_{ij} - \sum_{k=1}^{j-1} l_{ik} u_{kj} \quad \text{for } i = j, j+1, \dots, N \quad (\text{A.16})$$

$$u_{jk} = \frac{a_{jk} - \sum_{i=1}^{j-1} l_{ji} u_{ik}}{l_{jj}} \quad \text{for } k = j+1, j+2, \dots, N \quad (\text{A.17})$$

and

$$l_{NN} = a_{NN} - \sum_{k=1}^{N-1} l_{Nk} u_{kN} \quad (\text{A.18})$$

Once the matrix is decomposed, [L] and [U] can be employed to solve for [x]. This is accomplished in a two-step process. First Equation A.13 is employed to determine [d], for a particular [b], by forward substitution. This process can be represented concisely as:

$$d_1 = \frac{b_1}{l_{11}} \quad (\text{A.19})$$

$$d_i = \frac{c_i - \sum_{j=1}^{i-1} l_{ij} d_j}{l_{ii}} \quad \text{for } i = 2, 3, \dots, N \quad (\text{A.20})$$

Then Equation A.9 can be employed to compute, x, by back-substitution:



$$x_N = d_N \quad (\text{A.21})$$

$$x_i = d_i - \sum_{j=i+1}^N u_{ij}x_j \quad \text{for } i = N-1, N-2, \dots, 1 \quad (\text{A.22})$$

Just as for the elimination techniques, LU decomposition algorithms must employ partial pivoting to avoid division by zero, and to minimise round-off error. The pivoting is implemented immediately after computing each column of [L]. In contrast to the elimination techniques, the process is complicated by the fact that the right-hand side vector [b], is not operated on simultaneously with [A]. This means that the computer algorithm must keep track of any row switches that occur during the decomposition step. Such a scheme is employed in the LU decomposition routine presented in Press et al (1990).

## A.2 Non-Linear Modelling

Solving for a set of non-linear simultaneous equations requires a different approach to the methods that were described above, the principal method being iteration. Iteration is the process where the dependent variables are calculated with the required unknowns to be solved given a series of guessed values. After each calculation the calculated value for the dependent variable is checked against its desired value, and depending on the difference between these two values, new values are given to the unknowns and the process repeated. Eventually the calculated result matches the desired result and the values used for the unknowns on the last calculation are therefore the results. This technique relies on the fact that the true value of the dependent variable is always known in advance. For this reason the set of non-linear equations were re-arranged into the form shown in Equation A.23. The true value of the dependent variable was always known to be zero.

$$\begin{aligned}
 f_1(x_1, x_2, \dots, x_N) &= 0 = Y_1 \\
 f_2(x_1, x_2, \dots, x_N) &= 0 = Y_2 \\
 &\vdots \\
 &\vdots \\
 f_N(x_1, x_2, \dots, x_N) &= 0 = Y_N
 \end{aligned}
 \tag{A.23}$$

The solution of this set of simultaneous equations consists of a set of  $x$ 's that simultaneously result in all the equations equalling zero. One common approach is to reformulate the non-linear system as a single function:

$$F(x) = \sum_{i=1}^N [f_i(x_1, x_2, \dots, x_N)]^2 \tag{A.24}$$

where  $f_i(x_1, x_2, \dots, x_N)$  is the  $i$ th member of the original system of Equation A.23. The values of  $x$  that minimise this function also represent the solution of the non-linear system. This reformulation belongs to a class of problems called non-linear regression. As such, it can be approached with a technique such as the Levenberg-Marquardt algorithm.

### A.2.1 Levenberg-Marquardt Algorithm

Marquardt (1963) proposed a method, related to earlier suggestions by Levenberg, for varying smoothly between the extremes of two non-linear methods, the Hessian method and the steepest descent method. The Levenberg-Marquardt method is reported by Press et al (1990) to work very well in practice, and has become the standard of non-linear least squares routines.

If a model depends non-linearly on a set of  $M$  unknowns,  $a_k$ ,  $k=1,2,\dots,N$ , (in this case the unknowns are designated 'a', rather than 'x', to minimise possible confusion with the  $\chi$  (chi) symbol). The approach for solving for these unknowns is to define a  $\chi^2$  merit function, and by iteration determine best-fit values for the unknowns by its minimisation.



If the set of non-linear equations is of the general form:

$$\begin{aligned} y_1 &= f_1(a_1, a_2, \dots, a_N) \\ y_2 &= f_2(a_1, a_2, \dots, a_N) \\ &\vdots \\ y_N &= f_N(a_1, a_2, \dots, a_N) \end{aligned} \quad (\text{A.25})$$

The  $\chi^2$  merit function is:

$$\chi^2 = \sum_{i=1}^N \left[ \frac{y_{i,T} - y_{i,C}}{\sigma_i} \right]^2 \quad (\text{A.26})$$

Where

- $y_{i,T}$  = The true value of  $y$  of equation  $i$ .
- $y_{i,C}$  = The calculated value of  $y$  of equation  $i$ , using the present guessed values for the unknowns.
- $\sigma_i$  = The standard deviation for equation  $i$ .
- $N$  = The number of data points to be fitted.

The gradient of  $\chi^2$  with respect to the unknowns,  $a$ , which will be zero at the  $\chi^2$  minimum, has components:

$$\frac{\partial \chi^2}{\partial a_k} = -2 \sum_{i=1}^N \frac{[y_{i,T} - y_{i,C}]}{\sigma_i^2} \frac{\partial y_{i,C}}{\partial a_k} \quad k = 1, 2, \dots, M \quad (\text{A.27})$$

Taking an additional partial derivative reveals the Hessian matrix. The second derivative terms have been ignored as they can be considered to be negligible. Hence the Hessian matrix is:

$$\frac{\partial^2 \chi^2}{\partial a_k \partial a_l} = 2 \sum_{i=1}^N \frac{1}{\sigma_i^2} \left[ \frac{\partial y_{i,C}}{\partial a_k} \frac{\partial y_{i,C}}{\partial a_l} \right] \quad (\text{A.28})$$

It is conventional to remove the factors of 2 from equation's A.27 and A.28 by defining:

$$\beta_k \equiv -\frac{1}{2} \frac{\partial \chi^2}{\partial a_k} \quad \phi_{kl} \equiv \frac{1}{2} \frac{\partial^2 \chi^2}{\partial a_k \partial a_l} \quad (\text{A.29})$$

The Hessian method proposes that the increments  $\delta a_l$  are obtained from the solution of the following set of linear equations:

$$\sum_{l=1}^M \phi_{kl} \delta a_l = \beta_k \quad (\text{A.30})$$

While the steepest descent method suggests:

$$\delta a_l = \text{constant} \times \beta_l \quad (\text{A.31})$$

Marquardt proposed that the scale of the constant in Equation A.31 must be set by the reciprocal of the diagonal element of the  $[\phi]$  matrix. As the possibility remains that this scale might itself be too big, Marquardt suggested that it could be divided by some scaling factor  $\lambda$ , with the possibility of setting  $\lambda \gg 1$  to cut down the step. Equation A.31 can therefore be changed to:

$$\delta a_l = \frac{1}{\lambda \phi_{ll}} \beta_l \quad (\text{A.32})$$

Marquardt's second insight was that Equation A.30 and Equation A.32 could be combined if a new matrix  $[\phi']$  is defined in the following way:

$$\begin{aligned} \phi'_{jj} &\equiv \phi_{jj} (1 + \lambda) \\ \phi'_{jk} &\equiv \phi_{jk} \quad (j \neq k) \end{aligned} \quad (\text{A.33})$$

and then replace both Equation A.30 and Equation A.32 with the single equation:

$$\sum_{l=1}^M \phi'_{kl} \delta a_l = \beta_k \quad (\text{A.34})$$

When  $\lambda$  is very large, the matrix  $[\phi']$  is forced into being diagonally dominant, so Equation A.34 goes over to be identical to Equation A.32. On the other hand, as  $\lambda$  approaches zero, Equation A.34 goes over to Equation A.30.



Given an initial guess for the set of fitted unknowns,  $\mathbf{a}$ , the recommended Levenberg-Marquardt approach is as follows:

- i,      Compute  $\chi^2(\mathbf{a})$ .
- ii,     Pick a modest value for  $\lambda$ , say  $\lambda = 0.001$ .
- iii,    Solve the linear equations (Equation A.34) for  $\delta\mathbf{a}$  using a linear matrix solving technique such as LU decomposition, and evaluate  $\chi^2(\mathbf{a}+\delta\mathbf{a})$ .
- iv,     If  $\chi^2(\mathbf{a}+\delta\mathbf{a}) \geq \chi^2(\mathbf{a})$ , increase  $\lambda$  by a factor of 10 and go back to (iii).
- v,      If  $\chi^2(\mathbf{a}+\delta\mathbf{a}) < \chi^2(\mathbf{a})$ , decrease  $\lambda$  by a factor of 10, update the trial solution  $\mathbf{a}=\mathbf{a}+\delta\mathbf{a}$ , and go back to (iii).
- vi,     If the absolute value of  $(\chi^2(\mathbf{a}) - \chi^2(\mathbf{a}+\delta\mathbf{a})) < 0.1$ , convergence is close to occurring, therefore increment the variable 'ITST' by 1.
- vii,    If  $\text{ITST} < 3$ , return to (iii) to ensure convergence.
- viii,   If  $\text{ITST} = 3$ , the present values of,  $\mathbf{a}$ , are the final results.

### A.3 Bibliography for Appendix A

**Carnahan, B., H.A. Luther, and J.O. Wilkes.** (1969), *Applied Numerical Methods*, John Wiley and Sons.

**Chapra, S.C., and R.P. Canale.** (1985), *Numerical Methods for Engineers*, McGraw-Hill Book Co.

**LaFara, R.** (1973), *Computer Methods for Science and Engineering*, International Textbook Co. Ltd.

**Press, W.H., B.P. Flannery, S.A. Teukolsky, and W.T. Vetterling.** (1989), *Numerical Recipes, The art of Scientific Computing (FORTRAN version)*, Cambridge University Press.

**Shoup, T.E.** (1984), *Applied Numerical Methods for the Micro-Computer*, Prentice Hall.

## **Appendix B**

### **Lubricant Properties and General Modelling Data**



B.1 Grades of Oil

The American Society of Automotive Engineers (SAE) have divided oils into grades. The grades shown in Table B.1 have been taken from the SAE Handbook (1969, p. 324). The SAE viscosity grades in Table B.1 constitute a classification for engine oils of viscosity only. Other oil characteristics, such as those discussed in Appendix B.2, are not considered.

SAE viscosity number	Viscosity Units	Viscosity range			
		at -18°C (0°F)		at 99°C (210°F)	
		min.	max.	min.	max.
5W	Centipoises	-	1200	-	-
10W	Centipoises	1200	2400	-	-
20W	Centipoises	2400	9600	-	-
20	Centistokes	-	-	5.7	9.6
30	Centistokes	-	-	9.6	12.9
40	Centistokes	-	-	12.9	16.8
50	Centistokes	-	-	16.8	22.7

Table B.1. SAE viscosity numbers for crankcase oils

The classification is based on viscosities determined at 99 and -18°C (210 and 0°F). Viscosity grades with the letter W are based on -18°C (0°F) viscosities. Viscosity grades without the letter W are based on 99°C (210°F). A multi-viscosity graded oil, known simply as a multigrade, is one whose -18°C viscosity is within the prescribed range of one of the W grade classifications, and whose 99°C viscosity is within the prescribed range of one of the non-W grade classifications. For example a multigrade oil may fall into the 10W range at -18°C and SAE 30 at 99°C. For this reason it would be designated a 10W/30 multigrade.

The oil viscosity at 99°C is measured according to the American Society for Testing Materials (ASTM) D445, 'Method of Test for Kinematic Viscosity of Transparent and Opaque Liquids', and the results reported in centistokes. Viscosities so measured are useful as a guide in selection of the proper viscosity oil for use under normal engine operation.

The oil viscosity at -18°C is measured according to ASTM D2602, Method of Test for Apparent Viscosity of Motor Oils at Low Temperature Using the Cold Cranking Simulator, and the results reported in centipoises. Such measurements are intended to ensure that a given oil will permit satisfactory engine cranking under low ambient temperature conditions.

## B.2 Oil Additives

Typical chemicals used to enhance the performance of mineral oils in gasoline engines include:

- i, Detergents. These are used to prevent high temperature varnish deposits on pistons which may cause ring sticking. They are usually calcium, barium or magnesium oil soluble salts, or sometimes combinations of more than one. They are often mildly alkaline.
- ii, Dispersants. These prevent sludge deposits in the cooler parts of the engine by suspending dirt and combustion debris in the oil. They are often ashless (non-metallic) polymers dissolved in oil. Most dispersants have some detergent properties and visa versa, but in most formulations a combination of both is the most cost effective treatment.
- iii, Rust Inhibitors. These compounds reduce or eliminate rust in the engine



by neutralising strong acids and/or forming a protective barrier to keep water away from the metal surfaces.

- iv,     **Anti-Oxidants.** Oxidation inhibitors prevent oxygen from attacking the lubricant base fluid, thus preventing the formation of lacquers which may be acidic in nature. These weak acids may cause catastrophic corrosion of some bearing materials, notably unplated copper-lead.
- v,      **Anti-Wear (Extreme Pressure).** These prevent general cam and tappet distress and general metal to metal wear. At the rapid temperature rise which follows high load boundary lubrication but precedes possible welding, phosphorus and/or sulphur compounds react with the surfaces. This generates a film of solid lubricant which prevents catastrophic wear. The most common anti-wear additives are zinc diaryl dithiophosphates.
- vi,     **Anti-Foam.** It is often necessary to counteract the oils increased tendency to foam, which is induced by detergents and dispersants. A silicon fluid is usually used for this purpose, at very low concentrations of less than 20 parts-per-million. This additive functions by decreasing the surface tension of the oil. It keeps the lubricant from overflowing the sump and inhibits oxidation by reducing air/oil contact.
- vii,    **Pour Point Depressants.** These additives are used to control wax crystal growth at low temperatures. They keep the oil from solidifying and allow the lubricant to flow. Polymethacrylate polymers are usually used to modify the wax crystals and lower the temperature down to which an oil can be pumped to lubricate an engine.

- viii, Viscosity Index (VI) Improvers. VI improvers are oil soluble polymers that improve the viscosity-temperature characteristics of an oil. Simply put, they thicken the oil more at high temperatures than at low temperatures. By using a VI improver in a light base stock, the viscosity at low temperatures is not effected, but at high temperature the viscosity is more like that of a higher grade oil. The result is a multigrade oil.
- ix, Dyes. Dyes are often added in engine oils to aid identification or to make the oil more attractive to the consumer. Some also have antioxidant properties. They are usually inert, ashless, chemically complex materials used at very low concentrations.

A finished motor oil is a blend of a number of additives, some of which serve more than one function and the actions of which are preferably complementary to one another. The exact proportions and optimum chemical composition of each additive is determined from extensive bench and engine testing by the oil manufacturers.

The temperature v viscosity, and temperature v density properties of a BP 10W/30 motor oil (used in the AJ6 engine model) and 5W/40 oil (used in the V8 engine model) are presented in Appendix C.1.



B.3 Moody Chart

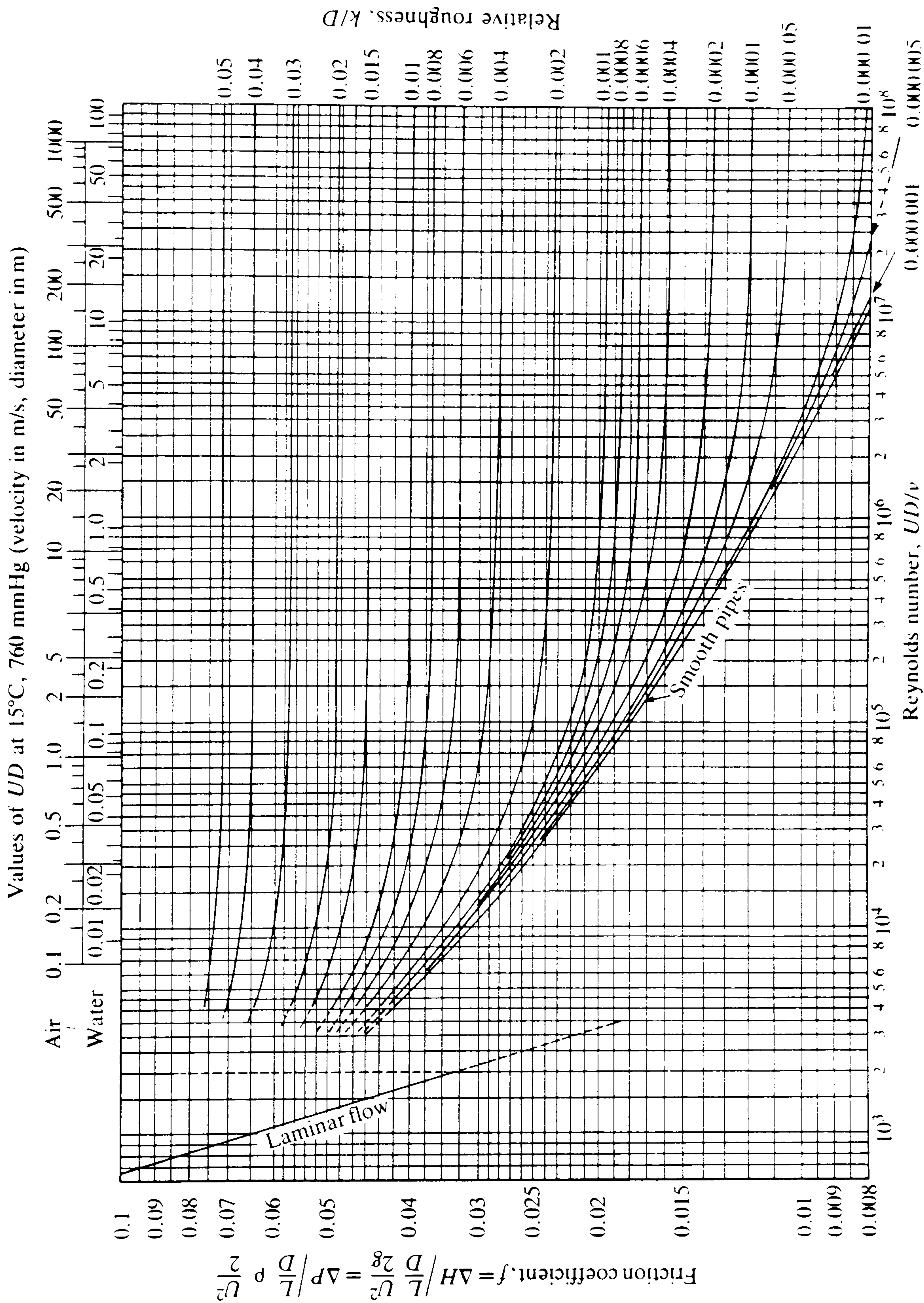


Figure B.1. Moody Chart - Friction Coefficient v Reynolds Number

B.4 Pipe Roughness Values

Table B.2 shows a selection of roughness values, *k*, for different types of pipes. The table was formulated from data published by Miller (1990).

Smooth pipes		
	Drawn brass, copper, aluminium, etc.	0.0025
	Glass, plastic, perspex, fibreglass, etc.	0.0025
Steel pipes		
	New smooth pipes	0.025
	Centrifugally applied enamels	0.025
	Light rust	0.25
	heavy rust	1.0
Other pipes		
	Sheet metal ducts with smooth joints	0.0025
	Galvanised metals, normal finish	0.15
	Galvanised metals, smooth finish	0.025
	Cast iron, uncoated and coated	0.15
	Asbestos cement	0.025
	Flexible straight rubber with smooth bore	0.025

Table B.2. Pipe roughness values, *k* (mm)



## B.5 Lubrication of Sliding Surfaces

An idealised lubrication diagram, showing the four different types of lubrication conditions, is given in Figure B.2. On the right hand side of the diagram is the desirable full fluid film or hydrodynamic lubrication regime. This regime offers low friction and wear with an oil film about 0.025 mm thick. The only relevant lubrication property in this regime is viscosity. Journal bearings and thrust pads operate in this regime.

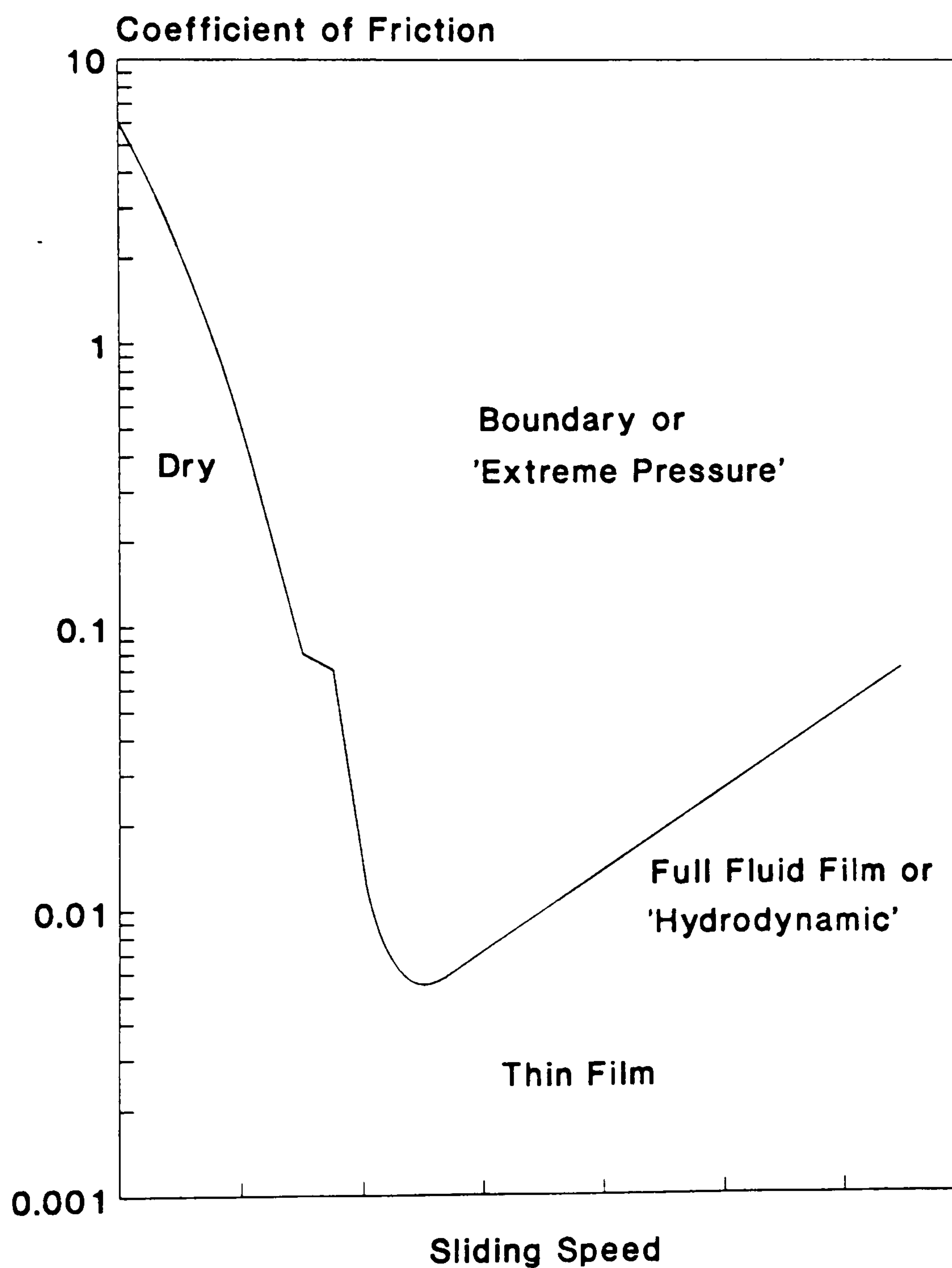


Figure B.2. Idealised lubrication regimes

As viscosity and/or sliding speed decreases, or load increases, lubrication moves into the thin film regime. Running gears, cams and tappets, and ball and roller bearings usually operate in this regime. Named "elastohydrodynamic lubrication" , the oil film thickness is down to 0.0025 - 0.000025 mm, and is dependent on elastic deformation of the surfaces to generate a film of lubricant.

At lower speeds yet, lubrication becomes "boundary". The limit here is not load but temperature. Unless chemical extreme pressure additives are used in the lubricant, temperatures in excess of 150-200°C cause adhesion and tearing, ie. scuffing rear. Cams and tappets and running hypoid gears operate in this region.

At still lower speeds, in outer space or at very high temperatures, the highly undesirable dry lubrication regime may be encountered. Friction coefficients ranging from 1 to 5 can cause high energy absorption and high wear rates.



## **Appendix C**

### **Component Performance Characteristics**

C.1 Thermal Properties of Lubricating Oil

The thermal properties of the BP SAE 10W/30 multigrade oil are shown in Table C.1. This grade of oil was used to model the lubrication system of the AJ6 engine. The density, viscosity, specific heat and prandtl number properties for this oil were provided by the suppliers.

Oil Property	Oil Temperature (°C)						
	40	60	80	100	120	140	160
Density (Kg/m <sup>3</sup> )	855	843	831	819	807	795	783
Dynamic Viscosity (Ns/m <sup>2</sup> )	0.064	0.029	0.017	0.01	0.066	0.0046	0.0033
Specific Heat Capacity (J/Kg°C)	1900	1980	2070	2150	2230	2310	2390
Prandtl Number	914	432	264	162	111	80	59

Table C.1. BP 10W/30 multigrade oil characteristics (AJ6 engine)

The properties of the ESSO SAE 5W/30 multigrade oil are shown in Table C.2. The oil used by Jaguar for development purposes was coded AL 3684/2. This grade of oil was used to model the lubrication system of the V8 engine.

The shaded portions in Table C.2 represent the measured oil properties which were provided by the supplier. The remaining properties were calculated using information contained in an Exxon publication (1990).



Oil Property	Oil Temperature (°C) (°F in brackets)								
	15 (59)	40 (104)	60 (140)	80 (176)	100 (212)	120 (248)	140 (284)	150 (302)	160 (320)
Oil Density (Kg/m³)	875.7	858.7	845.1	831.5	817.9	804.3	790.7	783.9	777.1
Kinematic Viscosity (m²/s)	115 x 10 <sup>-06</sup>	52.1 x 10 <sup>-06</sup>	28.0 x 10 <sup>-06</sup>	16.0 x 10 <sup>-06</sup>	9.97 x 10 <sup>-06</sup>	6.7 x 10 <sup>-06</sup>	4.6 x 10 <sup>-06</sup>	3.945 x 10 <sup>-06</sup>	3.35 x 10 <sup>-06</sup>
Dynamic Viscosity (Ns/m²)	0.1007	0.0447	0.02366	0.0133	8.154 x 10 <sup>-03</sup>	5.389 x 10 <sup>-03</sup>	3.637 x 10 <sup>-03</sup>	3.0924 x 10 <sup>-03</sup>	2.603 x 10 <sup>-03</sup>
Specific Heat Capacity (J/Kg°C)	1854.8	1938.6	2018.1	2097.7	2143.7	2240.1	2307.0	2340.5	2378.2
Thermal Conductivity (W/m°C)	1.0695	1.0548	1.0432	1.0316	1.0200	1.0083	0.9968	0.9908	0.9851
Prandtl Number	174.6	82.15	45.77	27.04	17.14	11.97	8.42	7.31	6.28

Table C.2. Esso 5W/30 multigrade oil characteristics (V8 engine)

The oil kinematic viscosities,  $\nu$ , were interpolated from the measured kinematic viscosities at 40, 100 and 150°C. The three known kinematic viscosities were plotted on an ASTM standard viscosity  $\nu$  temperature chart. The remaining viscosities were obtained from a best fit curve drawn through the three points. This curve is presented in Figure C.1.

The oil densities,  $\rho$ , were calculated from the following equation:

$$\rho_2 = \rho_1 - (0.00068 (t_2 - t_1))$$

(C.1)

Where

$t$  = Oil temperature (°C)

$\rho_1$  = Oil density at  $t_1$  (known to be 0.8757 Kg/l at 15°C)

$\rho_2$  = Desired oil density at  $t_2$  (Kg/l)



ASTM Viscosity-Temperature Chart – Centistokes

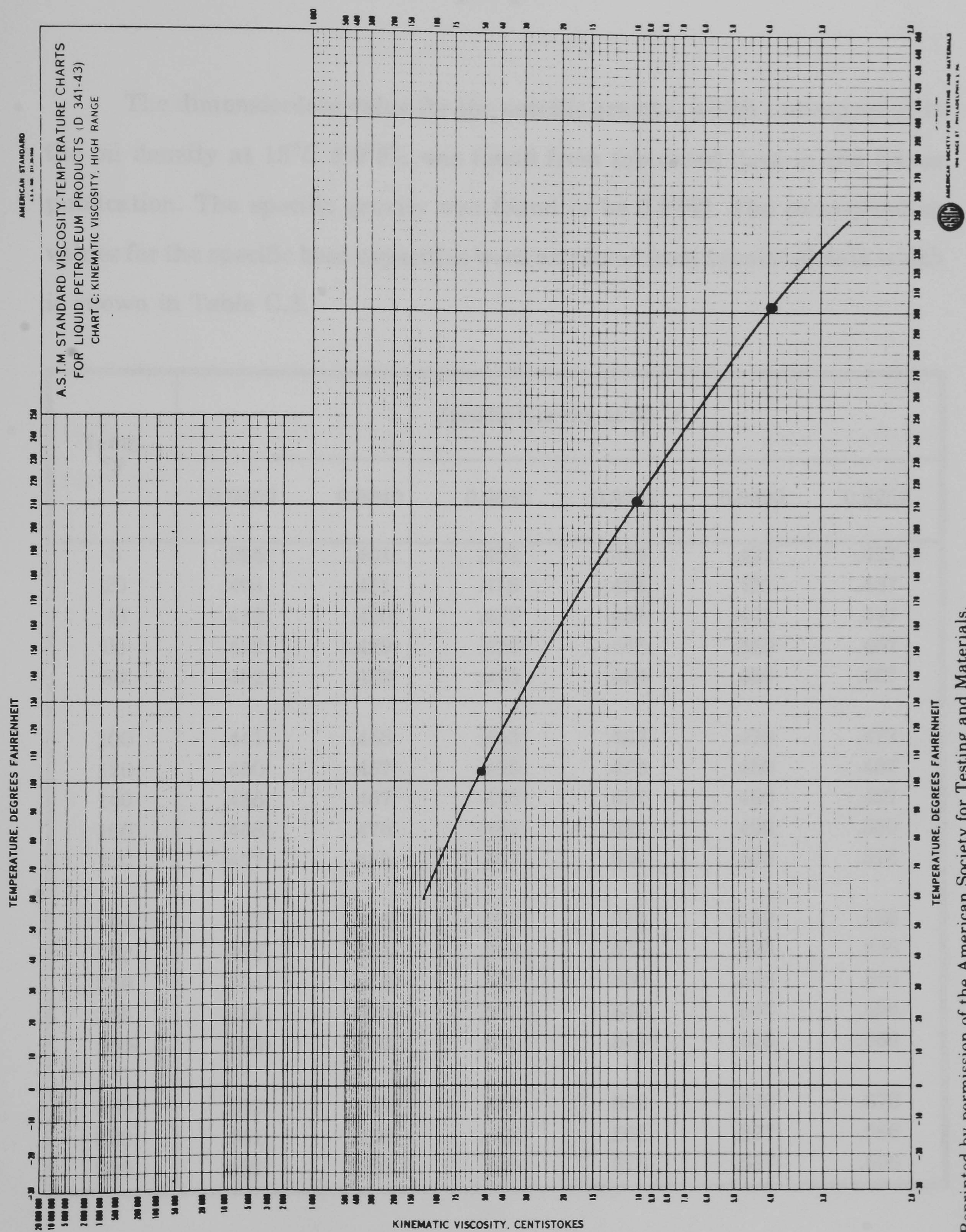


Figure C.1. Kinematic viscosities for an Esso 5W/30 multigrade oil plotted on a standard ASTM chart



The dynamic viscosities,  $\mu$ , were calculated from the simple relationship:

$$\mu = \rho \nu \tag{C.2}$$

The dimensionless value for the specific gravity, which corresponded to the oil density at 15°C (60°F), was found from tabulated data in the Exxon publication. The specific gravity was found to be 0.8762. The corresponding values for the specific heat capacities were extracted from tabulated data which is shown in Table C.3.

Temp. °F	Specific Gravity at 60 °F					
	0.9659	0.9340	0.9042	0.8762	0.8499	0.8251
0	.395	.401	.409	.415	.421	.427
20	.404	.411	.418	.424	.431	.437
40	.413	.420	.427	.434	.441	.447
60	.422	.429	.436	.443	.450	.457
80	.432	.439	.446	.453	.460	.467
100	.441	.448	.456	.463	.470	.477
120	.450	.457	.465	.472	.480	.487
140	.456	.467	.475	.482	.490	.497
160	.468	.476	.484	.491	.498	.560
180	.477	.485	.493	.501	.509	.516
200	.487	.495	.503	.511	.519	.526
220	.495	.504	.512	.520	.528	.536
240	.504	.513	.522	.530	.538	.546
260	.514	.523	.532	.540	.548	.556
280	.523	.532	.541	.549	.558	.566
300	.532	.541	.550	.559	.568	.576
320	.541	.550	.559	.568	.577	.586
340	.551	.560	.569	.578	.587	.596

Table C.3. Specific heats of lubricating oils (Btu per pound per °F)

The thermal conductivities,  $k$ , were calculated from the following expression:

$$k = \frac{0.813}{d} \times (1 - (0.0003(t - 32))) \quad (C.3)$$

Where:  $k$  = Thermal conductivity (Btu/h ft<sup>2</sup> °F/ft).  
 $d$  = Specific gravity at 60°F (previously found to be 0.8762).  
 $t$  = Oil temperature (°F).

Following the calculation of the densities, specific heat capacities and thermal conductivities, the prandtl numbers,  $Pr$ , were found from the general expression:

$$Pr = \frac{\mu C_p}{k} \quad (C.4)$$



C.2 Thermal Properties of Air

The thermal properties of dry air at atmospheric pressure are given in Table C.4. These properties were extracted from data published by Chapman (1987).

Air Property	Air Temperature (°C)						
	-20	0	20	40	60	80	100
Density (Kg/m³)	1.3944	1.2923	1.2042	1.1273	1.0596	0.9996	0.9460
Kinematic Viscosity (m²/s)	11.62 x 10 <sup>-6</sup>	13.31 x 10 <sup>-6</sup>	15.09 x 10 <sup>-6</sup>	16.96 x 10 <sup>-6</sup>	18.90 x 10 <sup>-6</sup>	20.92 x 10 <sup>-6</sup>	23.02 x 10 <sup>-6</sup>
Dynamic Viscosity (Ns/m²)	16.20 x 10 <sup>-6</sup>	17.20 x 10 <sup>-6</sup>	18.17 x 10 <sup>-6</sup>	19.11 x 10 <sup>-6</sup>	20.03 x 10 <sup>-6</sup>	20.92 x 10 <sup>-6</sup>	21.78 x 10 <sup>-6</sup>
Specific Heat Capacity (J/Kg°C)	1005.7	1005.7	1006.1	1006.8	1008.0	1009.5	1011.3
Thermal Conductivity (W/m°C)	22.49 x 10 <sup>-3</sup>	24.08 x 10 <sup>-3</sup>	25.64 x 10 <sup>-3</sup>	27.10 x 10 <sup>-3</sup>	28.52 x 10 <sup>-3</sup>	29.91 x 10 <sup>-3</sup>	31.27 x 10 <sup>-3</sup>
Prandtl Number	0.724	0.718	0.713	0.710	0.708	0.706	0.704

Table C.4. Thermal properties of dry air at atmospheric pressure

### C.3 Instantaneous Gas Temperature

The instantaneous gas temperatures for the combustion chamber of the Jaguar V8 engine are shown in Figure C.2. This data was extracted from the report published by Chang et al (1992).

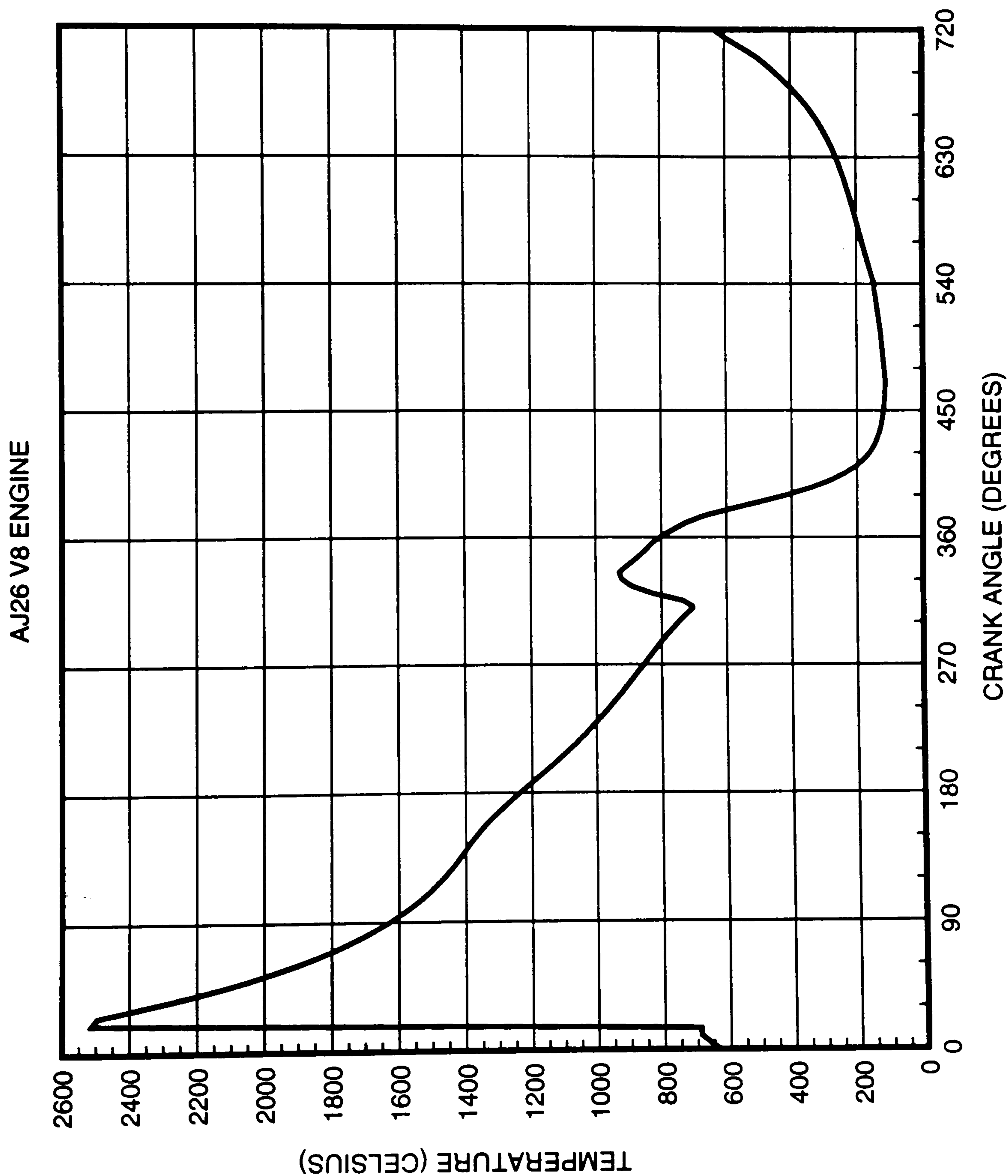


Figure C.2. Instantaneous gas temperatures for the combustion chamber of the V8 engine



C.4 Journal Centre Orbit Plots

AJ6 4.0 L Engine @ 2000 rpm—Cd = 0.025mm

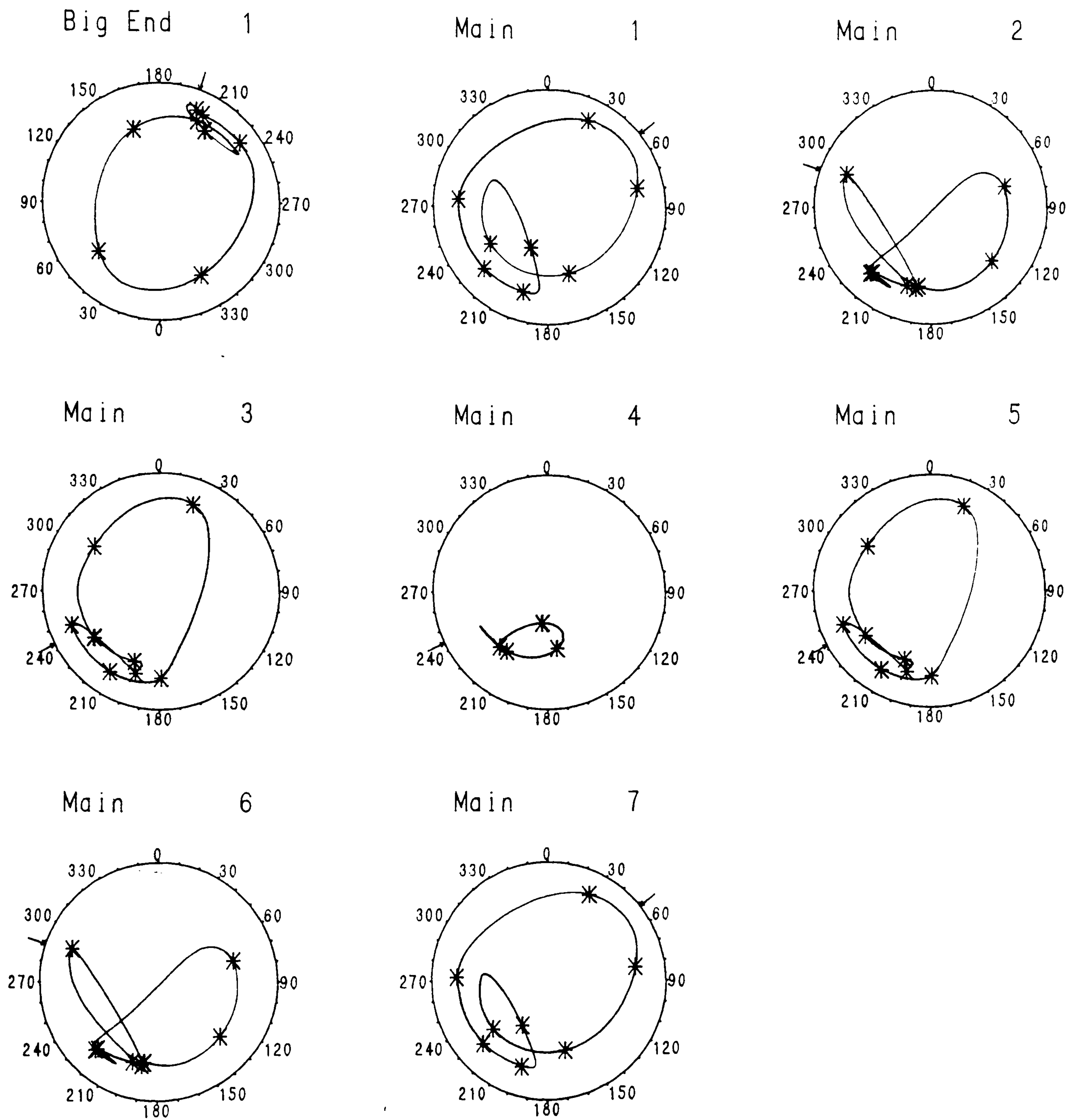


Figure C.3. Journal centre orbit plots for the main and big-end bearings of the Jaguar AJ6 engine

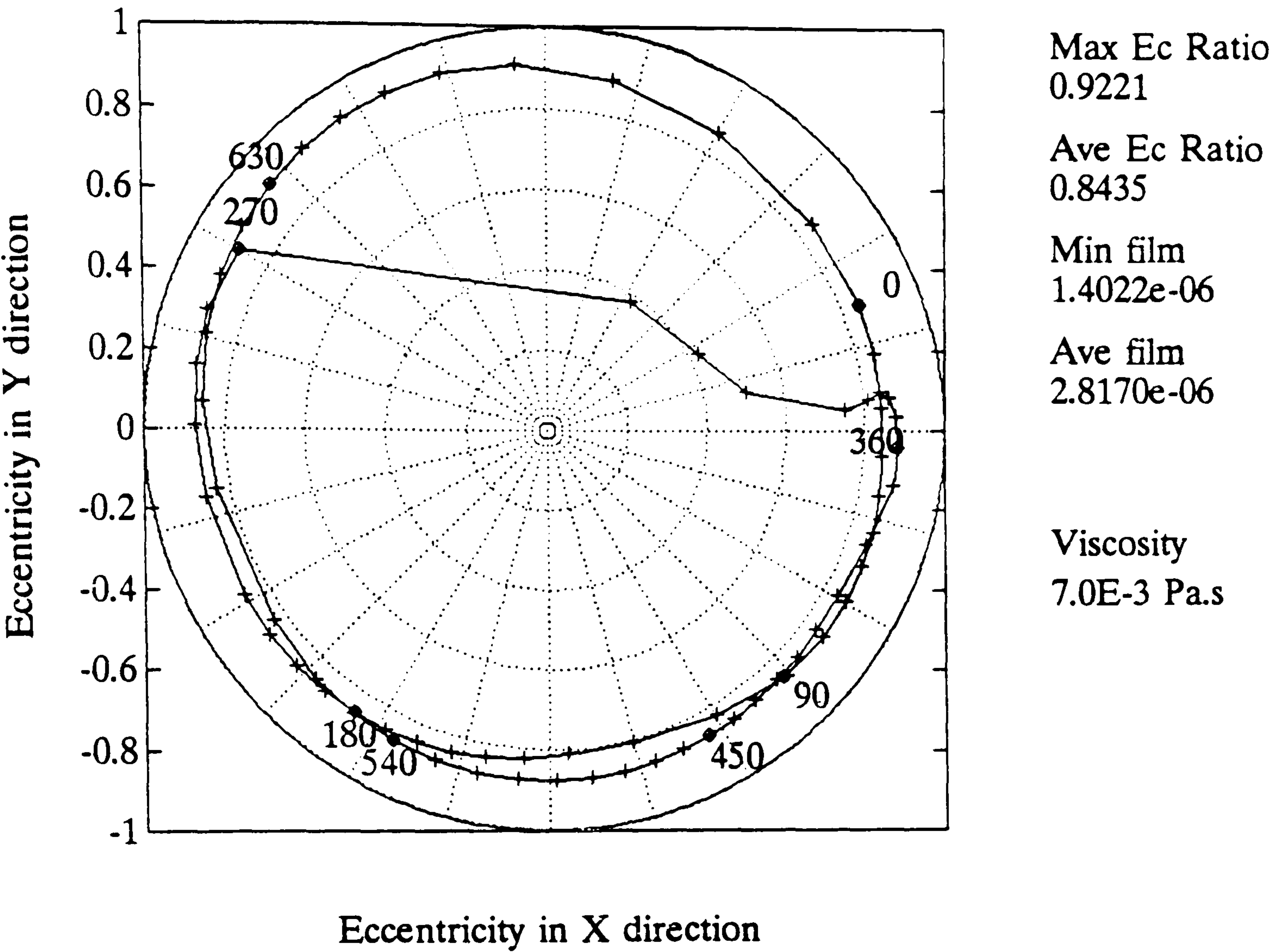


Figure C.4. Journal centre orbit plot for the No.2 main bearing of the V8 engine at 6000 rpm



## **Appendix D**

### **Supplementary Calculations**

## D.1 Oil Temperature Rise in the Pump

The change in the oil temperature within a typical Jaguar gear pump was estimated from the power consumption of the pump. The power consumption was calculated from a simple correlation which was extracted from Quale (1987):

$$q = \frac{QP}{\eta \times 10} \quad (D.1)$$

Where:

- q = The power consumption (KW).
- Q = The flow rate of the oil through the pump (m<sup>3</sup>/s).
- P = The pressure generated by the pump (N/m<sup>2</sup>).
- η = The pump efficiency in %.

Table D.1 shows the values which were selected for the variables listed above. These values were considered to be representative of the operating conditions within a Jaguar V8 engine, operating at 6000 rpm. Oil temperatures of 100°C and 15°C were selected to give an estimate of the power consumption within the pump over a reasonable operating oil temperature range. The resulting values for the power consumption, q, calculated from Equation D.1, are shown in the fifth column.

The oil temperature change, Δt, within the pump was estimated from the general expression shown in Equation D.2. The resulting values for the oil temperature rise within the pump are shown in the final column of Table D.1.



$$\Delta t = \frac{q}{\dot{m} C_p}$$

(D.2)

Where:         $\dot{m}$  = Mass flow rate of the oil, ie.  $Q \times \rho$ . (kg/s).  
                  $C_p$  = Specific heat capacity of the oil (J/Kg°C).

Sump Oil Temperature (°C)	Oil Flow Rate (m³/s)	Oil Pressure (N/m²)	Pump Efficiency (%)	Resulting Power Consumption (W)	Oil Temperature Rise (°C)
15	3.0 x 10 <sup>-4</sup>	5.25 x 10 <sup>5</sup>	80	196.8	0.37
100	2.5 x 10 <sup>-4</sup>	6.0 x 10 <sup>5</sup>	70	214.3	0.53

Table D.1.        Modelling conditions for the calculation of the oil temperature rise within a pump

## D.2 Typical Reynolds Number for a Falling Oil Film

The Reynolds number for a falling oil film was calculated from the expression:

$$Re = \frac{4 \dot{m}}{\mu C_w} \quad (D.3)$$

Where:  $\dot{m}$  = Mass flow rate of the falling oil film (kg/s).

$C_w$  = Width of the falling oil film (m).

It was assumed that a typical value for  $C_w$  would be half the circumference of a wetted liner. The oil flow rate,  $Q$ , which was splashed on to the surface, was assumed to be the flow rate through a single big-end bearing. The oil temperature was assumed to be 100°C. Thus:

$$\begin{aligned} Q &= 3.58 \times 10^{-6} \text{ m}^3/\text{s}, & C_w &= 0.1335 \text{ m.} \\ \mu &= 8.154 \times 10^{-3} \text{ Ns/m}^2, & \rho &= 817 \text{ Kg/m}^3 \end{aligned}$$

Therefore,

$$Re = \frac{4 \times 3.58 \times 10^{-6} \times 817.9}{8.154 \times 10^{-3} \times 0.1337} \quad (D.4)$$

Thus,

$$Re = 10.76$$



D.3 Oil Filter Characteristics

The following oil filter characteristics were plotted from Equation 4.45, for a wide range of oil flow rates. These characteristics were plotted using the variable values shown in Table D.2, for an oil at 100°C.

Variable	Notation	Value
Filter Bed Thickness	L	$6.35 \times 10^{-3} \text{ m}$
Fibre Diameter	$D_f$	$2.8 \times 10^{-6} \text{ m}$
Porosity	$\epsilon$	0.85 (dimensionless)
Projected Area of Fibres	$A_f$	$0.3584 \text{ m}^2$

Table D.2. Variable values used to plot the oil filter characteristics

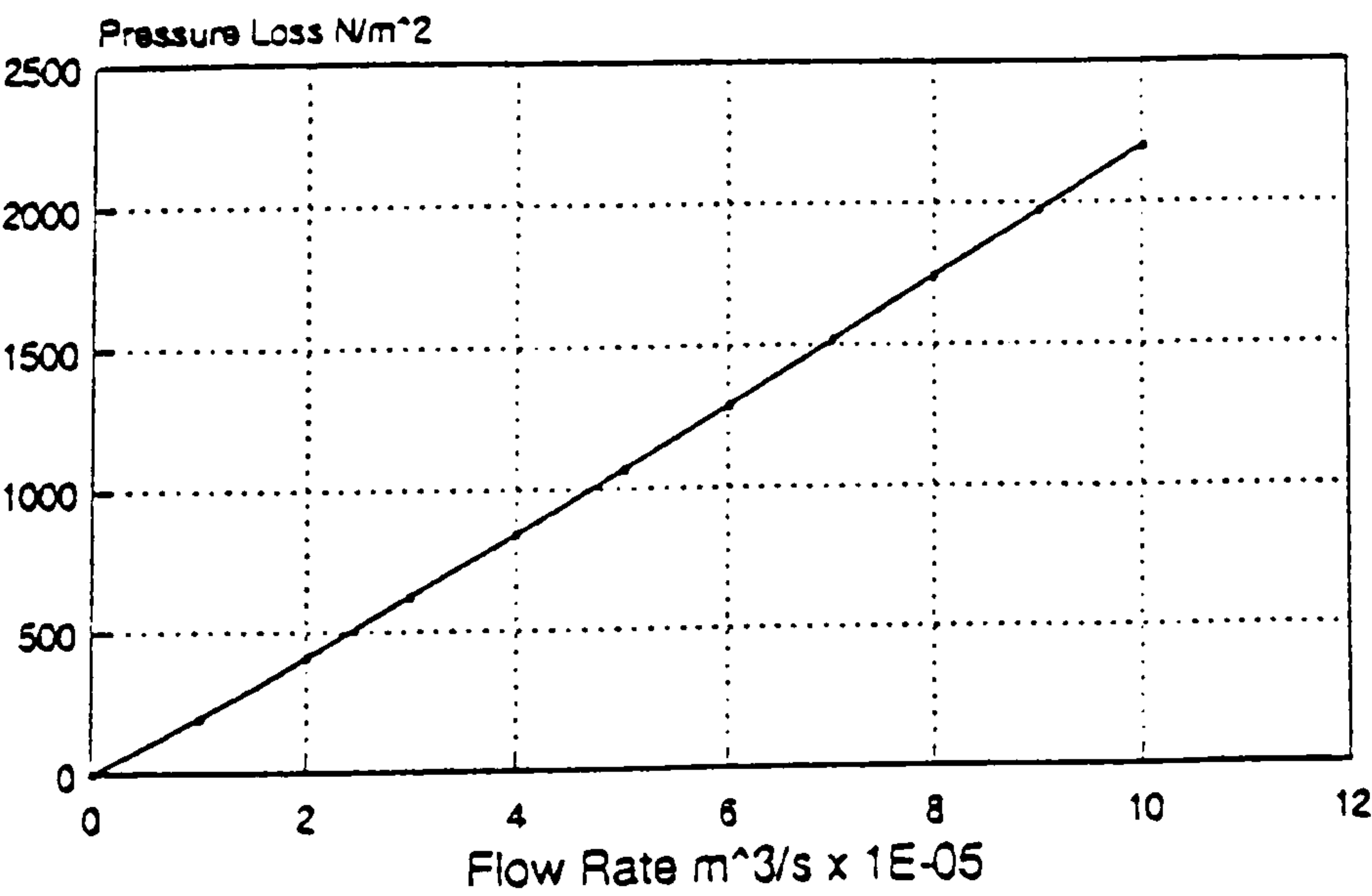


Figure D.1. Oil filter characteristics at low oil flow rates

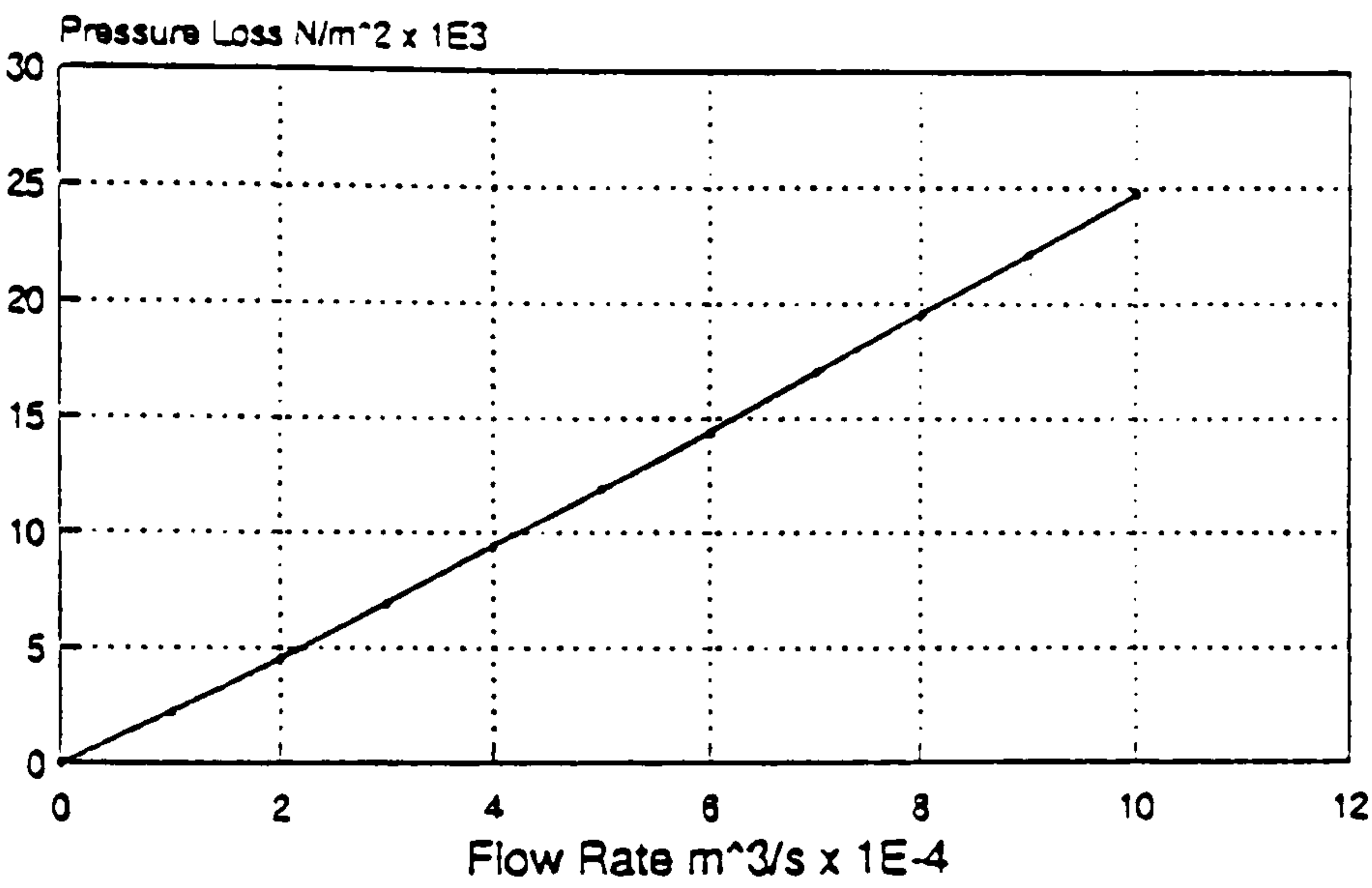


Figure D.2. Oil filter characteristics at medium oil flow rates

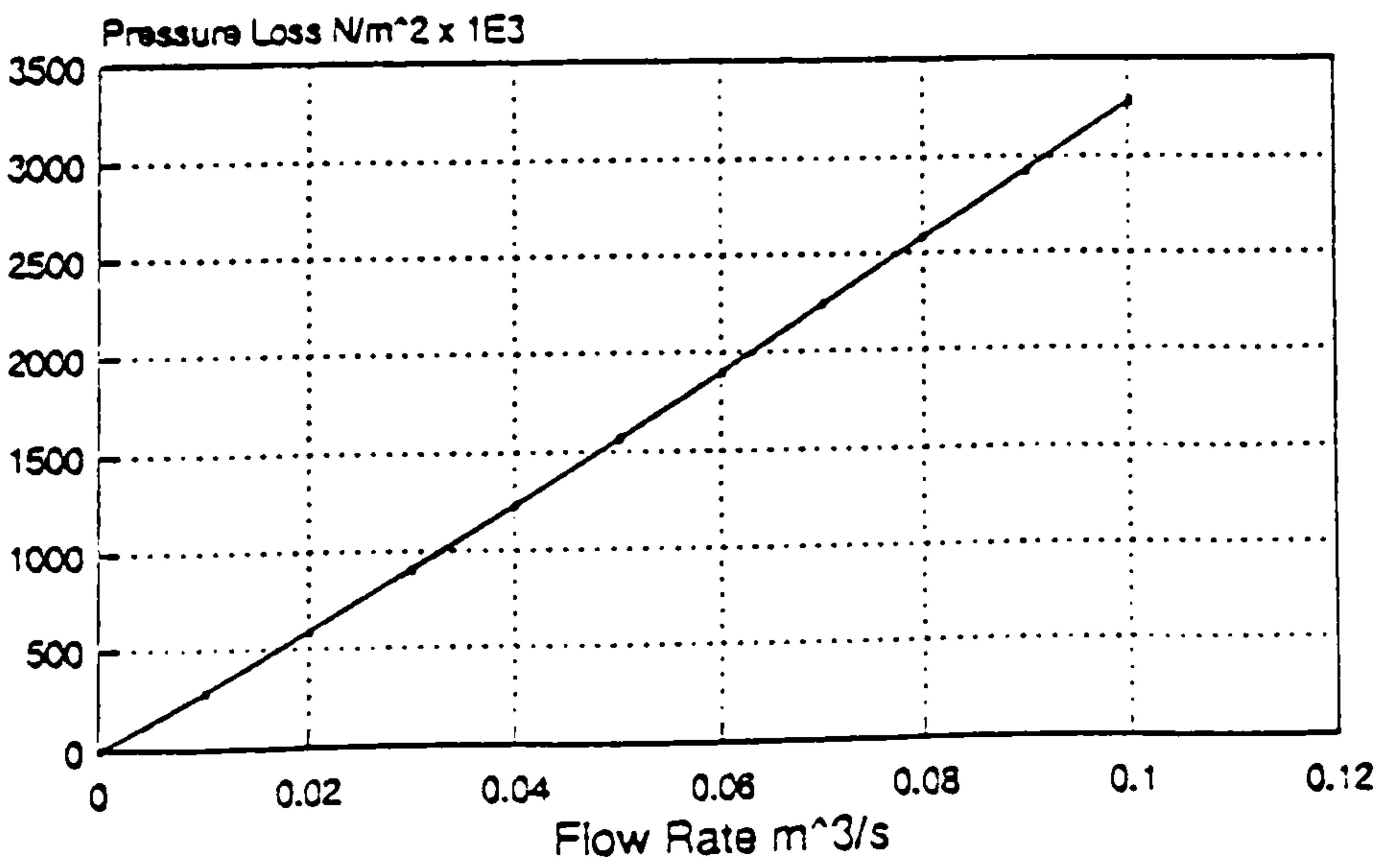


Figure D.3. Oil filter characteristics at high oil flow rates



D.4 Oil Cooler Dimensions

The dimensions of the oil cooler fitted to the Jaguar engines is shown in Table D.3.

Feature	Number	Length (m)	Height (m)	Width (m)
Tube or 'branch'	16	0.235	1.2x10 <sup>-3</sup>	36.4x10 <sup>-3</sup>
Manifold	2	0.122	28.0x10 <sup>-3</sup>	51.0x10 <sup>-3</sup>

Table D.3. Dimensions of the Jaguar oil cooler

$$Loss\ Ratio = \frac{total\ branch\ cross-sectional\ area}{manifold\ cross-sectional\ area}$$

(D.5)

$$Loss\ Ratio = \frac{16 \times 36.4 \times 10^{-3} \times 1.2 \times 10^{-3}}{51 \times 10^{-3} \times 28 \times 10^{-3}} = 0.49$$

(D.6)

$$Manifold\ length\ to\ branch\ length\ ratio = \frac{0.123}{0.235} = 0.52$$

(D.7)

## **Appendix E**

### **Experimental Investigation of the Jaguar AJ6 Engine**



## E.1 Introduction

A comprehensive experimental investigation was carried out on the Jaguar AJ6 4.0 litre engine, at the engine test facility of Jaguar Cars Limited in Coventry. The engine tests were carried out jointly with a researcher from Leeds University (Ref. Lai (1993)), who was conducting a detailed investigation of the engines main bearings. Oil pressure, oil flow rate and oil and metal temperatures were measured on the No. 4 and No. 7 main bearings. Additional oil flow rate, oil pressure and oil temperature measurements were made, for the purpose of this study, on the oil feed to the engine head. The total flow rate to the head was measured, as were the oil pressures and temperatures at the end of each cam-shaft.

The experiments were carried out in three parts. Different main bearing groove geometries were investigated in each part. These were:

- i, 180° groove on the top half (original arrangement).
- ii, Full circumferential groove.
- iii, 180° groove on the bottom half.

The results obtained during the first part of the experiment, with the main bearings in their original arrangement, were used for the purposes of this study.

The engine test cell at the Jaguar Engineering Centre was routinely instrumented for monitoring the operating condition of the test engine. This included the cylinder gas pressure, engine speed, engine torque, fuel consumption, coolant temperature and oil pump pressure. Additional instrumentation was added to measure the oil temperature, oil pressure, main

bearing metal temperature and the oil flow rate.

## E.2 Engine Modification and Instrumentation

All the temperature measurements were made using K-type thermocouples (Chromium/Aluminium). The temperature gradient across the shell of the main bearings was assumed to be small. Therefore, the thermocouples which measured the metal temperatures of the bearing shell were mounted on the engine block and bearing cap. The thermocouples were fixed with their junctions slightly raised above the metal surface. When the bearing shells were installed in position, the back of the shells were in contact with the thermocouple junctions. All the bearing metal temperatures were measured in this way.

The oil flow rates were measured using turbine flow meters. These meters were manufactured by Hydril UK Limited and designated as 'b-0.25-2'. The flow rates were measured by modifying the engine lubrication system. The oil supply drillings were plugged at several points, the drillings were tapped on either side of the plug and the oil flow was diverted externally through the turbine flow meters.

The two turbine flow meters which were used in the experiment were calibrated by AOT Systems Division, Hydril UK Limited. Calibration was carried out with an oil which had a specific gravity of 0.863 and a kinematic viscosity of  $110 \times 10^{-6} \text{ m}^2/\text{s}$  (15°C). The reported calibration data are recorded in Table E.1.



Flow Meter Identification	Turbine Flow Meter Output (Hz)	Oil Flow Rate (m <sup>3</sup> /s)
Turbine Flow Meter Ref. TS-10214. No. 4 Main Bearing (nodes 20 - 21)	131	1.7426 x 10 <sup>-5</sup>
	399	4.6597 x 10 <sup>-5</sup>
	807	9.1072 x 10 <sup>-5</sup>
	1200	13.4183 x 10 <sup>-5</sup>
	1486	16.6005 x 10 <sup>-5</sup>
Turbine Flow Meter Ref. TS-10213. No. 7 Main Bearing (nodes 25 - 26) or Flow to the Head (nodes 48 - 49)	131	1.8032 x 10 <sup>-5</sup>
	406	4.6672 x 10 <sup>-5</sup>
	807	9.0617 x 10 <sup>-5</sup>
	1206	13.0167 x 10 <sup>-5</sup>
	1484	16.6308 x 10 <sup>-5</sup>

Table E.1. Turbine flow meter calibration data

### E.3 Test Procedure

The engine was tested over a range of operating conditions. The effects on the temperature, pressure and flow rates in the lubrication system were investigated with the variation of the following operating parameters.

- i, Engine speed (2000 to 5000 rpm).
- ii, Engine load (see Table E.3).
- 3, Oil gallery temperature (the oil passed through an external oil cooler and the oil temperature was controlled through the operators console).

The Engine load was controlled through a dynamometer in the engine test cell. The load was measured in terms of the brake torque of the crankshaft. The magnitude of the brake torque at different engine speeds is shown in Table E.2.

Before any experiments were conducted, the test engine underwent a

Engine Speed (rpm)	Engine Load (Nm)			
	25%	50%	75%	Full
2000	82	164	246	328
3000	88	175	262	349
4000	93	159	279	372
5000	80	159	239	318

Table E.2. Brake torque of the Jaguar AJ6 4.0 litre engine

five hour running-in process, with different rotational speeds and loading conditions. During the test procedure, the required engine speed, load and oil gallery temperature were set at the control console. Experimental readings were recorded when the oil gallery and the sump temperatures reached stable values. All the recorded data was averaged for 20 seconds before being stored on the VAX computer. In general, after a test variable was altered, the time required by the test engine to reach thermal equilibrium state varied between 5 and 15 minutes. Each set of tests were repeated, a varying number of times, in order to assess the repeatability of the results. The test schedule for the first series of tests is shown in Table E.3.



Layout 1						
Test Number	Date	Time	Engine Speed (rpm)	Engine Load	Notes	Total Number of Tests
1	9-6-92	15.03	-	-	Run-In	3
2	9-6-92	15.41	3000, 4000	-	Run-In	2
3	10-6-92	08.49	3000, 3500, 4000	-	Run-In	3
4	10-6-92	13.04	2000, 3000, 4000, 5000	25%, 50%, 75%	Natural Oil Temperatures	12
5	11-6-92	08.02	0	0	Calibration Test	1
6	11-6-92	08.53	2000, 3000, 4000, 5000	25%, 50%, 75%	Natural Oil Temperatures	12
7	11-6-92	11.15	2000, 3000, 4000, 5000	25%, 50%, 75%	60°C Oil Temperature	14 (10 & 12 repeat)
8	11-6-92	14.17	4000, 5000	25%, 50%, 75%	Natural Oil Temperature	6
9	11-6-92	15.57	2000, 3000, 4000, 5000	25%, 50%, 75%	60°C Oil Temperature	13 (7 repeat)
10	12-6-92	10.32	2000	25%, 50%	Natural Oil Temperatures	2
11	12-6-92	11.15	2000, 3000, 4000, 5000	25%, 50%, 75%	Natural Oil Temperatures	12
Layout 2						
Test Number	Date	Time	Engine Speed (rpm)	Engine Load	Notes	Total Number of Tests
12	15-6-92	14.53	2000, 3000, 4000, 5000	25%, 50%, 75%	Natural Oil Temperatures	12
13	16-6-92	09.04	2000, 3000, 4000, 5000	25%, 50%, 75%	60°C Oil Temperature	12
14	16-6-92	10.42	2000, 3000, 4000, 5000	25%, 50%, 75%	Natural Oil Temperatures	14 (4 & 13 repeat)
15	16-6-92	13.30	2000, 3000, 4000, 5000	25%, 50%, 75%	60°C Oil Temperature	14 (3 & 6 repeat)
16	16-6-92	14.42	5000	50%	Various Oil Temperatures. 60°C - 120°C	8

Table E.3. Test schedule for first series of AJ6 engine tests (main bearings 180° groove on the top half)

## **Appendix F**

# **Experimental Investigation of the Jaguar V8 Engine**



F.1 Test Schedule

Oil Survey Test Engine No. 1013. V8 4.0 litre				
Test No.	Date	Time	Oil Temperature (°C)	Notes
1	20-08-92	10:32	70	No Load
2	20-08-92	12:12	70	WOT
3	30-08-92	07:24	100	WOT
4	03-09-92	11:21	130	WOT
5	09-09-92	11:01	70	No Load. Relief Valve Shut
6	09-09-92	14:02	70	WOT. Relief Valve Shut
7	09-09-92	14:36	100	WOT. Relief Valve Shut
8	11-09-92	09:12	130	WOT. Relief Valve Shut
9	14-09-92	10:29	130	WOT. Relief Valve Shut. Flow Meter Removed. Oilfin/Oilfout Adaptor Fitted
10	16-09-92	10:22	130	WOT. Relief Valve Open. Else Test 9
11	17-09-92	07:41	70	WOT. 4 Litres Oil in Sump. As 10
12	17-09-92	09:20	100	WOT. As 11
13	17-09-92	10:21	130	WOT. 4 Litres Oil in Sump. Else Test 10
14	17-09-92	14:42	Min. Temp	No Load. 6 Litres Oil in Sump

Table F.1. Test schedule for V8 engine oil system tests